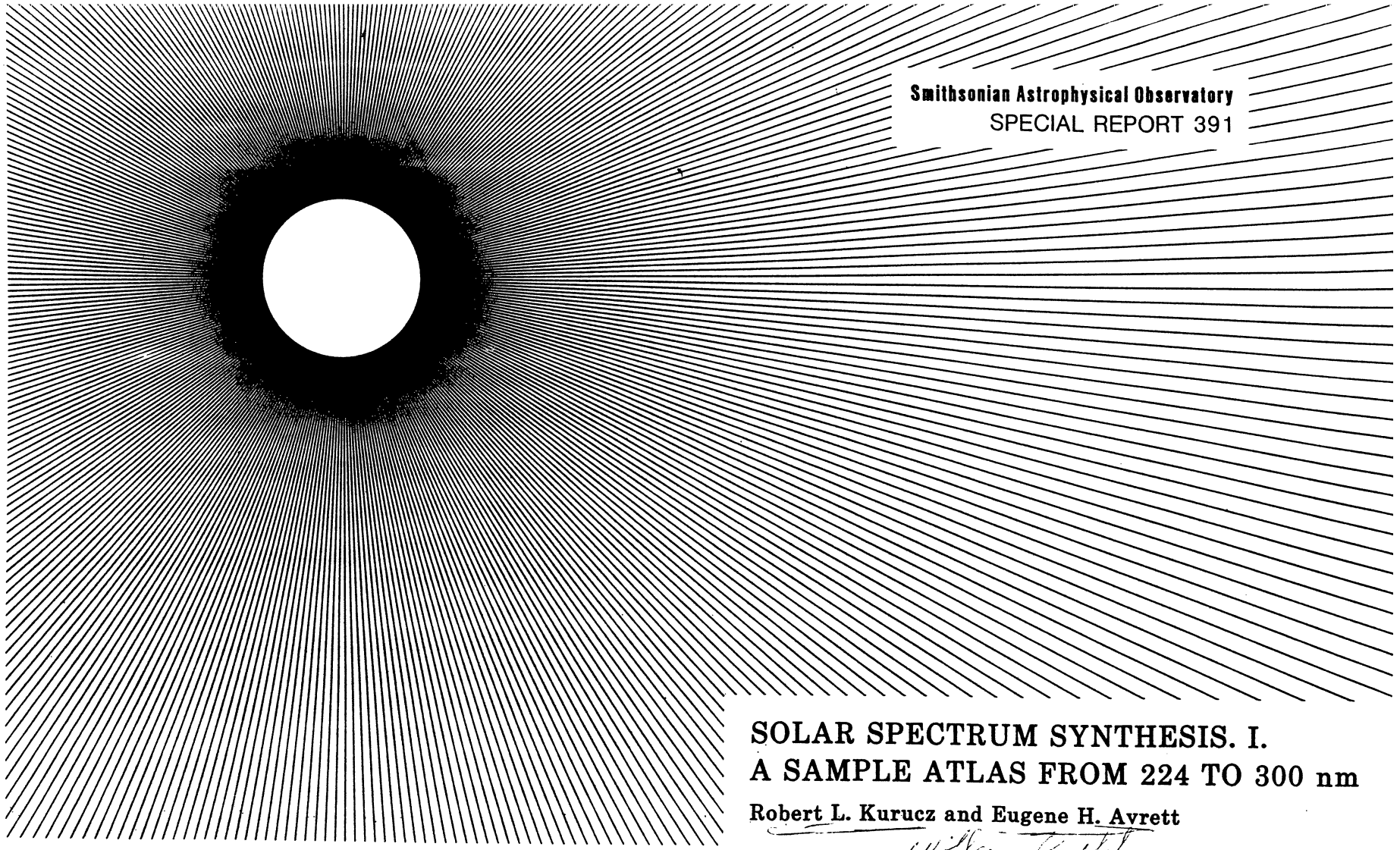

Smithsonian Astrophysical Observatory
SPECIAL REPORT 391

SOLAR SPECTRUM SYNTHESIS. I. A SAMPLE ATLAS FROM 224 TO 300 nm

Robert L. Kurucz and Eugene H. Avrett

Research in Space Science
SAO Special Report No. 391

SOLAR SPECTRUM SYNTHESIS. I.
A SAMPLE ATLAS FROM 224 TO 300 nm

Robert L. Kurucz and Eugene H. Avrett
Harvard-Smithsonian Center for Astrophysics

May 1981

Smithsonian Institution
Astrophysical Observatory
Cambridge, Massachusetts 02138

TABLE OF CONTENTS

FIGURES

ABSTRACT

We have developed sophisticated computer programs for determining solar and stellar atmospheric structure through the analysis of spectra. These programs allow us to treat the spectrum as a whole and to draw much stronger conclusions than would be apparent from individual spectral features.

For a given LTE or non-LTE model atmosphere, the programs compute the emergent flux or the specific intensity at up to 20 angles. The spectrum can be broadened by macroturbulence and rotation; it can be modified by transmission through the Earth's atmosphere; it can be convolved with the instrumental profile; and it can finally be plotted together with the observed spectrum with each line labeled. In the opacity calculation, the lines are broadened by radiative, Stark, and van der Waals damping, and they can have isotopic and hyperfine splitting, autoionization, partial redistribution, or be merged into a continuum. The departure coefficients for ions treated in non-LTE in the model atmosphere calculation can be used in the spectrum synthesis programs for all lines of these ions, and highly ionized lines can be treated in the coronal approximation. The model atmosphere can have depth-dependent doppler shifts corresponding to large-scale motions.

Using the Vernazza, Avrett, and Loeser models for the average quiet sun, we have computed theoretical solar spectra that include all available atomic and molecular line data. In this atlas we compare with the best available observed spectra in the 224- to 300-nm wavelength range, namely, the Kohl, Parkinson, and Kurucz (Harvard) center and limb rocket spectra in the range 224 to 300 nm; the Allen, McAllister, and Jefferies (Hawaii) disk center rocket spectrum for 268 to 293 nm; and the Brault and Testerman disk center spectrum taken at Kitt Peak for 294 to 300 nm. We also compare the observed spectra with each other.

The existing spectra are noisy and do not have adequate resolution, so that it is difficult or impossible to identify weak features, to resolve blends, to study velocity fields, to search for variability, or to do any of the projects that can be routinely done

in the visible where high quality spectra are available. Because the ultraviolet spectrum provides diagnostics for the upper photosphere, the temperature minimum, and the chromosphere, our understanding of these regions of the solar atmosphere is seriously impaired.

One-half the lines in the observed spectrum are not identified. The overall level of the calculation lies considerably above the observed. The discrepancy is caused mainly by missing atomic and molecular lines and possibly by errors in the measured continuum opacities. Laboratory spectral analyses are seriously incomplete, especially for the iron group atoms and for high J and V molecular levels of CO, SiO, and the hydrides. Any model atmosphere or non-LTE rate calculation that depends directly on available ultraviolet opacities should not be trusted.

1981SAOSR.391.....K

SOLAR SPECTRUM SYNTHESIS. I.
A SAMPLE ATLAS FROM 224 TO 300 nm

Robert L. Kurucz and Eugene H. Avrett

1. INTRODUCTION

The goal of the research reported here is to determine the temperature and density structure of the solar atmosphere through computer simulation of the spectrum, based on detailed non-LTE model calculations. We take an assumed variation of temperature with height, compute the spectrum, and compare it with ground-based, rocket, and satellite observations. We study the differences between the computed and observed spectra, first to determine whether the basic physics of our computer calculations is sufficiently complete and realistic, and then to determine the physical conditions for the atmospheric region under study. These detailed models provide not only the temperature and density stratification but also the internal radiation field, a description of the excitation and ionization of the various atomic and molecular constituents, and other data needed for a basic physical understanding of the structure and behavior of the solar atmosphere.

Our studies of the computed and observed spectra have led us to introduce many changes and improvements in our computer programs. As a result, we are now able to compute quiet-sun models (Vernazza, Avrett, and Loeser, 1973, 1976, 1981) that match observations in much greater detail than has been possible before. The computer program development and the analysis of observations required for the completion of this phase of the research have been of a general nature so that we can construct models of coronal holes, sunspots, active regions, and flares in a similar way as a routine continuation of the present research effort.

This work was supported in part by National Aeronautics and Space Administration grant NSG-7054 and by a grant of computer time at the National Center for Atmospheric Research, which is sponsored by the National Science Foundation.

We compute the model atmospheres with the PANDORA non-LTE computer program, which solves the radiative transfer, statistical equilibrium, and hydrostatic equilibrium equations for H, He, C, Mg, Al, Si, Ca, and other constituents. (See Vernazza, Avrett, and Loeser, 1981, and references therein.)

In this paper we describe the spectrum synthesis programs and present sample calculations in the form of an atlas. One of the objectives of these calculations is to find the shortcomings and errors in our line data so that we can improve the data and consequently the modeling. When we find particular problems in the spectrum of some ion or molecule, we introduce improvements in the physics that affect the whole spectrum at once. We do not try to force individual lines to match because, with the noisiness and low resolution of the available spectra, we frequently cannot distinguish whether an error in a feature is caused by an incorrect gf value or by a bad damping constant or by blending with other lines that have not been included. Because many of these blends can be high J molecular lines that have a temperature, optical depth, and limb darkening behavior radically different from atomic lines, we could introduce significant physical errors in our models by forcing a match to the wrong data. Our approach is to compute the spectrum as best we can, to encourage new laboratory work on atomic and molecular spectra, to improve the reduction of the existing observed solar spectra, and to encourage new observations.

The problem of the so-called "missing" solar opacity has been investigated by Dragon and Mutschlecner (1980), and they include a discussion of earlier work. They studied the "missing" opacity at relatively low resolution by comparing atomic and statistical molecular calculations to intensity and flux measurements of varying resolution. For atomic data they used the Kurucz and Peytremann (1975) line list, while for molecular data they investigated nearly all possible bands, estimating constants when necessary. Because they worked statistically, they were able to use very approximate smeared line expressions for the opacities. They found a match in the overall level somewhat better than we do because they included molecular lines to high V and high J. They found, as we do, a large discrepancy between 230 and 260 nm.

Dragon and Mutschlecner made a number of simplifications in their calculations that we do not have to make. By treating the spectrum directly instead of statistically,

we can compare the calculated and observed spectra line by line and ascertain whether discrepancies come from missing lines, or from bad damping constants, or from lines that are computed to be too strong or too weak. By including the molecular lines explicitly we get an opacity that is much more accurate than a band model, and the line by line comparison allows us to check level populations and relate the molecular line strengths to the structure of the solar model. Dragon and Mutschlecner used the approximation of a damping constant ten times the classical value, but we are able to treat damping more realistically. We can study the center-to-limb decrease in the van der Waals broadening, which is proportional to number density.

The comparison of detailed calculated spectra with the observed spectra provides us with much more information about the structure of the solar atmosphere and the sources of the ultraviolet opacity, and allows us to draw much stronger conclusions, than is possible with simplified approaches. A calculated spectrum can be a helpful guide to reducing observed spectra and setting wavelength scales and can also indicate errors in the observations.

In Section 2 we describe our spectrum synthesis computer programs. In Section 3 we compare our calculated spectra with the observed spectra and the observed spectra with each other, and discuss the comparisons. Section 4 summarizes our current and future work.

1981SAOSR.391.....K

2. SPECTRUM SYNTHESIS PROGRAMS

The spectrum synthesis computer programs have been under development since 1965 and have been described by Kurucz and Furenlid (1980). The algorithms for computing the total line opacity are extremely fast because maximum use is made of temperature and wavelength factorization and pretabulation. In the work described here, we had access to computers with large real or virtual memories and have modified the programs to allow the computation of up to 500,000 wavelength points in one run. We have removed a number of approximations where mean wavelengths or frequencies had been used earlier because the wavelength intervals can be quite long. A detailed description of these programs follows.

The spectrum calculations require a pre-existing model atmosphere. The model can be empirical, such as one of the solar models of Vernazza, Avrett, and Loeser (1981; hereinafter VAL), or theoretical, such as the radiative and convective equilibrium models of Kurucz (1979) or Gustafsson, Bell, Eriksson, and Nordland (1975). The VAL model C, including departure coefficients, was used in the calculations described here. Quantities that need be computed only once for the model atmosphere are pretabulated. The model is read in, including departure coefficients if the model was computed in non-LTE. The continuum opacity is tabulated at wavelength points on both sides of every photoionization edge and throughout the Balmer and Paschen continua for later use in estimating the strength of line wings relative to the continuum. The atomic and molecular number densities divided by partition functions are pretabulated for later use in Boltzmann equations. Doppler velocities are also pretabulated for each atom and molecule with allowance for depth-dependent microturbulence.

Line data are divided into two groups for treatment. In the first group, the source function for the lines is the Planck function B_ν or some other specified function that approximately accounts for non-LTE effects in the surface region. In the work reported here the line source function was taken to be the continuum source function of the ground level of Si I, which approaches the Planck function in the photosphere. Program SYNTHE processes this first group of lines to produce a summed line absorption coefficient for the wavelength interval of interest, which may be specified for either air or vacuum wavelengths.

In the second group of lines, we calculate a source function for each line, which reduces to B_ν in LTE. In this calculation the source functions are computed from the departure coefficients of the VAL Model C. Program SPECTR processes this group of lines by directly summing the line opacity and source function contributions at every wavelength and combining these results with the line opacity and source function obtained from SYNTHE.

We have used the Kurucz and Peytremann (1975) basic line list with corrections and deletions together with many additional lines from the literature. Included in this calculation were H_2, CO (Kurucz, 1977), SiO (Kurucz, 1980), and Fe II (Kurucz, 1981). There are two versions of these line lists, lines with real wavelengths between known energy levels, and lines with approximate wavelengths between predicted energy levels. Only lines with real wavelengths were used in this calculation. The line data are being constantly improved so that those used here are a year out of date as of this writing. At the present time we also have compiled line data for CH and OH and are working on all the hydrides.

The program SYNTHE extracts a smaller list of lines that fall in or overlap the wavelength interval. For each line, the air or vacuum wavelength, the exact upper and lower energy levels, and the gf value must be given. Other data may also be specified, such as the upper and lower J, labels for the upper and lower level, radiative, Stark, and van der Waals damping constants, fractional isotopic abundances for treating isotopic lines, comments, and references. Departure coefficient indices for the upper and lower levels, line strength, partial redistribution, and autoionization parameters may also be specified for later use in the individual line calculations. Coronal lines may also be designated for later treatment in the coronal approximation. Pseudolines may be read in for photoionization edges that serve to move the edge to the wavelength at each depth where the line series merges into a continuum.

Damping constants are treated as follows:

Radiative: If Γ_R is not specified for a line, the classical value is assumed,

$$\Gamma_R = 2.223\text{E}13/\lambda^2 \quad \text{for} \quad \lambda \text{ in nm} \ ;$$

Stark: Γ_S/N_e is assumed to be a constant. If Γ_S/N_e is not specified, we use the approximation

$$\Gamma_S/N_e = 1.0E\text{-}8\ n_{eff}^5 \quad ,$$

which is a fit by Peytremann (1972) to detailed calculations by Sahal-Brechot and Segre (1971). Here, n_{eff} is the effective quantum number of the upper state,

$$n_{eff}^2 = \frac{R\ Z_{eff}^2}{E_{ion} - E_{upper}} \quad ,$$

where R is the Rydberg energy, Z_{eff} is the effective charge (= 1 for Fe I, 2 for Fe II, etc.), and E_{ion} is the ionization potential. If the upper level is above the ionization potential because it ionizes to an excited level of the parent, n_{eff} is set to 5. For molecules we arbitrarily adopt $\Gamma_S/N_e \equiv 1.0E\text{-}5$.

van der Waals: Starting with the treatment in Aller (1963) and taking into account the polarization of H, He, and H_2 we adopt

$$\Gamma_W = 17\left[\frac{8\,kT(1/A+1/1)}{\pi M}\right]^{0.3}\left[6.63E\text{-}25\,\frac{e^2}{h}\left(\langle r^2\rangle_{up} - \langle r^2\rangle_{lo}\right)\right]^{0.4} N_H$$
$$+17\left[\frac{8\,kT(1/A+1/4)}{\pi M}\right]^{0.3}\left[2.07E\text{-}25\,\frac{e^2}{h}\left(\langle r^2\rangle_{up} - \langle r^2\rangle_{lo}\right)\right]^{0.4} N_{He}$$
$$+17\left[\frac{8\,kT(1/A+1/2)}{\pi M}\right]^{0.3}\left[8.04E\text{-}25\,\frac{e^2}{h}\left(\langle r^2\rangle_{up} - \langle r^2\rangle_{lo}\right)\right]^{0.4} N_{H_2} \quad .$$

Then, assuming that the atomic weight A is much greater than 4, and that the mean-square-radius of the lower level $\langle r^2\rangle_{lo}$ is small compared to $\langle r^2\rangle_{up}$, we obtain

$$\Gamma_W = 4.5E\text{-}9\ \langle r^2\rangle^{0.4}\left[N_H + 0.42\ N_{He} + 0.85\ N_{H_2}\right]\left(\frac{T}{10000}\right)^{0.3} \quad .$$

These approximations assume a single optical electron, and that the f sum rule yields 1, which is not in fact the case for the d^n levels of the iron group.

In practice, the coefficient $4.5E\text{-}9\ \langle r^2\rangle^{0.4}$ in the expression for Γ_W, which is also Γ_W/N_H at 10,000 K for pure hydrogen, is specified in the input or calculated, and the He and H_2 dependencies are computed. If this coefficient is not specified, we compute it from the following expressions for $\langle r^2\rangle$. For iron group elements, assuming that strong lines have a 4p upper level, we have computed values of $\langle r^2\rangle$ from our previously calculated 4p wavefunctions, and fit these values with the expression

$$\langle r^2\rangle = (45\text{-}S)/Z_{eff} \quad ,$$

where S is the atomic number of the sequence, i.e., 26 for the iron sequence. For other atoms the hydrogenic form is used:

$$\langle r^2\rangle = 2.5\left(\frac{n_{eff}^2}{Z_{eff}}\right)^2 \quad .$$

If the upper level is above the ionization potential, $\langle r^2\rangle \equiv 25$. For molecules we arbitrarily adopt the constant

$$\Gamma_W/N_H \equiv 1.0E\text{-}7/Z_{eff}$$

in the above expression for Γ_W.

The program makes a new smaller list of lines that fall within the wavelength interval or overlap the ends of the interval. For each depth in the model, the program reads the pretabulated number densities divided by partition functions, N/U, and the doppler velocities. A buffer is set up that represents the whole wavelength interval plus 1000 points at each end for overlapping lines. A 100-nm interval in the ultraviolet with a point spacing of 0.5 pm thus has a 102,001-point buffer. The program goes through the line list rounding the line center wavelength to the nearest point in the buffer so that each line is symmetric about the central point and only one wing need be computed. This approximation also means that the spectrum can be computed only in high resolution. The line absorption coefficient is divided into four factors,

$$\ell_\nu = \left[\frac{\pi e^2}{mc}\,\frac{N}{U}\,\frac{1}{\rho}\,gf\,\frac{1}{\sqrt{\pi}\,\Delta\nu_D}\right]\left[e^{-E/kT}\right]\left[H(a,v)\right]\left[1-e^{-h\nu/kT}\right] \quad ,$$

the second, third, and fourth of which are expensive to compute and are less than or equal to 1. Here N and U are the number density and partition function for the atom or molecule, ρ is the mass density, g is the statistical weight of the lower energy level, f is the absorption oscillator strength, $\Delta\nu_D$ is the doppler width in frequency units,

1981SAOSR.391.....K

E is the lower energy level, H(a, v) is the Voigt function, and ν is the frequency. The line absorption coefficient is initially set to the first factor, which is an upper limit. If this value is less than 0.001 times the pretabulated approximate continuum opacity, the line is discarded from the current depth. The Boltzmann factor is otherwise multiplied in and the test is repeated. If the line passes, the damping parameter

$$a = \frac{\Gamma_R + \Gamma_S + \Gamma_W}{4\pi \Delta\nu_D}$$

is evaluated and the Voigt function is computed at successive steps away from line center for $v = \Delta\lambda/\Delta\lambda_D$ until the wings fall below 0.001 of the continuum. Table lookup is used to find $H(a, v) \simeq H_0(v) + aH_1(v)$, where H_0 and H_1 are pretabulated to give an accuracy better than 2% for $a < 0.1$. An upper limit of 0.25 is placed on a, but typical values range from 0.01 to 0.001. The program saves the line-center absorption coefficient and all the parameters for every line used. After going through all the layers in the model atmosphere, an array of, say, 100,001 by 64, has been computed. This is transposed, multiplied by the stimulated emission factor, and written out one wavelength at a time for use in computing the spectrum. The line center opacity is also written out for each line for subsequent computation of the central depth of each line.

The next stage of the calculation uses the program SPECTR, which is based on a version, ATLAS7, of the model atmosphere program ATLAS (Kurucz, 1970), to compute the non-LTE opacity and source function, to add in the LTE opacity and source function from SYNTHE, to add the continuum opacity and source functions, and then to compute the intensity or flux at each wavelength point. This procedure is also repeated for each line center. In ATLAS7, departure coefficients have been inserted in the partition functions, the Saha and Boltzmann equations, and the opacities as follows.

Partition functions:

$$U = \sum g_i e^{-E_i/kT} \rightarrow \sum g_i b_i e^{-E_i/kT} ,$$

where g_i and E_i are the statistical weight and energy for each level.

Boltzmann factors:

$$\frac{N_i}{N} = \frac{g_i}{U} e^{-E_i/kT} \rightarrow \frac{b_i g_i}{U} e^{-E_i/kT} ,$$

where N and N_i are the total and level i number densities.

Stimulated emission:

$$1 - e^{-h\nu/kT} \rightarrow 1 - \frac{b_{up}}{b_{lo}} e^{-h\nu/kT} ,$$

where up and lo refer to the upper and lower levels. For ionization, up refers to the ground state of the ion. (Note that these departure coefficients are not normalized so that $b_{ion} \equiv 1$.)

Source functions:

$$S(lo \rightarrow up) = \frac{2h\nu^3}{c^2} \left[e^{h\nu/kT} - 1\right]^{-1} \rightarrow \frac{2h\nu^3}{c^2} \left[\frac{b_{lo}}{b_{up}} e^{h\nu/kT} - 1\right]^{-1} .$$

In practice, b's are calculated only for the low terms, so for higher levels, b's are assumed to have the same value as the b for the lowest level of the ion. If the model atmosphere is assumed to be in LTE, the departure coefficients are all set to unity in the calculation.

ATLAS7 is designed to be accurate in treating continuum opacities. Edges are put in at their exact positions specified in wavenumbers and with individual cross sections. Thus, for example, for C I or Si I, ionization from the neutral ground term ^3P to the ionized ground term ^2P actually forms six continua,

$$^3P_J \rightarrow {}^2P_{1/2} , \quad {}^3P_J \rightarrow {}^2P_{3/2} , \quad J = 0, 1, \text{ and } 2 ,$$

all of which are treated explicitly. The one exception to this accurate treatment is Fe I for which the cross sections and their wavelength dependence are so poorly known that the cross sections are assumed to be parabolic in frequency space with a maximum of 3 Mb for every level. This maximum is roughly that found in calculations by Merts quoted by Dragon and Mutschlecner (1981). Since there are so many levels, the net effect is to produce a smooth photoionization continuum with the correct LTE Boltzmann dependence. Provision has not yet been made to include departure coefficients.

To save computation in SPECTR, continuum quantities are pretabulated at the middle and ends of the wavelength interval, or for any subinterval formed by an opacity discontinuity, and interpolated to each wavelength parabolically. In complete redistribution the following source function is used,

$$S_\nu = \left[\kappa_\nu \bar{S}_\nu + \sigma_\nu J_\nu + \ell_\nu(1-f)\, S_\nu^L + \ell_\nu f J_\nu + \Sigma\, \ell_\nu^i S_\nu^i\right] / (\kappa_\nu + \sigma_\nu + \ell_\nu + \Sigma\, \ell_\nu^i) \quad ,$$

where κ_ν and $\bar{S}_\nu$ are the continuum absorption coefficient and continuum source function, σ_ν is the scattering coefficient, ℓ_ν and S_ν^L are the summed line opacity (which has been calculated by SYNTHE) and its source function, ℓ_ν^i and S_ν^i are the individual line absorption coefficients and source functions produced in this stage of the calculation, and f is a depth-dependent function that allows treatment of part of the line opacity as scattering. We normally make the approximation that J_ν is computed only for the continuum and that f = 0, so that the source function is

$$S_\nu = \left[(\kappa_\nu + \sigma_\nu)\, S_\nu^{cont} + \ell_\nu S_\nu^L + \Sigma\, \ell_\nu^i S_\nu^i\right] / (\kappa_\nu + \sigma_\nu + \ell_\nu + \Sigma\, \ell_\nu^i) \quad ,$$

with

$$S_\nu^{cont} = (\kappa_\nu \bar{S}_\nu + \sigma_\nu J_\nu)/(\kappa_\nu + \sigma_\nu) \quad .$$

Before the point-by-point calculation begins, the program reads the non-LTE line list in wavelength order to select lines in the wavelength interval and lines outside the wavelength interval having wings that might extend into the interval. Each line is stored in one of seven groups based on a strength parameter that limits the extent of its wings to 100., 30., 10., 3., 1., 0.3, or 0.1 nm. As the opacity at each point in the wavelength interval is computed, only those lines close enough to contribute to the opacity are considered.

Lines included in the non-LTE list at the time of this calculation were H, He, C, Mg, Al, and Si, with line series extrapolated to high n so that lines merge smoothly into continua. There were also a few lines of other elements. Each important continuum has a series of lines converging up to it. The lines merge into a quasi-continuum at an upper energy or upper quantum number determined by Stark and van der Waals broadening, because lines are no longer visible when the width exceeds the line spacing. In practice, at each depth in the atmosphere, we compute the energy at which individual lines are no longer visible and extend each continuum redward at a constant level to this point. This technique smooths the transition from one continuum to another even if no lines are included explicitly.

For Al I and Mg I we were able to compute Rydberg series to high n (80), and to find or estimate the radiative, Stark, and van der Waals broadening for each line. For Si I and C I there is so much configuration interaction that extrapolated energy levels can be off by up to 2 cm^{-1} unless great effort is made to include the interaction effects. For Si I, however, energy levels have been observed up to n = 56 although many of them were unclassified. We were able to pick out the interacting levels by estimating the mutual repulsion, so we could assign each level to an LS series. Then we estimated LS f values by extrapolating each series. These f values will be correct for many of the lines but wrong for the strongly interacting lines. However, the total f values spread over all transitions should be correct because configuration interaction only redistributes the line strengths.

H I lines are tabulated to n = 80. Profiles are computed using a new routine from Peterson (1979) that approximates the Vidal, Cooper, and Smith (1973) profiles, works to high n, and includes doppler broadening, resonance broadening, van der Waals broadening, and fine-structure splitting. Autoionization lines have Shore parameter Fano profiles (Shore, 1968). Other lines have Voigt profiles that are computed accurately for any a. The lines occur at their exact wavelengths. Departure coefficients for levels that are higher than have been computed are assumed to be the same as those for the ground state of the next higher stage of ionization. Strong lines can be treated with approximate partial redistribution effects but the computer cost increases dramatically. It is also possible to use the coronal approximation and ionization tables for highly ionized lines if the model has a corona. Neither partial redistribution nor the coronal approximation was used in the present calculations.

Either surface flux or surface intensity at up to 20 angles can be computed. When there is a subsequent calculation of rotational broadening, 17 angles are used from μ = 1.0 to 0.01. In the calculation reported here, we computed disk center and several limb positions. For each wavelength both the spectrum and the continuum level are determined. Finally, the line center residual intensity is computed for all the lines that were used in the calculation.

The spectrum can be rotationally broadened using program ROTATE. At each wavelength the spectrum is interpolated to 100 values of μ evenly spaced from 0.995 to

0.005. A rectangular grid is placed over the stellar disk and, for the given V sin i, the μ index and the doppler shift in wavelength steps are computed for each point. These pairs of numbers are sorted in $\Delta\lambda$, summed, and normalized to obtain the flux. For V sin i = 0 this simply amounts to computing flux integration weights. A buffer is then set up that is longer than the spectrum; the intensity-interpolated spectrum is read in, one wavelength at a time, distributed among the neighboring wavelengths according to the broadening indices, and added to the buffer. For normal spherical stars, symmetries are used to reduce the number of calculations but the method will work for any shape star and even for binaries. To compute a solar flux spectrum we first compute the intensity spectrum at 17 angles, then pass it through ROTATE.

Macroturbulent and instrumental broadening are treated in similar fashion using program BROADEN. The broadening function is defined at integral values of the point spacing. Then the spectrum is read in, one wavelength at a time, redistributed among neighboring wavelengths, and added to the buffer for the new spectrum. To minimize blending we have not included macroturbulence or instrumental broadening in the plots shown here.

Other complications that can be introduced in the spectrum synthesis are interstellar or terrestrial atmospheric absorption and a depth-dependent doppler shift.

The most important step in the spectrum synthesis is the final preparation of plots, which allow information to be displayed for a number of purposes: to study the spectrum as a whole; to compare with one or more observed spectra; to study individual features in detail; and to identify lines and the composition of blends. Figures 1 to 4 are examples of plots that can be simply produced with program PLOTSYN on our VAX computer. More complicated plots can be made that also show various degrees of broadening.

1981SAOSR.391.....K

3. COMPARISON WITH OBSERVED SPECTRA

In this section we compare our calculated spectra in the range 224 to 300 nm with the best available observed spectra and compare the observed spectra with each other. Figure 1 shows the two Harvard photoelectric disk center spectrum scans (Kohl, Parkinson, and Kurucz, 1978) for the interval 224 to 300 nm that were taken from a rocket. Our computed spectrum and continuum are shown on the same plot. The calculated lines are labeled if their residual intensity is less than 0.98. Figure 2 shows the Harvard disk center ($\mu = 1.00$) and limb ($\mu = 0.23$) scans and our center and limb calculation. Figure 3 shows the Hawaii (Allen, McAllister, and Jefferies, 1978) photographic echelle disk center rocket spectrum for the interval 268 to 293 nm that was normalized to the Harvard spectra. Figure 3 also shows our calculated spectra and the Harvard spectra for comparison. Figure 4 is similar to Figure 3 but shows the disk center photoelectric spectrum taken from Kitt Peak by Brault and Testerman (1972) for the interval 294 to 300 nm. We have roughly normalized the Kitt Peak spectrum to the Harvard spectrum. All these spectra will be treated together below in discussing the absolute calibration, wavelength scale, signal to noise, noise features, resolution, the line data, and the photoionization cross sections.

3.1 Absolute Calibration

We are not able to draw any conclusion about the absolute calibration. The claimed error in the Harvard calibration is ± 12%. As the Hawaii and Kitt Peak spectra have been adjusted to match the Harvard calibration, they do not add any information. Our calculated spectra are systematically higher than the observed spectra, but there are so many lines missing from the calculated spectrum that the difference may be totally accounted for by the missing lines and, in some cases, improvements in damping constants. The position of the Harvard limb spectrum is uncertain by ± 0.04 in μ so that the limb spectrum may have been calculated at the wrong position for comparison, and thus may have a systematic error in intensity as large as 25%. The solar model atmospheres are still relatively uncertain as well and introduce some error in the level of the calculated spectra. One of the purposes of these calculations and comparisons is to find ways to improve the models. Any conclusion about the calibration will have to wait until we can add many more lines to the calculated spectrum and until we can refine the model calculations.

3.2 Wavelength Calibration

There is remarkable disagreement in the wavelength scales among all these spectra. The Harvard spectra are claimed to have a wavelength accuracy of ± 0.002 nm and the Hawaii spectra are claimed to be accurate to ± 0.0015 nm. We do not know the accuracy of the Kitt Peak wavelengths but we assume them to be exact for this discussion. The calculated wavelengths are derived by differencing the known energy levels and converting from vacuum to air. However, in the calculation of the spectrum, the line centers are moved to coincide with one of the computed points so that the profile is symmetric and only one wing need be calculated. In the calculation reported here the adopted point spacing was 0.0005 nm so the uncertainty is at least ± 0.00025 nm. The error in many energy levels can be larger than this value, and we estimate a wavelength error of, say, ± 0.0005 nm for the computed spectra. However, this error has little to do with determining the wavelength scale of the observed spectra. Every feature in the solar ultraviolet is significantly blended, so that the wavelength of a feature is generally different from that of its component lines. Until we can compute a spectrum that can reproduce the observed spectrum feature for feature, the wavelength scale actually depends on the errors in the strengths of the lines that are the components of the blends. At present many of the lines are missing altogether. In the calculation we also find lines in the wrong places, but such errors usually are obvious and can be corrected; this is one of the reasons for making this calculation and comparison. Working with all the spectra shown here, we plan a series of further corrections. Making the wavelength scales consistent will also effectively increase the signal-to-noise ratio when co-adding the spectra.

The noisiness and low resolution of the Harvard and Hawaii spectra are serious problems in trying to fix the wavelength scale. Because of these uncertainties one has to be very careful about identifying weak features on the basis of wavelength, or about trying to determine abundances from such features. These wavelength uncertainties also affect the calculation of the absorption of solar radiation by terrestrial atmospheric lines because of changes in the relative positions of maxima and minima.

3.3 Signal-to-Noise Ratio

The Harvard and Hawaii spectra are noisy so that it is difficult or impossible to identify weak features, to resolve blends, to determine abundances, to study velocity fields, to search for variability, i.e., to carry out research routinely done in the visible where high quality spectra are available. For the Harvard spectra we estimate a signal-to-noise ratio of 50 for disk center and 25 for the limb at a resolution of 90,000. For the Hawaii data we estimate a signal-to-noise ratio of 50 at their claimed resolution of 200,000. However, as we discuss below, their actual resolution is about one-half this figure, so they have about twice the signal to noise of the Harvard spectra at the same resolution. There is a further complication in that the signal to noise is much higher for features at the center of an echelle order than for those at the edges, so that the signal to noise varies with wavelength in the rectified spectrum. The Mg II h and k lines are much less noisy in the Hawaii spectrum than in the Harvard spectra because they were centered in an echelle order to maximize the signal.

For the Kitt Peak atlas the signal to noise is well over 1000 at 300 nm at a resolution of 400,000 and deteriorates toward shorter wavelengths as ozone blocks the signal.

Our whole knowledge of solar spectrum shown in this atlas below 294 nm is based on 5 minutes worth of observation. These spectra are too noisy to show weak features or to interpret adequately the blended features. Figure 4 shows occasional features that seem to be present in both Harvard scans but are spurious because they do not appear in the Kitt Peak spectrum. One cannot tell if weak features in the wings of the Mg II h and k lines shown in the Harvard spectrum in Figure 3 are absorption lines, emission lines, or noise. Our understanding of the solar atmosphere will be greatly improved when spectra with signal to noise greater than 1000 at a resolution of 400,000 become available from space.

3.4 Noise Features

The actual uncertainty, as opposed to the statistical signal to noise, of an observed spectrum can be much greater than expected due to the presence of noise spikes, dropouts, cosmic rays, transmission errors, recording errors, etc. The Harvard spectrum has both noise spikes and dropouts. Because there are two scans at the center and two at the limb, and because it is possible to compare the Harvard spectra with the Hawaii spectrum, with the Kitt Peak spectrum, and with the calculated spectra, it is sometimes possible to determine that only one of the Harvard scans is affected by noise and to use the other. For this reason, regions in which the two scans disagree have not been eliminated, as was done in the atlas of Kohl, Parkinson, and Kurucz (1976). One has to worry whether these noise features might be present at a low level that is not detectable because of the low statistical signal to noise. There are examples in the Harvard spectra of accidentally corresponding noise spikes in different scans. Thus one cannot always trust that weak features are real, even if they appear on both scans. It should be noted that there are inhomogeneities and scratches in photographic emulsions that may produce noise features in the Hawaii data as well. Noise features limit the accuracy to which one can degrade the resolution of these spectra, and still maintain the calibration, for comparison with lower resolution spectra that show solar variability.

We plan to "reprocess" these rocket data as much as possible to remove noise features. When the calculation can better reproduce the observed spectrum, it should be possible to use the calculated spectrum to interpolate through noise regions.

We recommend that in future space observations designed to produce reliable, high-resolution spectra, any given scan must be repeated at least three times to allow for the removal of nonstatistical noise.

3.5 Resolution

The resolution of the Kitt Peak spectrum shown in Figure 4 is about 400,000. The effects of this resolution compared to the Harvard resolution of 90,000 can be seen at 298.0 and 298.2 where the Kitt Peak spectrum shows deeper minima, narrower features, and higher maxima. At other places in the spectrum the increased resolution reveals substructure in blended features that is not visible at the lower resolution, although the noisiness makes such comparisons difficult.

The nominal resolution of the Hawaii spectrum is 200,000. However, when we compare the Hawaii and Harvard spectra in Figure 3, we find no examples of

demonstrably sharper features in the Hawaii spectrum as we could find in the Kitt Peak spectrum. Thus the effective resolution appears to be less than 200,000.

If these rocket spectra were co-added to improve the signal to noise, the resolution would be decreased because of wavelength misalignments.

To emphasize the individual line contributions to blends, the calculated spectra in this atlas have not been broadened by macroturbulence or an instrumental profile. Since the instrumental broadening in the Kitt Peak atlas produces only a small effect on the spectrum, the difference in the widths of the calculated and observed features in Figure 4 indicates the effect of macroturbulence (and missing blends). For the Harvard and Hawaii spectra the instrumental broadening has a large effect. In working with the spectra we can make large-scale plots that show both the unbroadened and broadened spectra simultaneously.

3.6 Line Data

The most obvious conclusion to be drawn from the comparison of the calculated spectra to the observed is that roughly half the lines are missing from the calculated spectra. We know that many of these are atomic and molecular lines with high-lying upper energy levels that have not yet been observed in the laboratory. Also near 300 nm there are lines of diatomic hydrides that were not included in our line list at the time these calculations were made. For energy levels that occur in known atomic configurations or in analyzed molecular electronic states, we have predicted the energies and the wavelengths and gf values for all possible lines. In future calculations we will include all these predicted lines, whose wavelengths are very uncertain, together with the known lines, to see if we can match the overall level in a statistical sense. There are still many other atomic and molecular configurations for which no data exist. Either new laboratory work or purely theoretical calculations are necessary before we can predict these additional lines.

As an example, consider Fe II. Many of the strong features in Figures 1 and 2 between 230 and 260 nm are Fe II lines. In some intervals they produce 80 to 90% blocking. The known configurations, i.e., the configurations for which even one level is given by Johansson (1978) are d^7, $d^6 4s$, 5s, 6s, 4p, 5p, 4d, 5d, 4f, $d^5 4s^2$, 4s5s, 4s4p, 4s4d, and $4p^2$, but we know that the configurations 7s, 6p, 7p, 6d, 7d, 5f, 6f, 7f, 4s5p, etc. exist and produce significant lines. We plan to make Hartree-Fock calculations for these configurations so that we can add them to our predicted line list. We now have (Kurucz, 1981) 22,000 significant Fe II lines between known levels, and over 400,000 lines between predicted levels; and future calculations should bring the total to over 1,000,000 lines. The same deficiency applies to other iron group atoms and ions. Further laboratory work is urgently needed.

Diatomic molecules are also incompletely analyzed. The sun is a very high temperature source by laboratory standards. High V and high J levels are populated and produce significant opacity, but in current laboratory studies only low V and low J levels have been observed. Many excited electronic states that could produce significant solar opacity have not been analyzed at all. Thorough laboratory analyses are required.

As this is an exploratory calculation, the reader should not be surprised to find mistakes in our line data. One of our main goals in making this comparison is to find and correct such mistakes. Some lines may have been accidentally omitted. If there was a typographical error in an energy level, or if an energy level was reported that does not actually exist, hundreds of lines could be put in at the wrong wavelengths.

Besides mistakes, there is the normal large scatter in the accuracy of the measured and, especially, the calculated gf values. Thus the computed lines can be too weak or too strong. Macroturbulence and instrumental broadening will considerably raise lines that are narrow in the plots; thus a line that appears too deep does not necessarily mean that it is too strong. Also, if a blend is too weak, it is not obvious which component or components are at fault.

There are so many lines missing that it is difficult to draw any conclusions about damping. For example, in the region around 260 nm in Figure 2 one could improve the match in the regions between strong lines for the disk center spectrum by increasing the van der Waals broadening. However, if all the lines that are clearly present

in the observed spectrum were included in the calculation, the currently used damping might be just right. If the center and limb spectra are compared, for example at 260 nm, the damping seems reasonable at the limb. We plan to check all the strong lines to see if any improvement is necessary. Obviously, better observed spectra at the center and limb would help.

In the present calculation the cores of the Mg II h and k lines were not included in order to avoid partial redistribution calculations that require much computer time.

3.7 Photoionization Cross Sections

One source of uncertainty in our calculated spectra is the Mg I ^{3}P photoionization cross section, which strongly affects the spectrum shortward of 252 nm. We use the cross section measured by Botticher (1958), which has a ν^{-14} dependence down to 238 nm, and we assume the same dependence at shorter wavelengths where the cross section has never been measured. If the cross section falls off less rapidly, it could be twice as large at 225 nm. A larger cross section there would bring the mean level of our calculated spectra into better agreement with the observed spectra. However, because there are so many missing lines, we cannot conclude that the cross section is in error. Measurement of the photoionization cross section is urgently required.

1981SAOSR.391.....K

4. CURRENT AND FUTURE WORK

We plan to continue to work on the observed spectra shown in this atlas. We expect at least to put the different spectra all on the same wavelength scale and to remove noise features.

A second atlas comparing our calculations with observed spectra below 225 nm is in preparation, which will include NRL rocket spectra by Moe, van Hoosier, Bartoe, and Brueckner (1976) for 118 to 210 nm; several Harvard rocket spectra by Kohl, Parkinson, and Reeves (1975) for 140 to 225 nm; and OSO-8 spectra for the interval 169 to 186 nm (Chipman, 1981). We are determining the Harvard and OSO-8 wavelength scales by adjusting the spectra to match our calculations.

Our current plans for improving the atomic and molecular line data are the following. We will continue to correct errors we find by comparing the calculated and observed spectra. We will continue to collect all published data on gf values and update our line list using newer data in place of our current data whenever the newer data seem more reliable. We have begun to recompute the Kurucz and Peytremann line list by taking into account new laboratory analyses; we plan to extend that work to heavier elements and higher stages of ionization. In addition, we plan to include calculations using a Hartree-Fock program written by Robert Cowan of Los Alamos so that we will not be restricted to observed configurations. We are making a list of all diatomic molecular lines significant in the sun, but we are hampered by poor laboratory data. We are reanalyzing existing data and trying to encourage new measurements.

We expect these additional lines to have a significantly different temperature and depth dependence in the solar atmosphere than the existing lines, which are relatively strong atomic lines. Thus they should produce mean intensities significantly different from those we are now using in our non-LTE calculations, and produce significantly different center-to-limb behavior. We plan to compute mean intensities for the whole ultraviolet solar spectrum, which can be used to produce accurate radiative rates for non-LTE calculations.

Once we can make reliable calculations in the ultraviolet, we can investigate the changes to be expected from small modifications in the structure of the solar atmosphere and thereby try to interpret observations of solar variability.

As always, the rate of progress in this research depends on access to large computers.

5. REFERENCES

ALLEN, M.S., McALLISTER, H.C., and JEFFERIES, J.T.
1978. High Resolution Atlas of the Solar Spectrum 2678-2931 A. Institute for Astronomy, University of Hawaii, Honolulu, 58 pp.

ALLER, L.H.
1963. The Atmosphere of the Sun and Stars. 2nd ed., The Ronald Press Co., New York, 650 pp.

BOTTICHER, W.
1958. Quantitative messung des 3^3P-Seriengrenzkontinuums von Mg. Zeit. f. Phys., vol. 150, pp. 336-345.

BRAULT, J. and TESTERMAN, L.
1972. Preliminary Kitt Peak Photoelectric Atlas. Kitt Peak National Observatory, Tucson, 623 pp.

CHIPMAN, E.G.
1981. Personal communication.

DRAGON, J.N. and MUTSCHLECNER, J.P.
1980. The solar ultraviolet continuum. Astrophys. Journ., vol. 239, pp. 1045-1069.

GUSTAFSSON, B., BELL, R.A., ERIKSSON, K., and NORDLUND, A.
1975. A grid of model atmospheres for metal-deficient giant stars I. Astron. Astrophys., vol. 42, pp. 407-432.

JOHANSSON, S.
1978. The spectrum and term system of Fe II. Phys. Scripta, vol. 18, pp. 217-265.

KOHL, J.L., PARKINSON, W.H., and KURUCZ, R.L.
1978. Center and Limb Solar Spectrum in High Spectral Resolution: 225.2 to 319.6 nm. Harvard-Smithsonian Center for Astrophysics, Cambridge, Mass., 365 pp.

KOHL, J.L., PARKINSON, W.H., and REEVES, E.M.
1975. (See Vernazza, Avrett, and Loeser, 1976).

KURUCZ, R.L.
1970. ATLAS: A computer program for computing model stellar atmospheres. Smithsonian Astrophys. Obs. Spec. Rep. No. 309, 291 pp.
1977. The fourth positive system of carbon monoxide. Smithsonian Astrophys. Obs. Spec. Rep. No. 374, 170 pp.
1979. Model atmospheres for G, F, A, B, and O stars. Astrophys. Journ. Suppl., vol. 40, pp. 1-340.
1980. SiO in the ultraviolet solar spectrum (abstract). Bull. Amer. Astron. Soc., vol. 11, p. 710.
1981. Semiempirical calculation of gf values, IV: Fe II. Smithsonian Astrophys. Obs. Spec. Rep. No. 390, 319 pp.

KURUCZ, R.L. and FURENLID, I.
1980. A sample spectral atlas for Sirius. Smithsonian Astrophys. Obs. Spec. Rep. No. 387, 142 pp.

KURUCZ, R.L., and PEYTREMANN, E.
1975. A table of semiempirical gf values. Smithsonian Astrophys. Obs. Spec. Rep. No. 362 (in 3 parts), 1219 pp.

MOE, O.K., van HOOSIER, M.E., BARTOE, J.-D.F., and BRUECKNER, G.E.
1976. A Spectral Atlas of the Sun between 1175 and 2100 Angstroms. Naval Research Laboratory Report 8057, 49 pp.

PETERSON, D.M.
1979. Personal communication.

PEYTREMANN, E.
1972. Theoretical effect of various broadening parameters on ultraviolet line profiles. Astron. Astrophys., vol. 17, pp. 76-82.

SAHAL-BRECHOT, S. and SEGRE, E.
1971. Semi-classical calculations of electron and ion collisional broadening of the strongest U.V. ionic lines of astrophysical interest. Astron. Astrophys., vol. 13, pp. 161-168.

SHORE, B.W.
1968. Parameterization of absorption-line profiles. Phys. Rev., vol. 171, pp. 43-54.

VERNAZZA, J.E., AVRETT, E.H., and LOESER, R.

1973. Structure of the solar chromosphere. I. Basic computations and summary of the results. Astrophys. Journ., vol. 184, pp. 605-631.

1976. Structure of the solar chromosphere. II. The underlying photosphere and temperature-minimum region. Astrophys. Journ. Suppl. Ser., vol. 30, pp. 1-60.

1981. Structure of the solar chromosphere. III. Models of the EUV brightness components of the quiet sun. Astrophys. Journ. Suppl. Ser., vol. 45, pp. 619-725.

VIDAL, C.R., COOPER, J., and SMITH, E.W.

1973. Hydrogen Stark broadening tables. Astrophys. Journ. Suppl., vol. 25, pp. 37-136.

Figure 1. The observed Harvard disk center spectrum in the wavelength range 224 to 300 nm compared with our calculated spectrum, with identifications of the calculated lines. Each page shows 1.7 nm in two 0.9-nm panels with a 0.1-nm overlap. The two heavy lines are disk center scans from Kohl, Parkinson, and Kurucz (1978) and the thin line is our calculated spectrum. The sloping line near the top of each panel is the computed continuum level. The intensity in ergs $cm^{-2} s^{-1} sr^{-1} nm^{-1}$ at the top of each panel is given on the left. The intensity varies linearly between this value at the top and zero at the bottom of each panel. All the observed data are plotted including noise spikes and dropouts. The first reliable data start at about 224.5 nm. Lines in the calculated spectrum that have residual intensities less than 0.98 are labeled. For atoms the identification consists of the last three digits of the wavelength, the element and ion code, the lower energy level in cm^{-1}, and the residual intensity in per mil at line center if the line were computed in isolation. For molecules the identification consists of the last three digits of the wavelength, the molecule code, the lower and upper V of the transition, the lower J, the branch, and the residual intensity in per mil at line center if the line were computed in isolation. The first two labels above the first panel can be translated as follows:

005 25.01 41182 796	means	005	wavelength 244.0005,
		25	atomic number for Mn,
		.01	charge Mn^{+} = Mn II,
		41182	lower energy level in cm^{-1},
		796	0.796 residual intensity;
084 814 1- 4 29R 929	means	084	wavelength 244.0084,
		814	atomic number of constituent atoms, 8=O, 14 = Si, meaning SiO,
		1	V_{lower},
		4	V_{upper},
		29	J_{lower},
		R	branch,
		929	0.929 residual intensity.

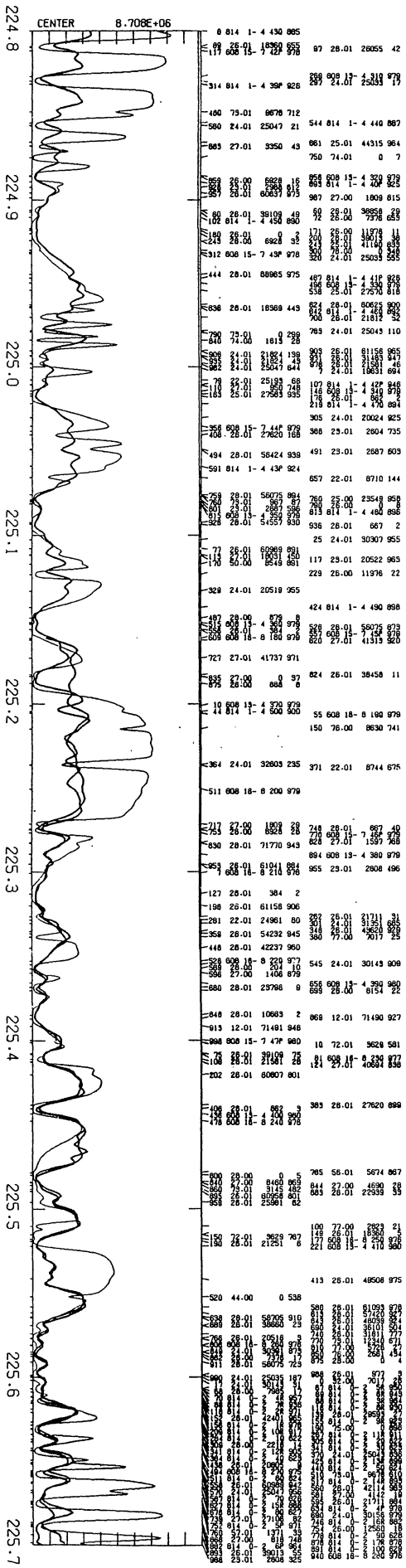

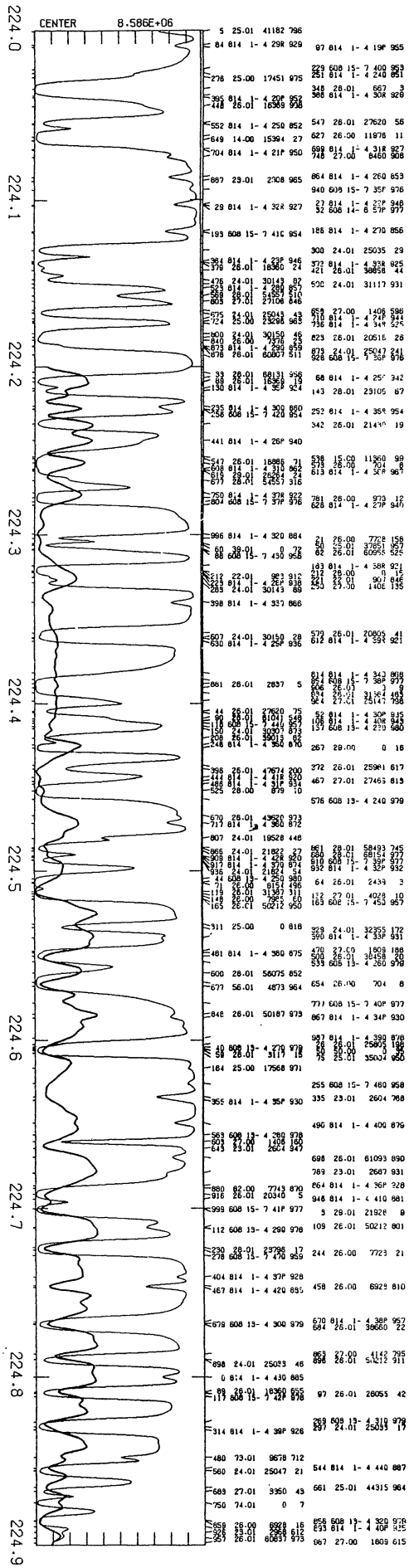

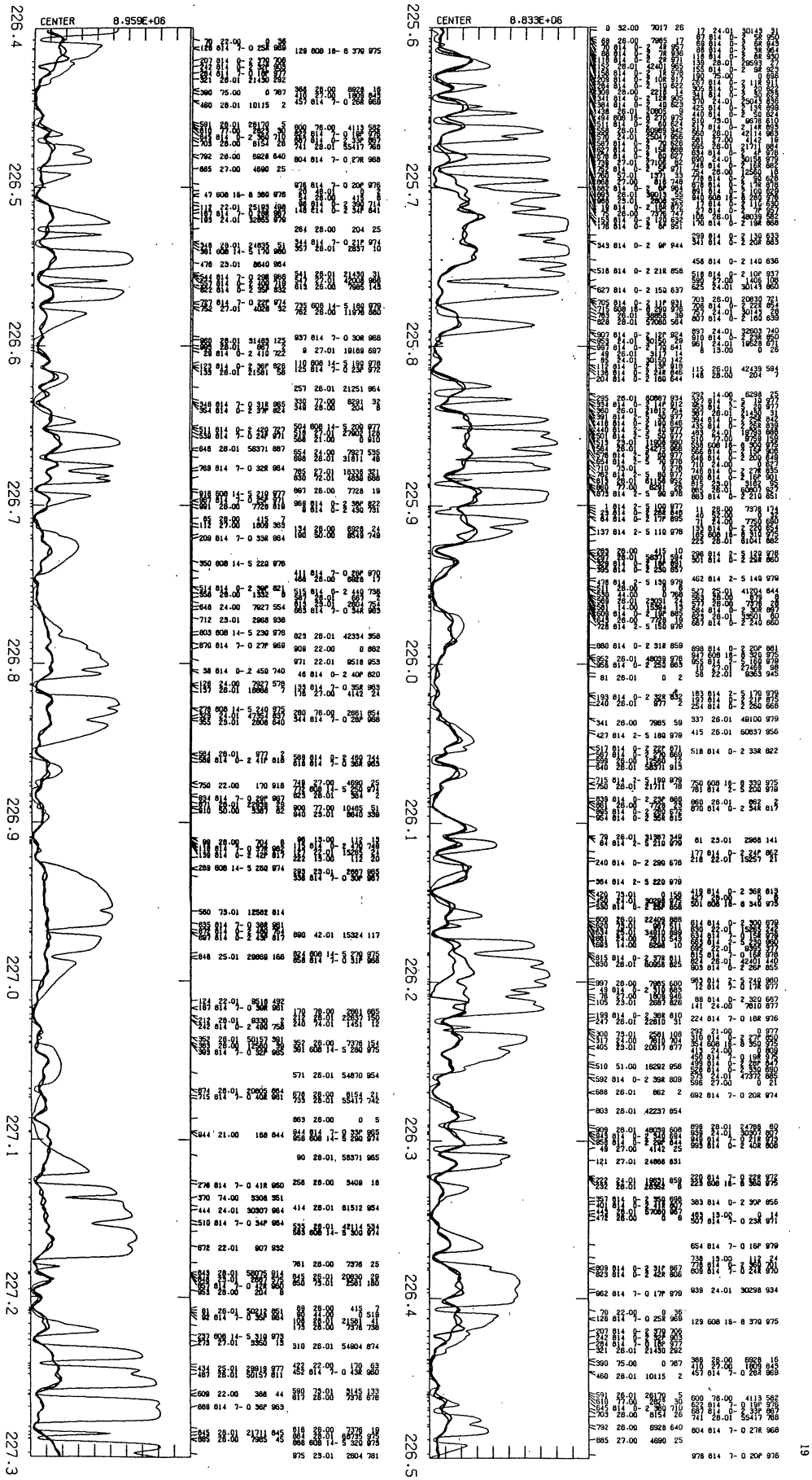

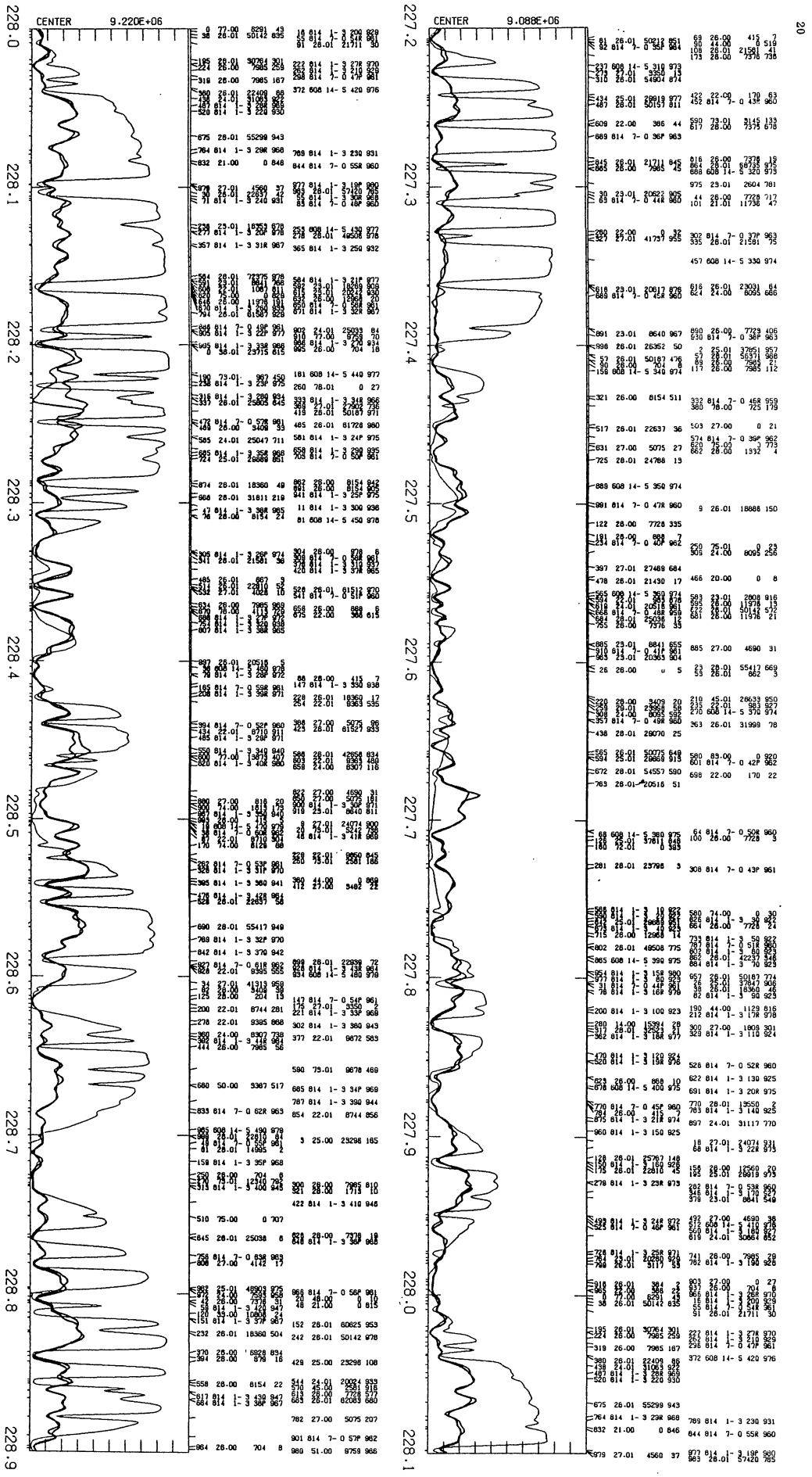

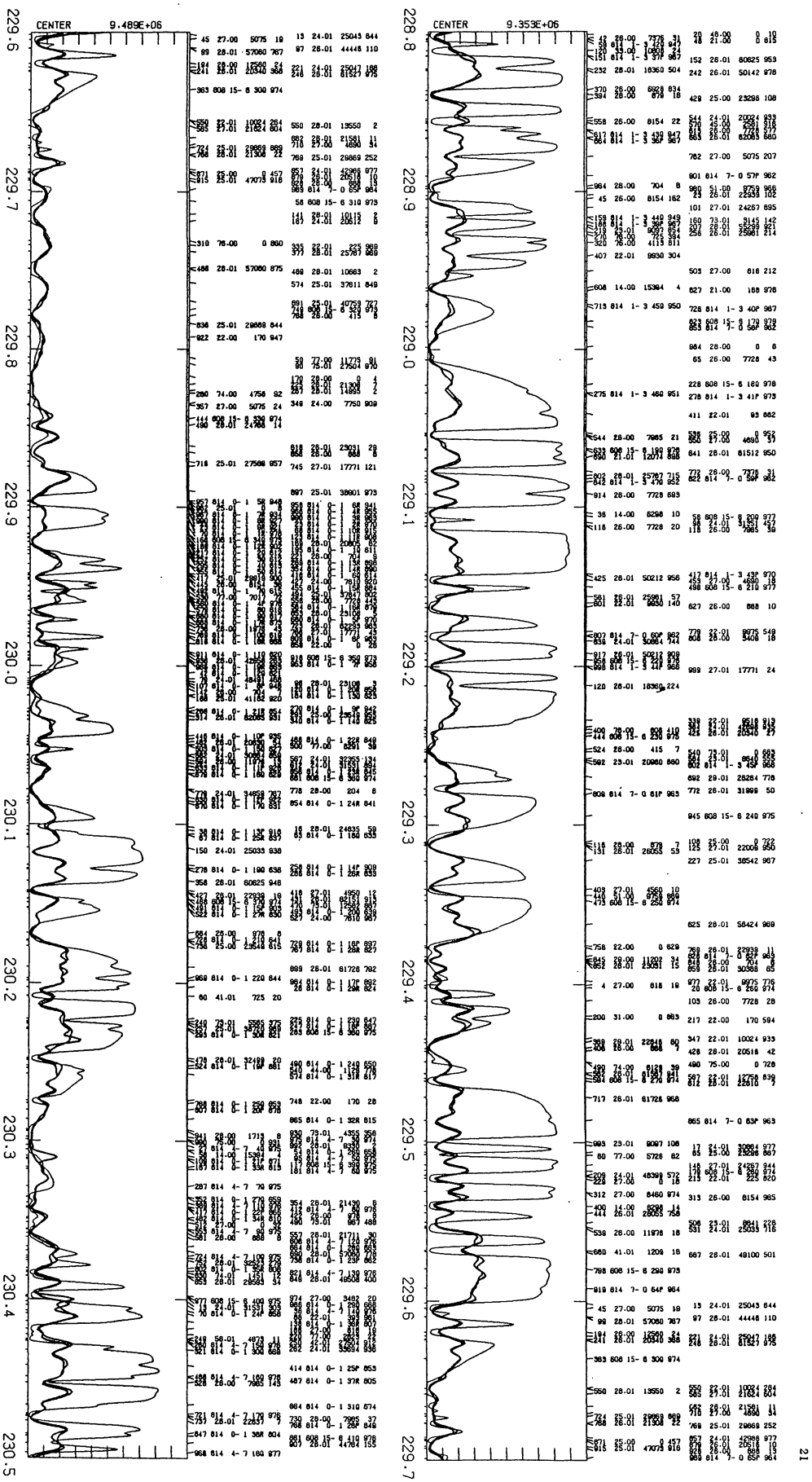

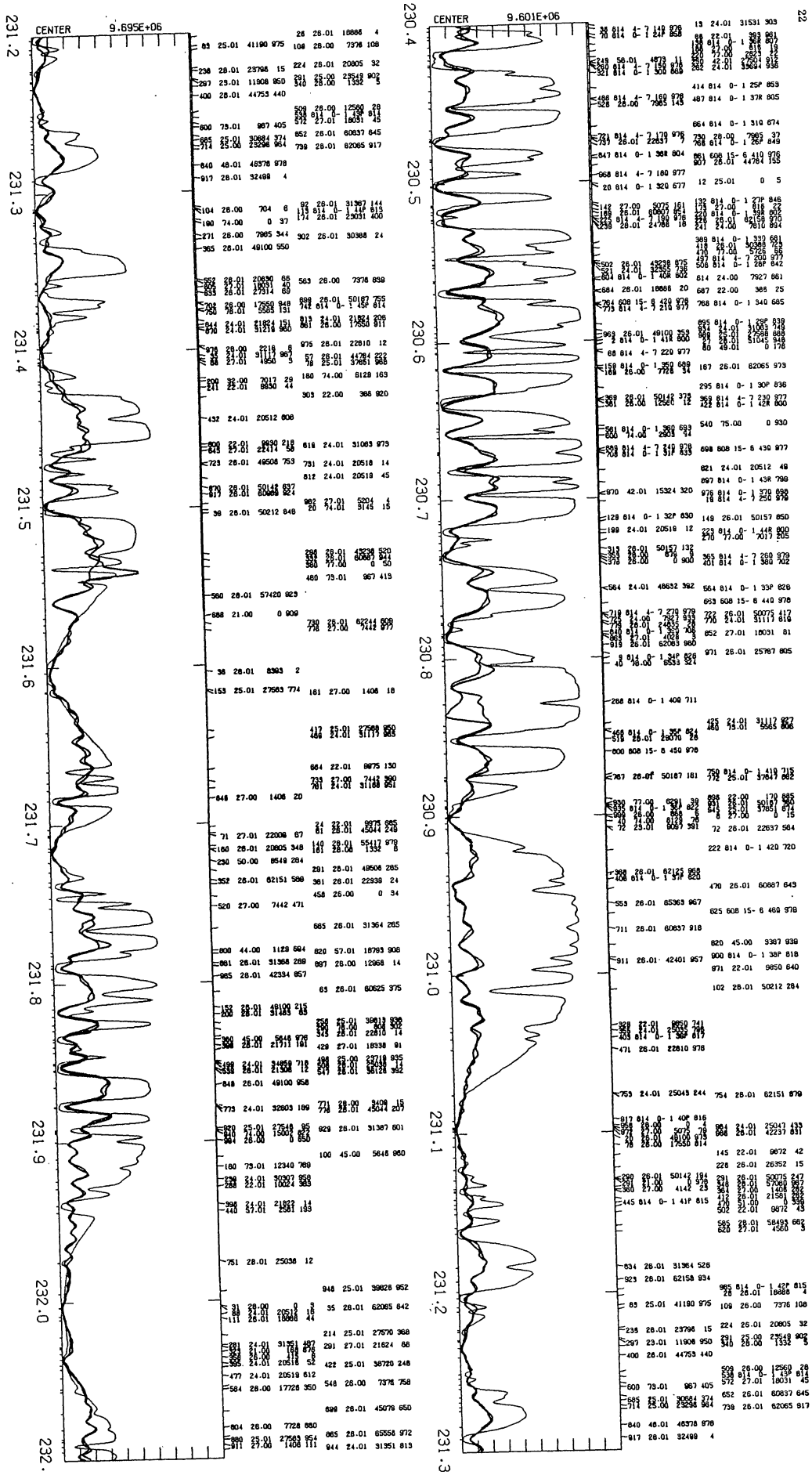

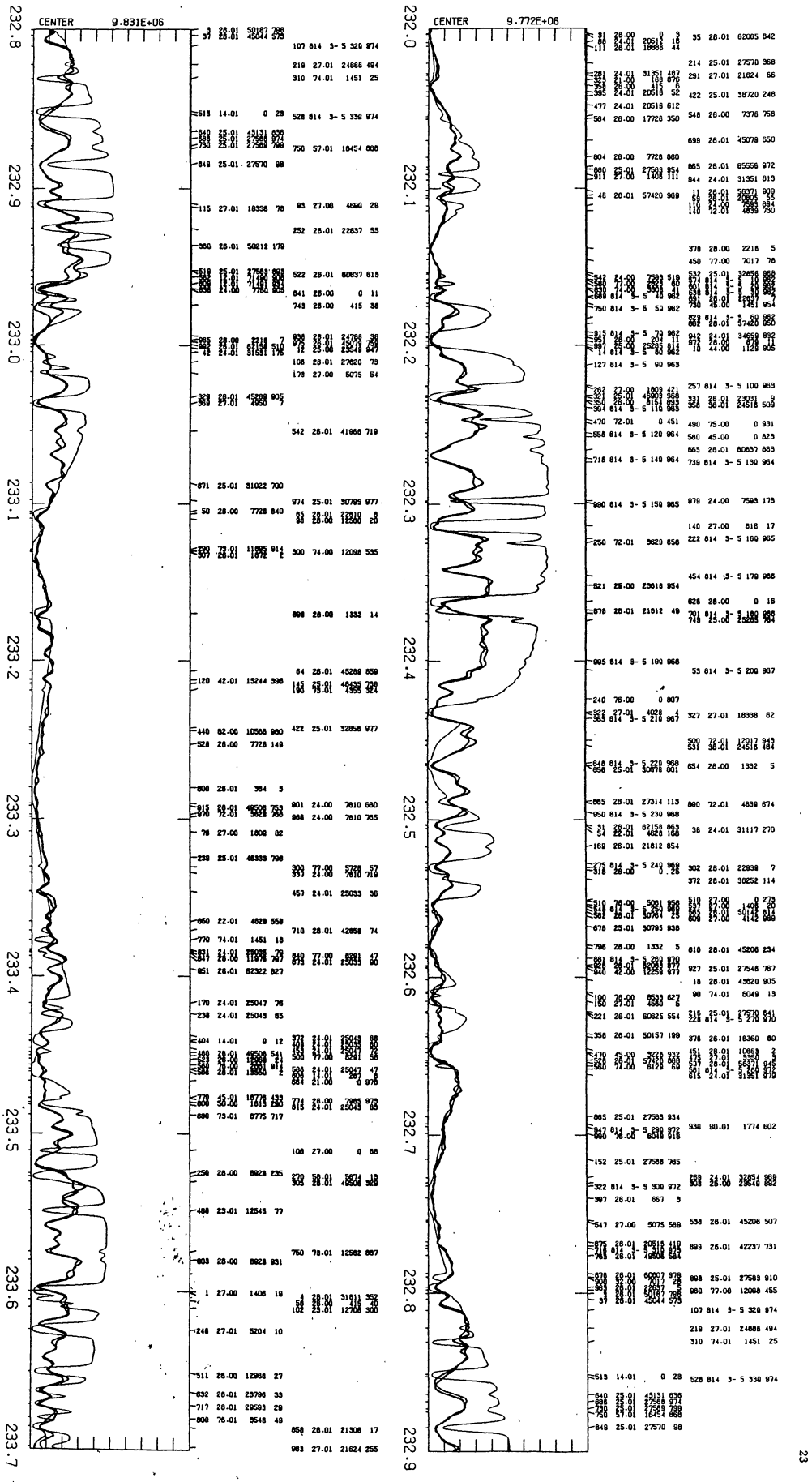

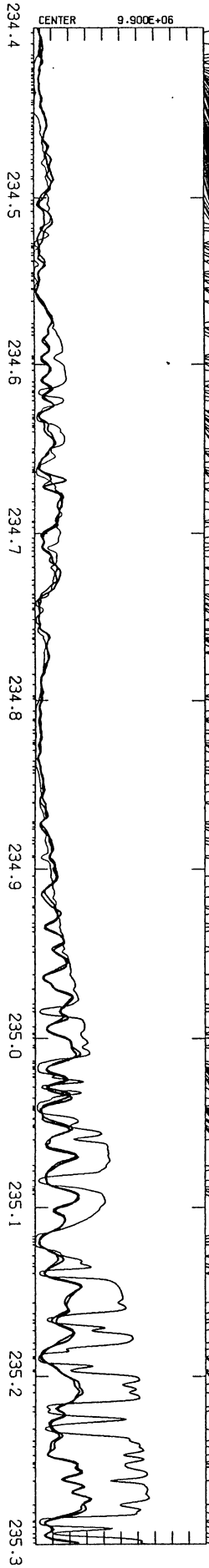

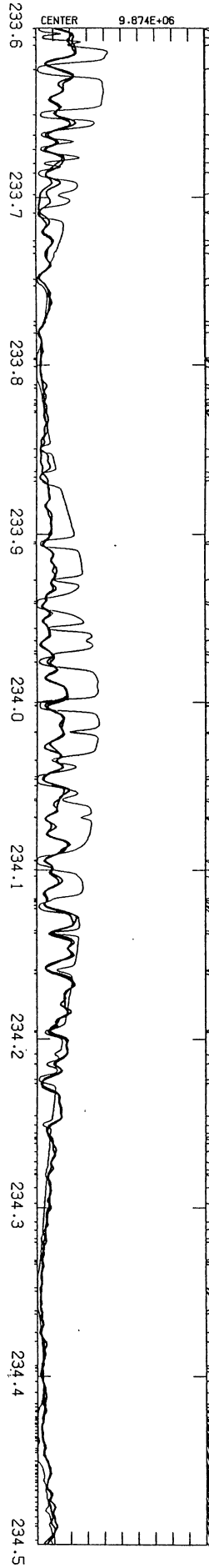

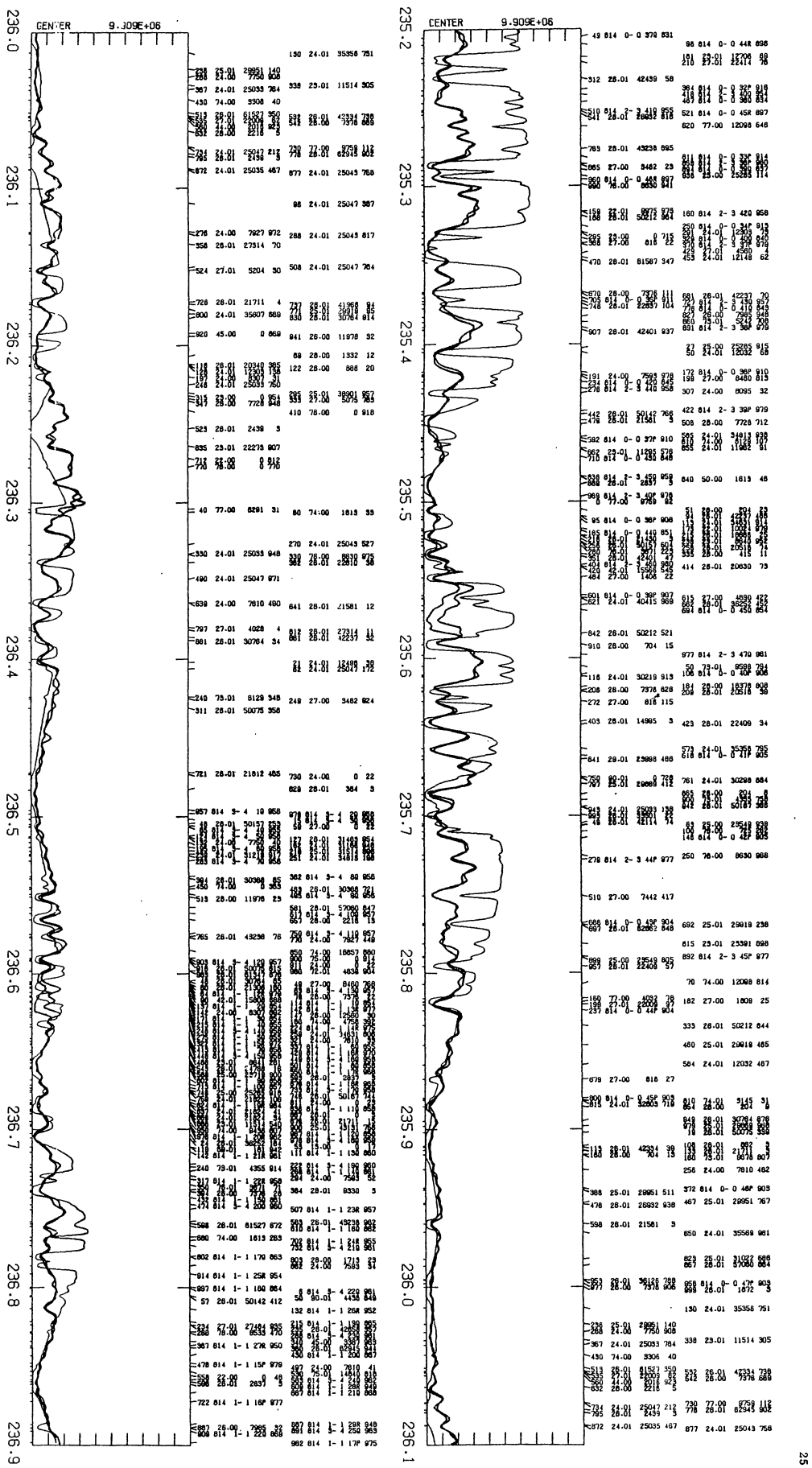

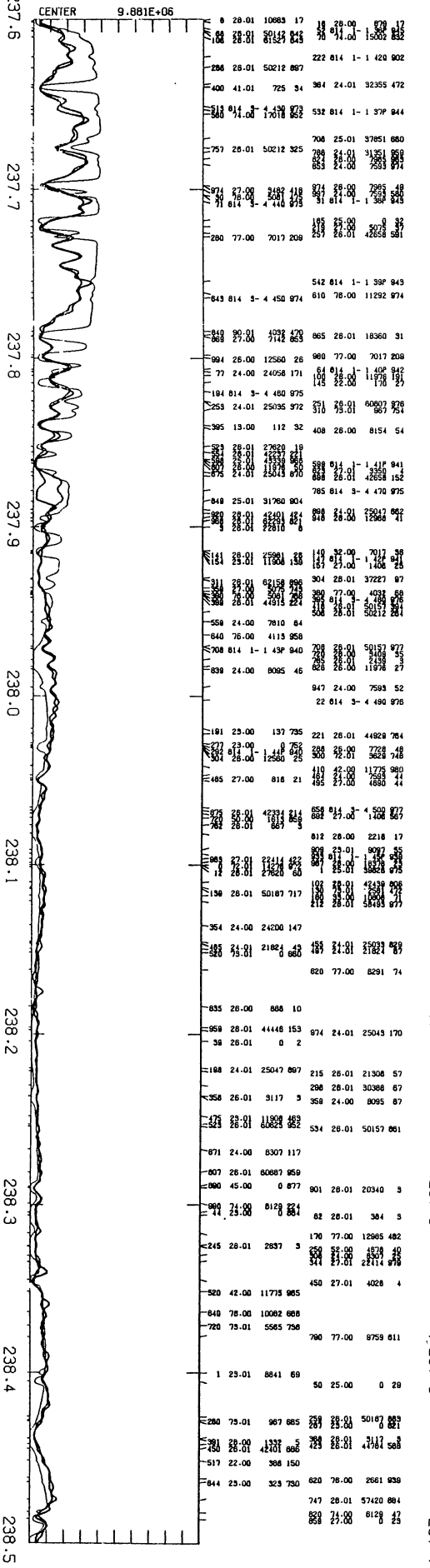

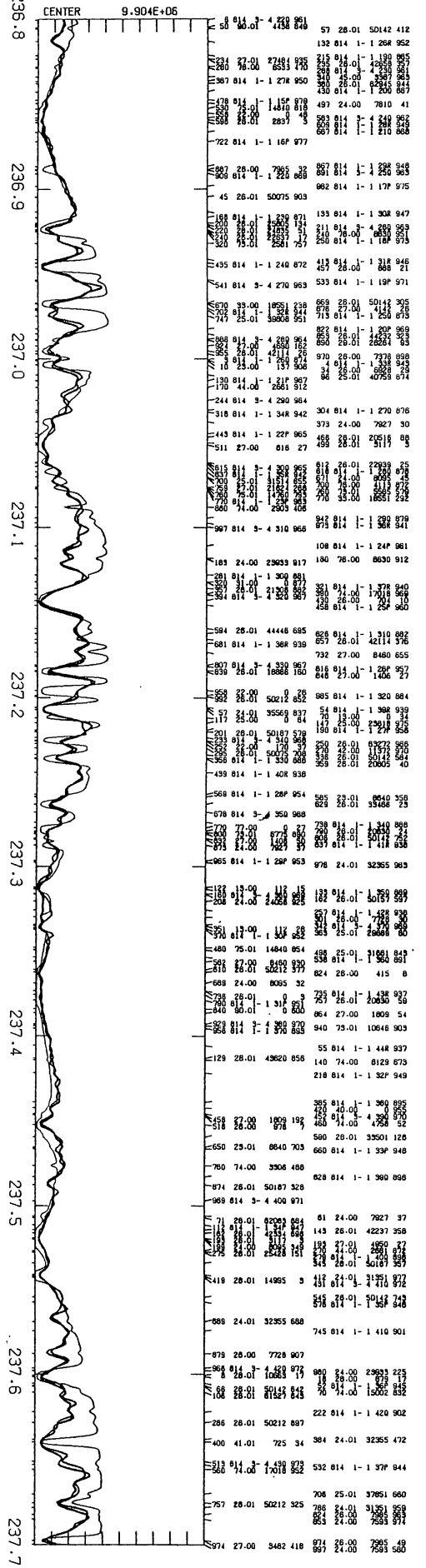

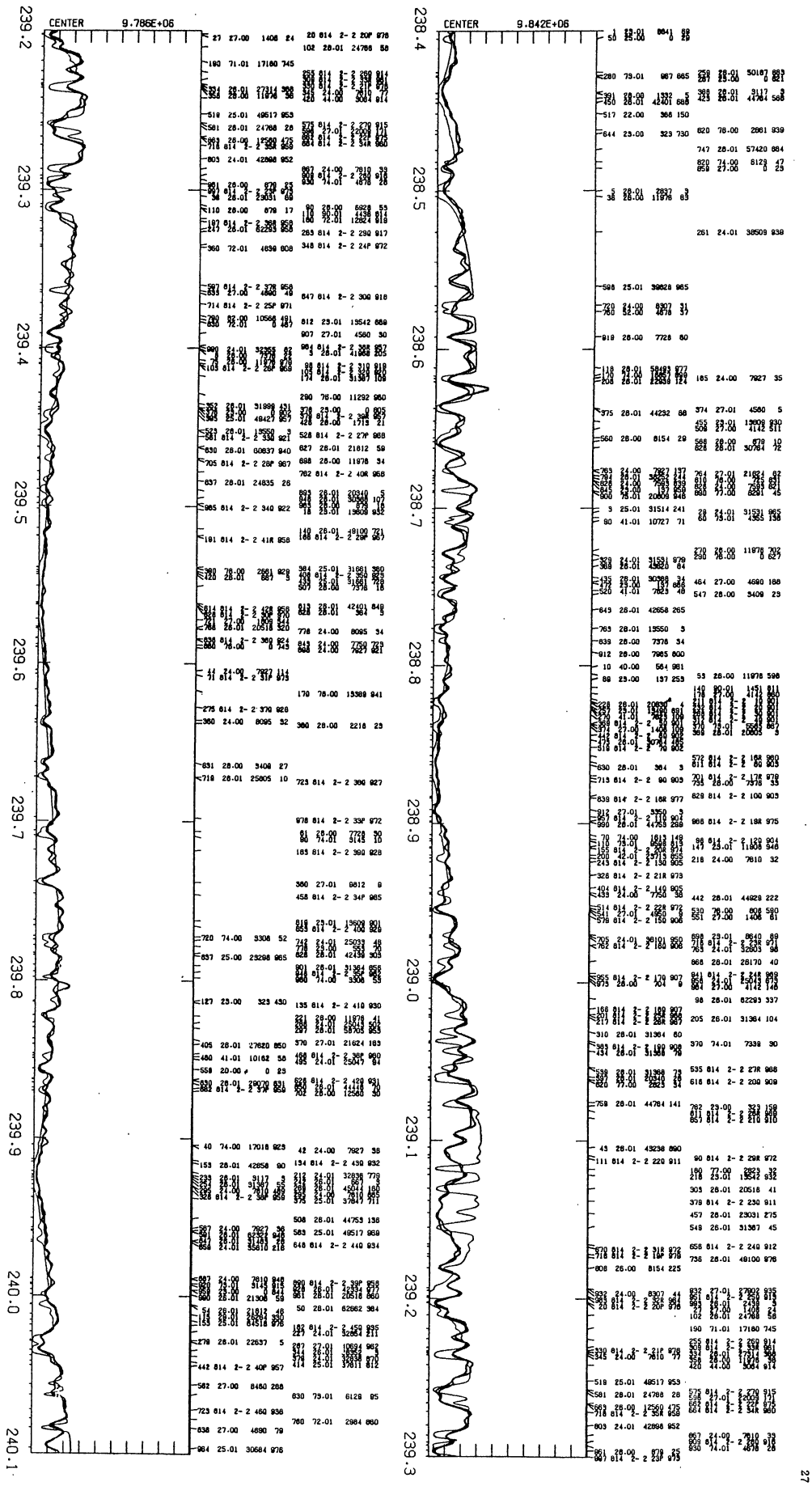

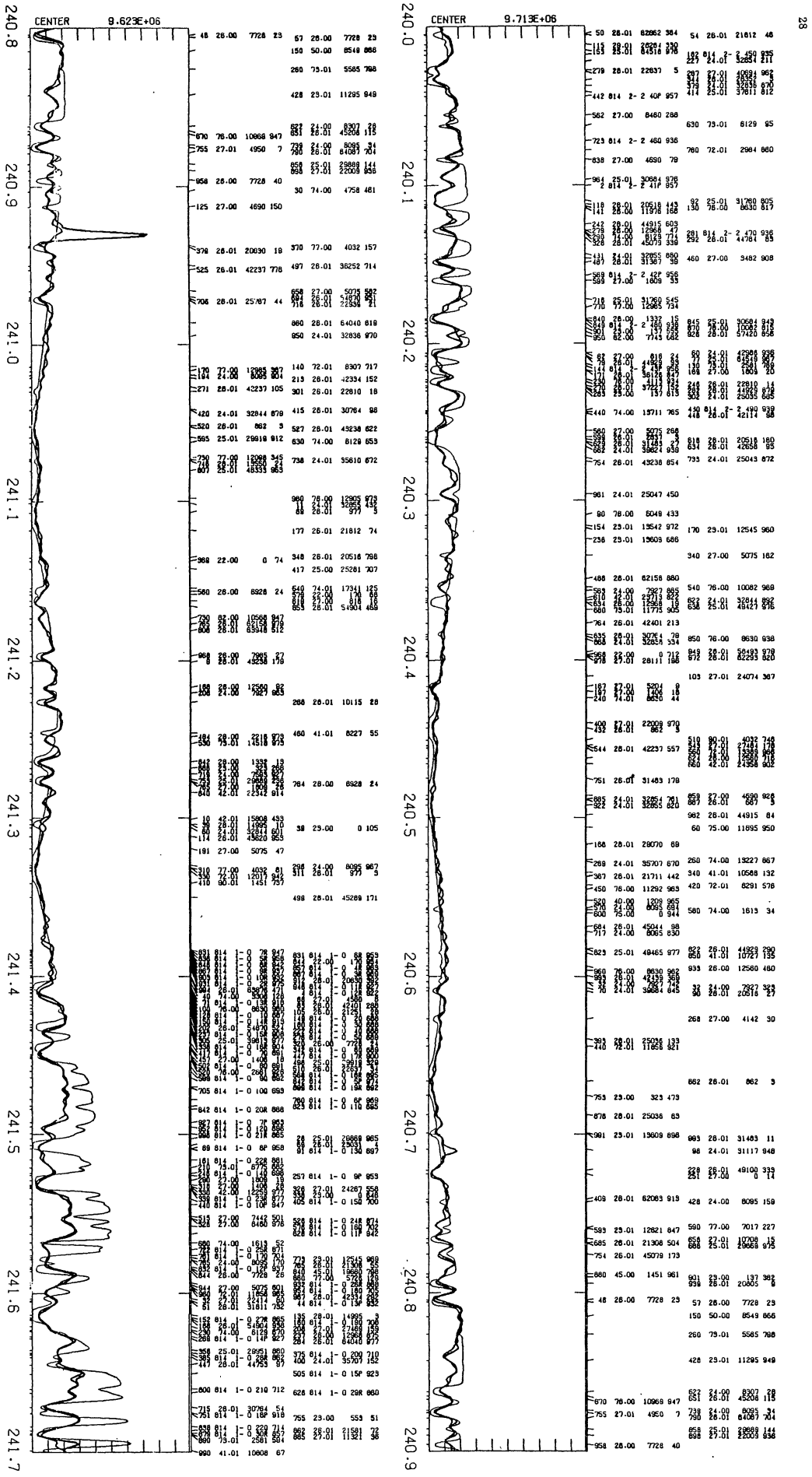

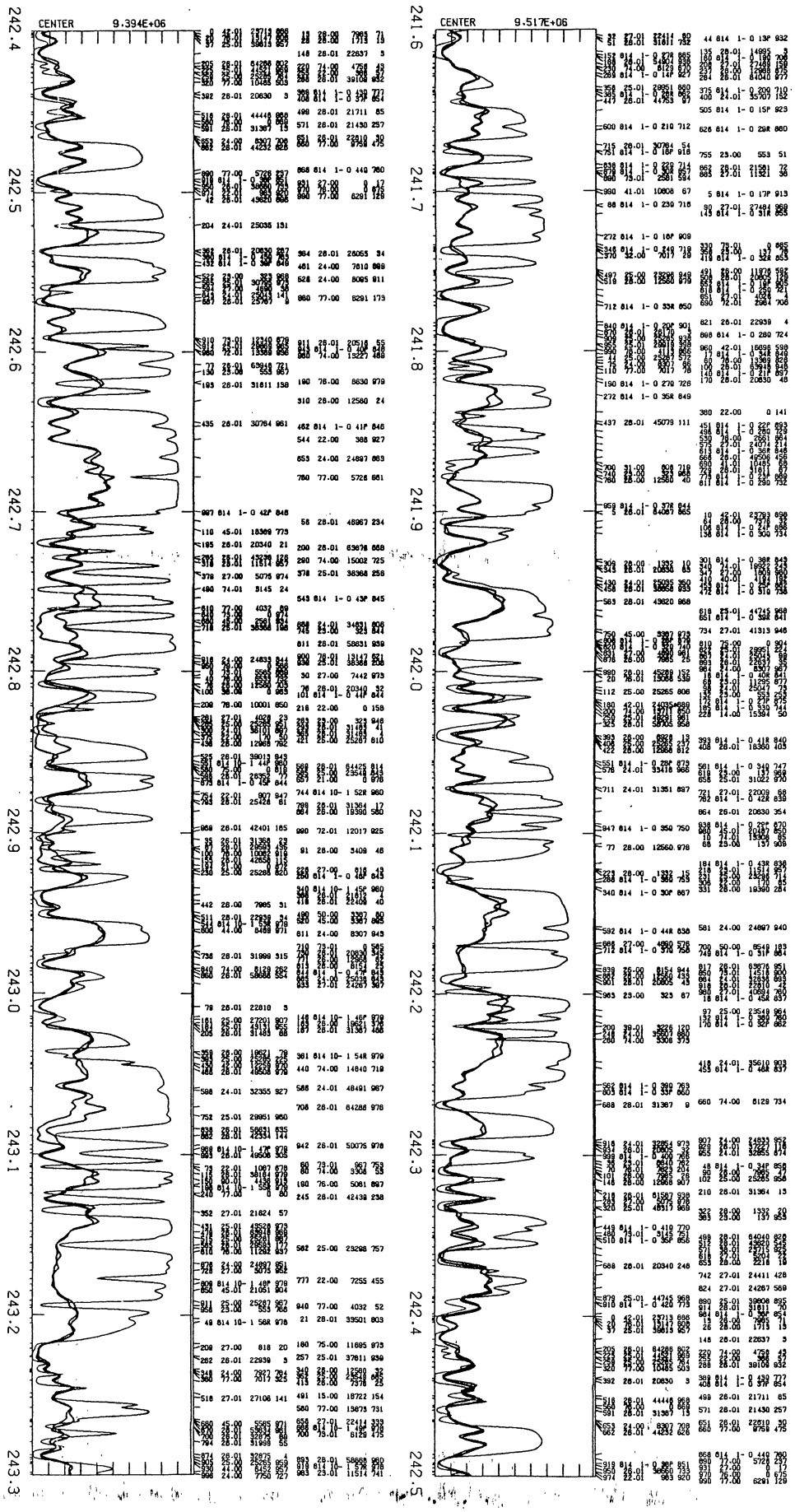

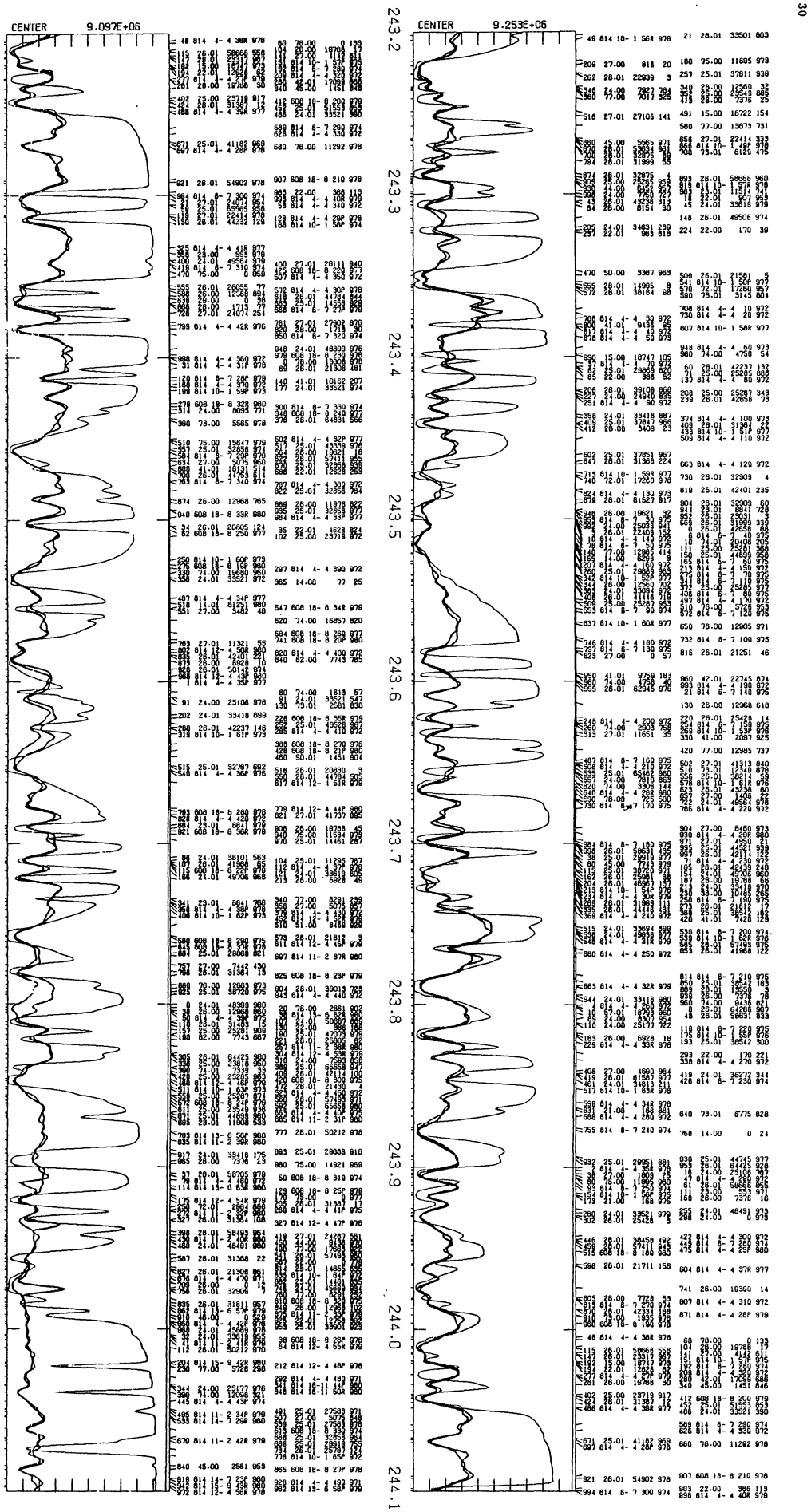

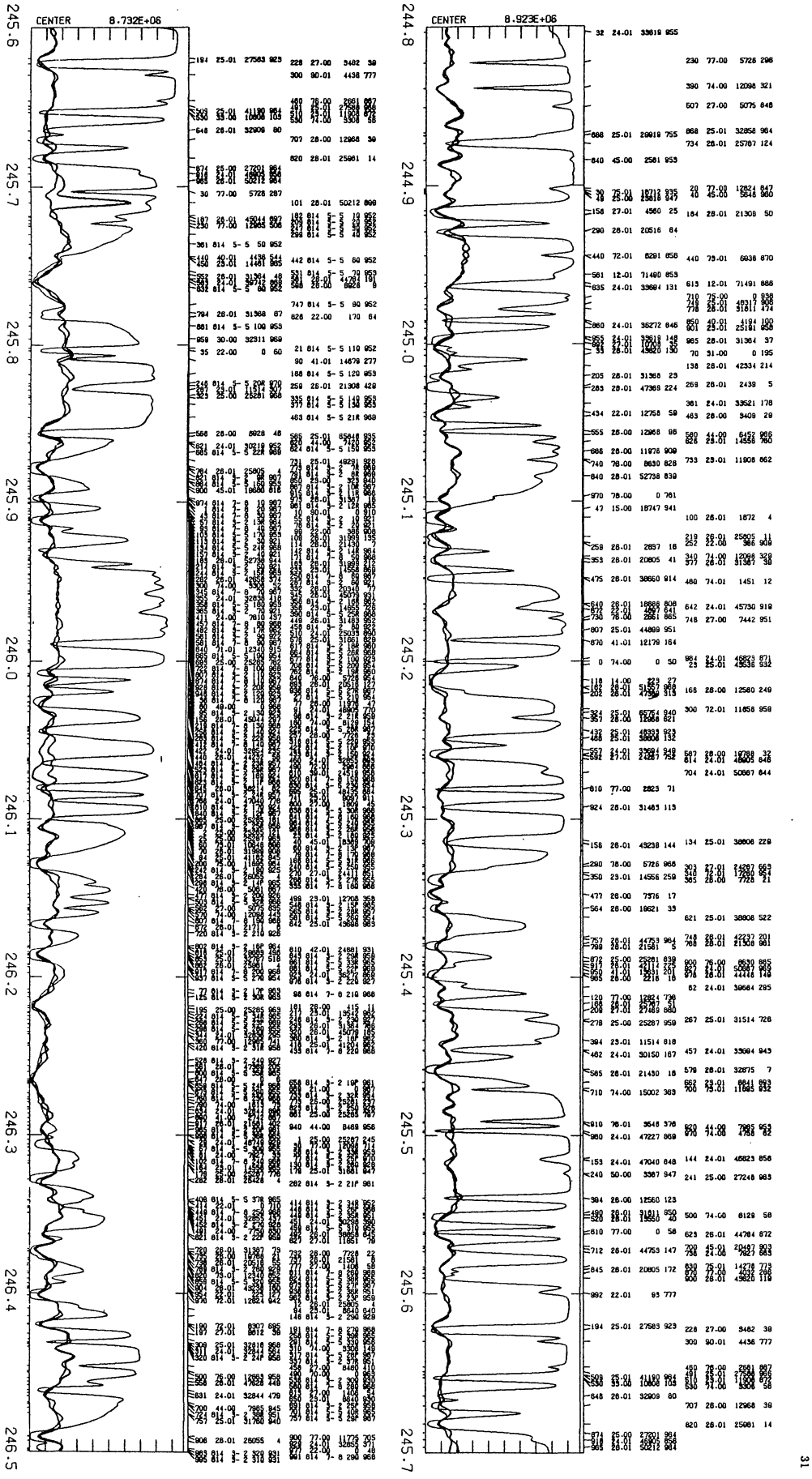

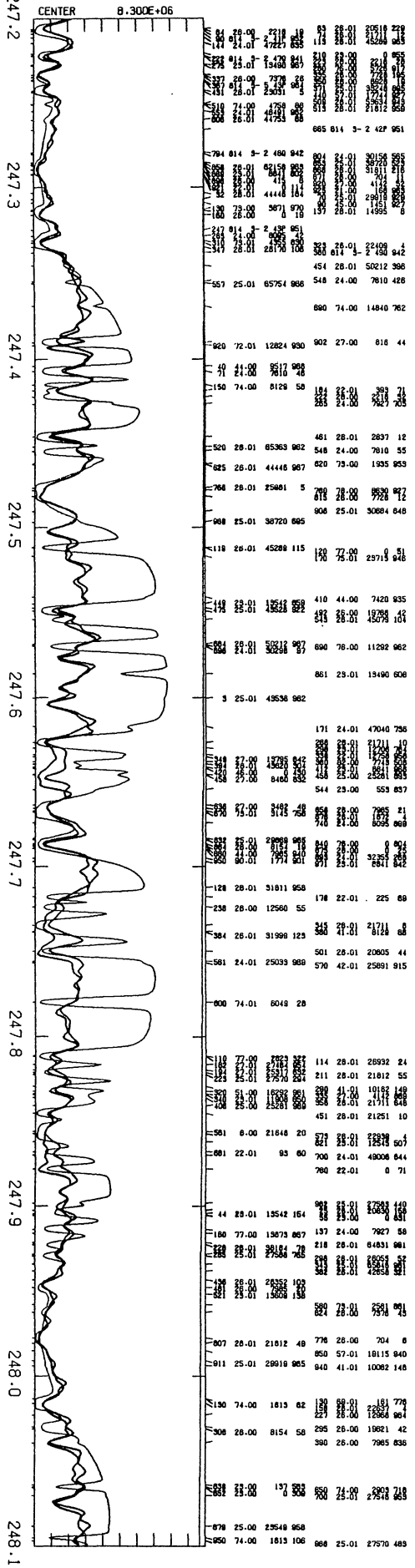

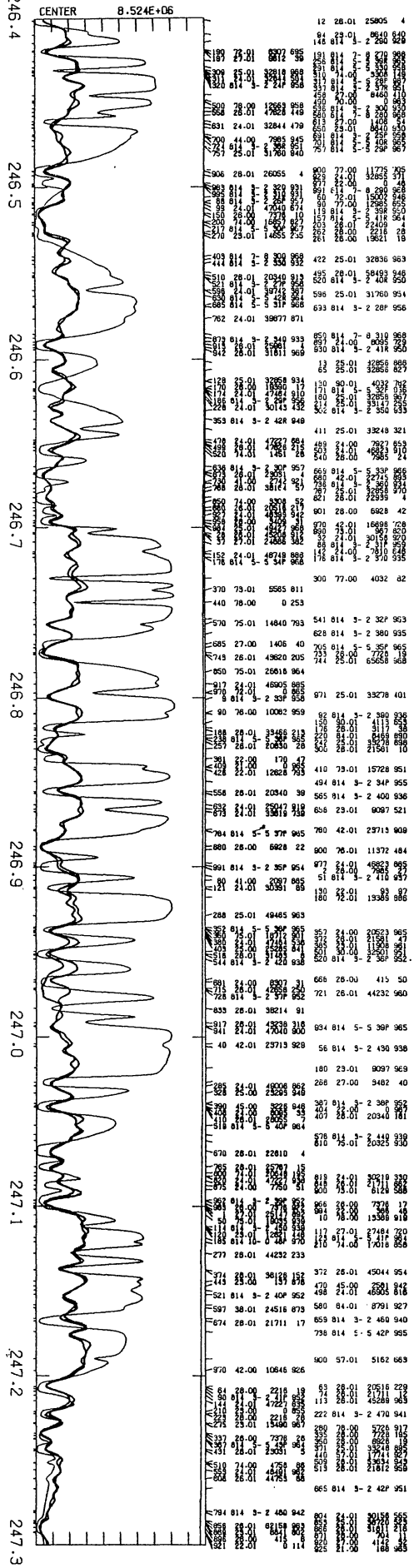

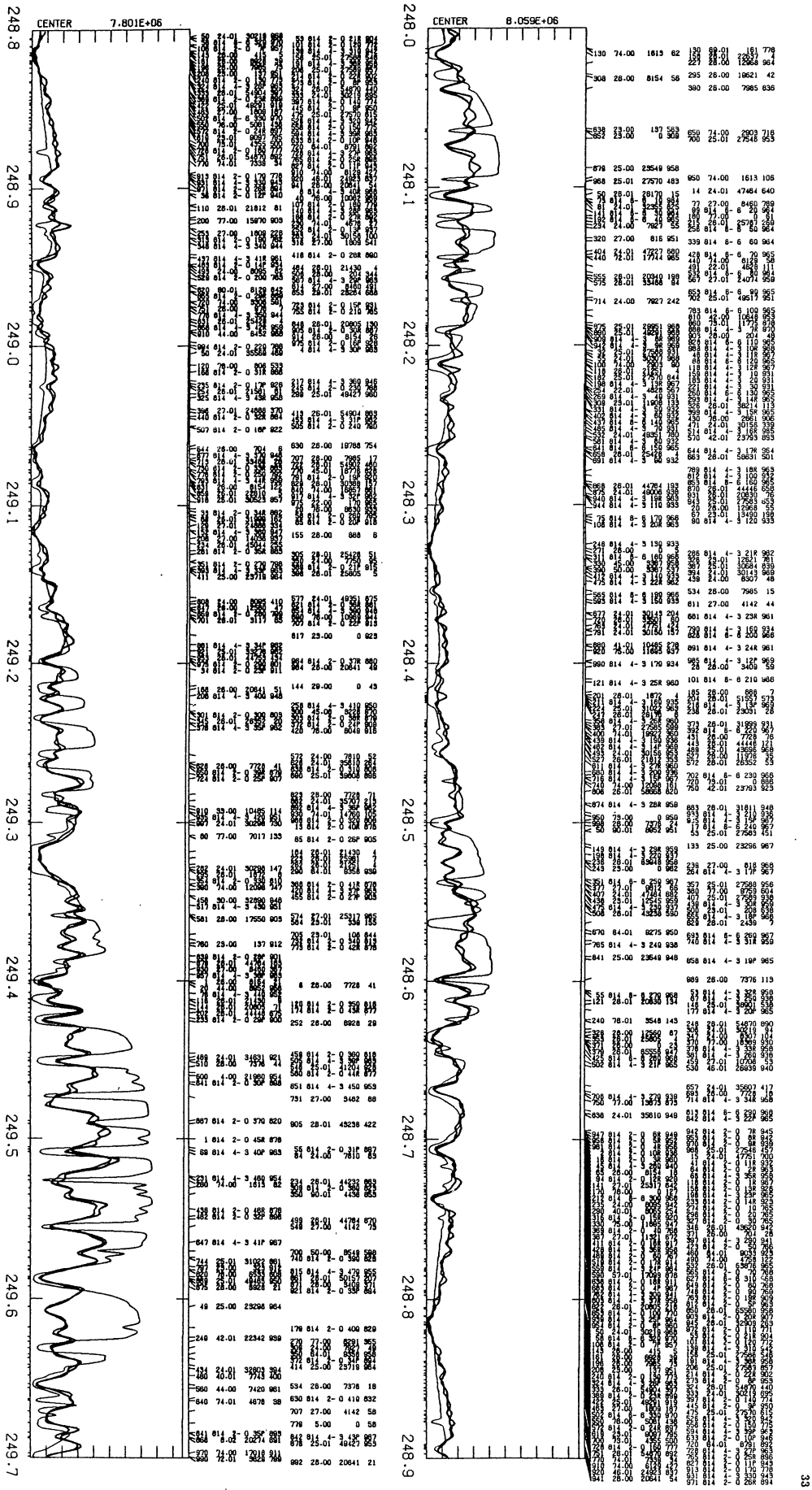

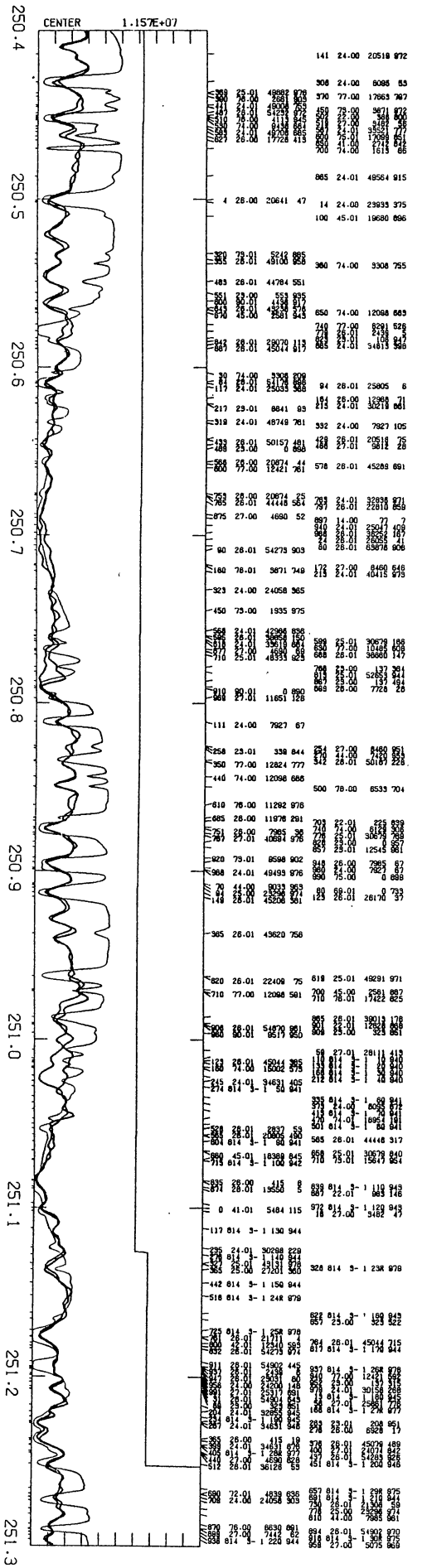

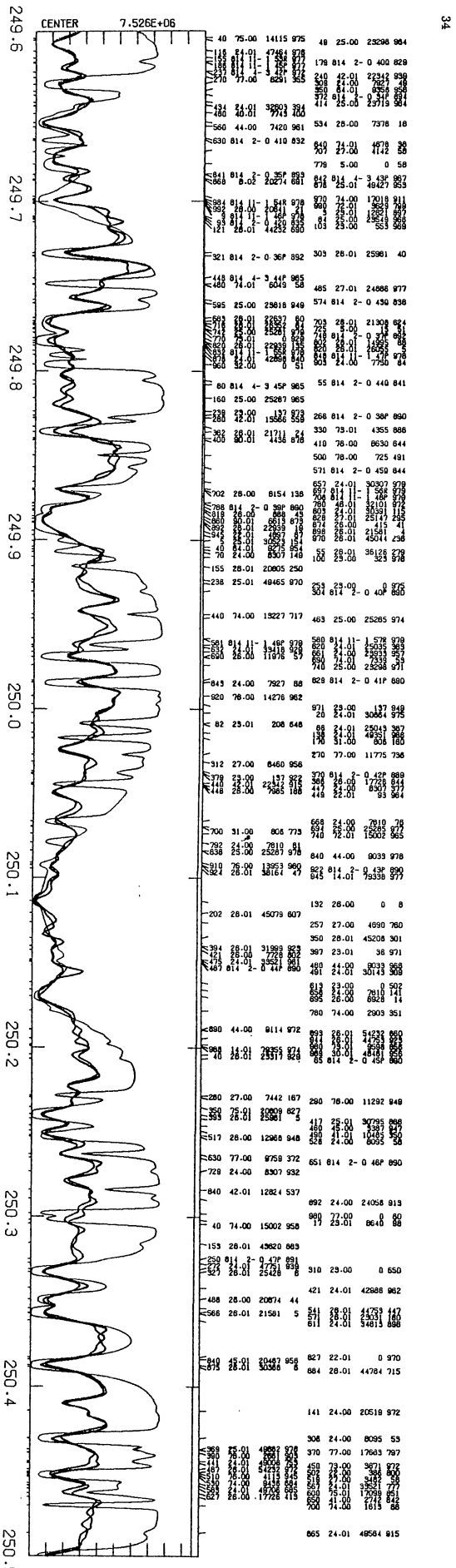

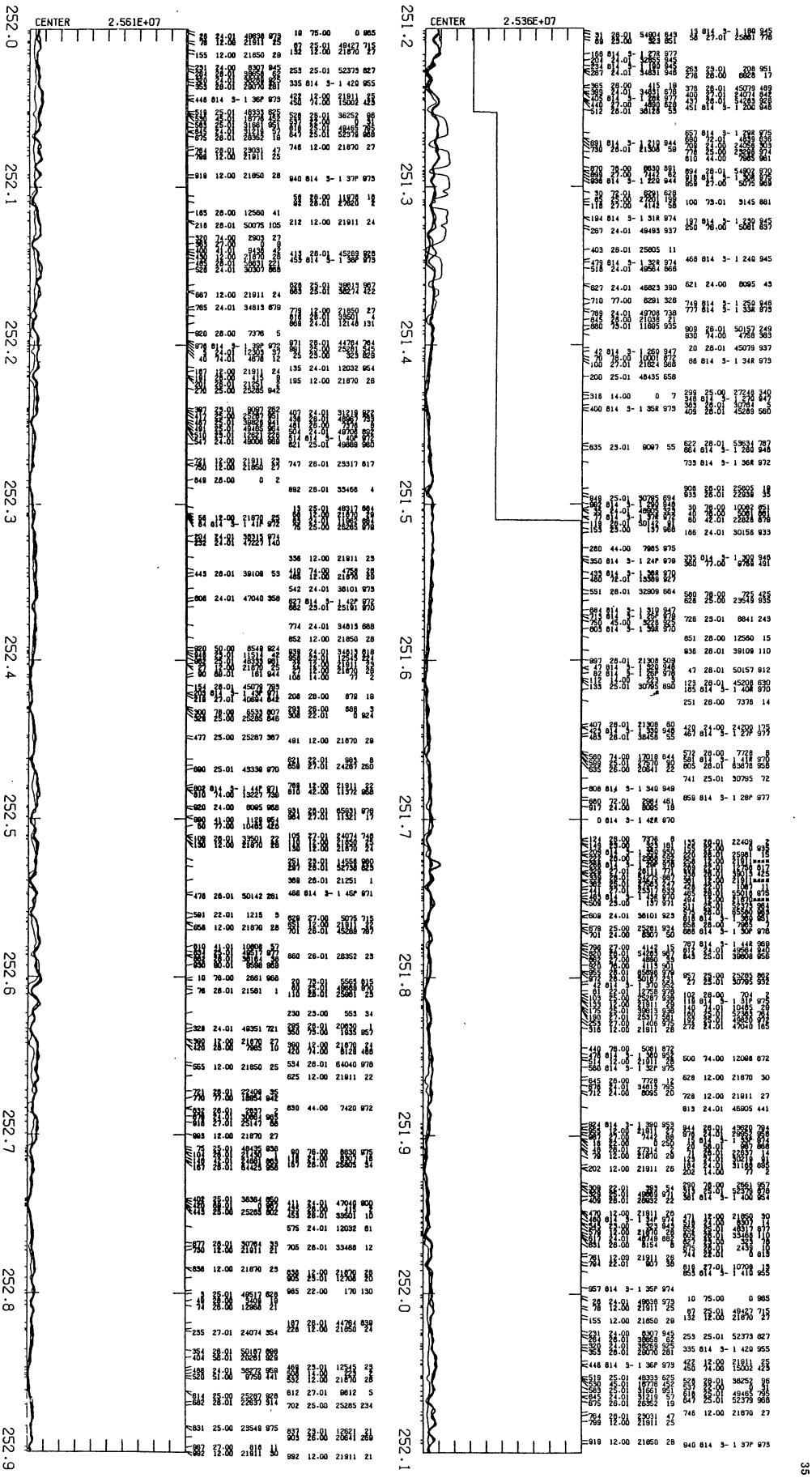

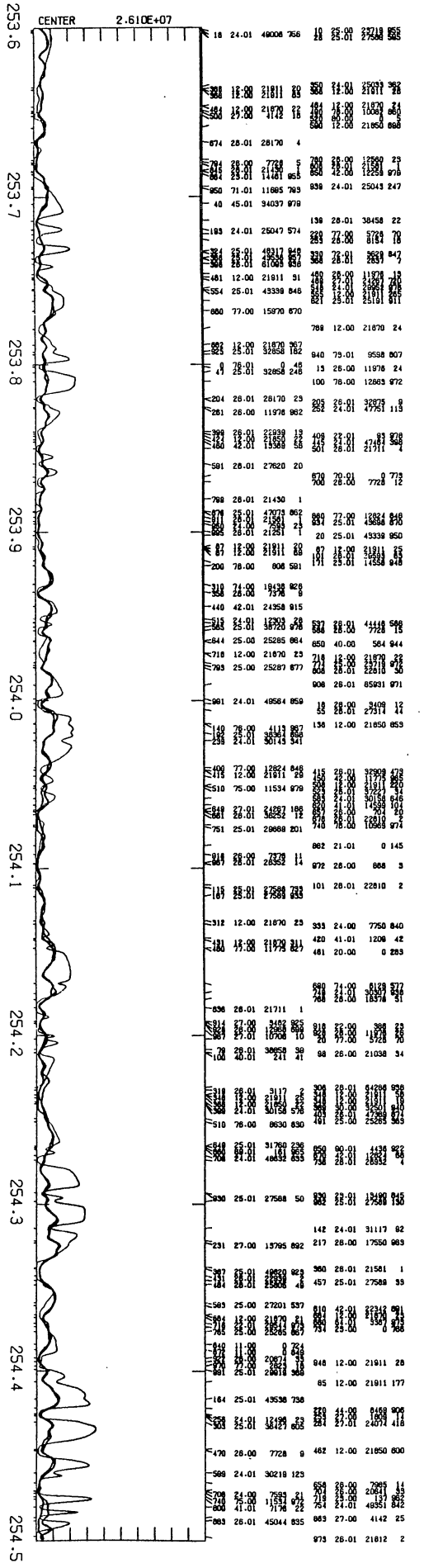

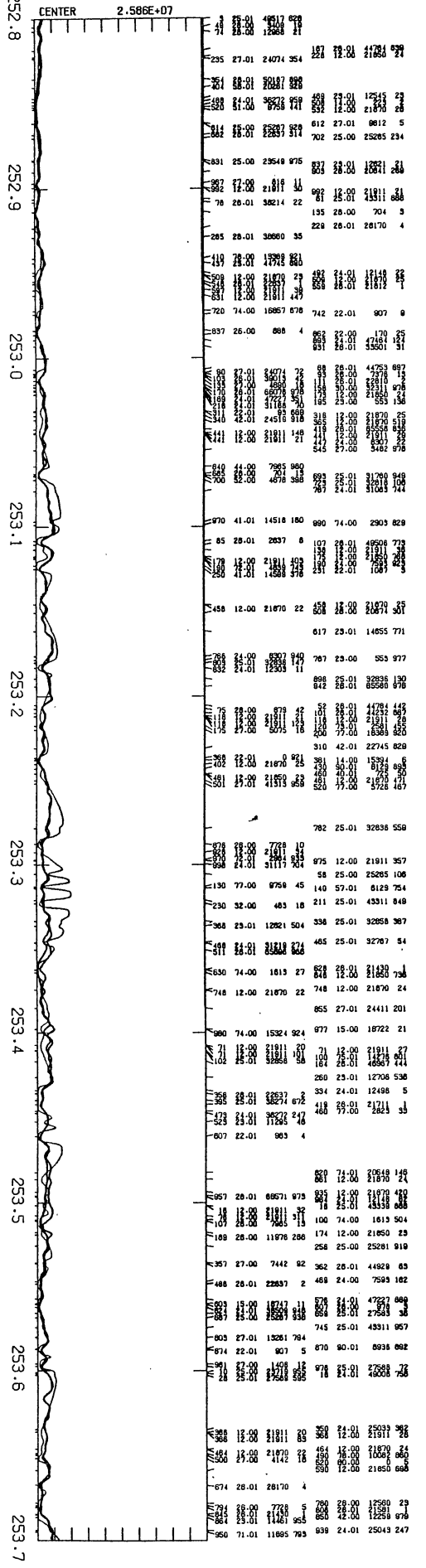

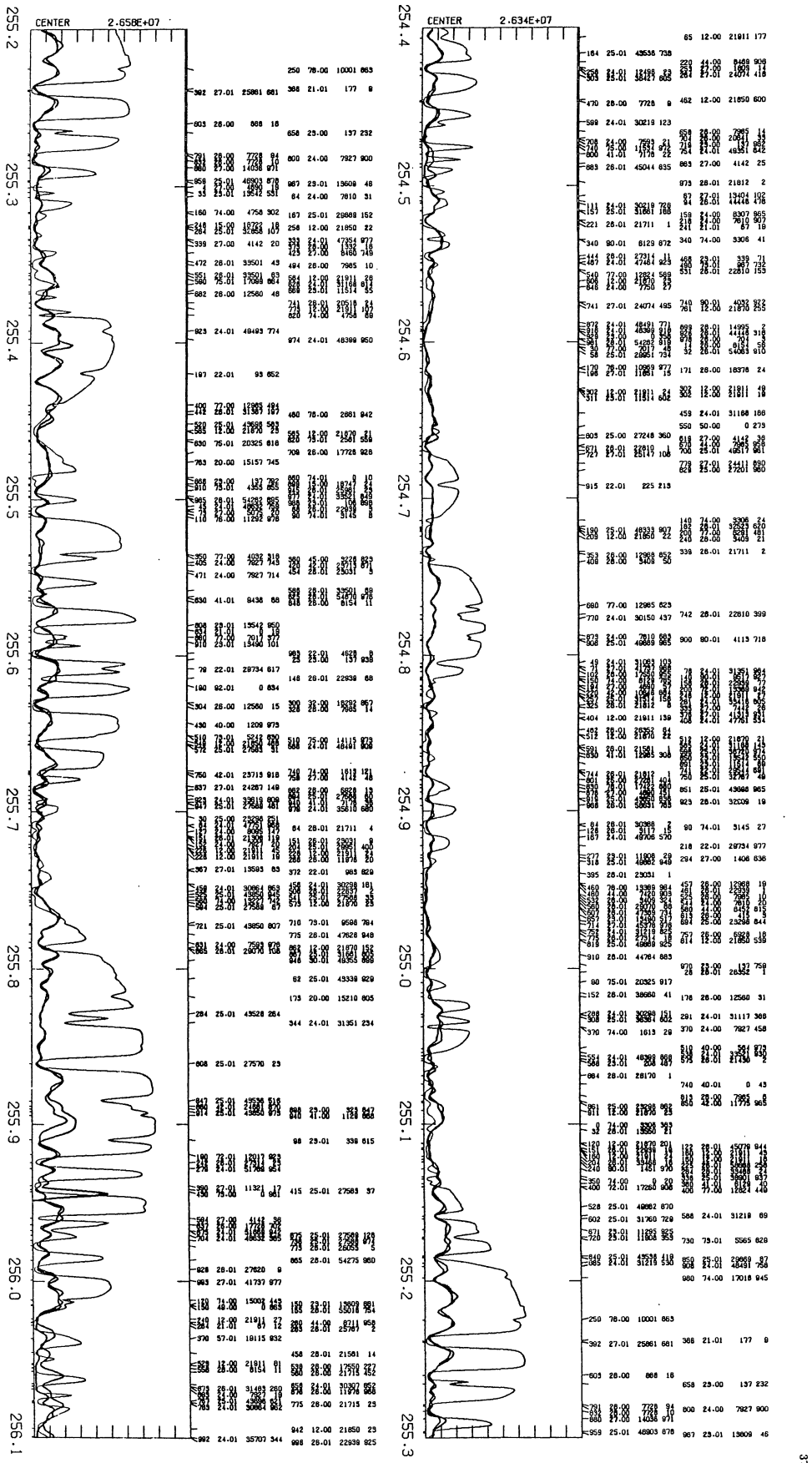

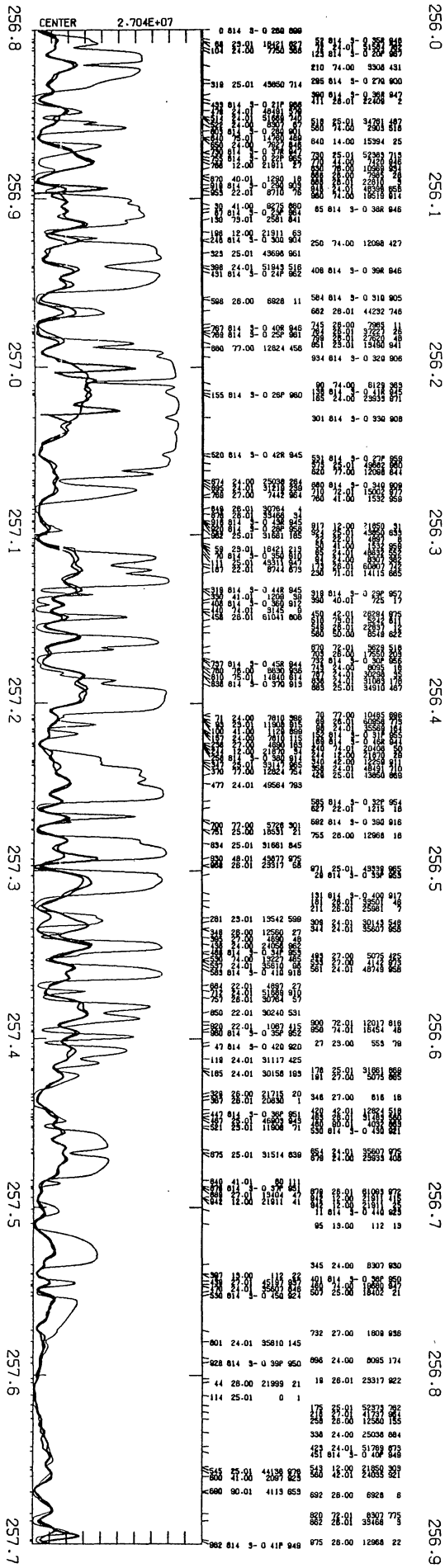

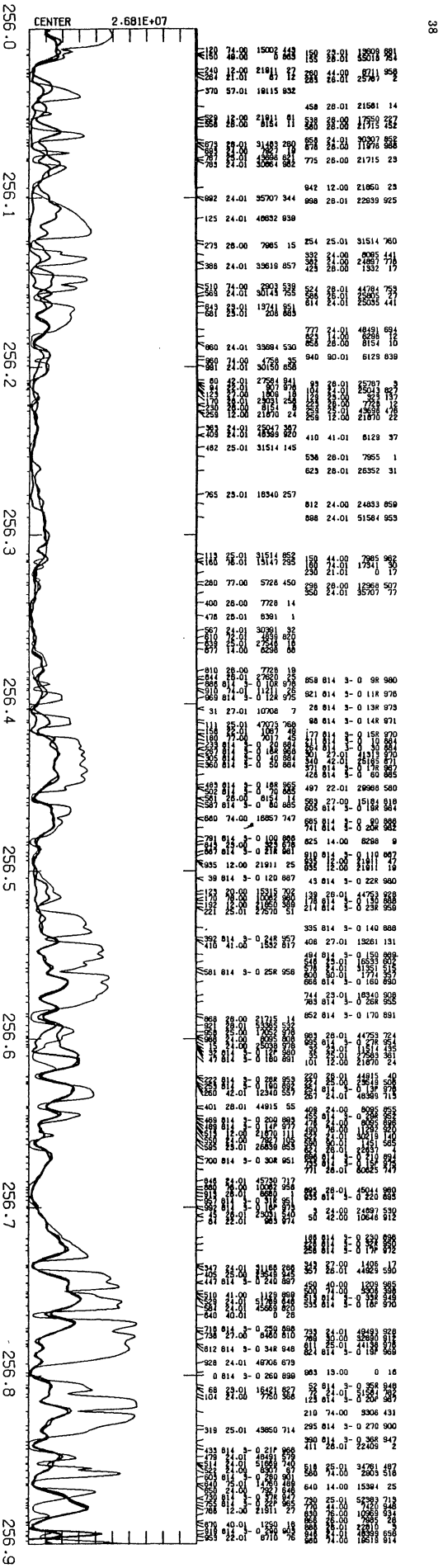

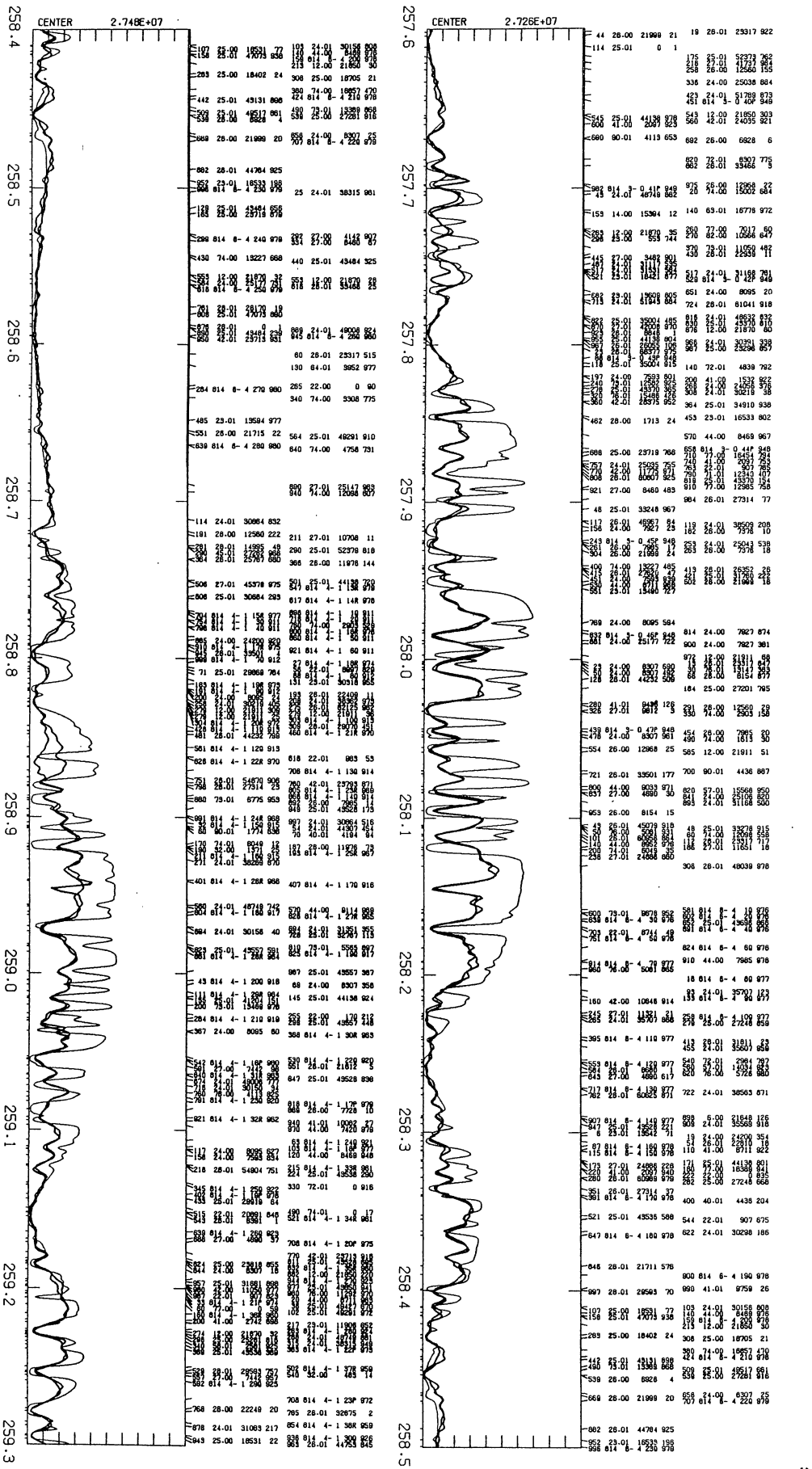

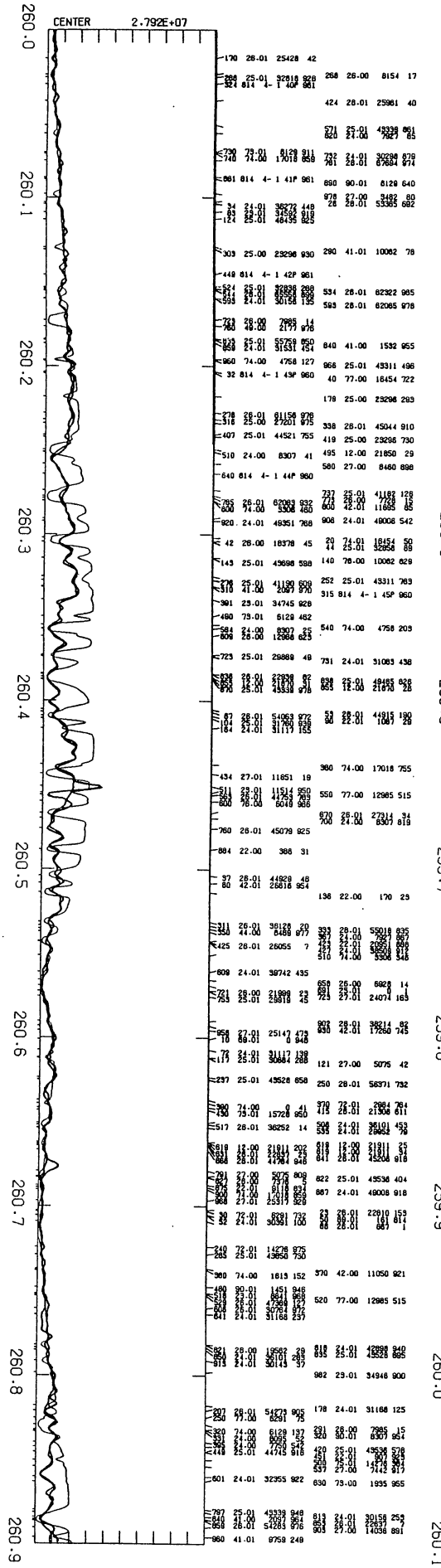

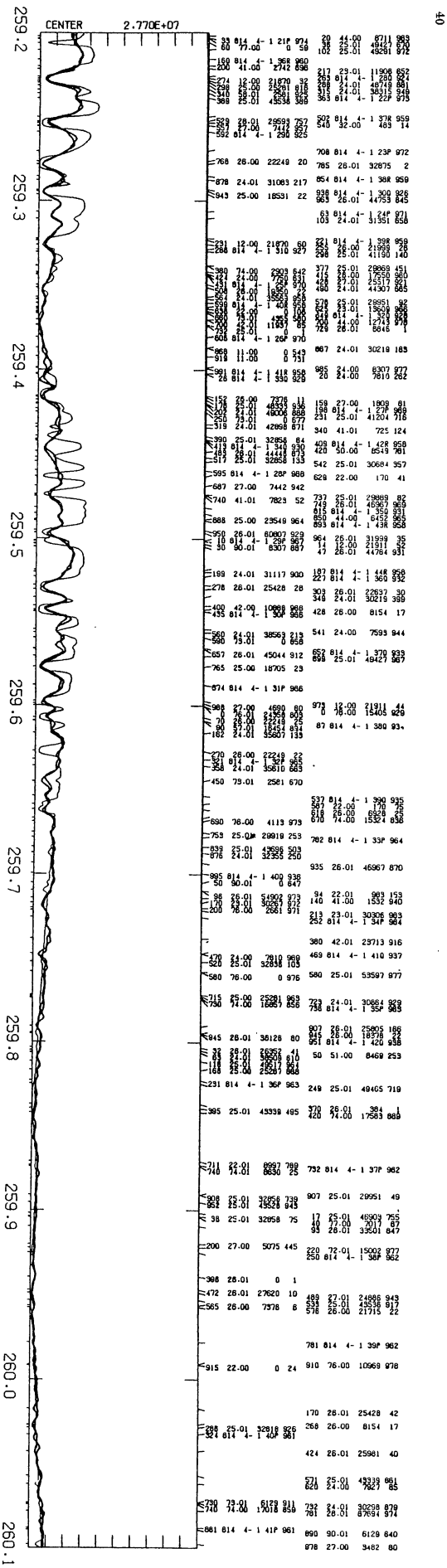

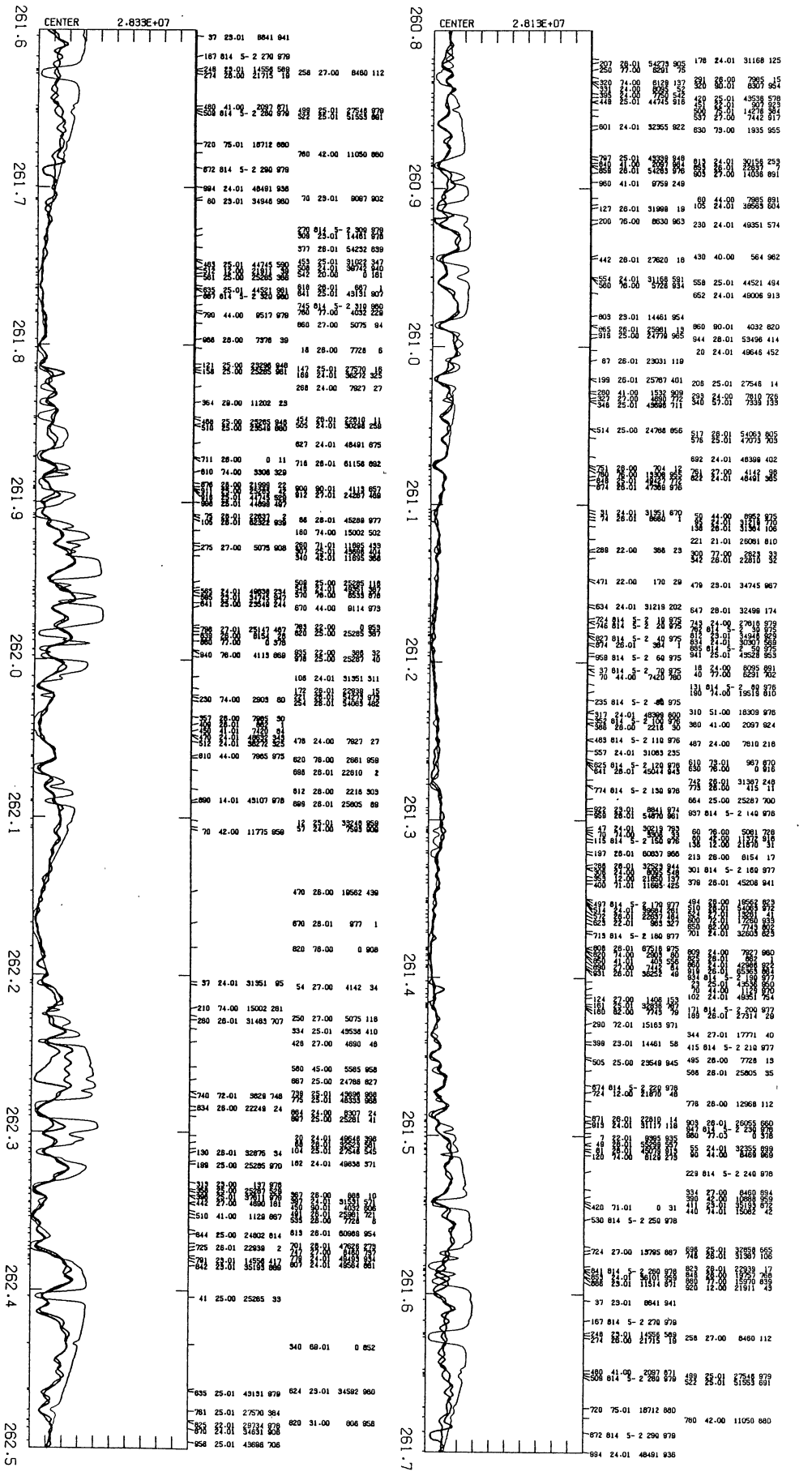

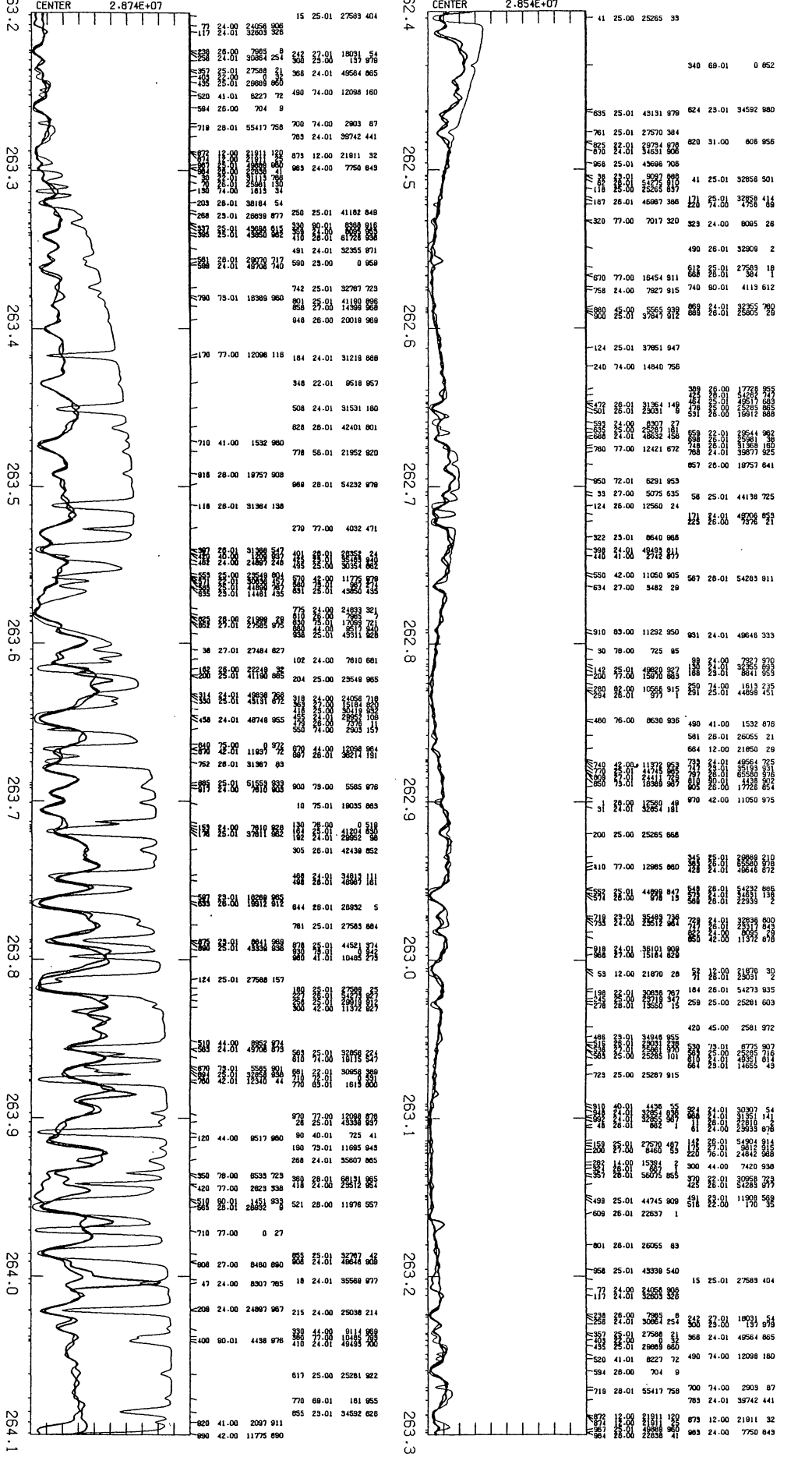

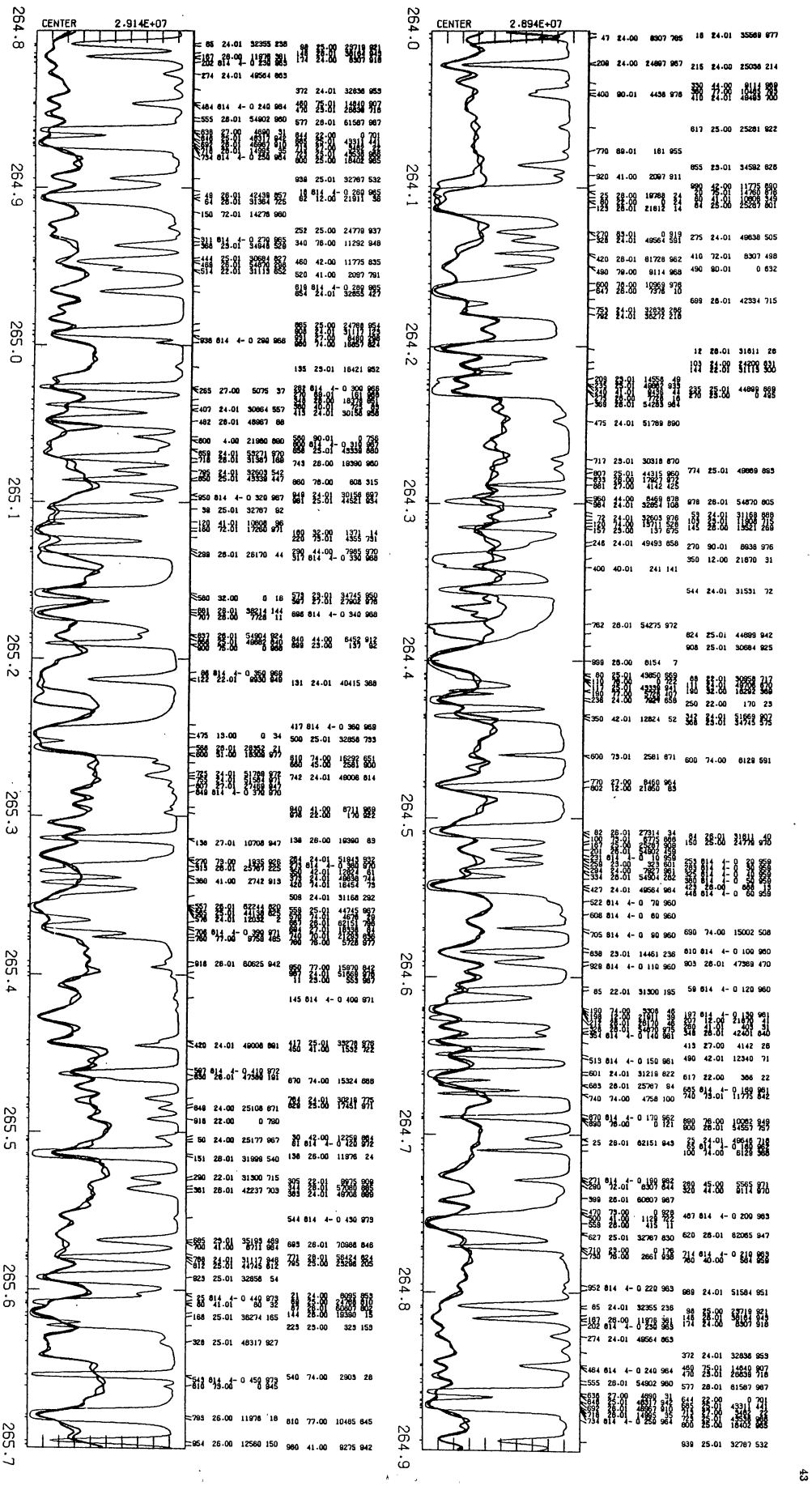

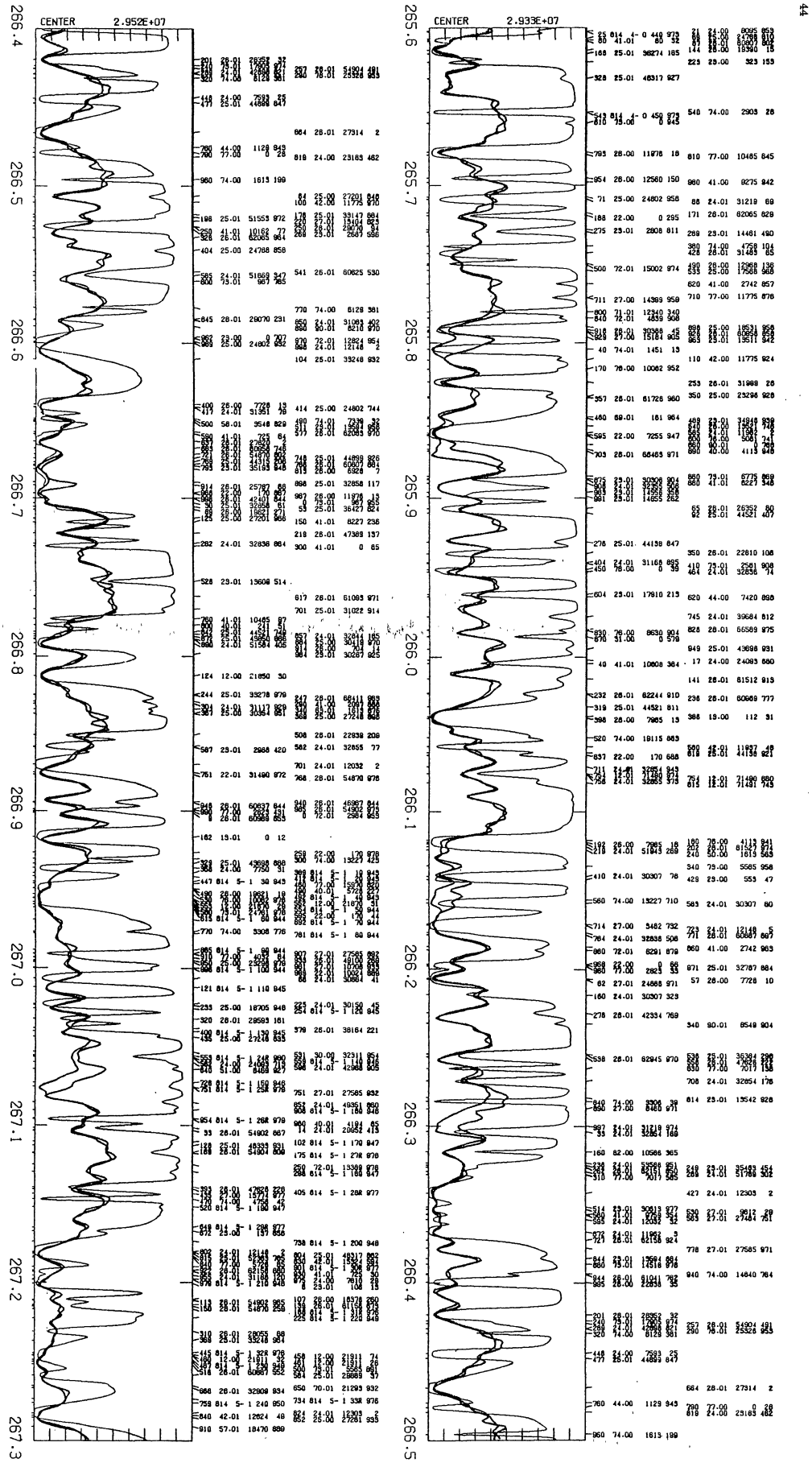

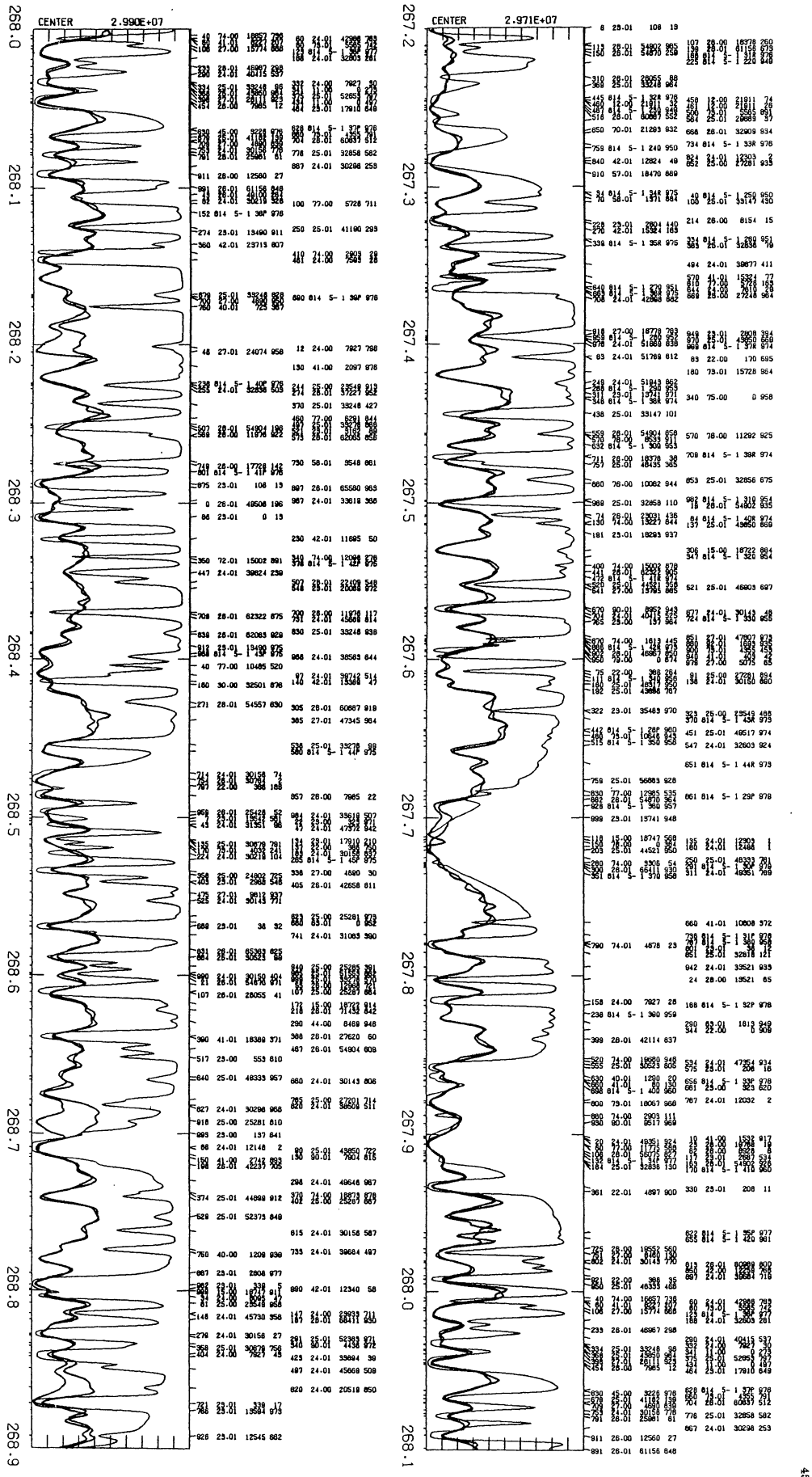

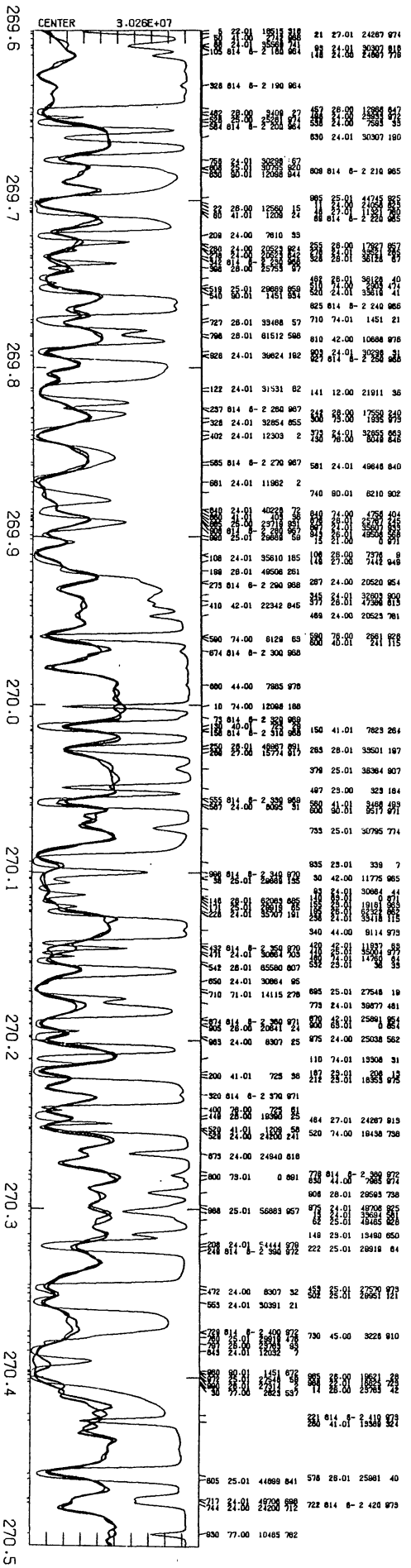

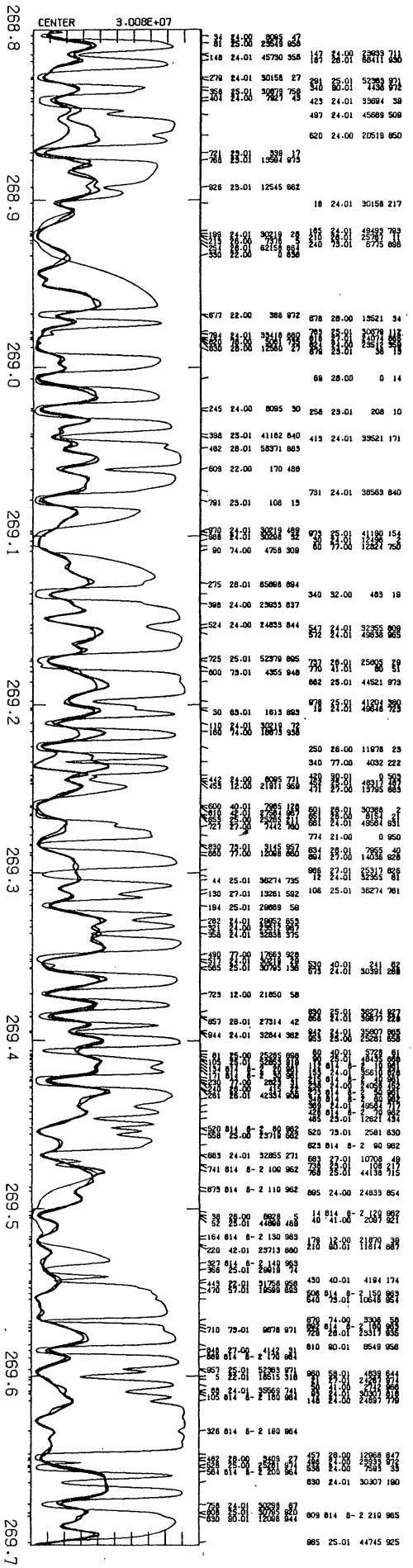

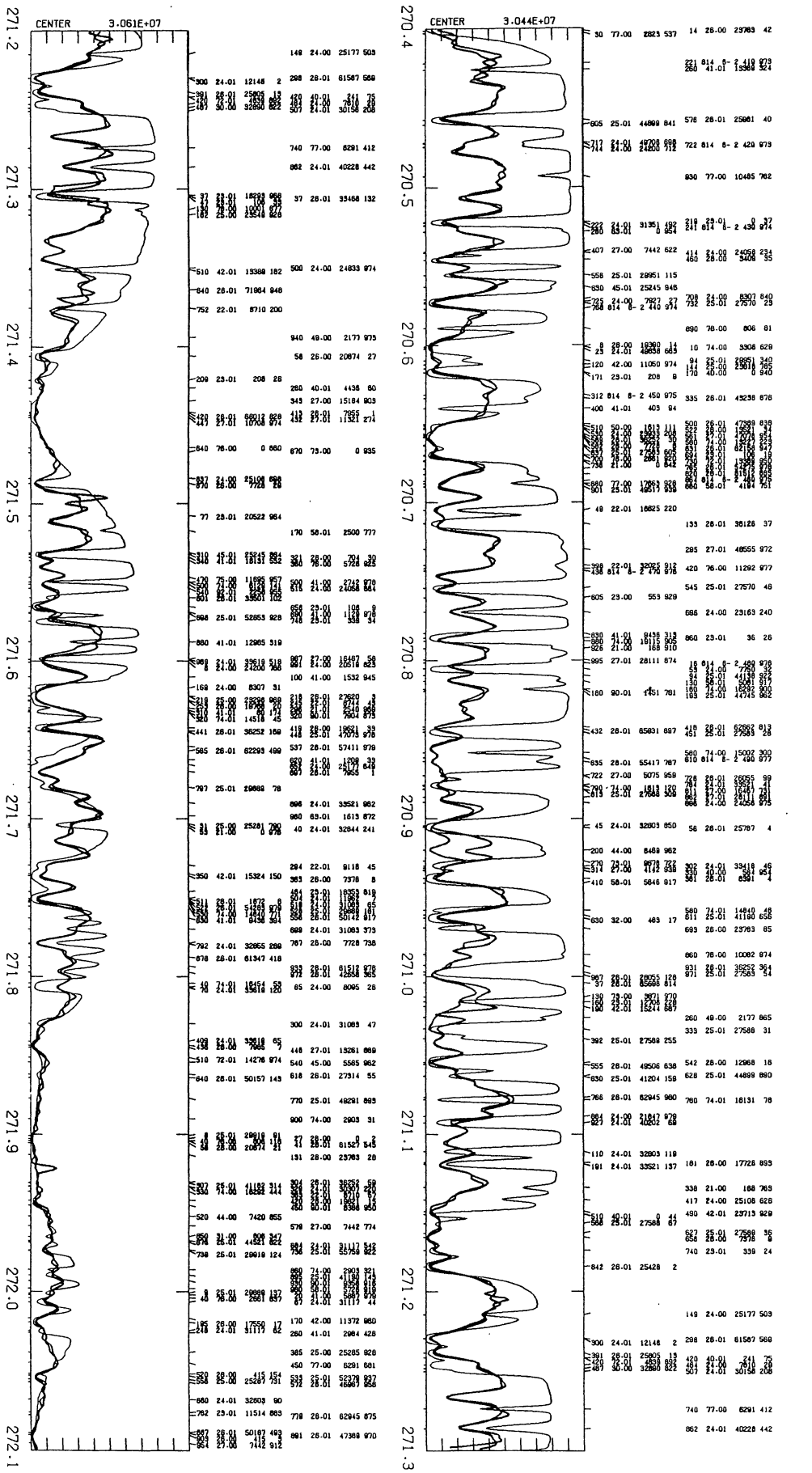

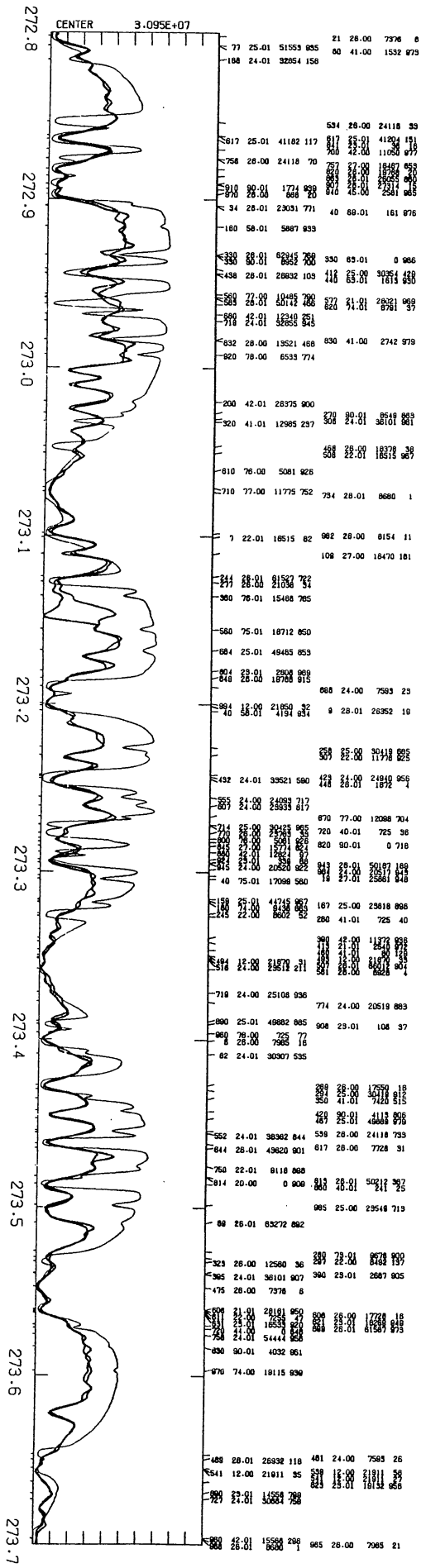

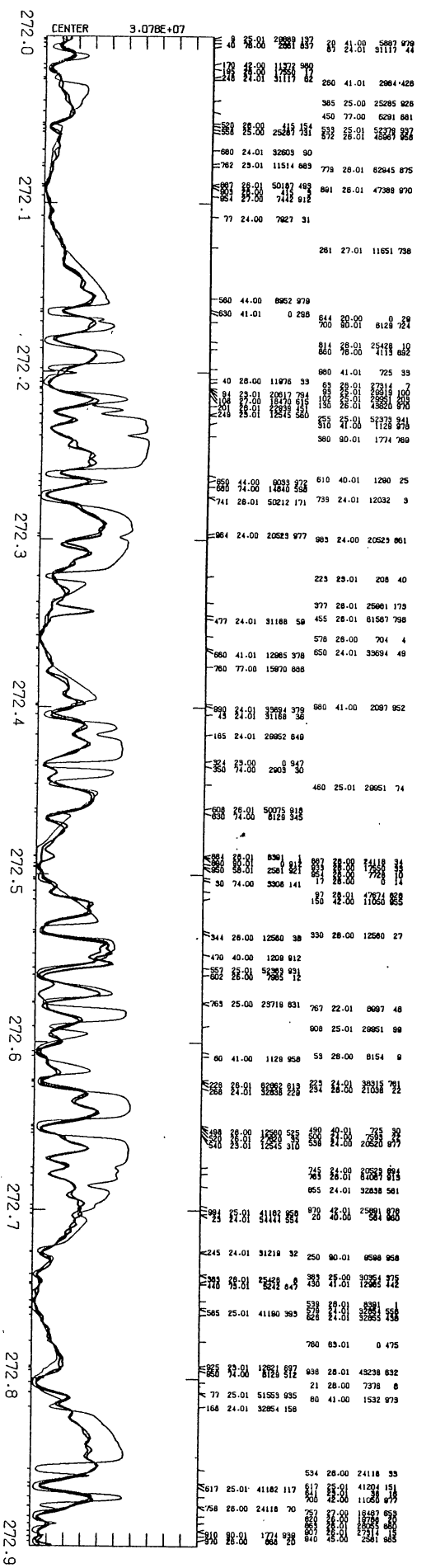

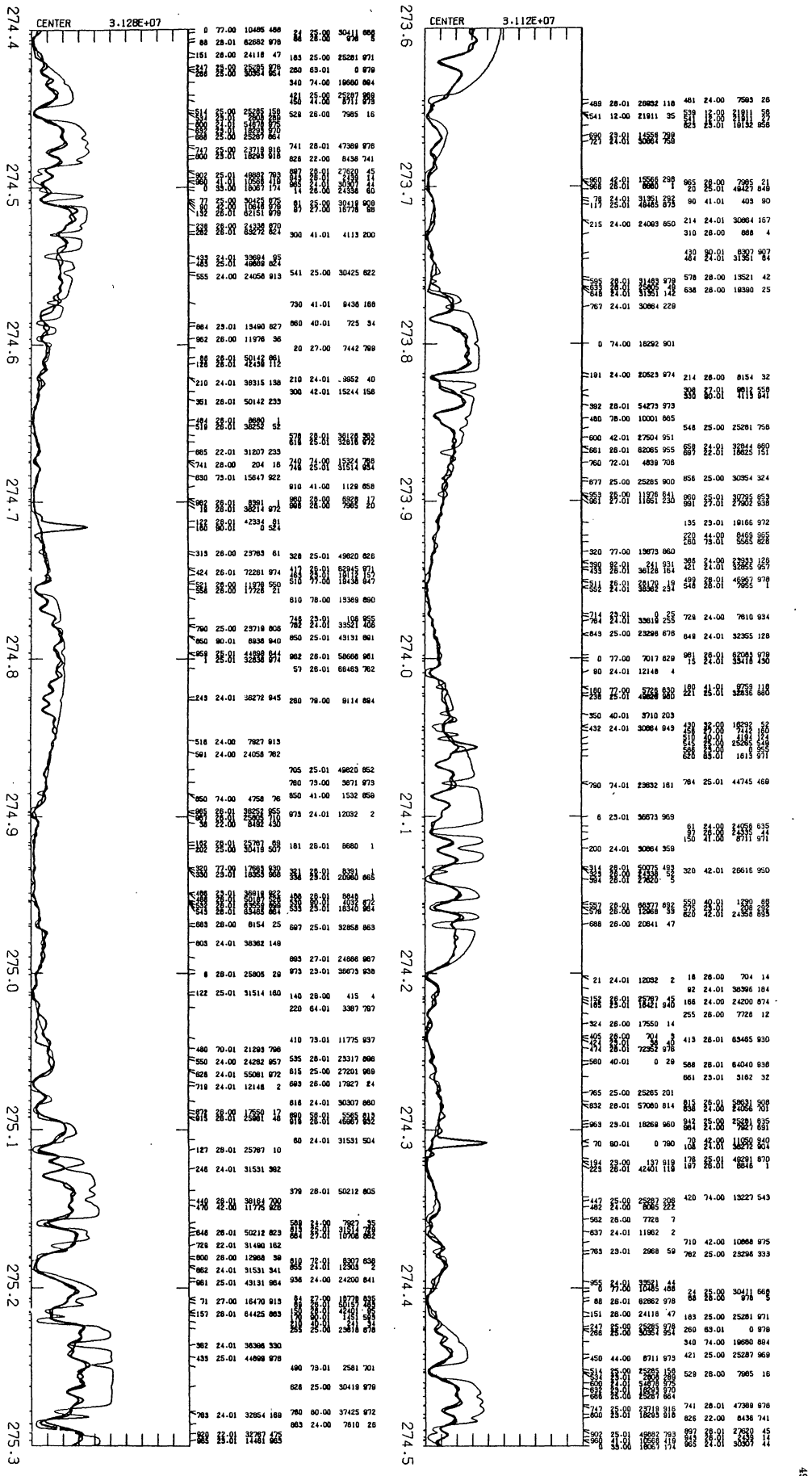

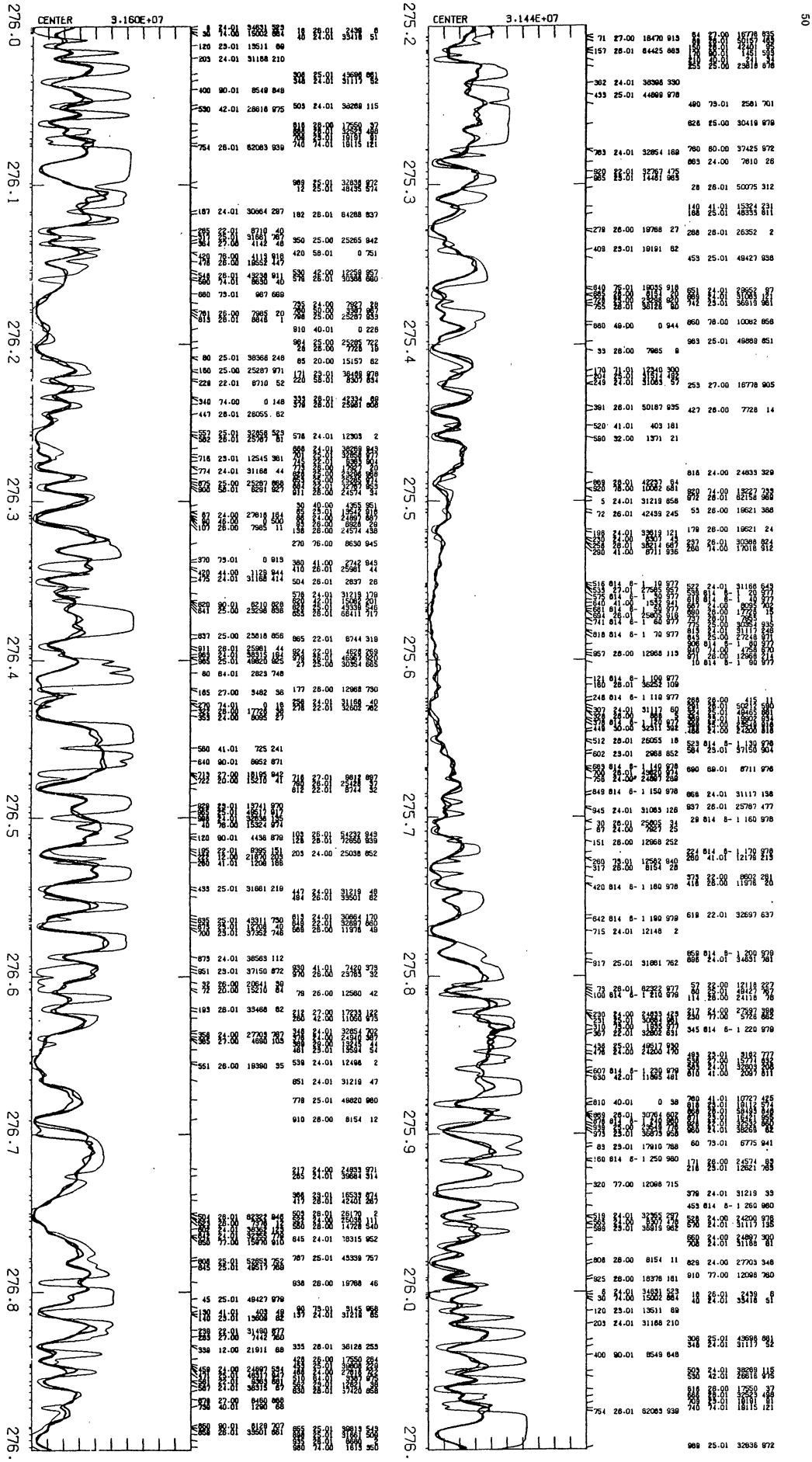

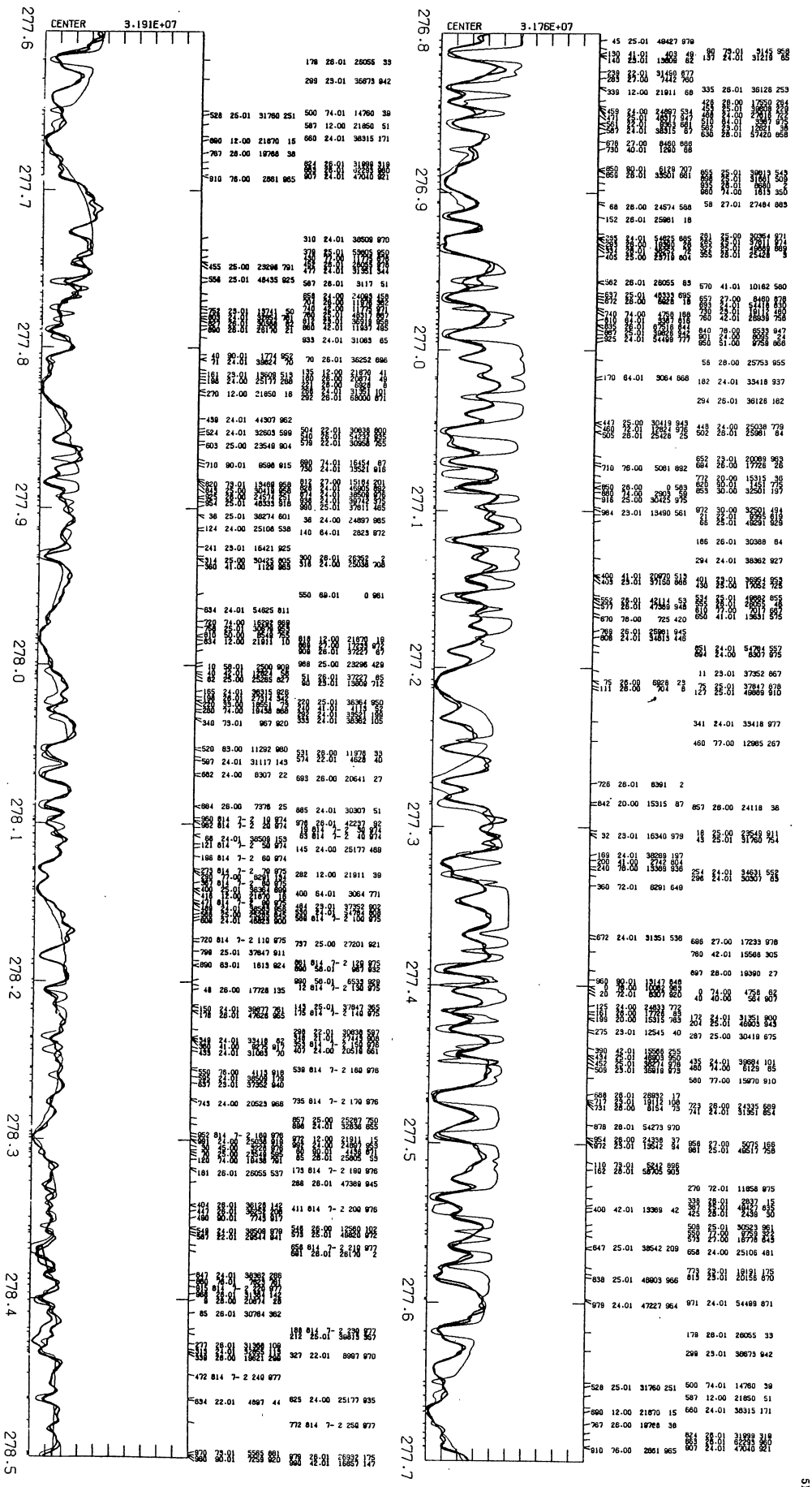

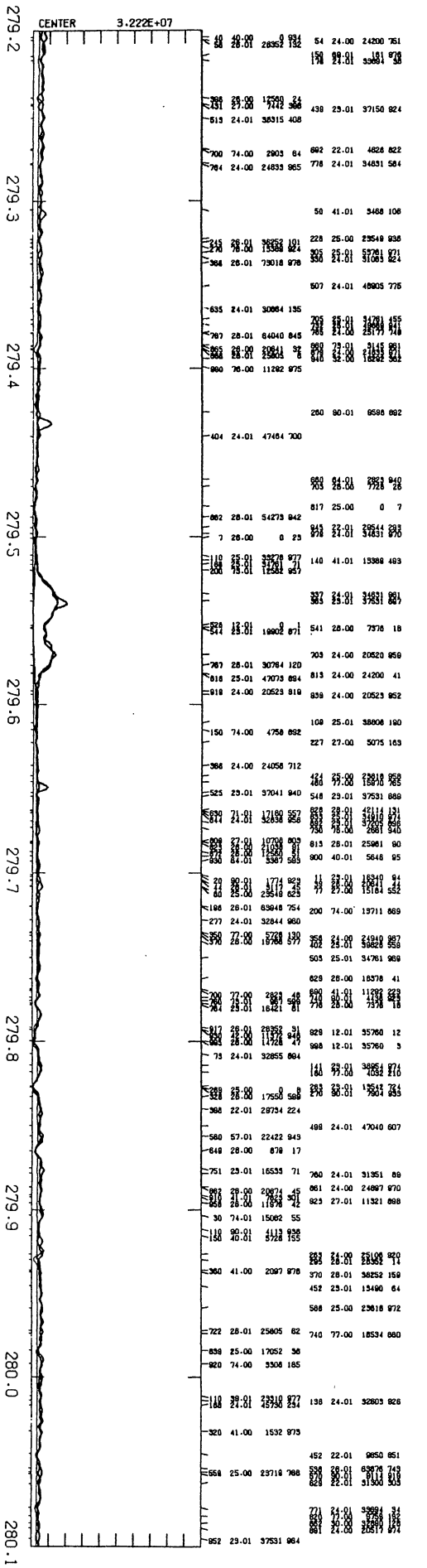

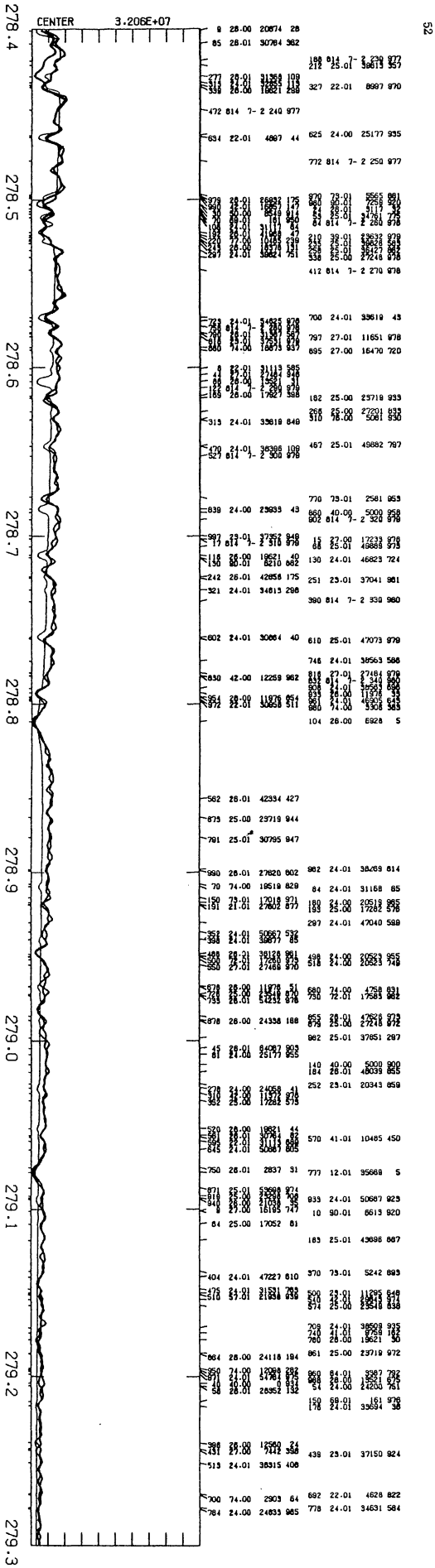

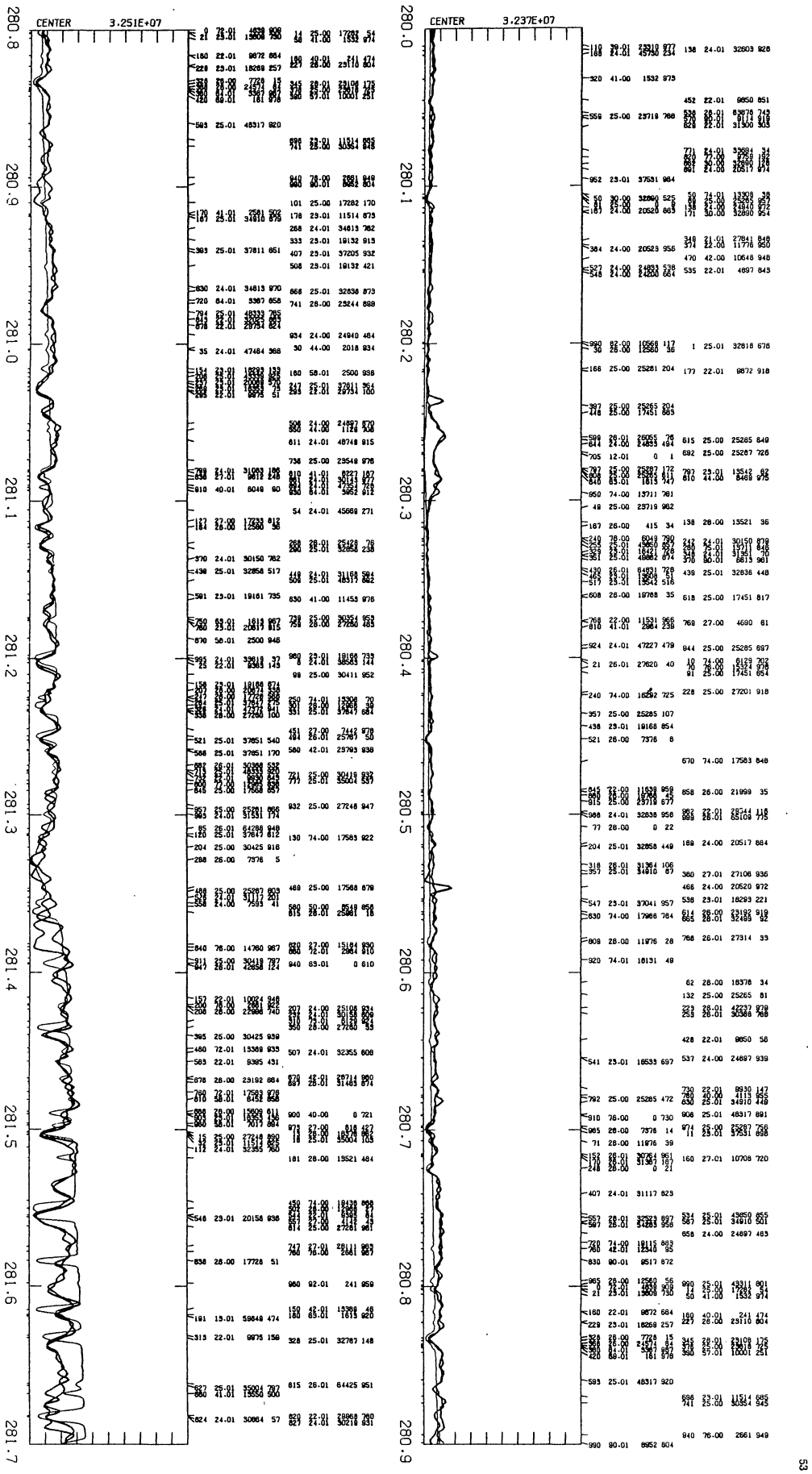

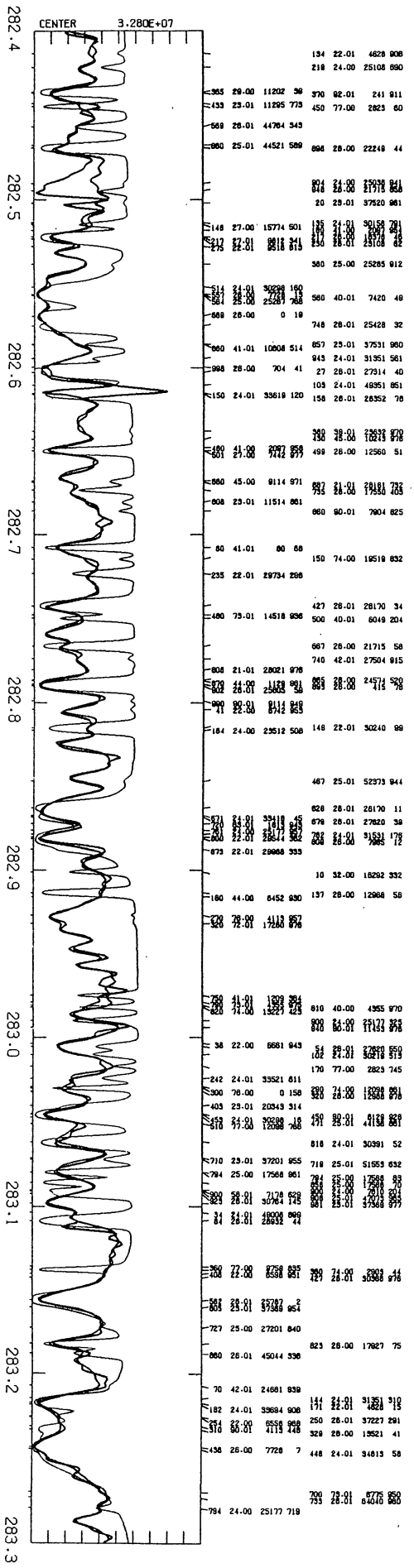

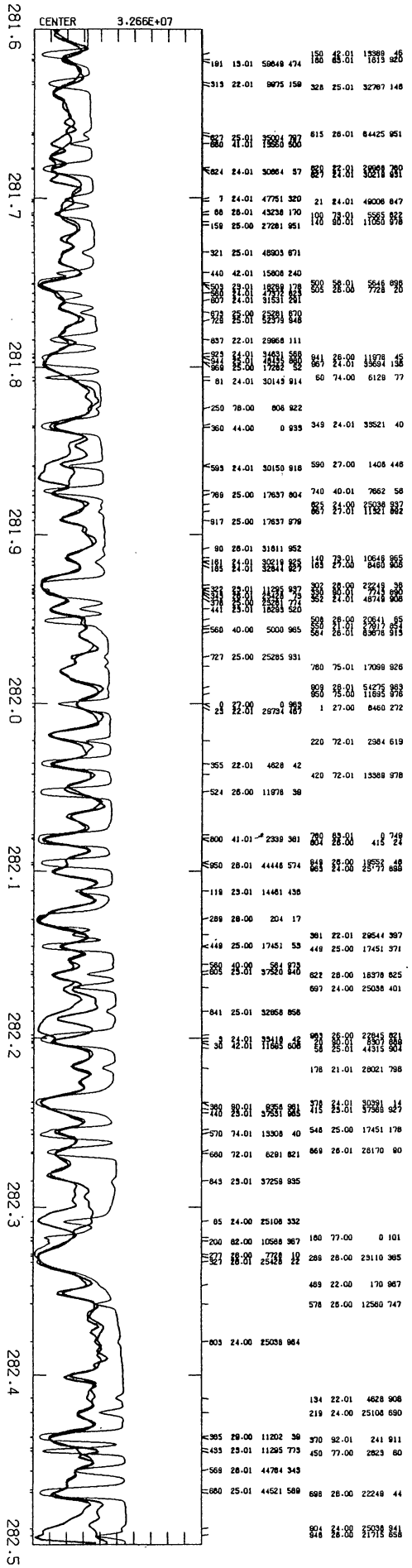

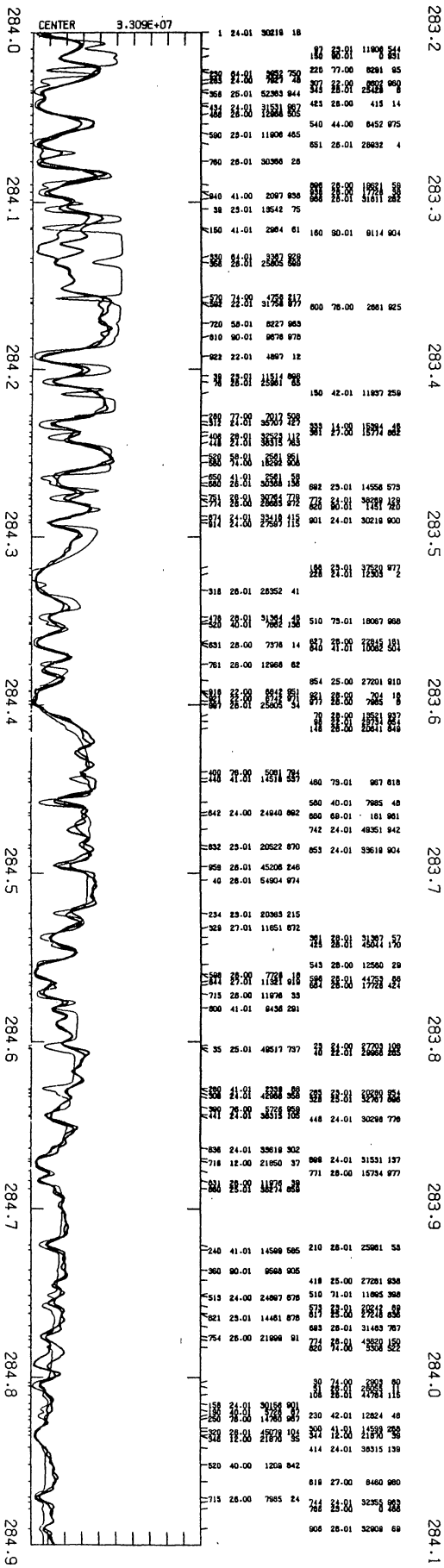

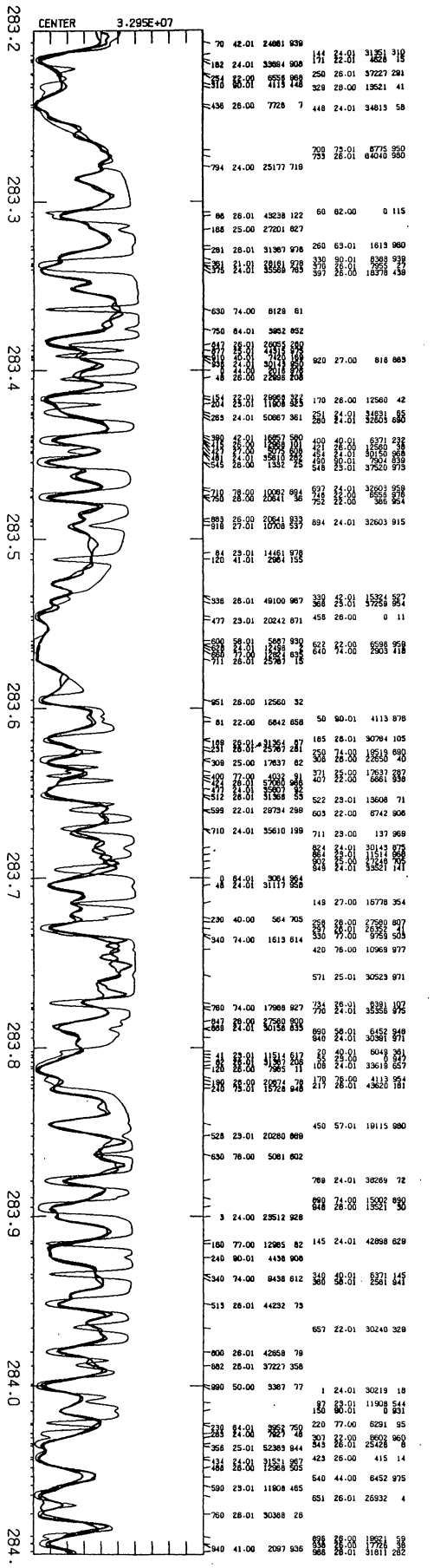

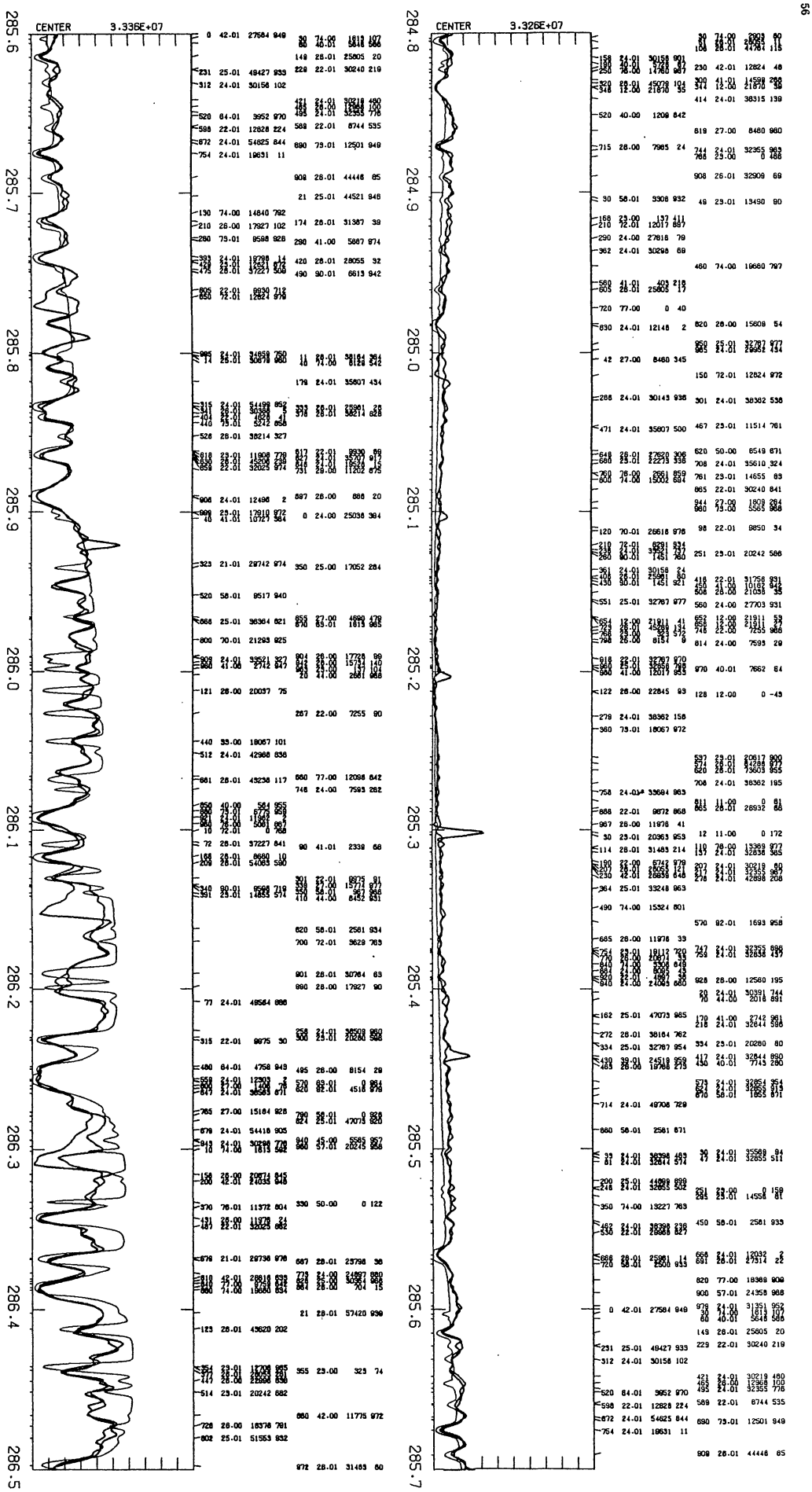

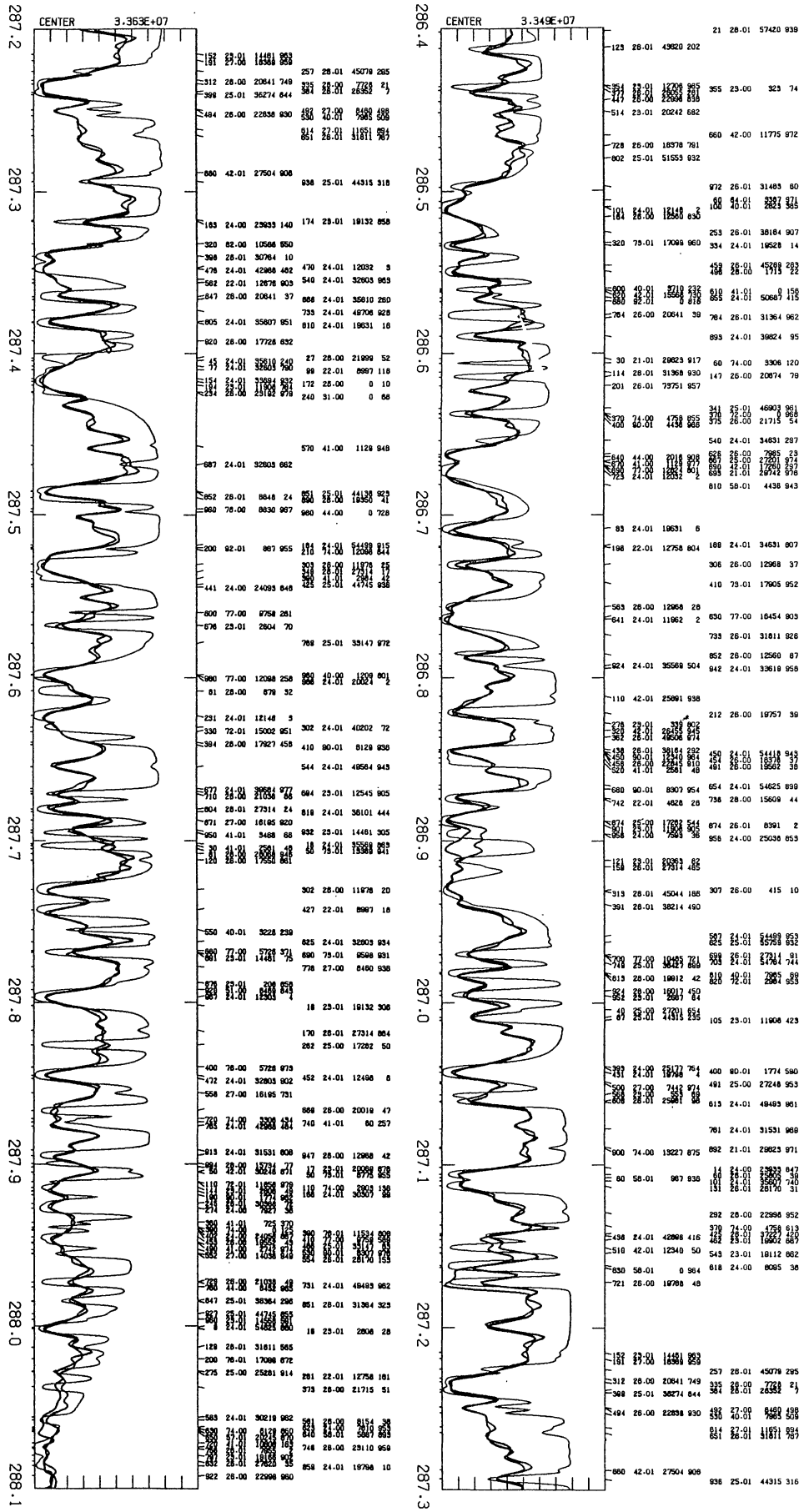

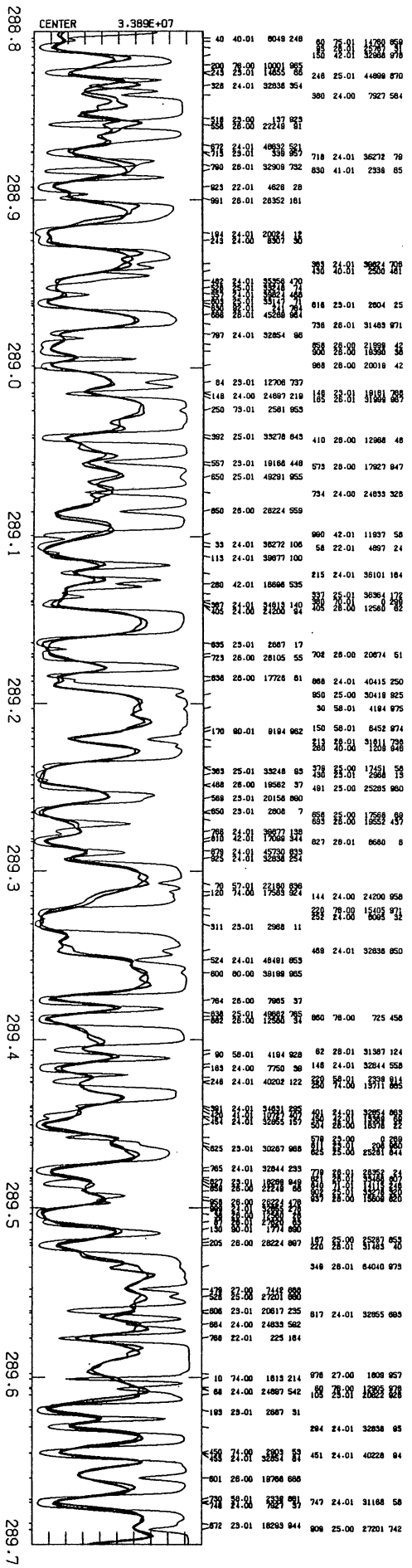

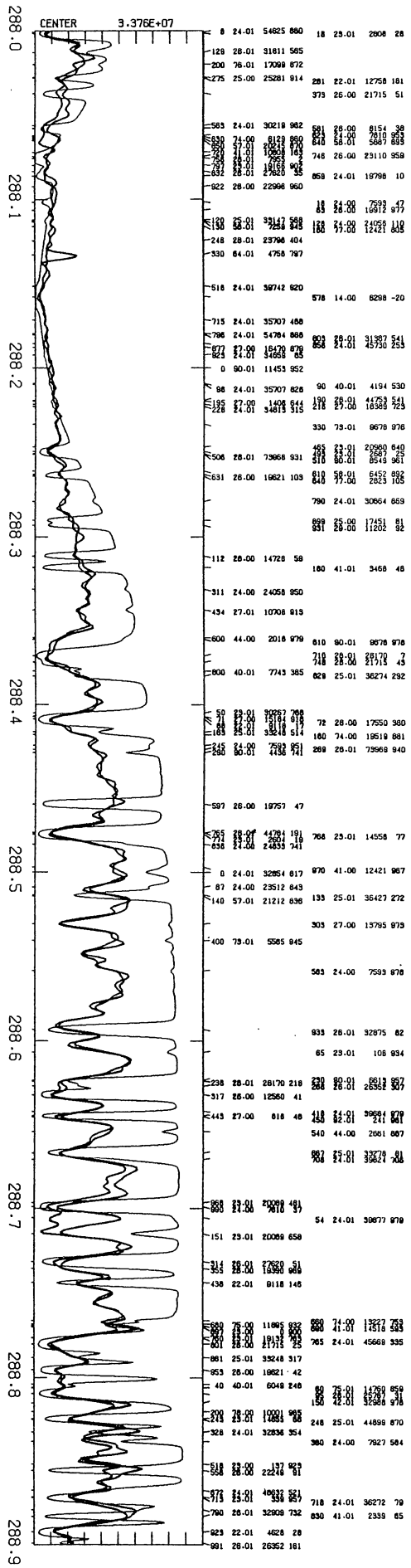

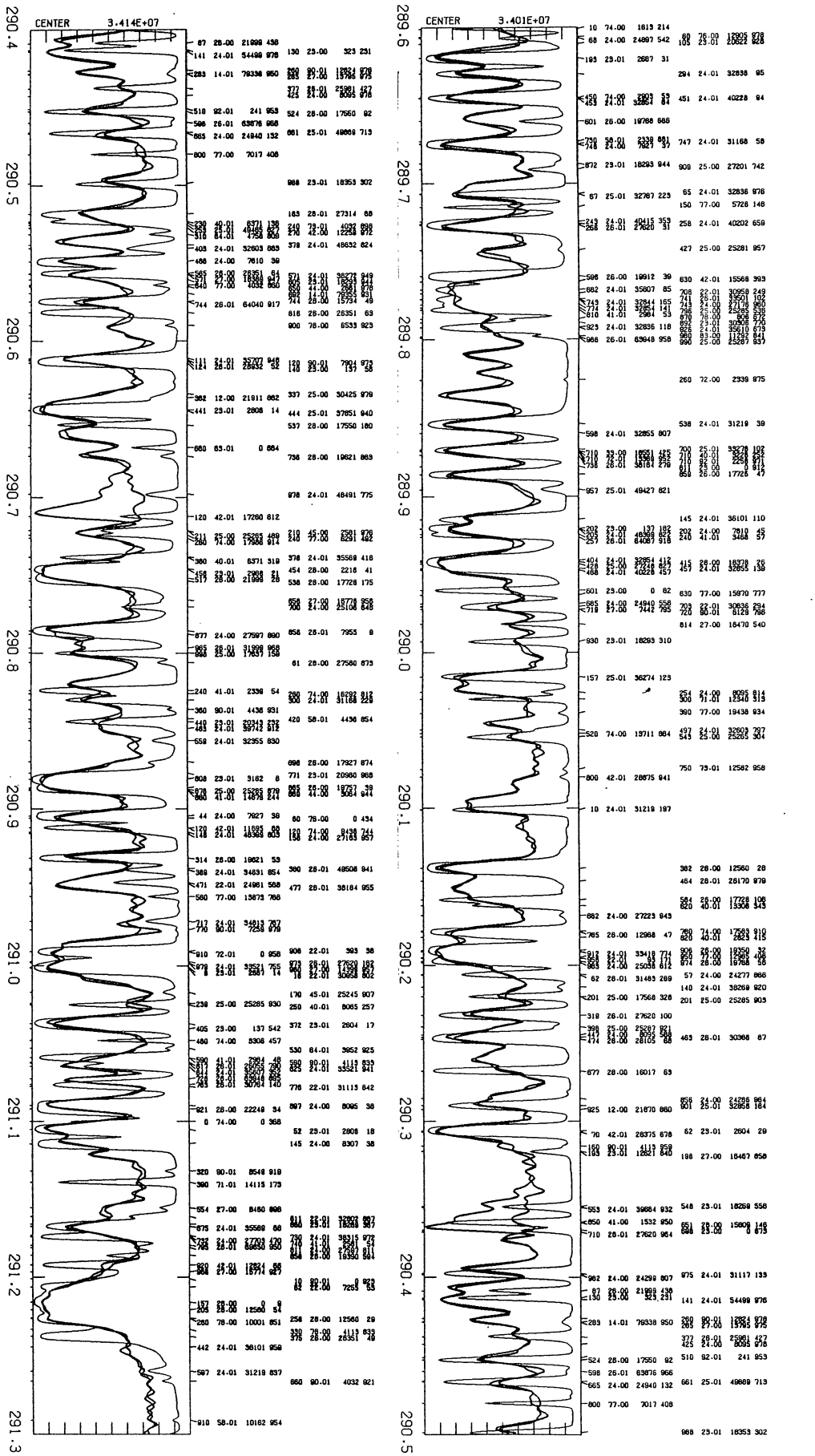

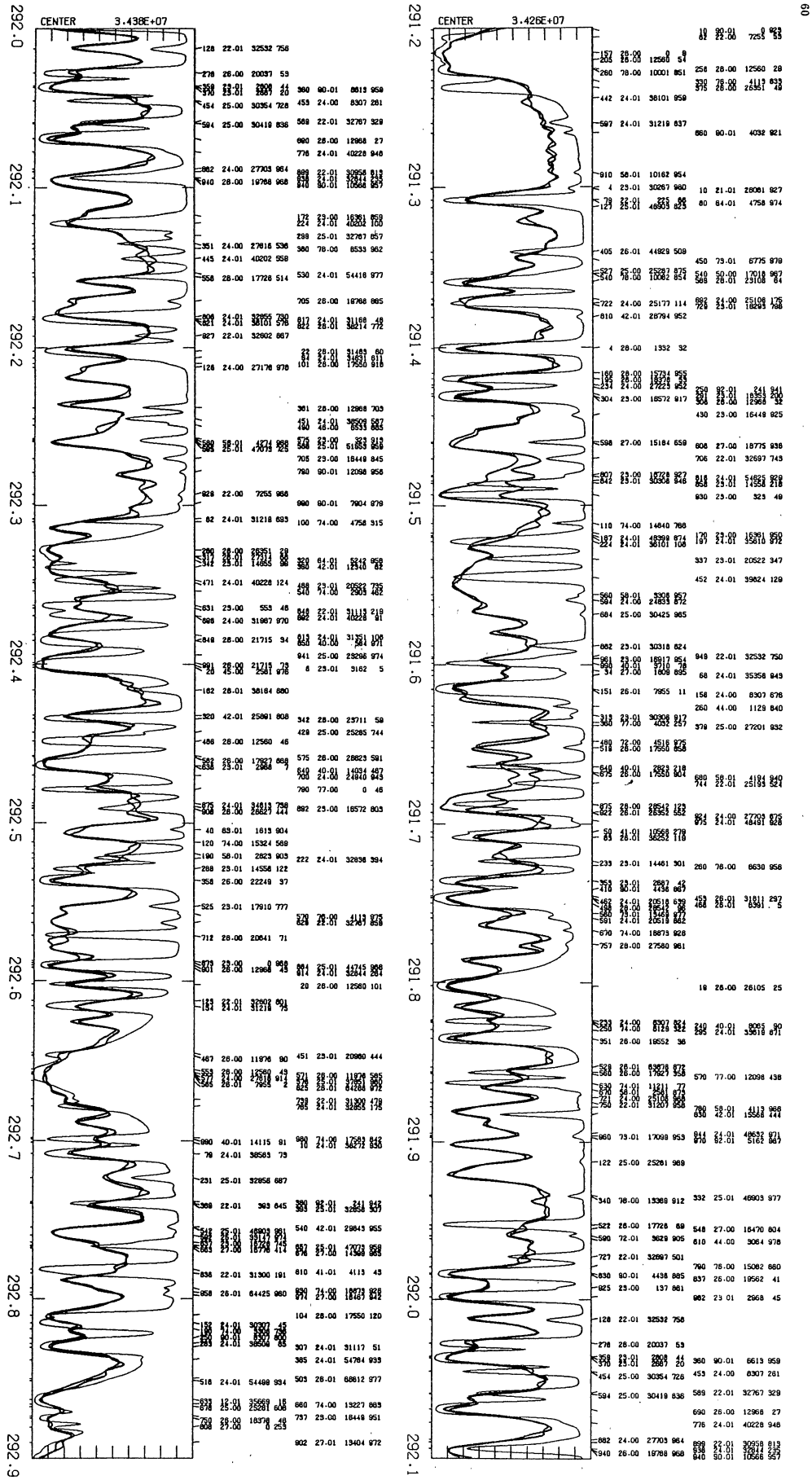

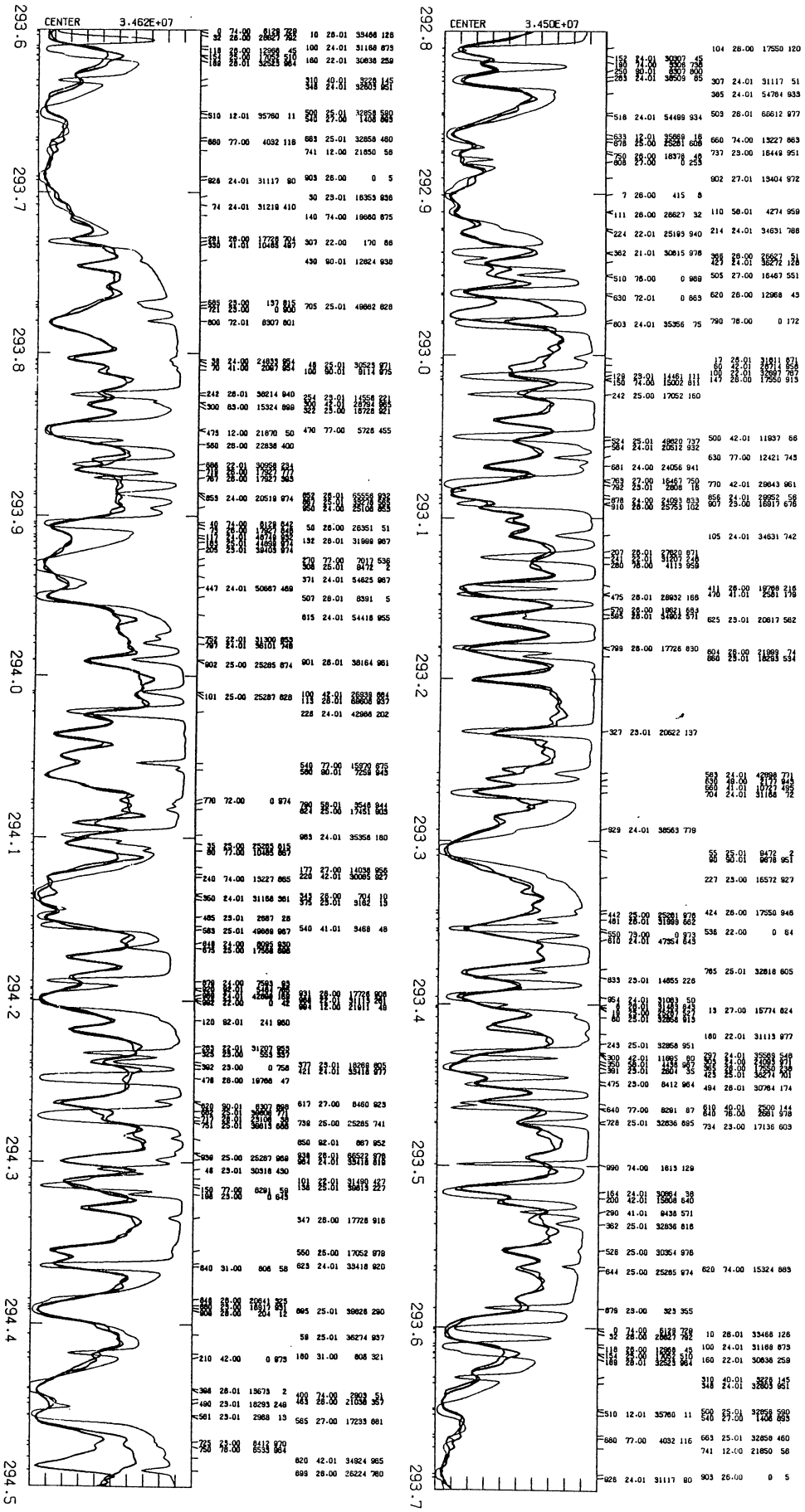

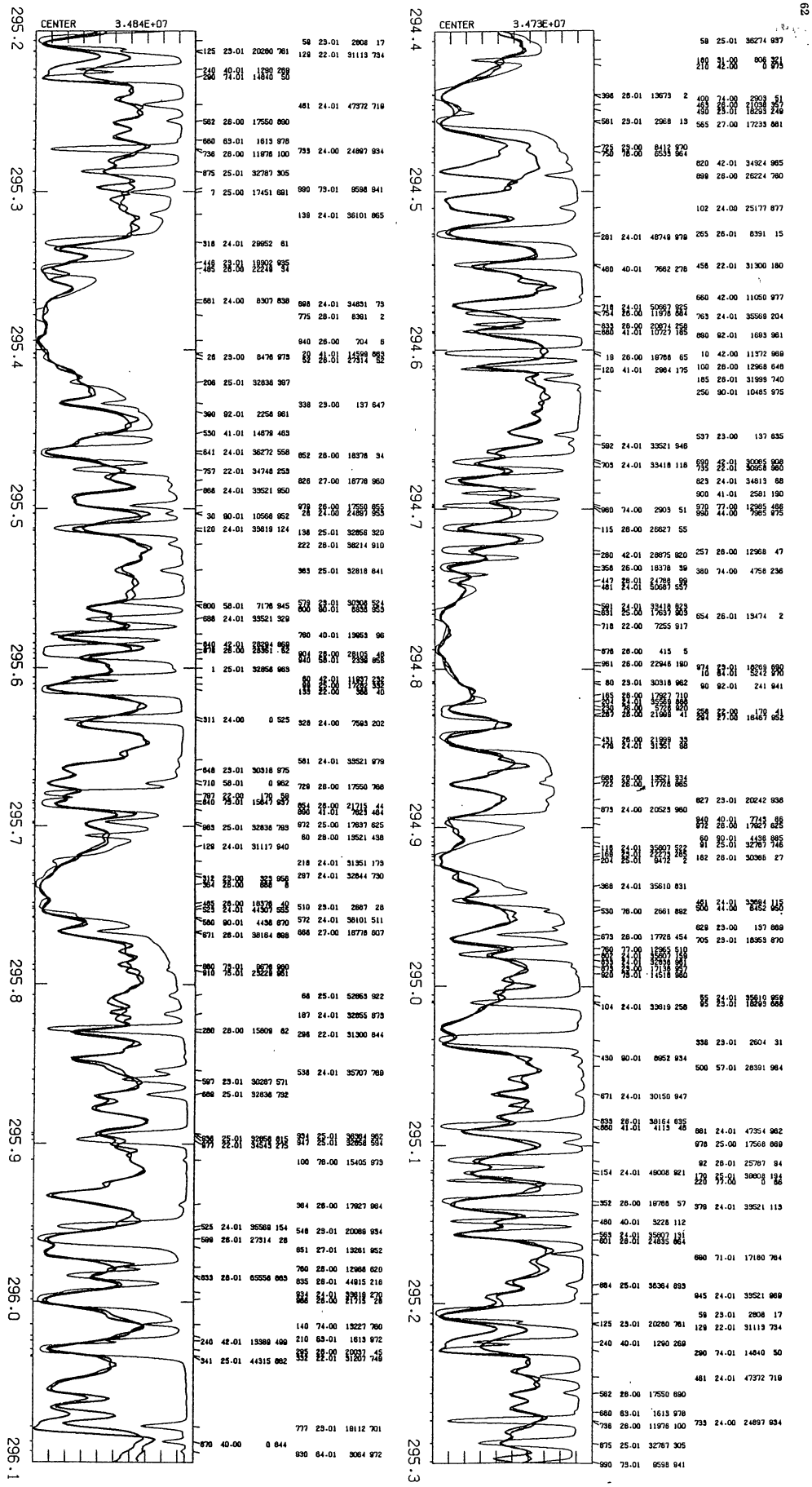

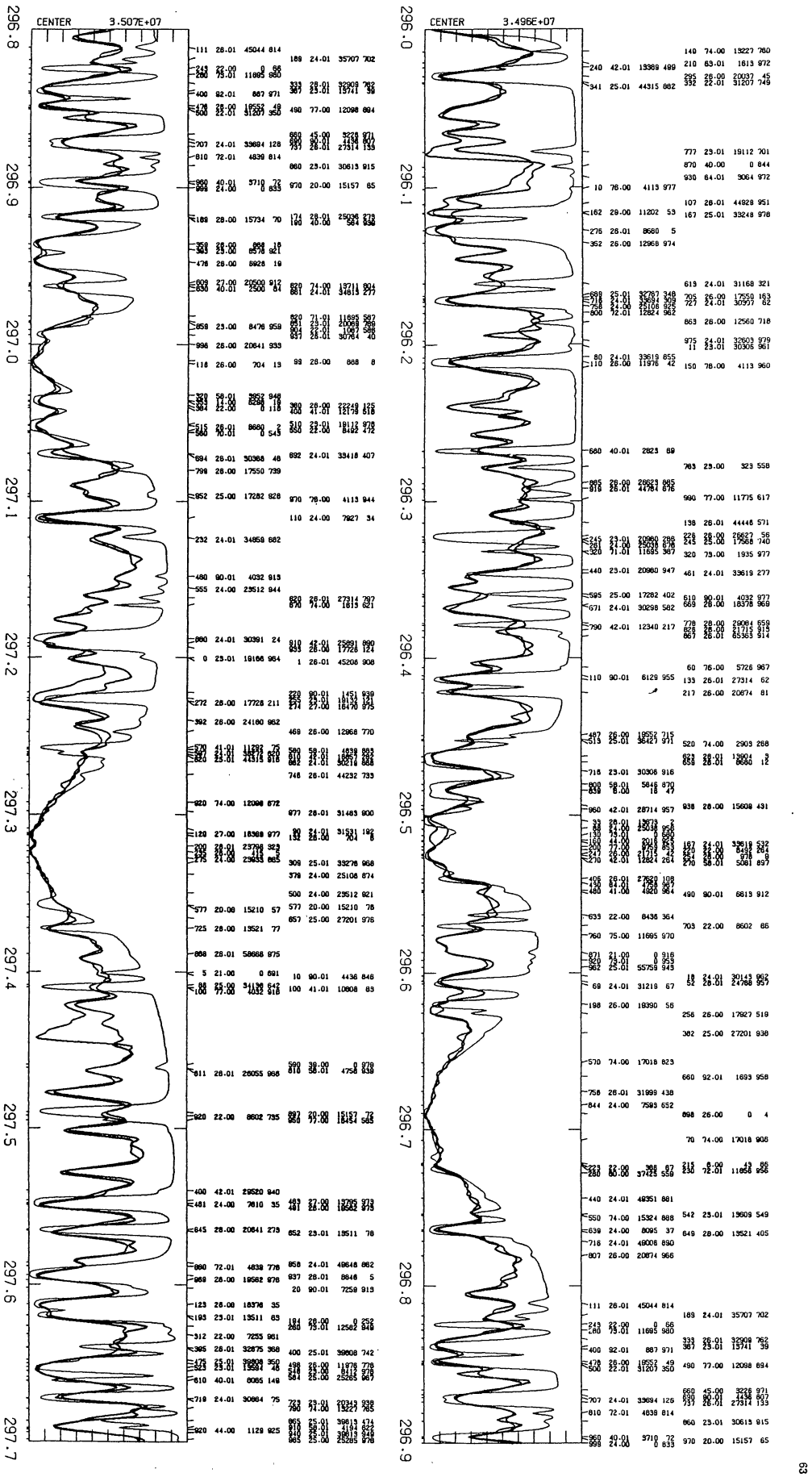

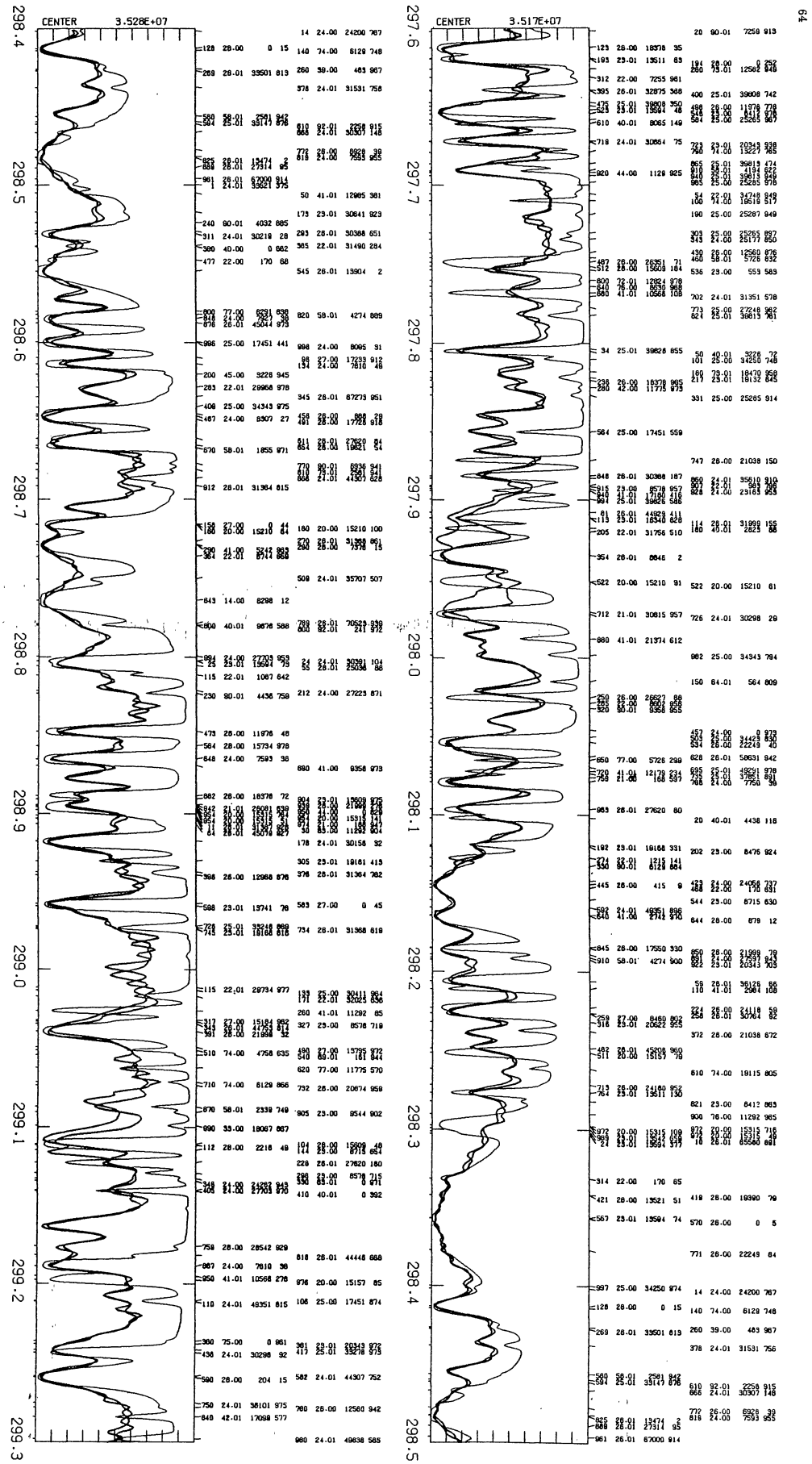

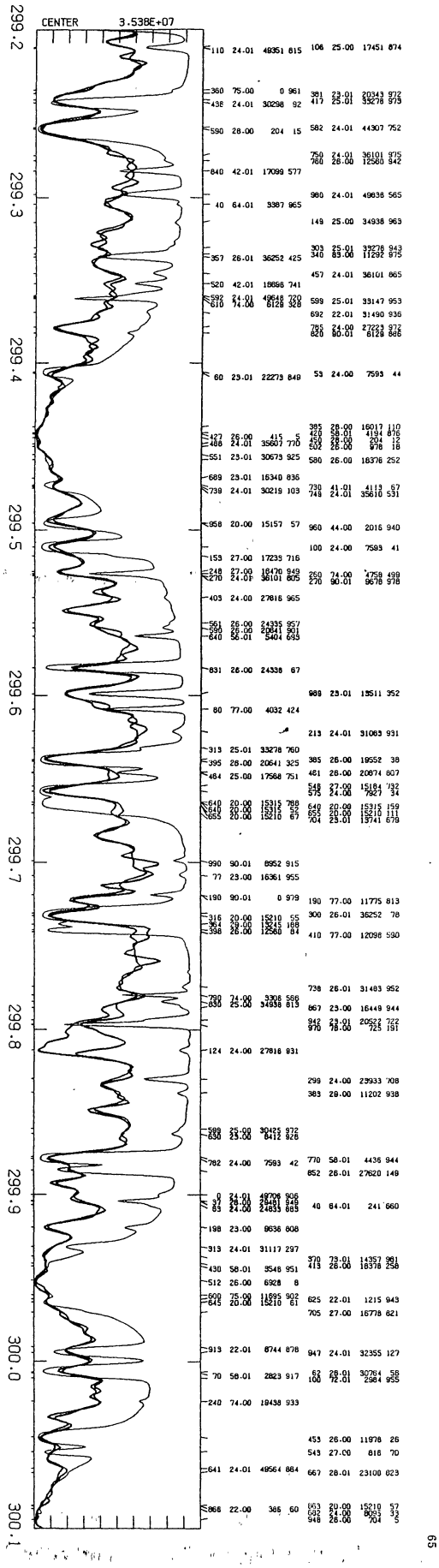

Figure 2. Harvard center and limb spectra in the wavelength range 224 to 300 nm compared with our calculated spectra. The lower half panels showing observed and calculated disk-center spectra are the same as the corresponding panels in Figure 1. As in Figure 1, each page shows 1.7 nm in two 0.9-nm panels with a 0.1-nm overlap, with the spectra from the limb shown in the upper half of each panel and that from the disk center shown in the lower half. The heavy lines are disk center and limb ($\mu = 0.23$) scans from Kohl, Parkinson, and Kurucz (1978). The thin lines are our calculated spectra. The sloping line near the top is the computed continuum level. The intensity in ergs $cm^{-2}\,s^{-1}\,sr^{-1}\,nm^{-1}$ at the top of each half panel is given on the left. The intensity varies linearly between this value at the top and zero at the bottom. All the observed data are plotted including noise spikes and dropouts. The first reliable data start at about 224.5 for the center and 225.6 for the limb.

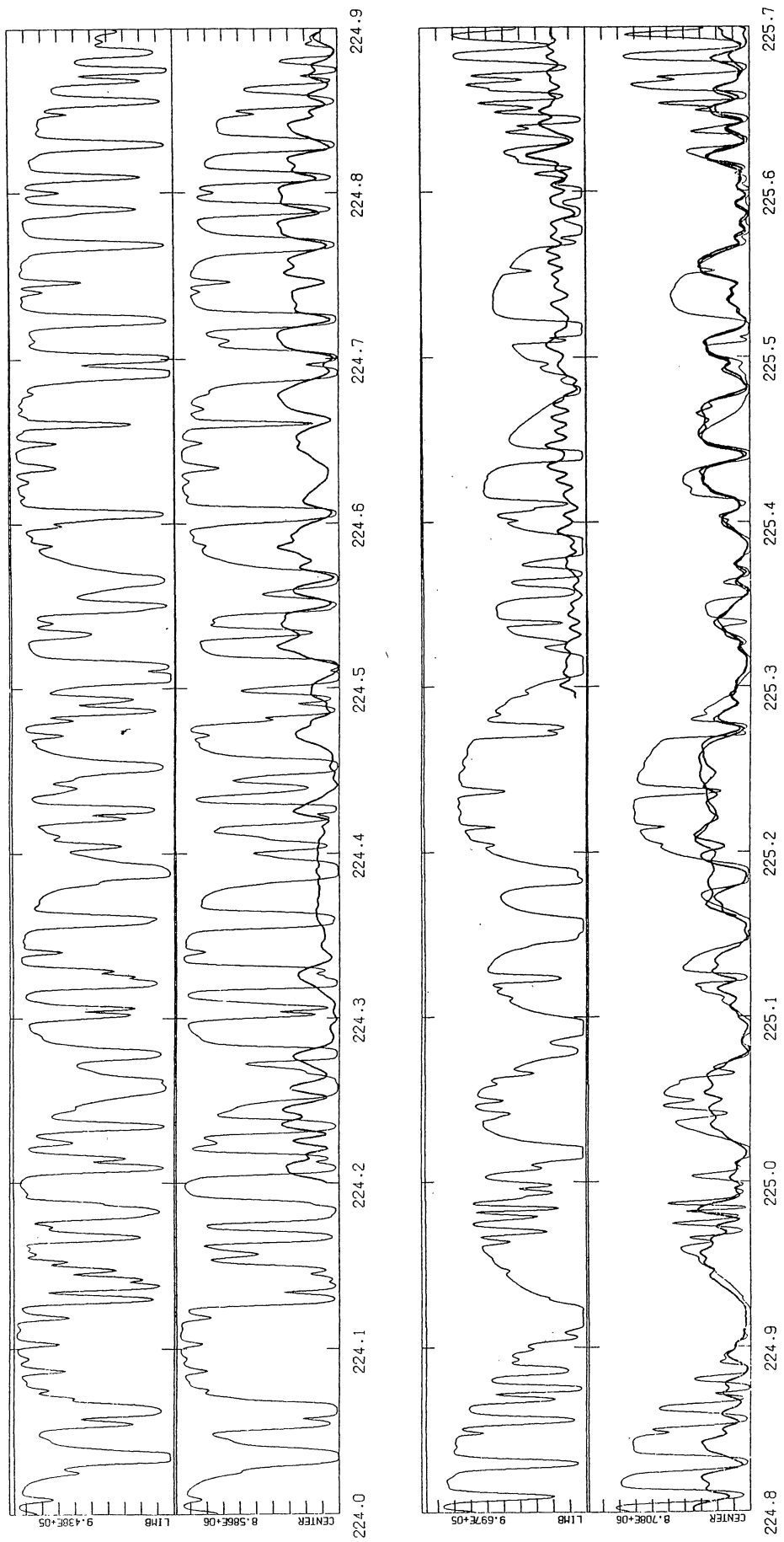

1981SAOSR.391.....K

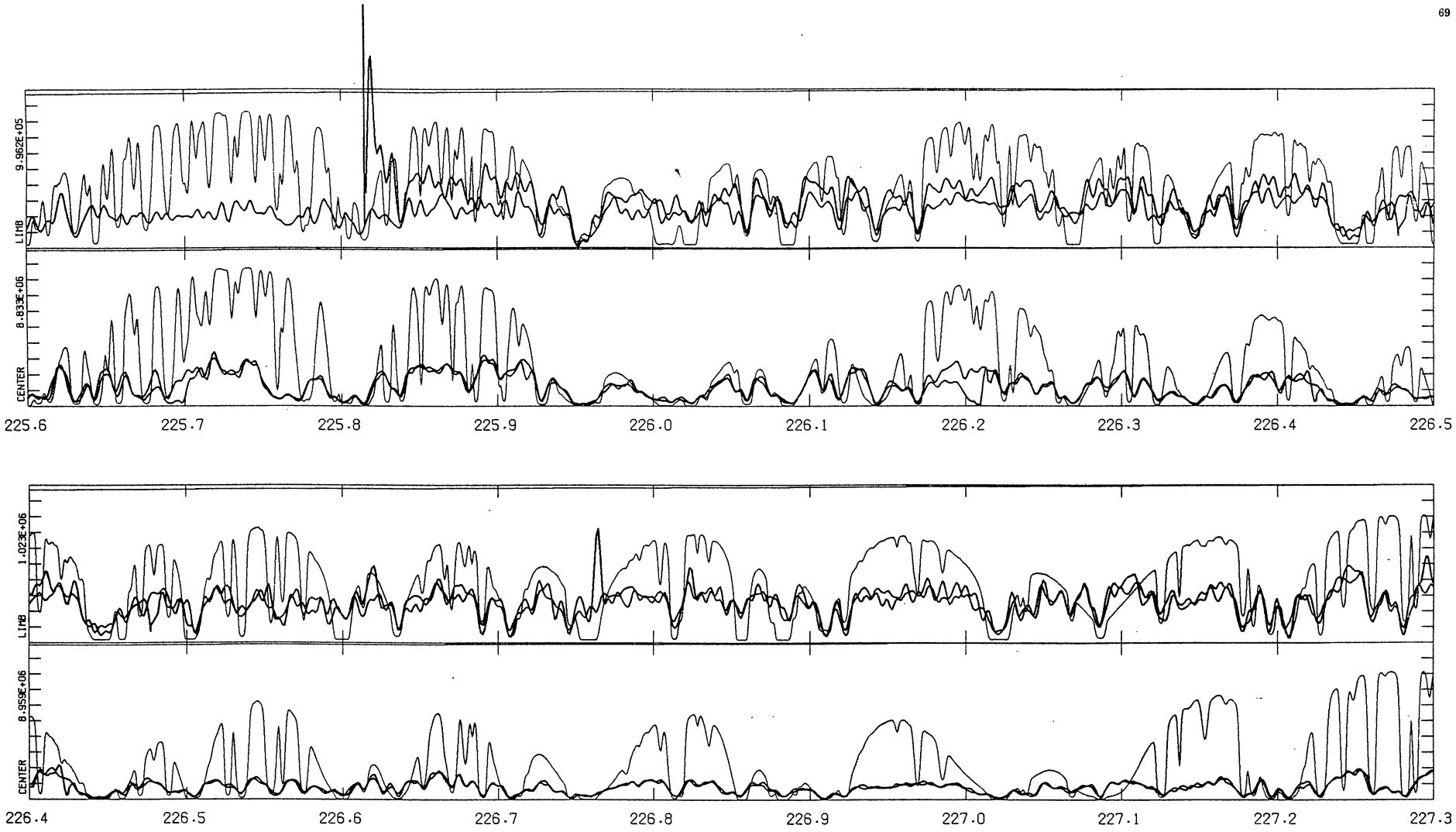

1981SAOSR.391.....K

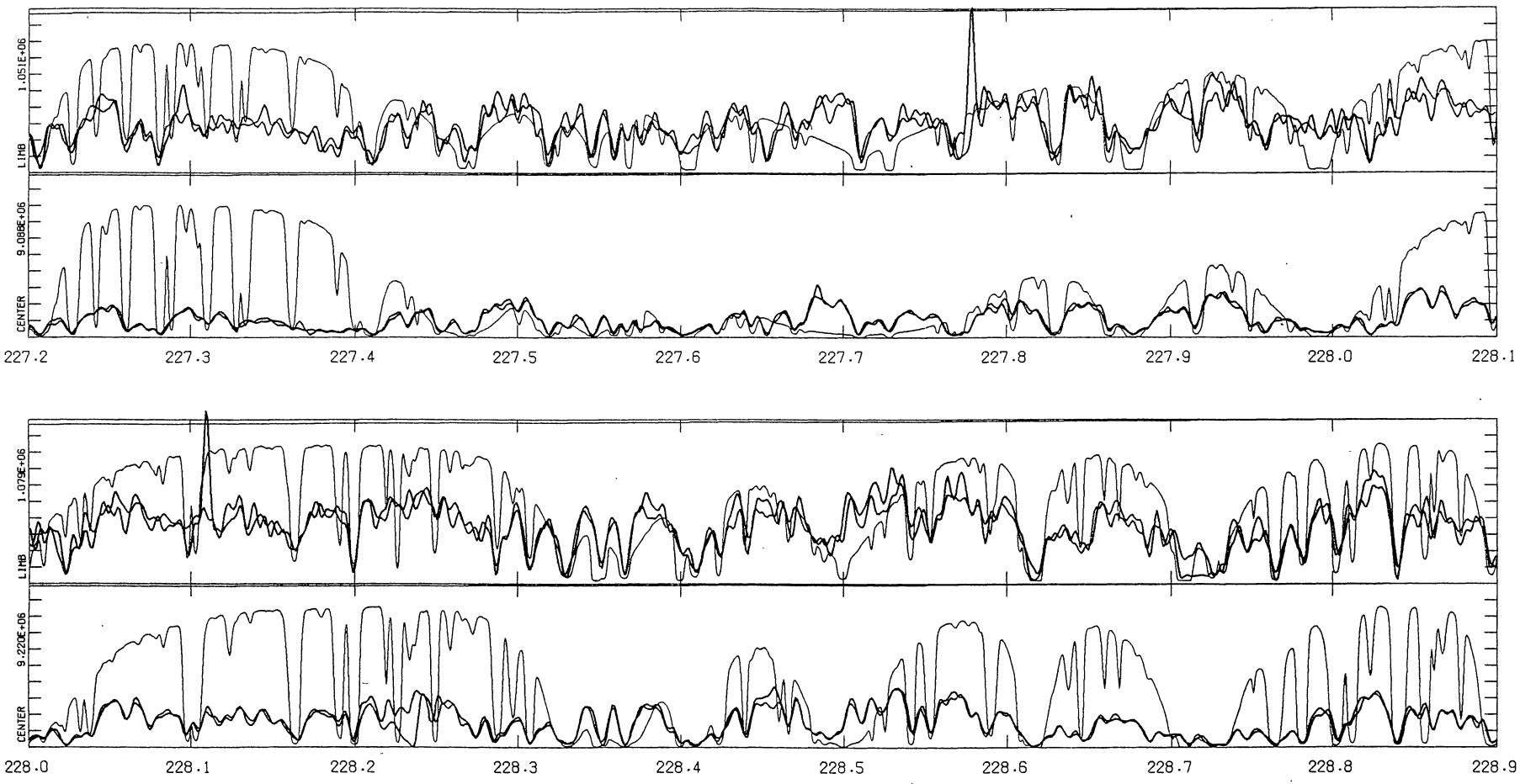

1981SAOSR.391.....K

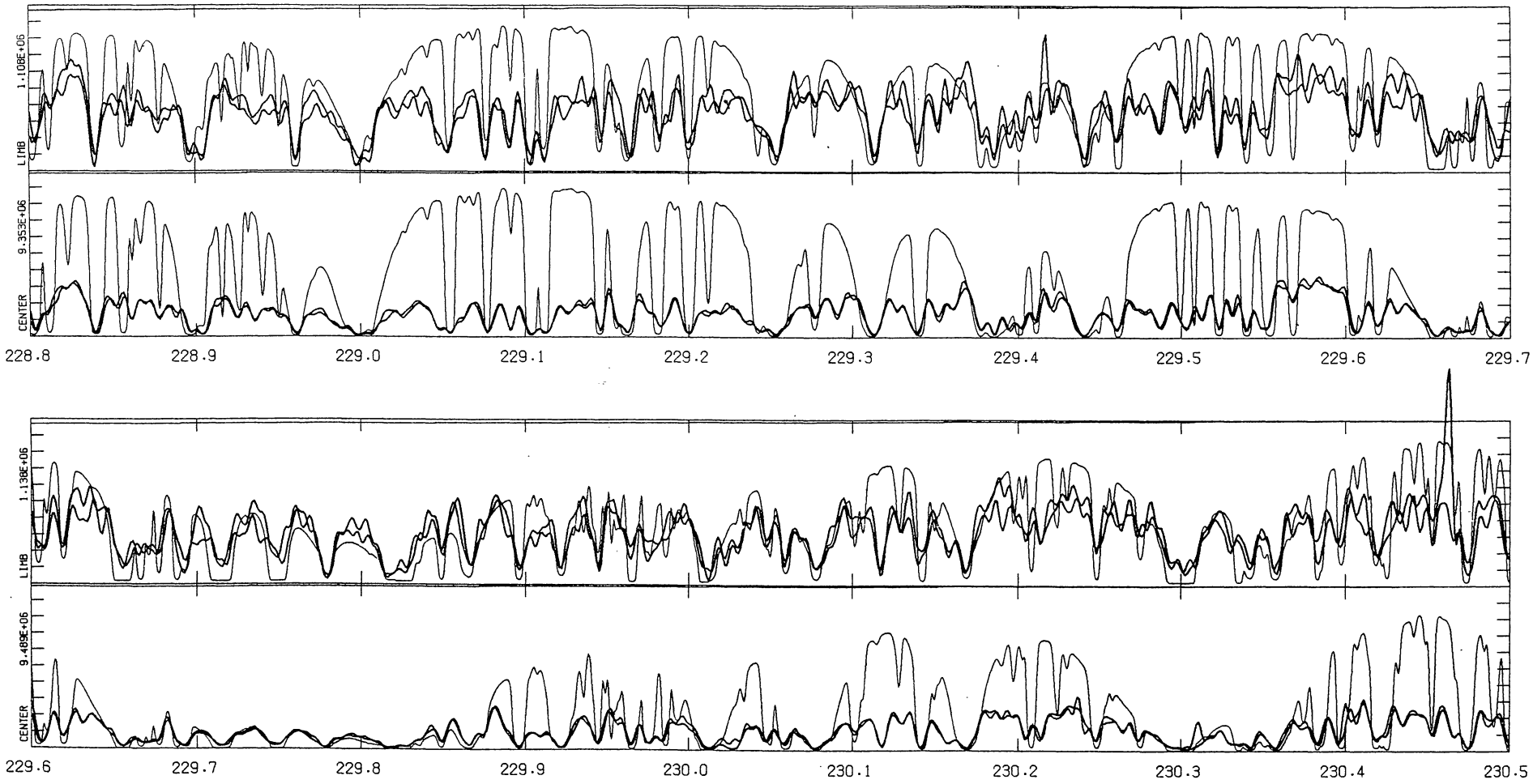

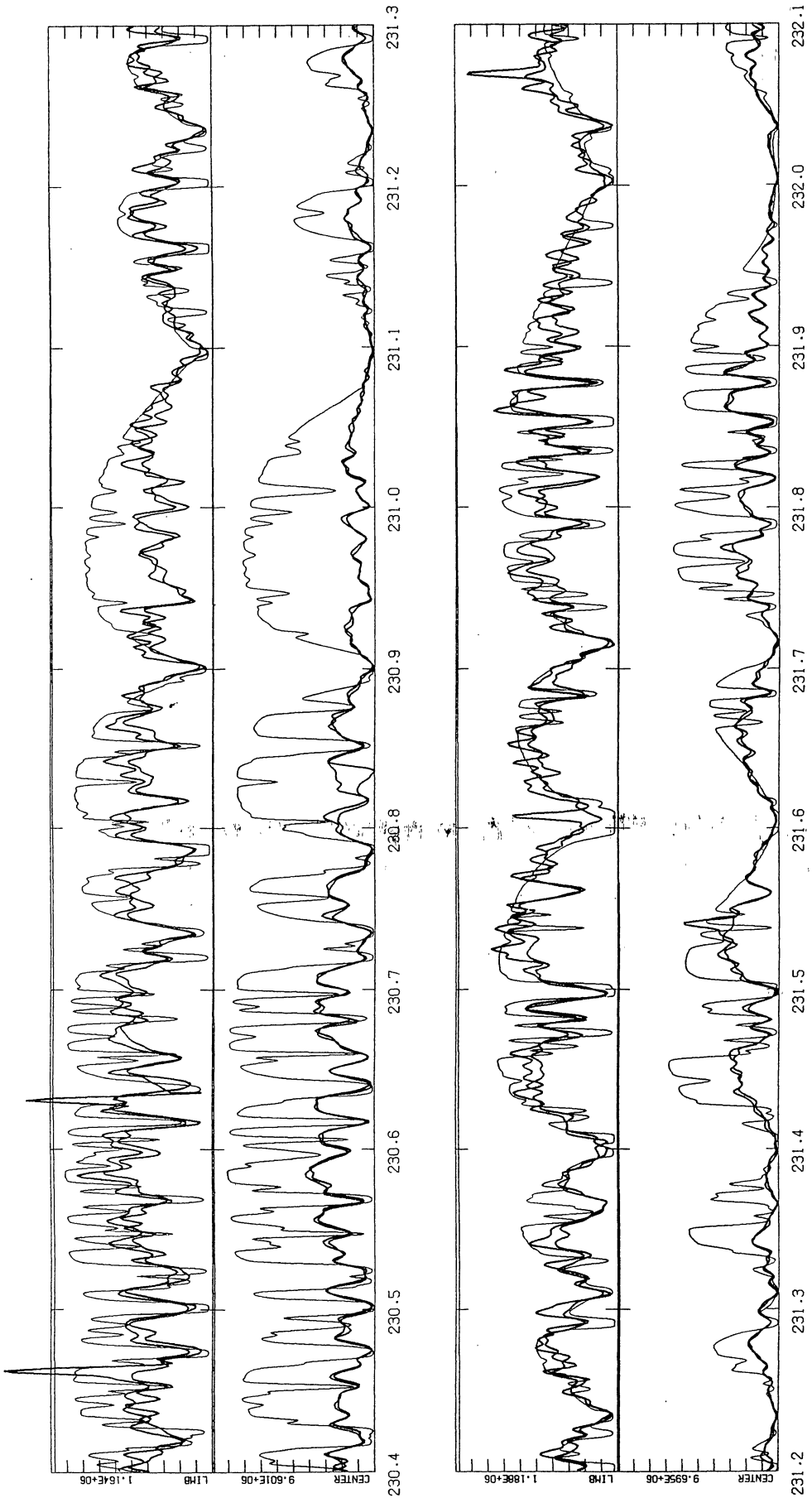

1981SAOSR.391.....K

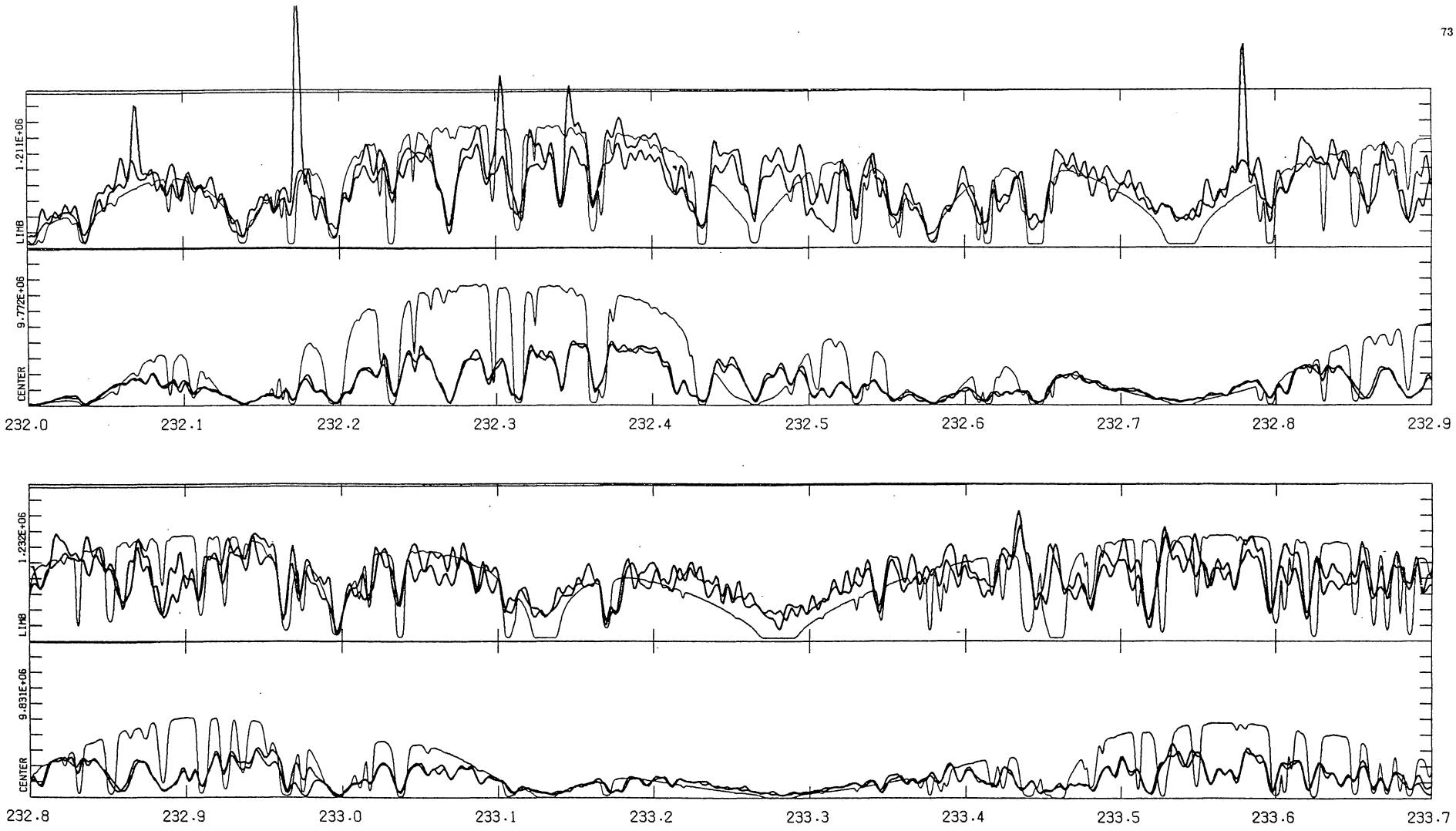

1981SAOSR.391.....K

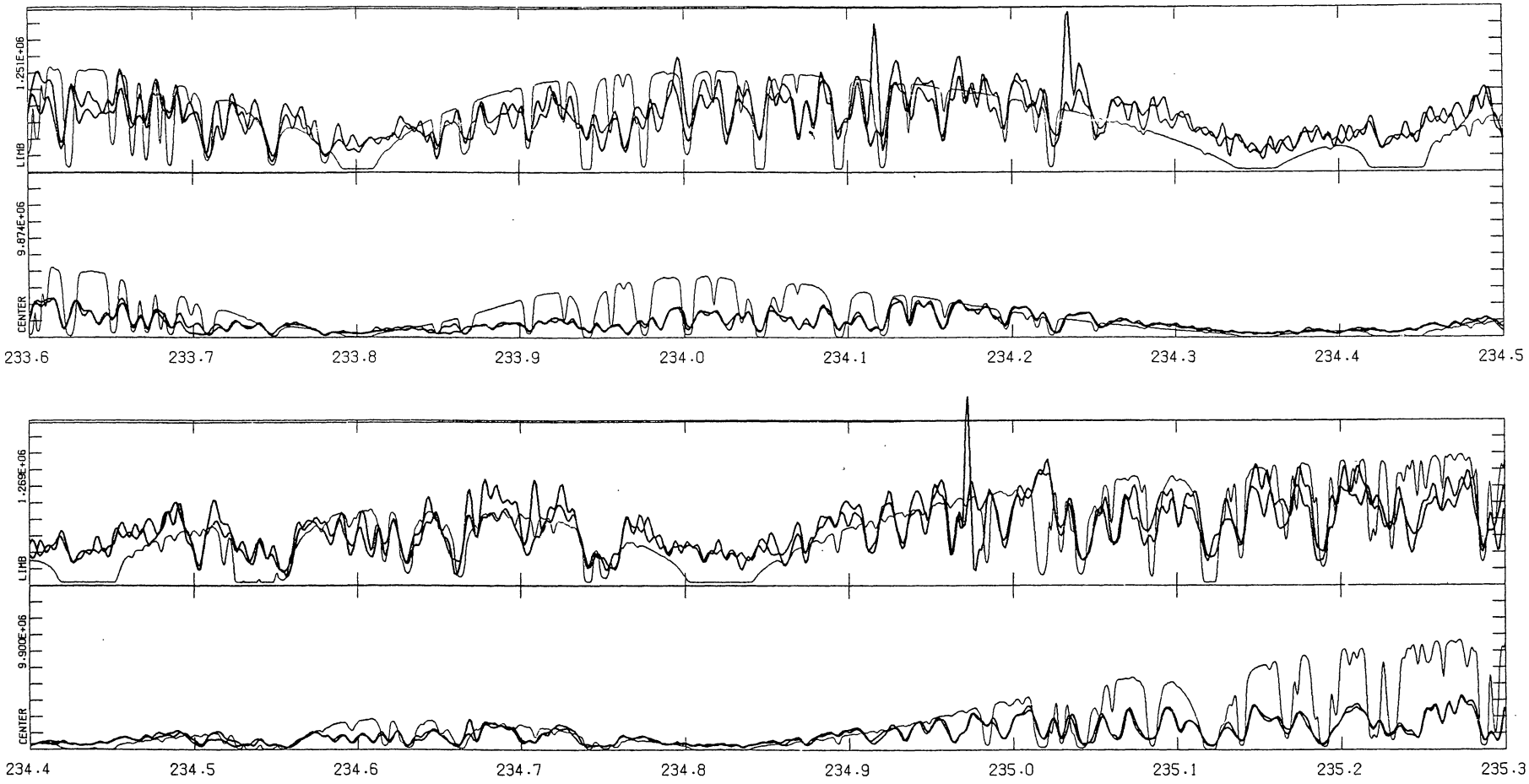

1981SAOSR.391.....K

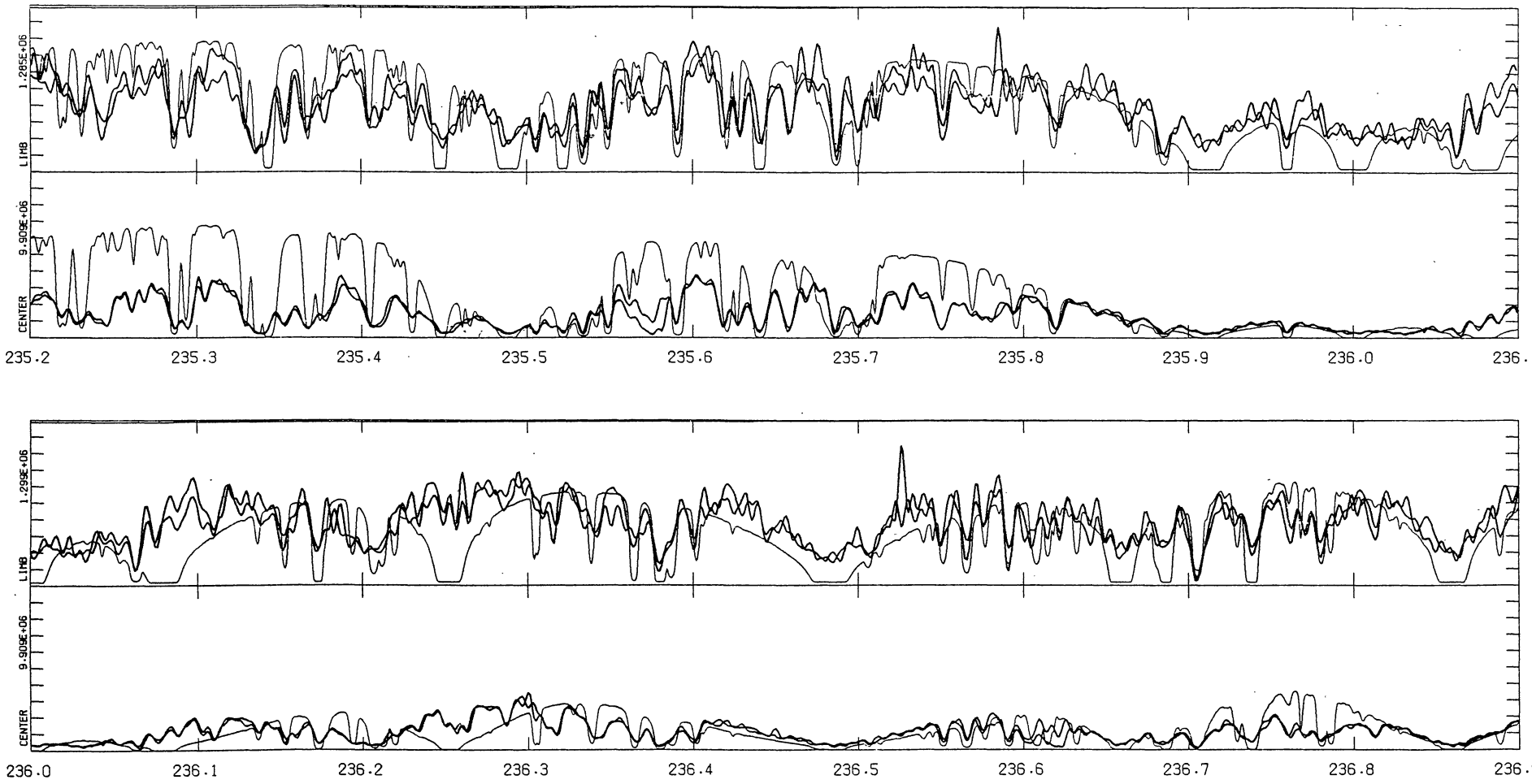

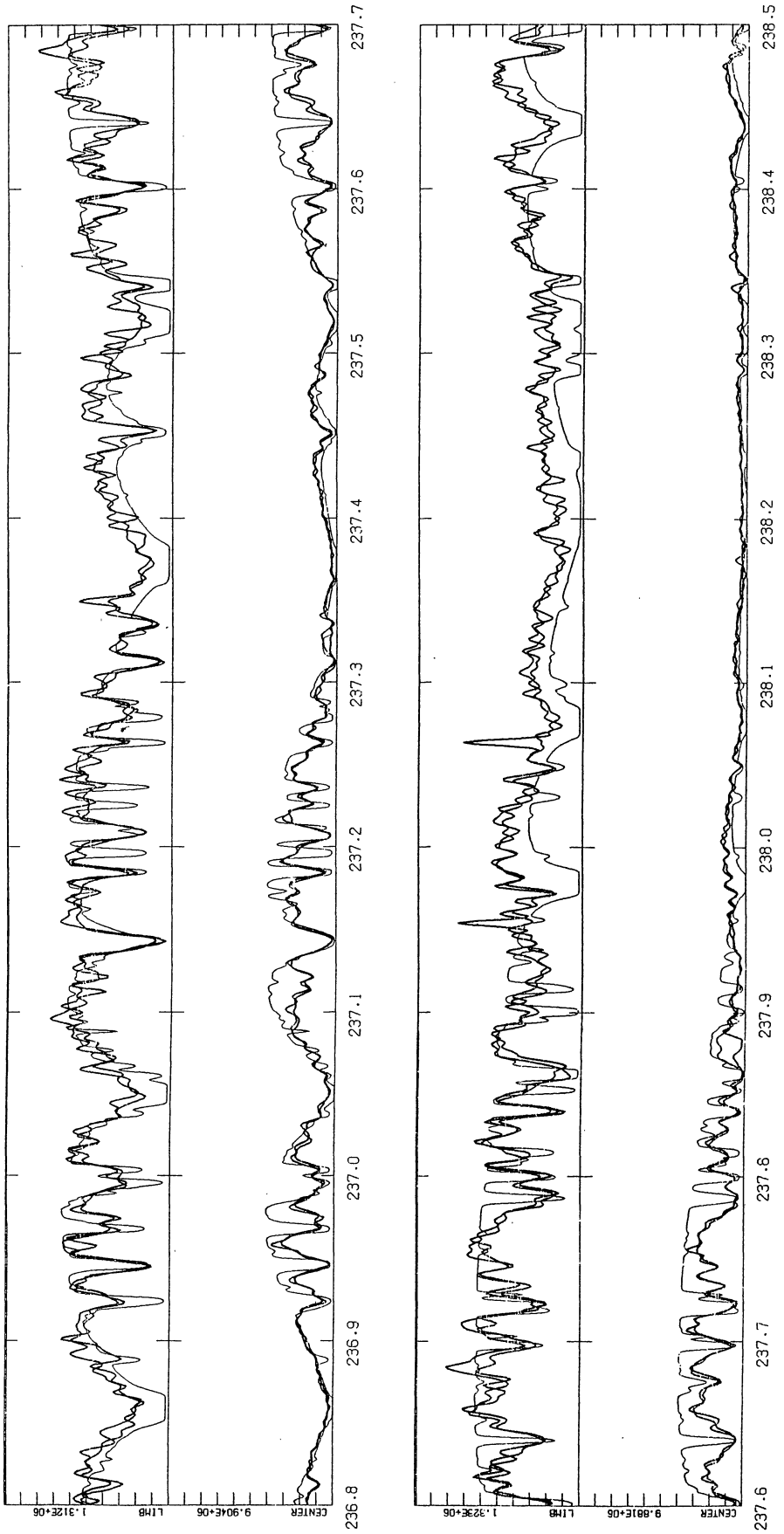

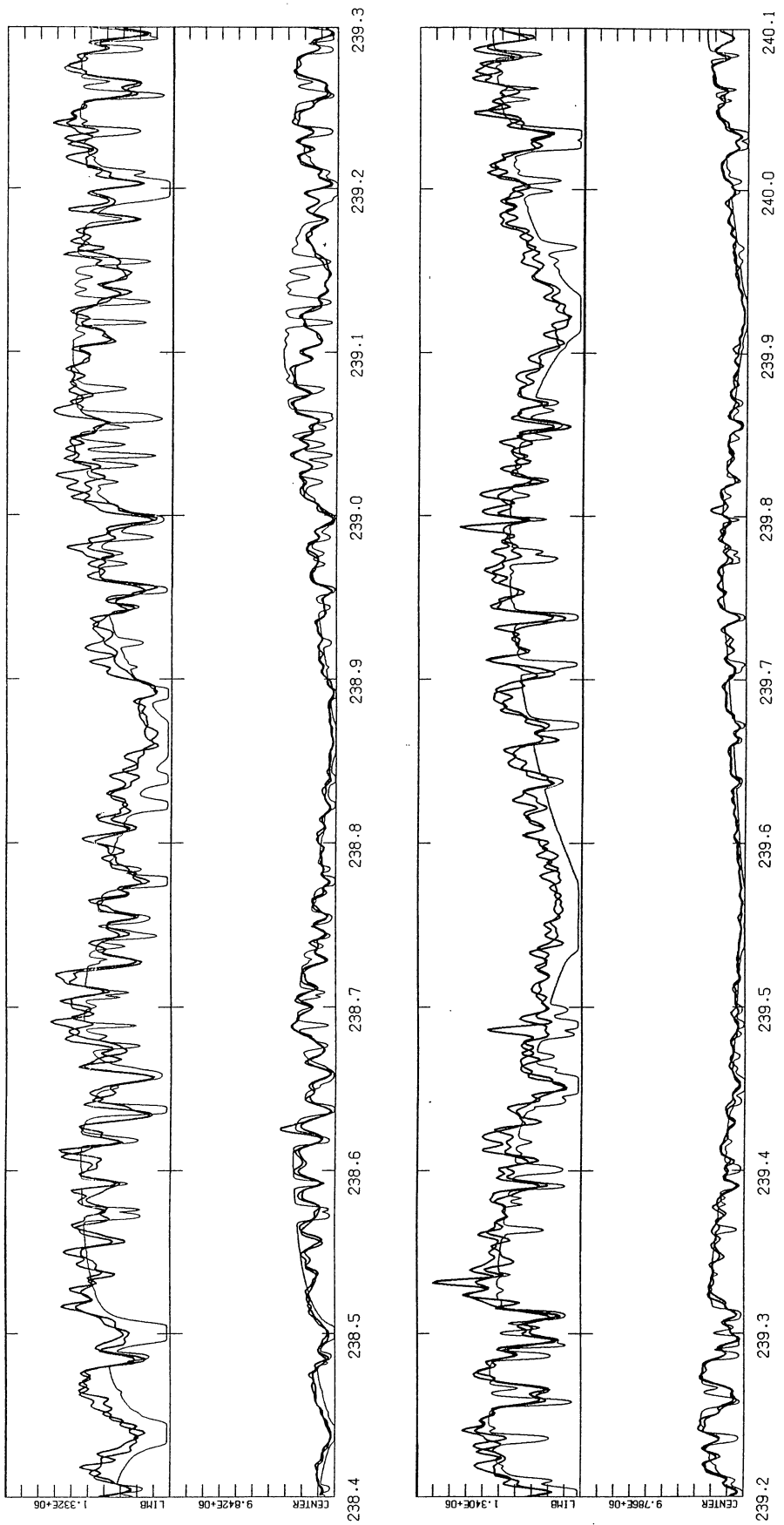

1981SAOSR.391.....K

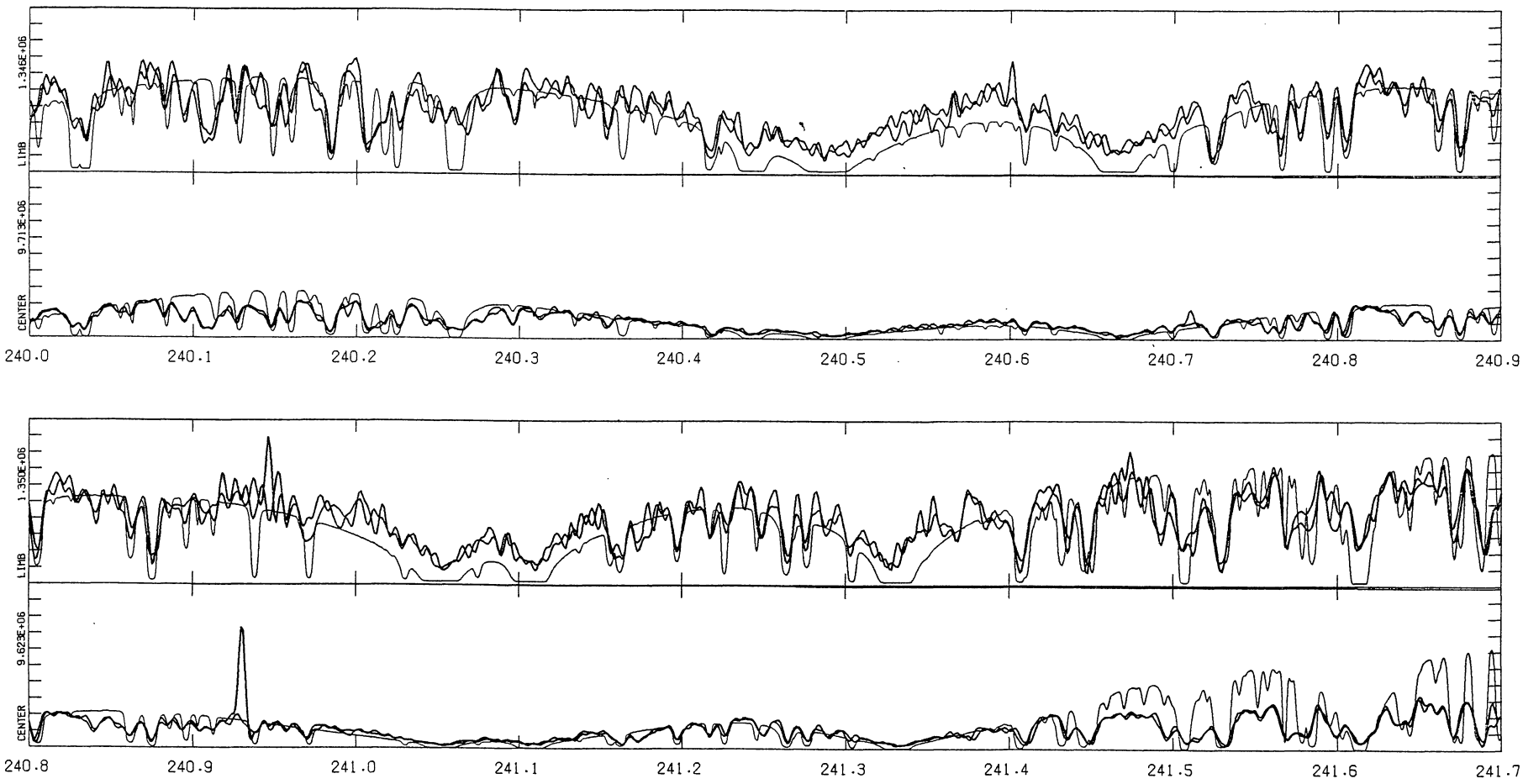

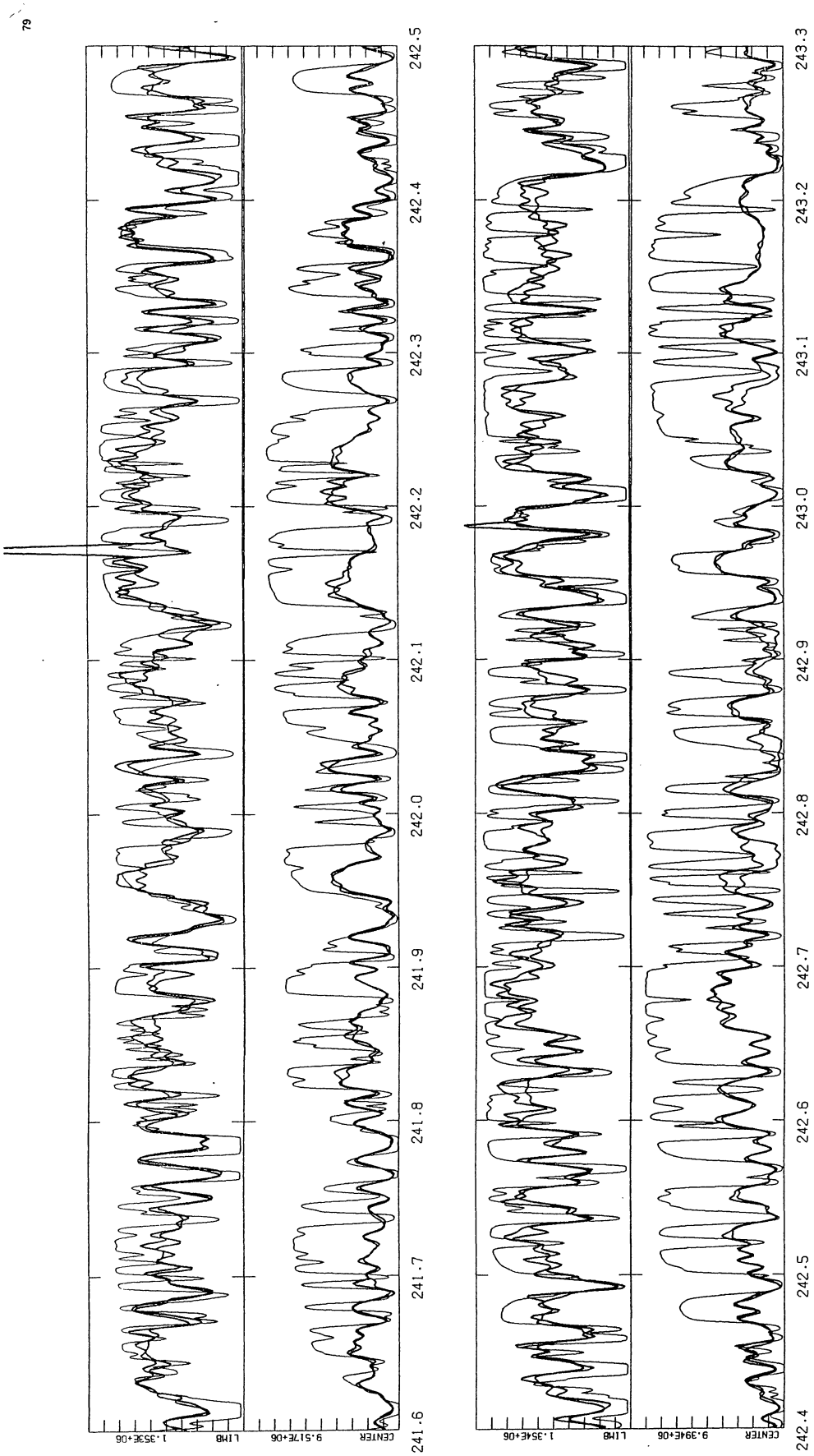

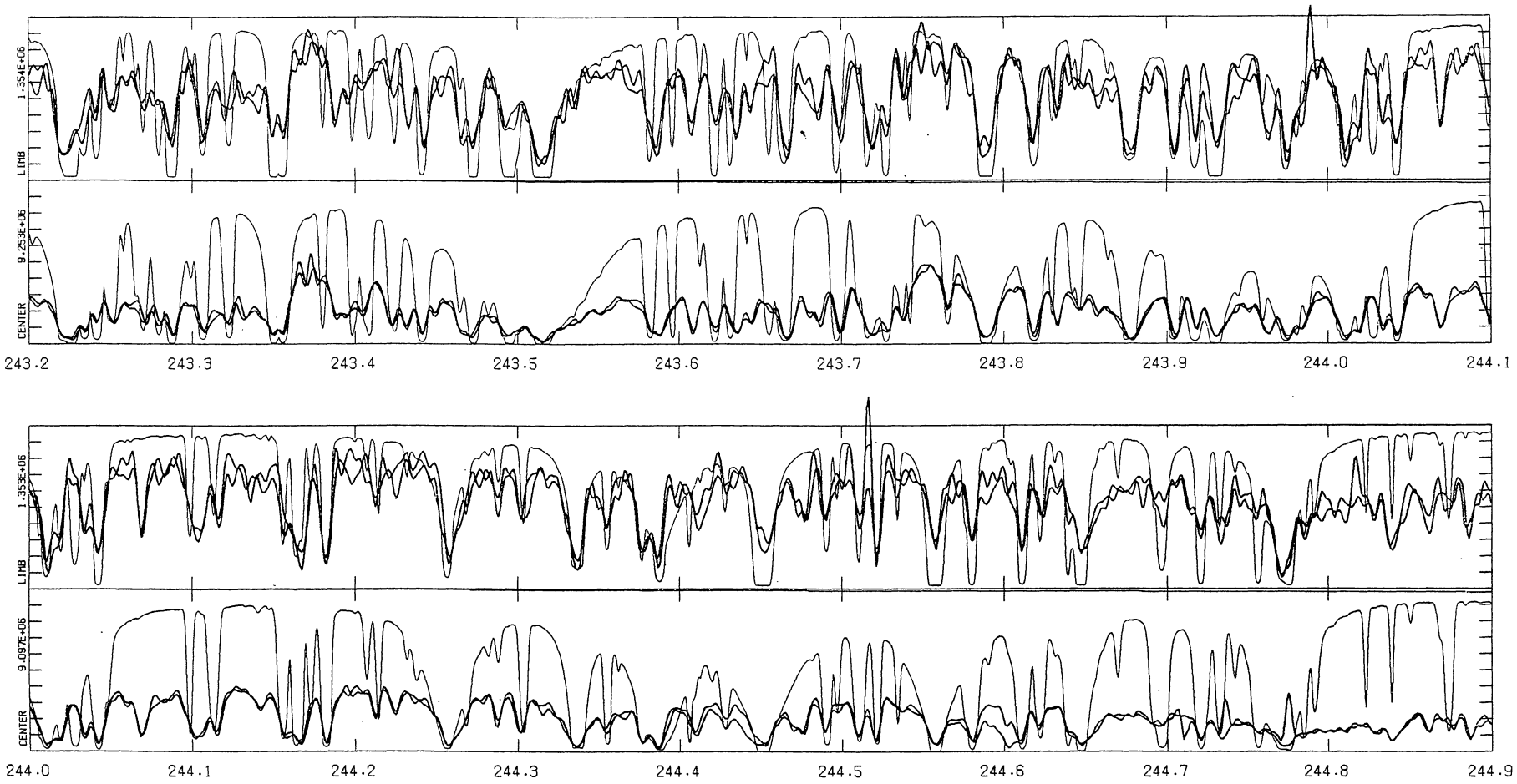

1981SAOSR.391.....K

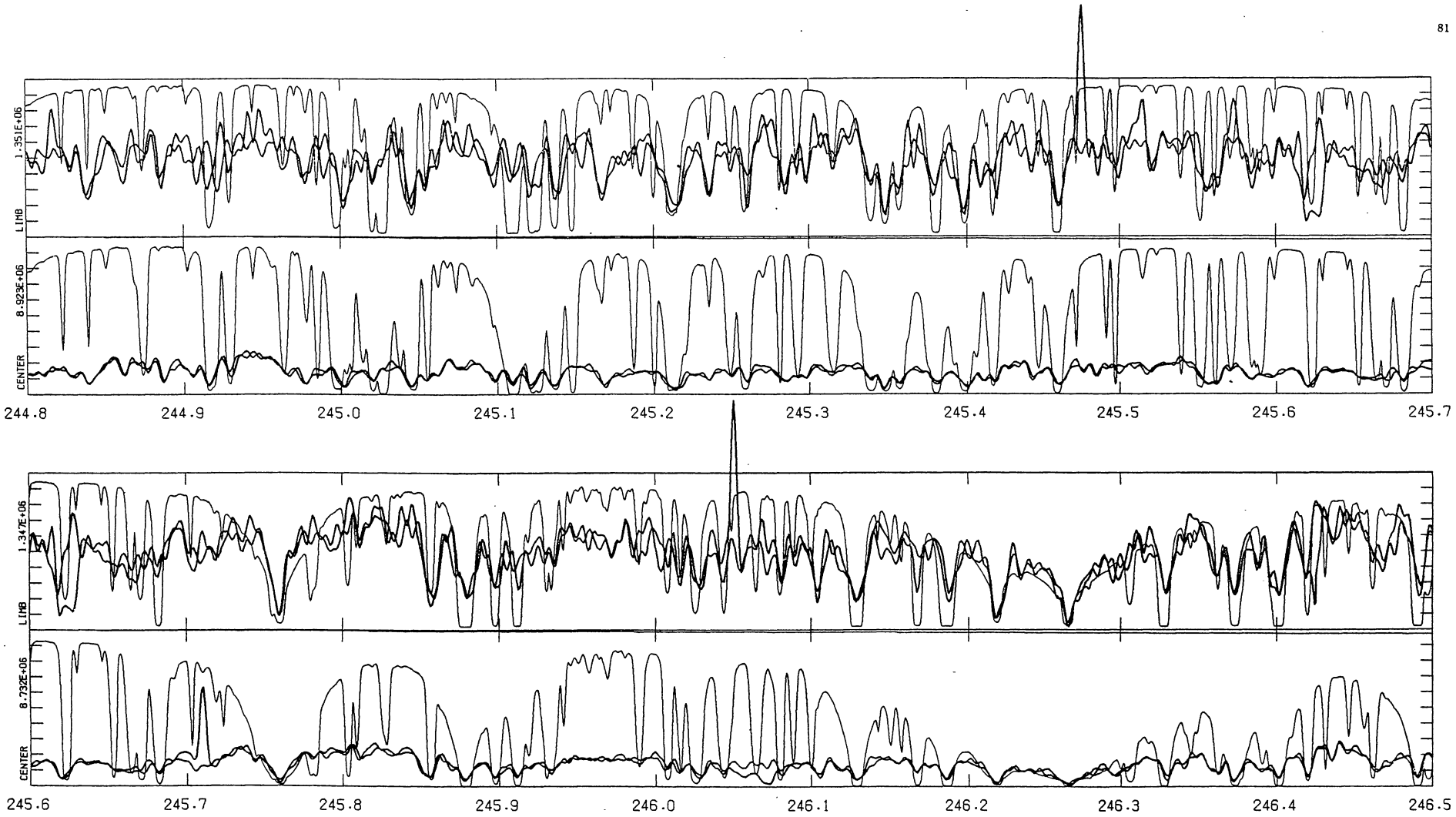

1981SAOSR.391.....K

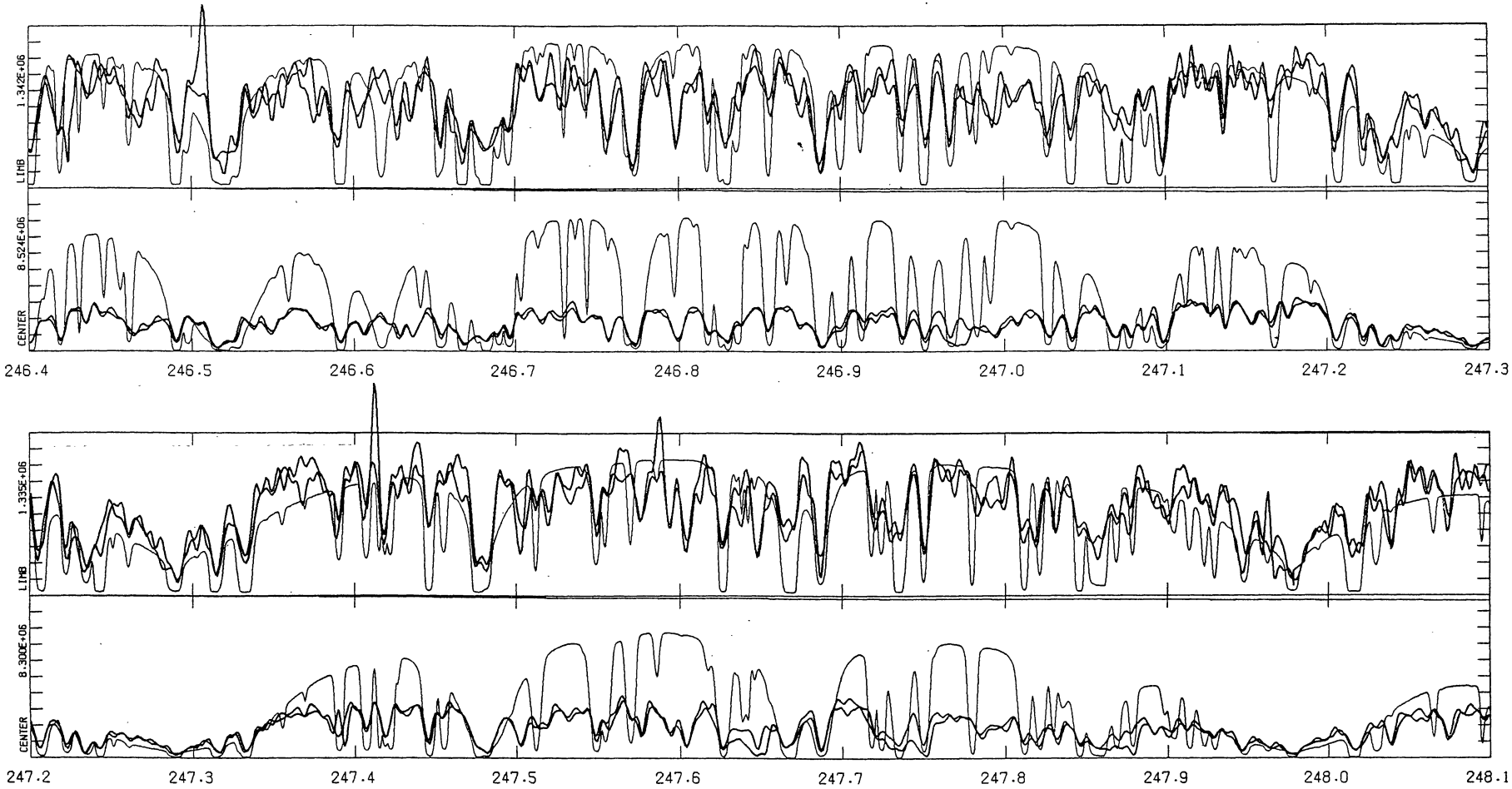

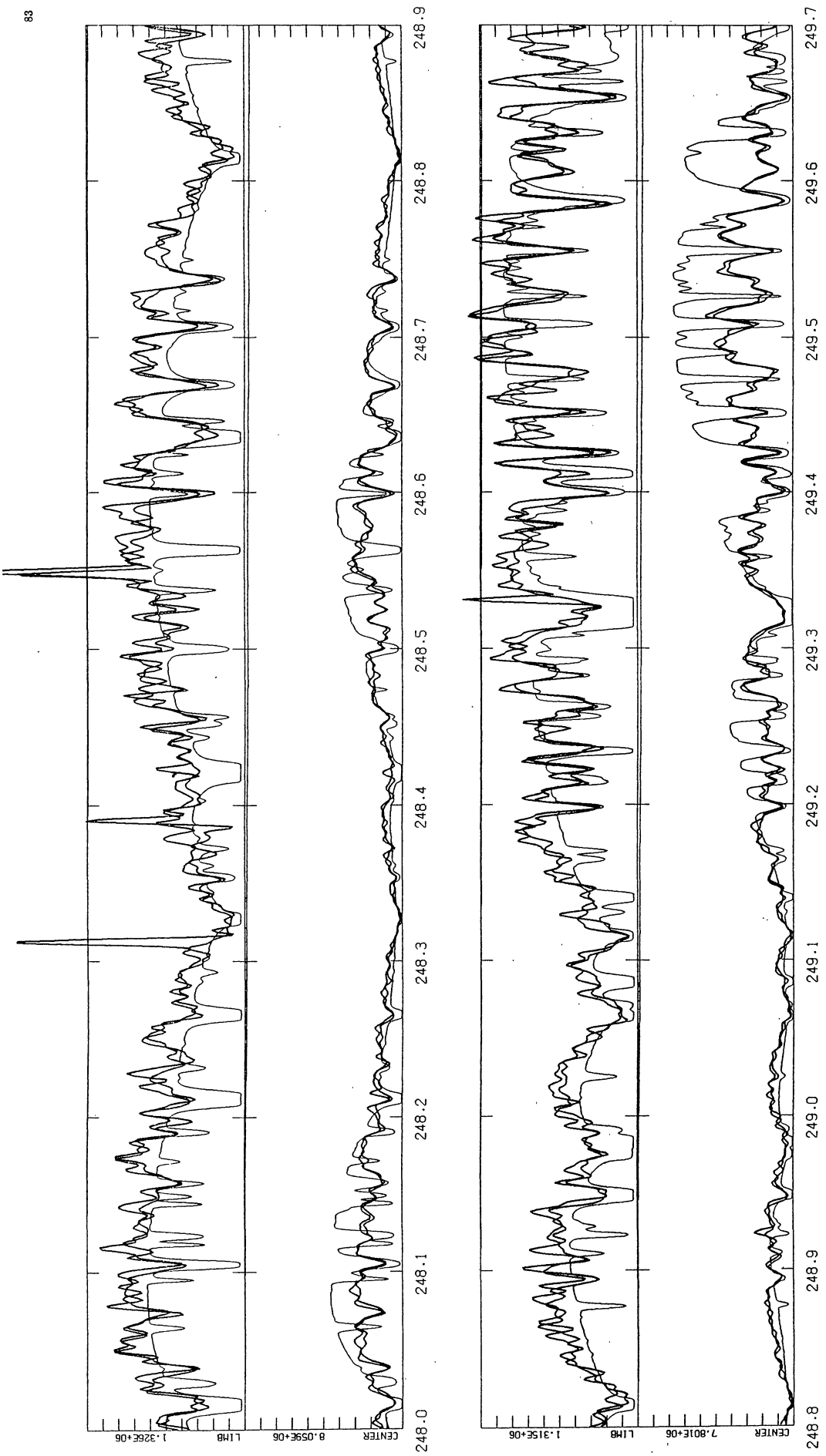

1981SAOSR.391.....K

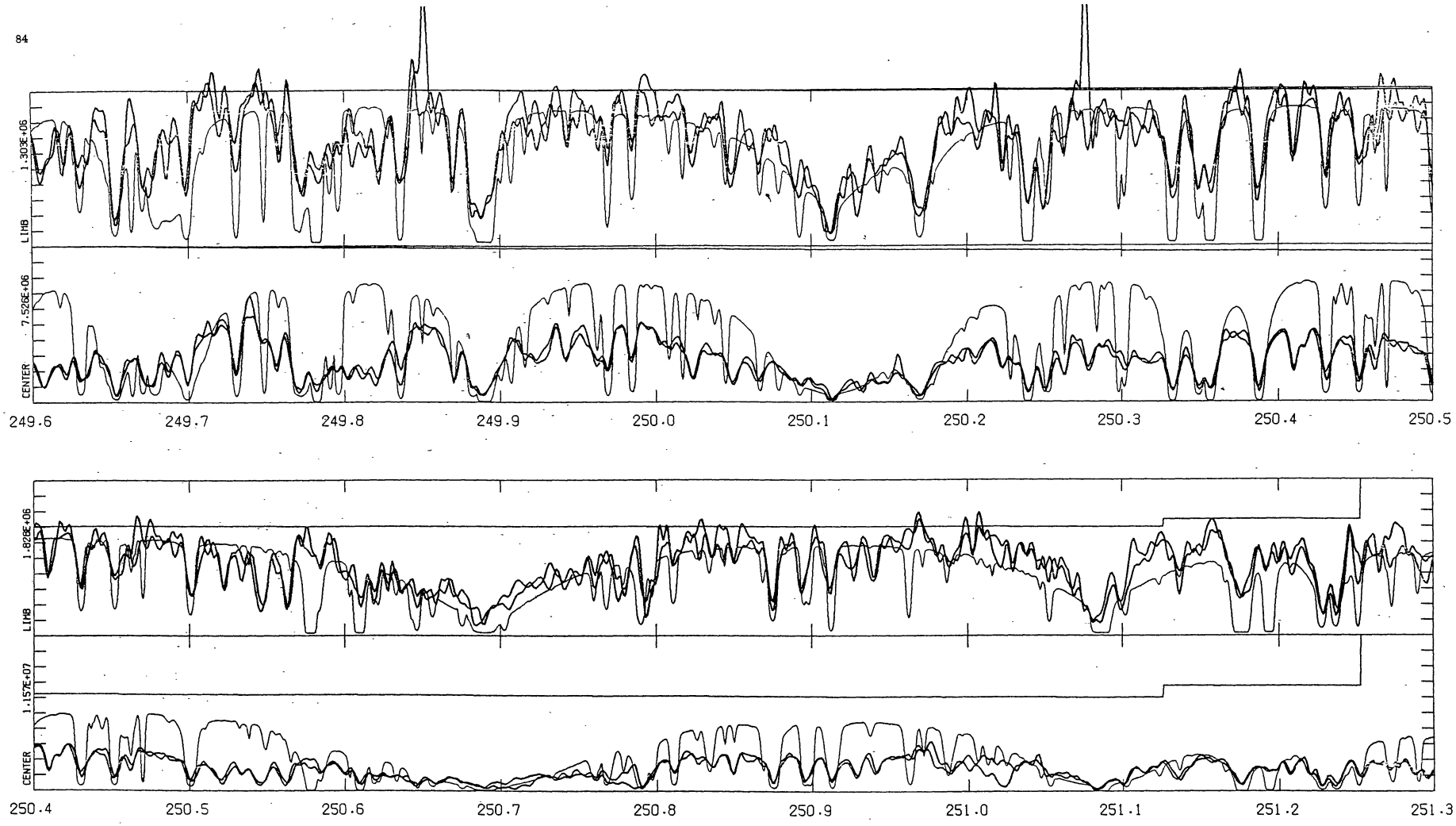

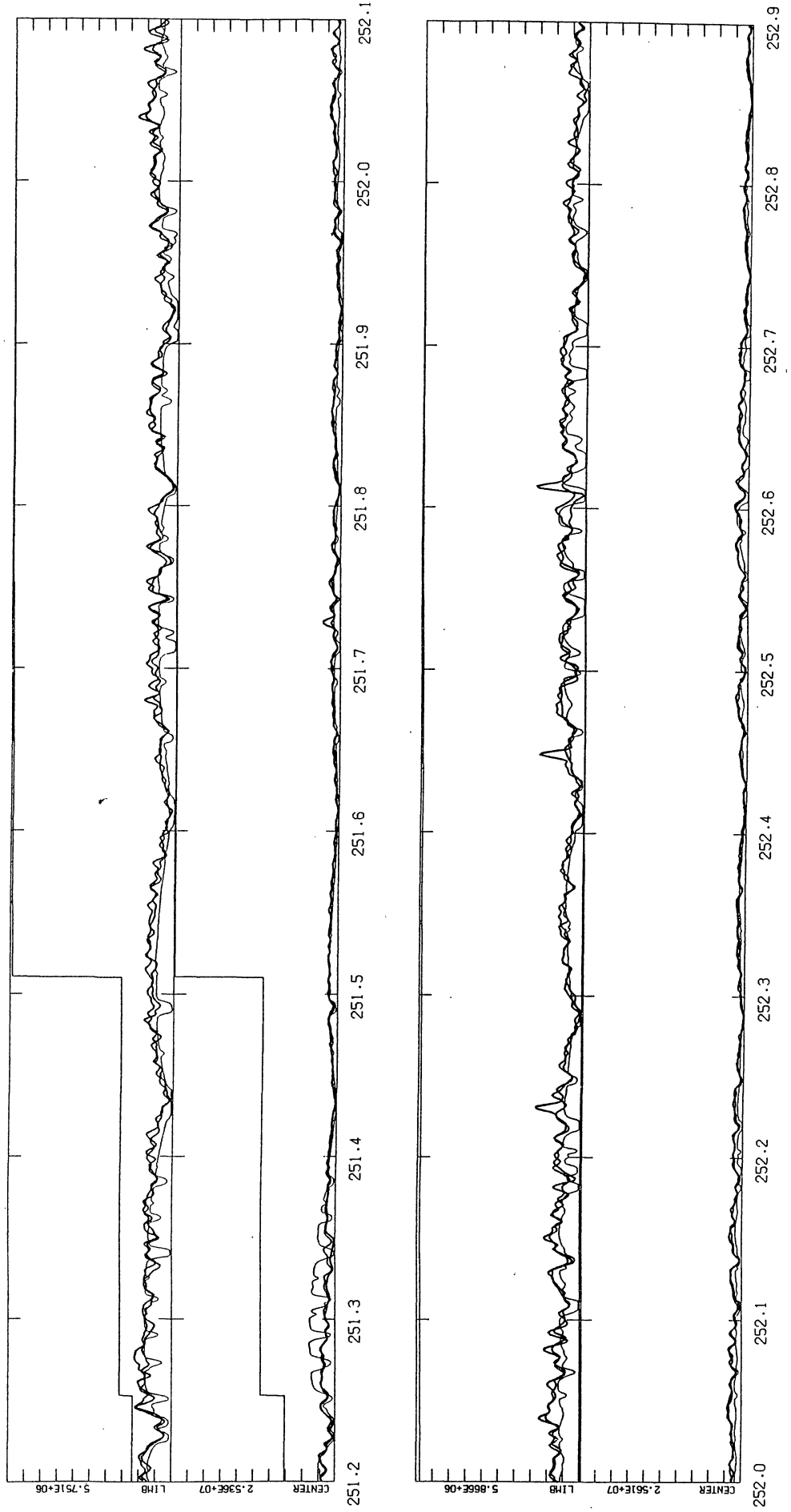

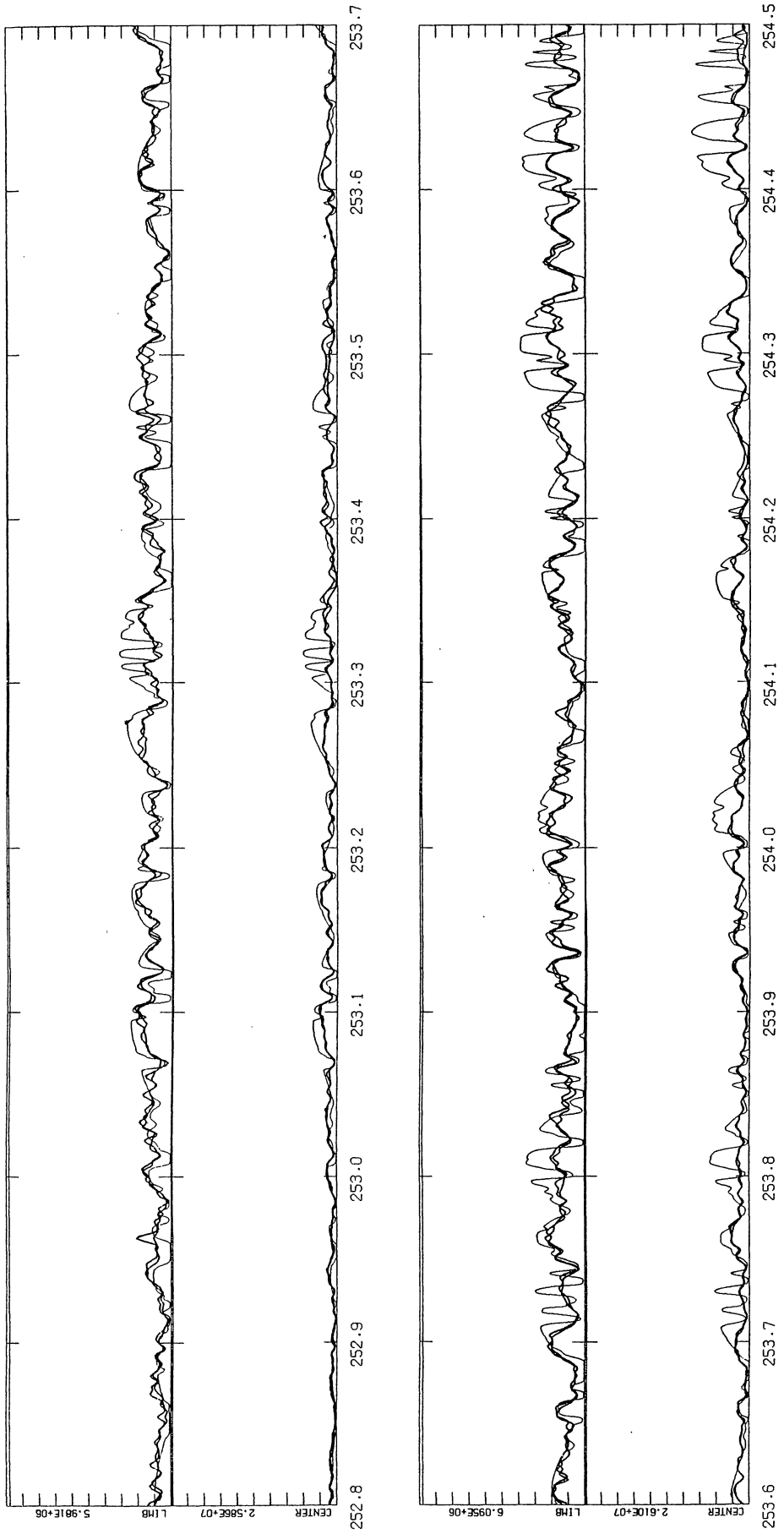

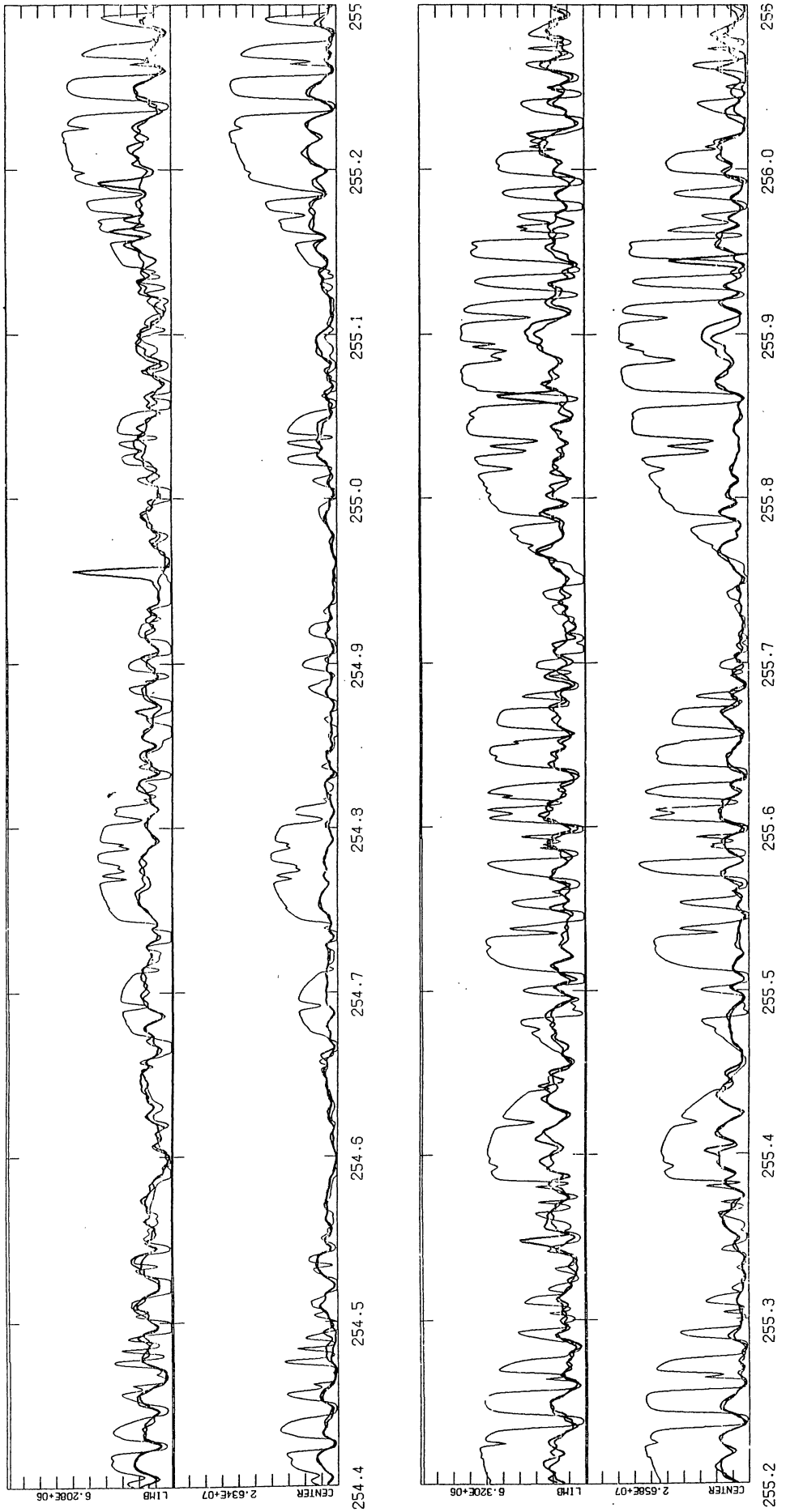

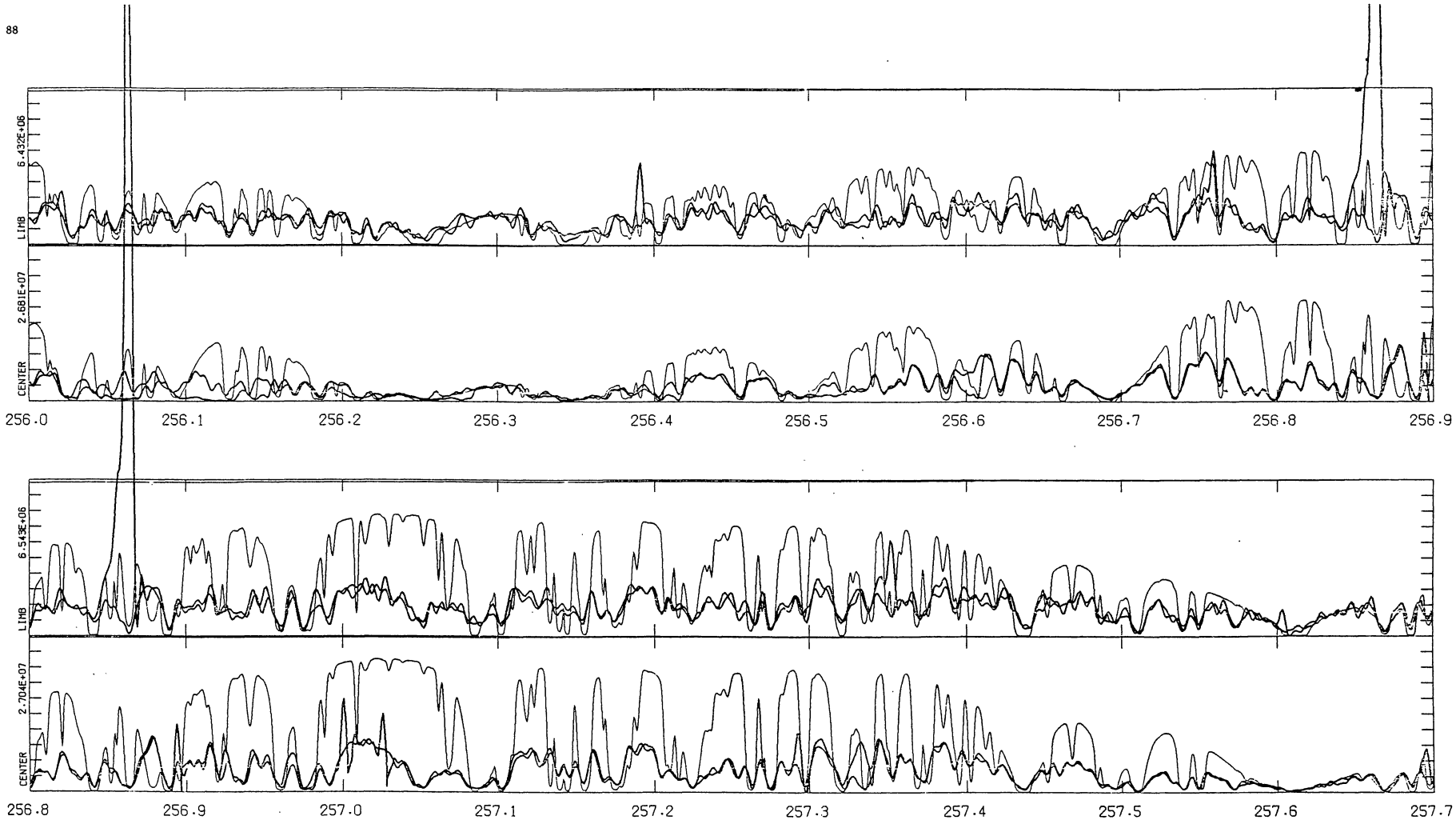

1981SAOSR.391.....K

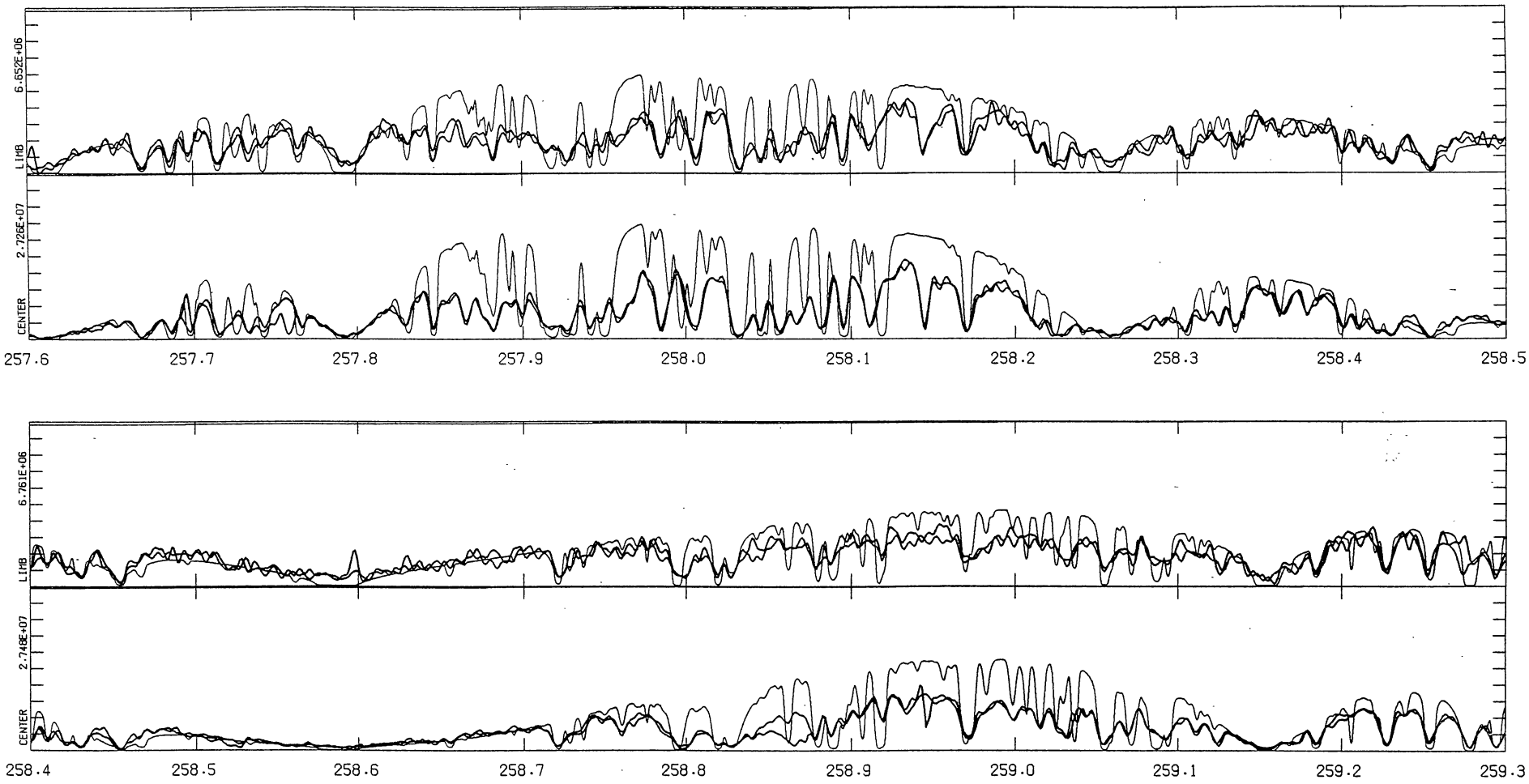

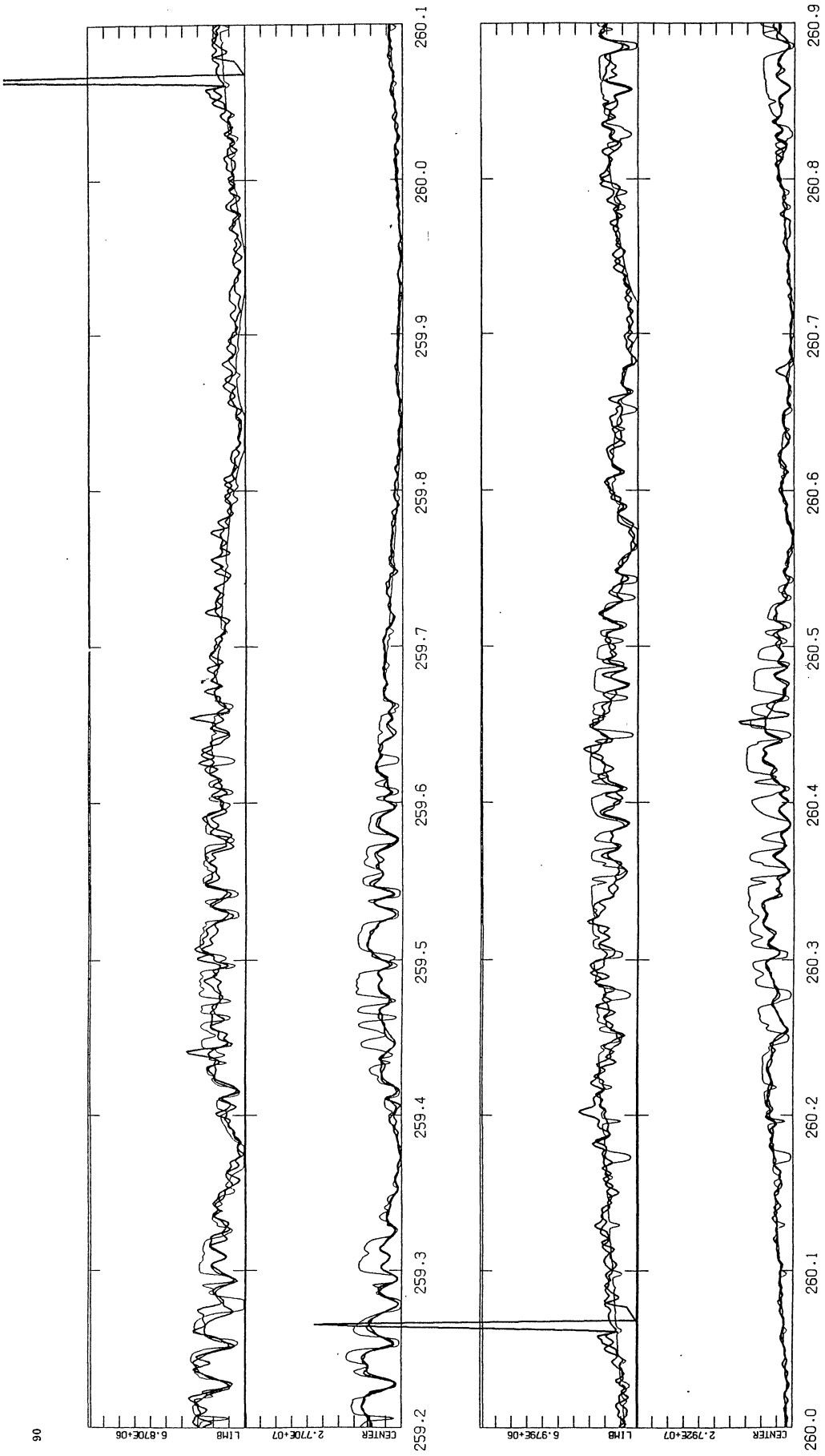

1981SAOSR.391.....K

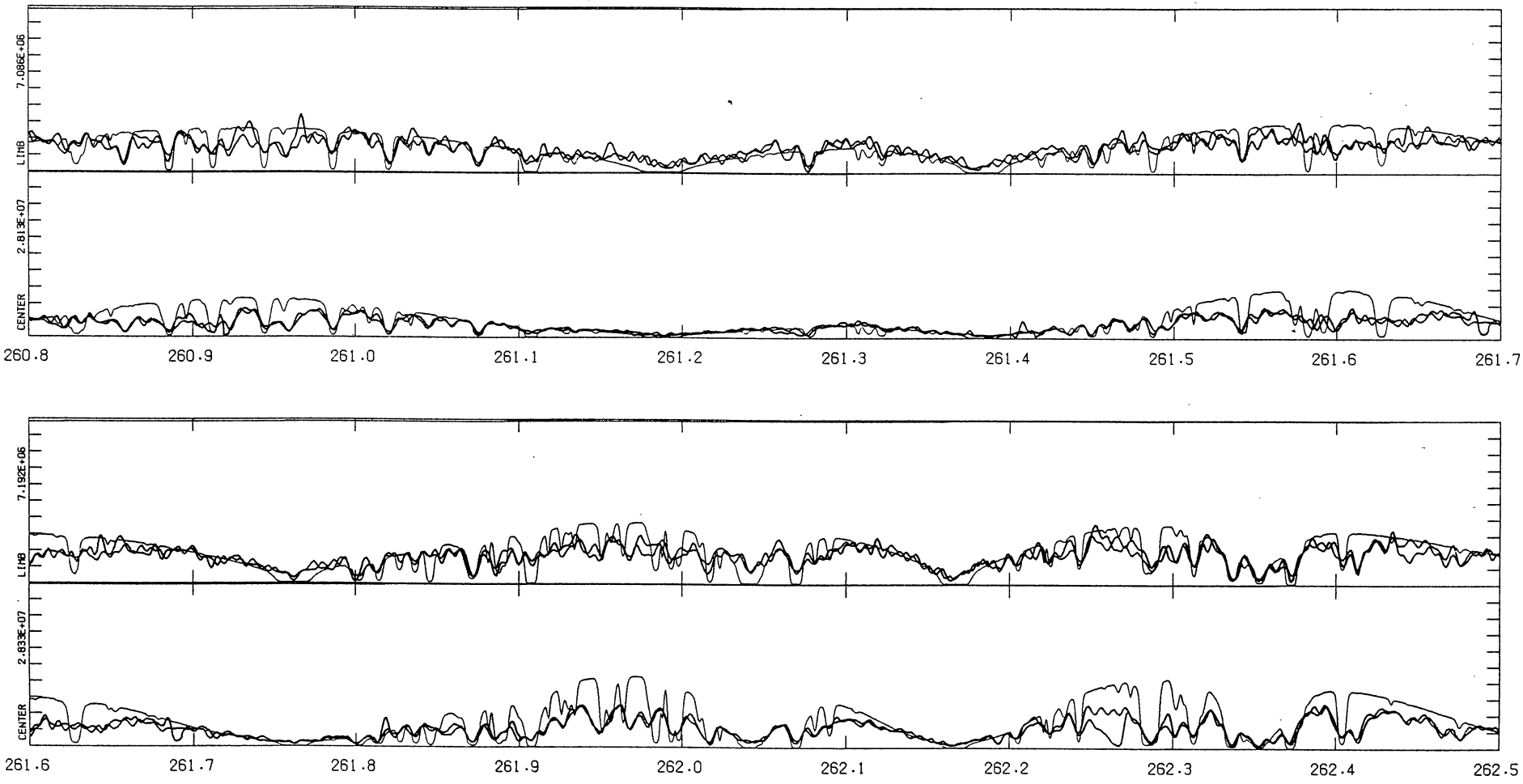

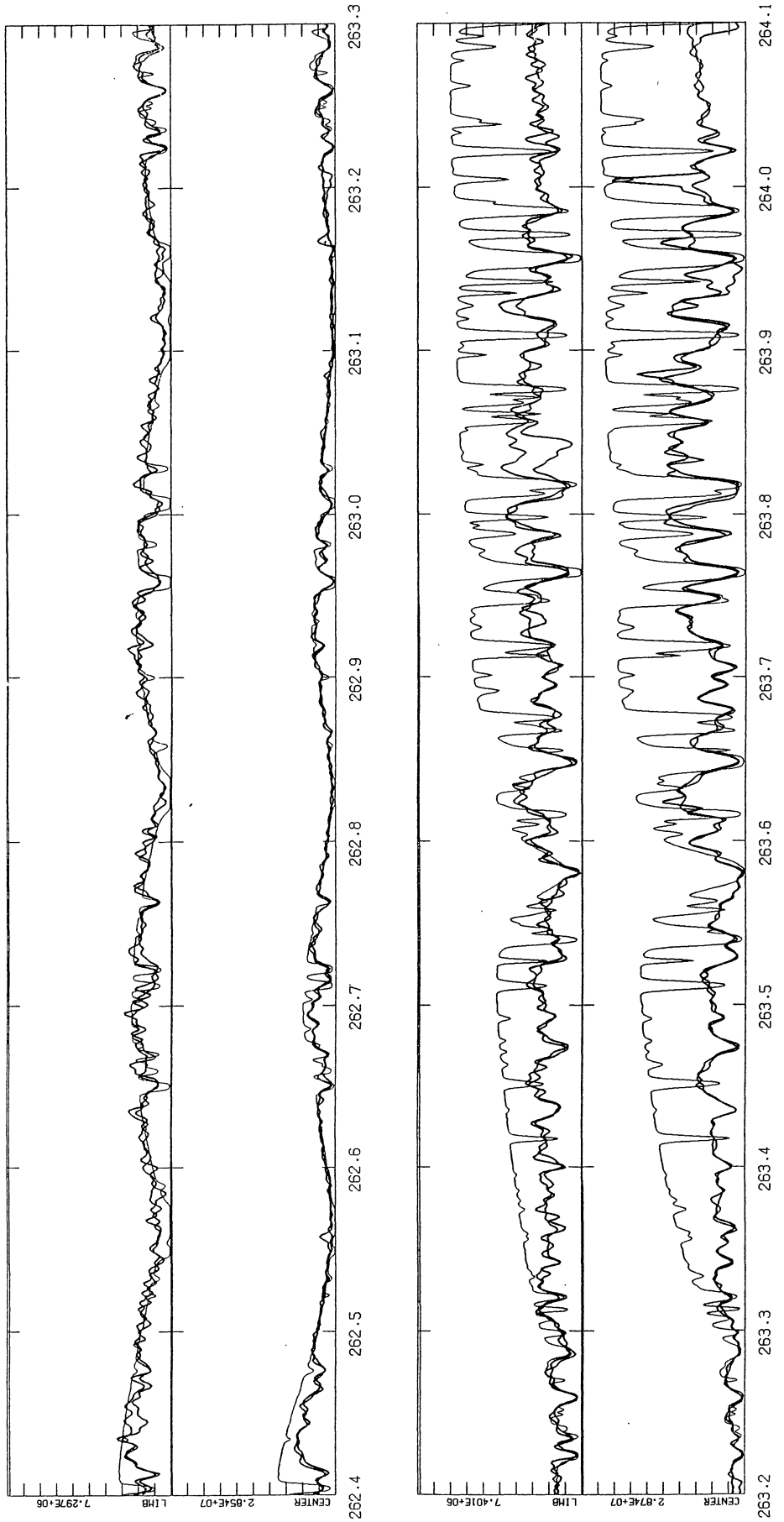

1981SAOSR.391.....K

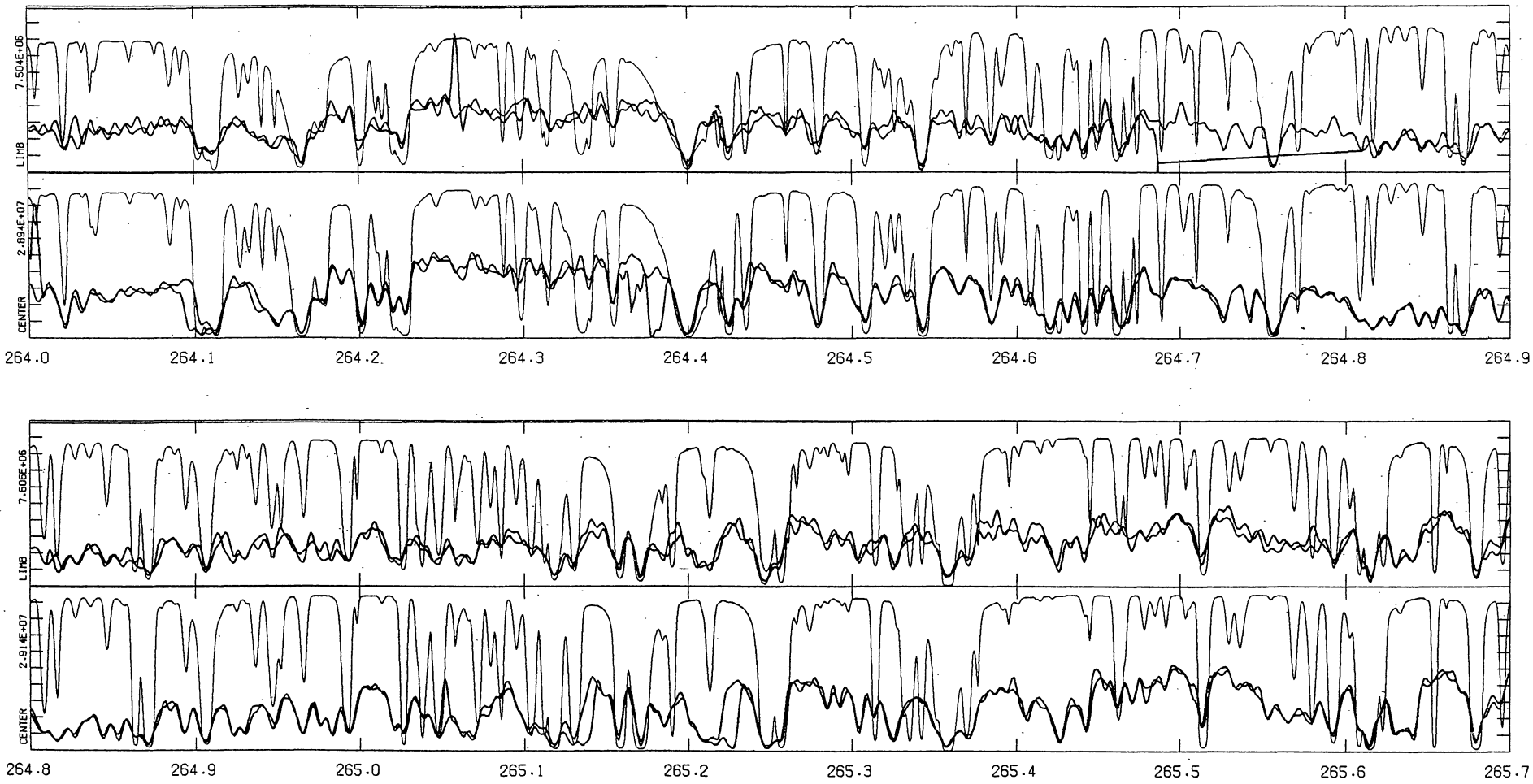

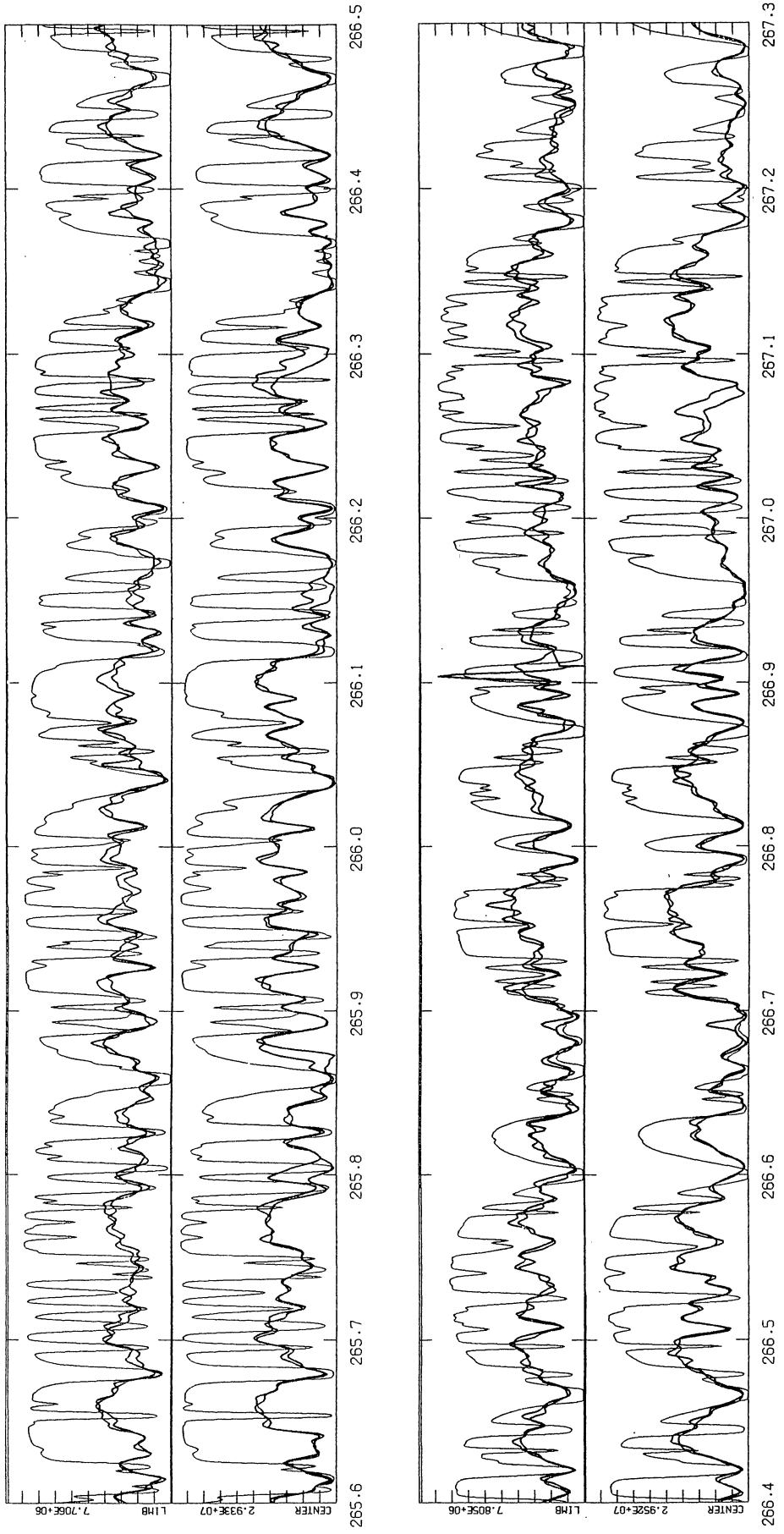

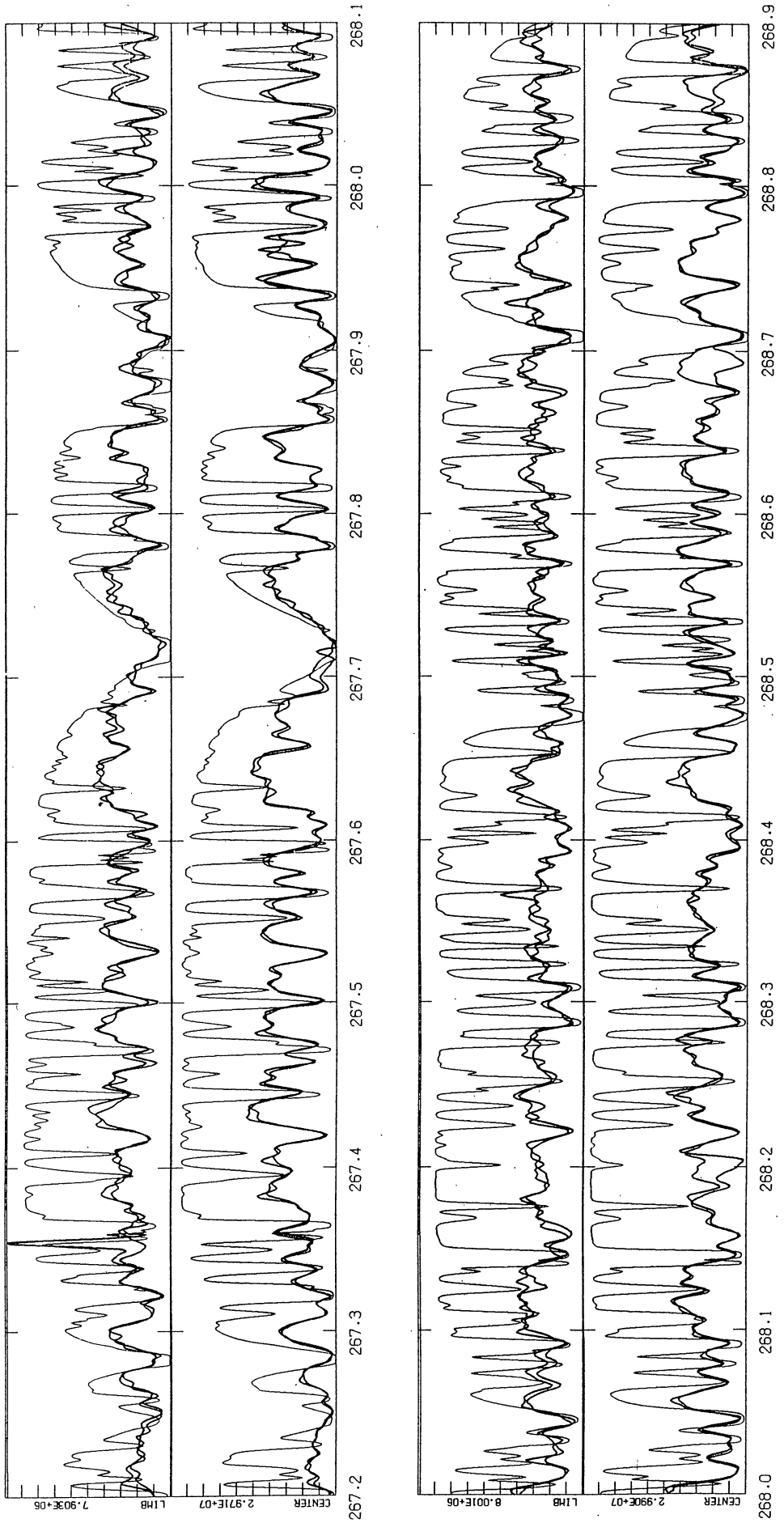

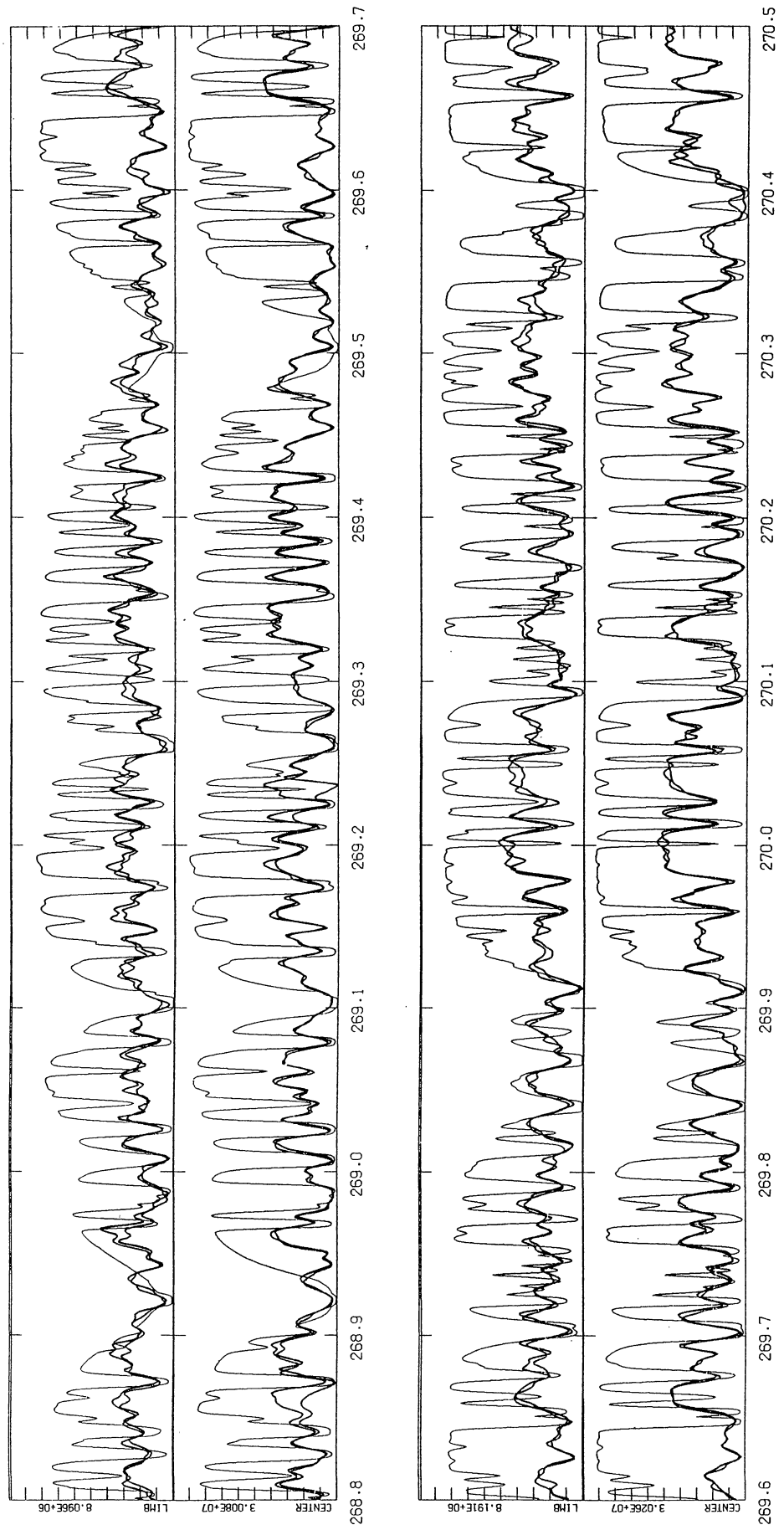

1981SAOSR.391.....K

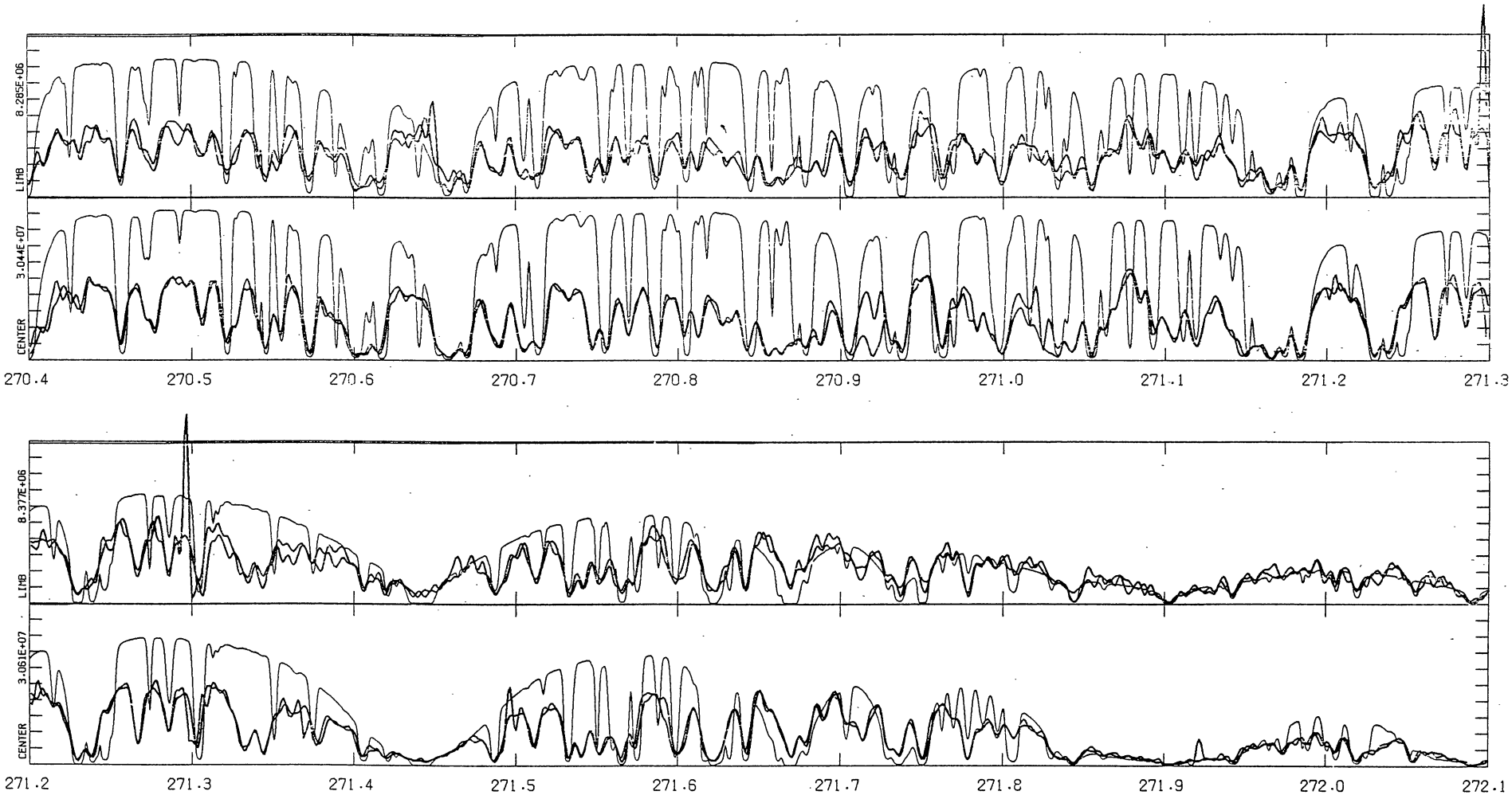

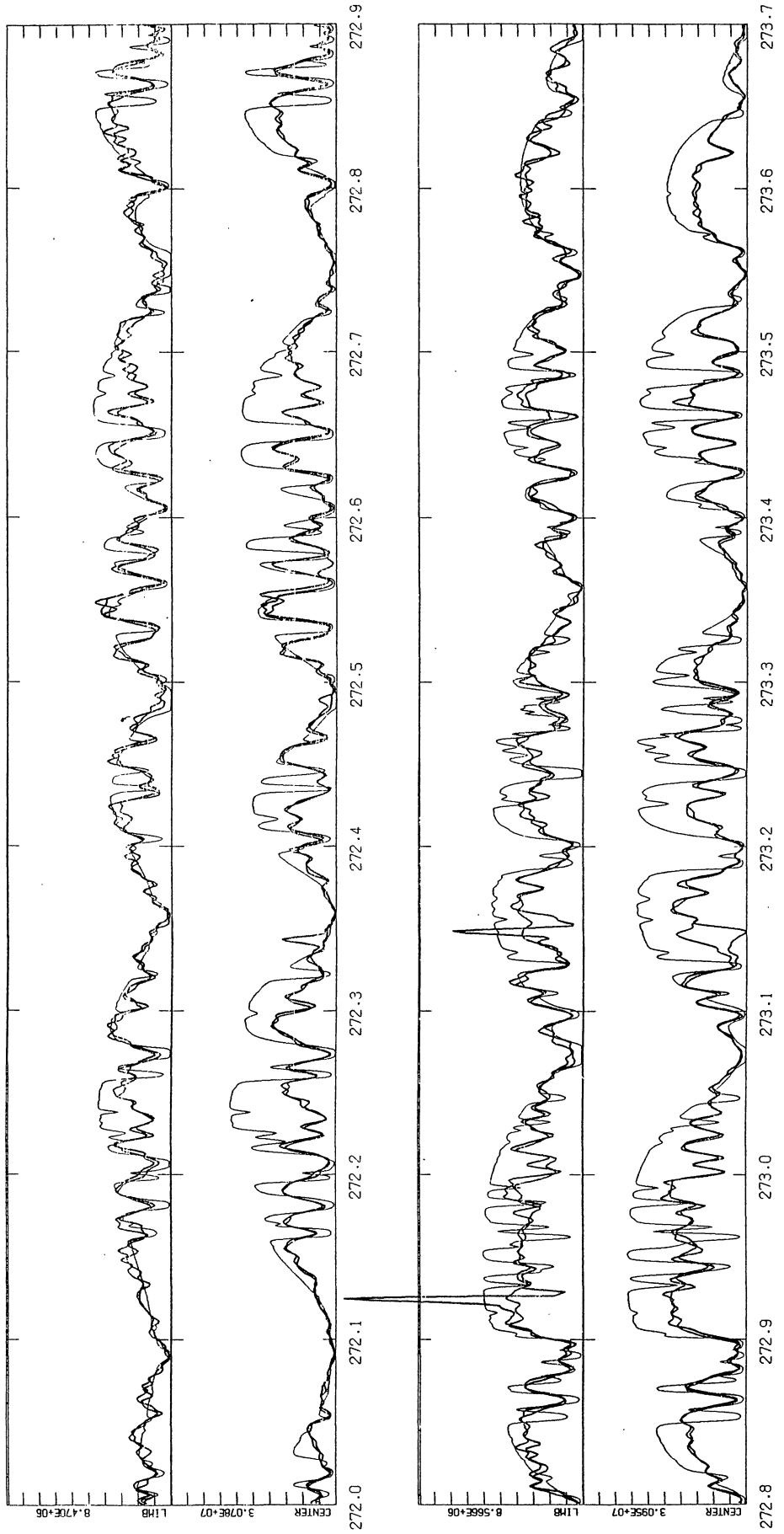

1981SAOSR.391.....K

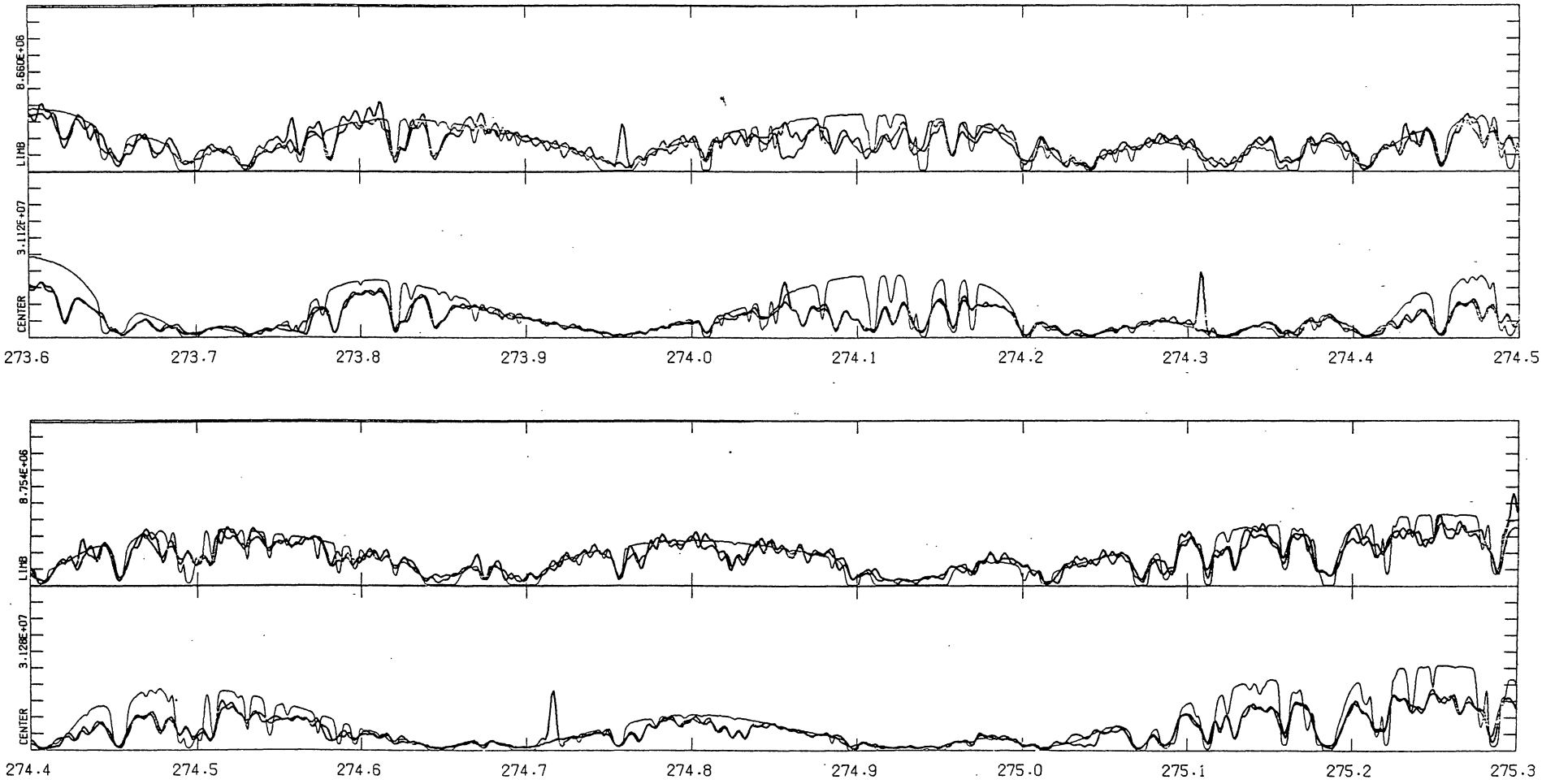

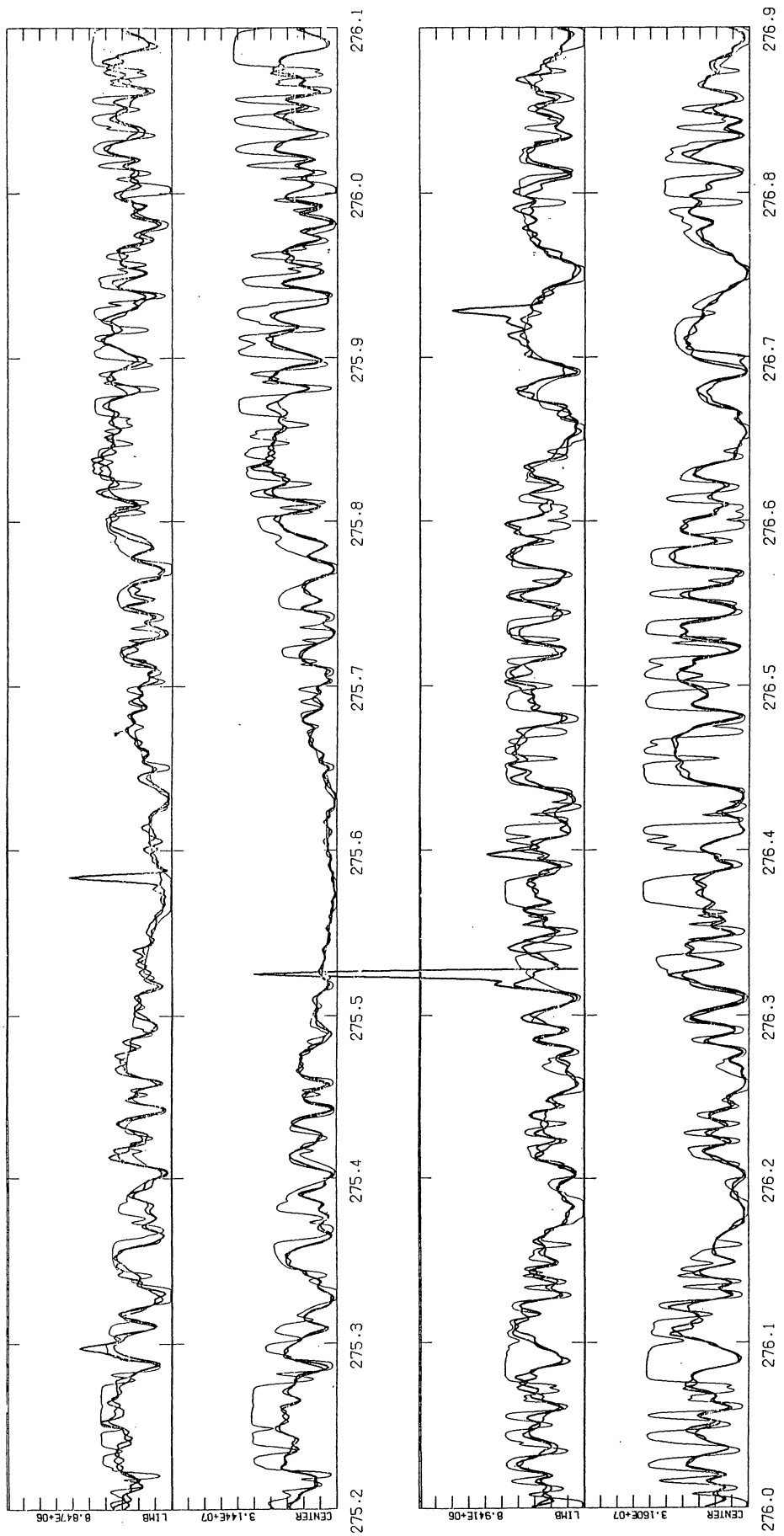

1981SAOSR.391.....K

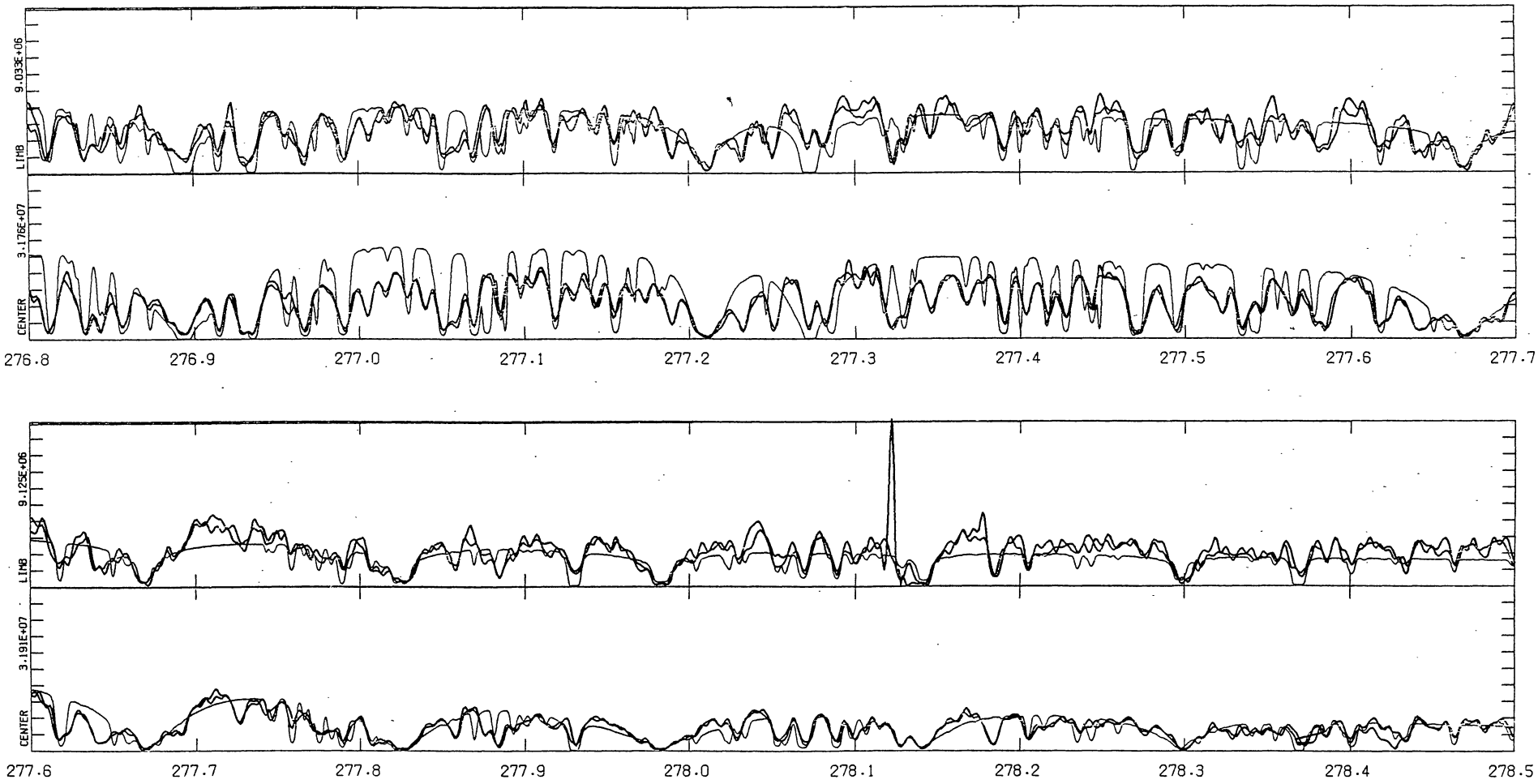

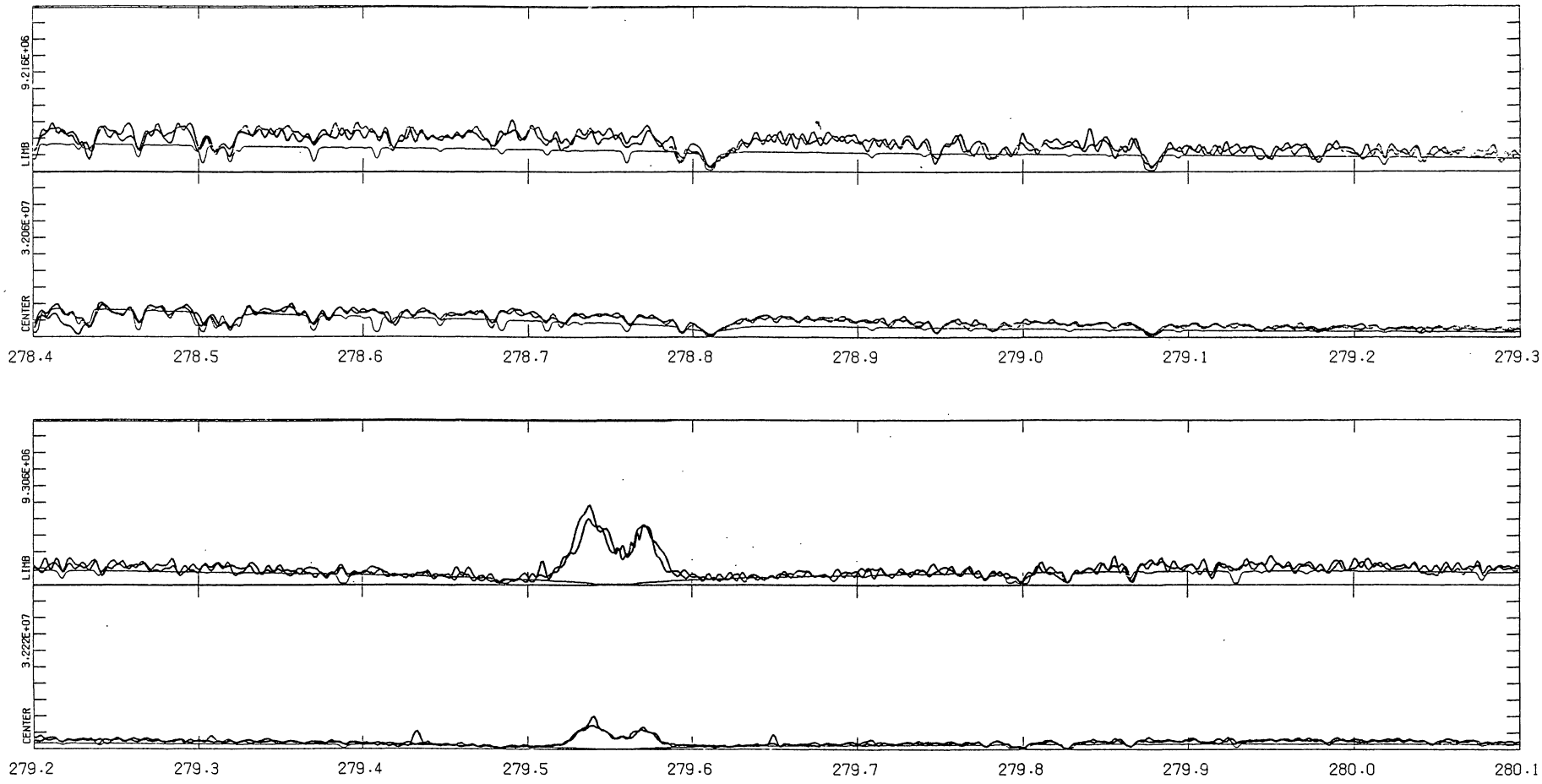

1981SAOSR.391.....K

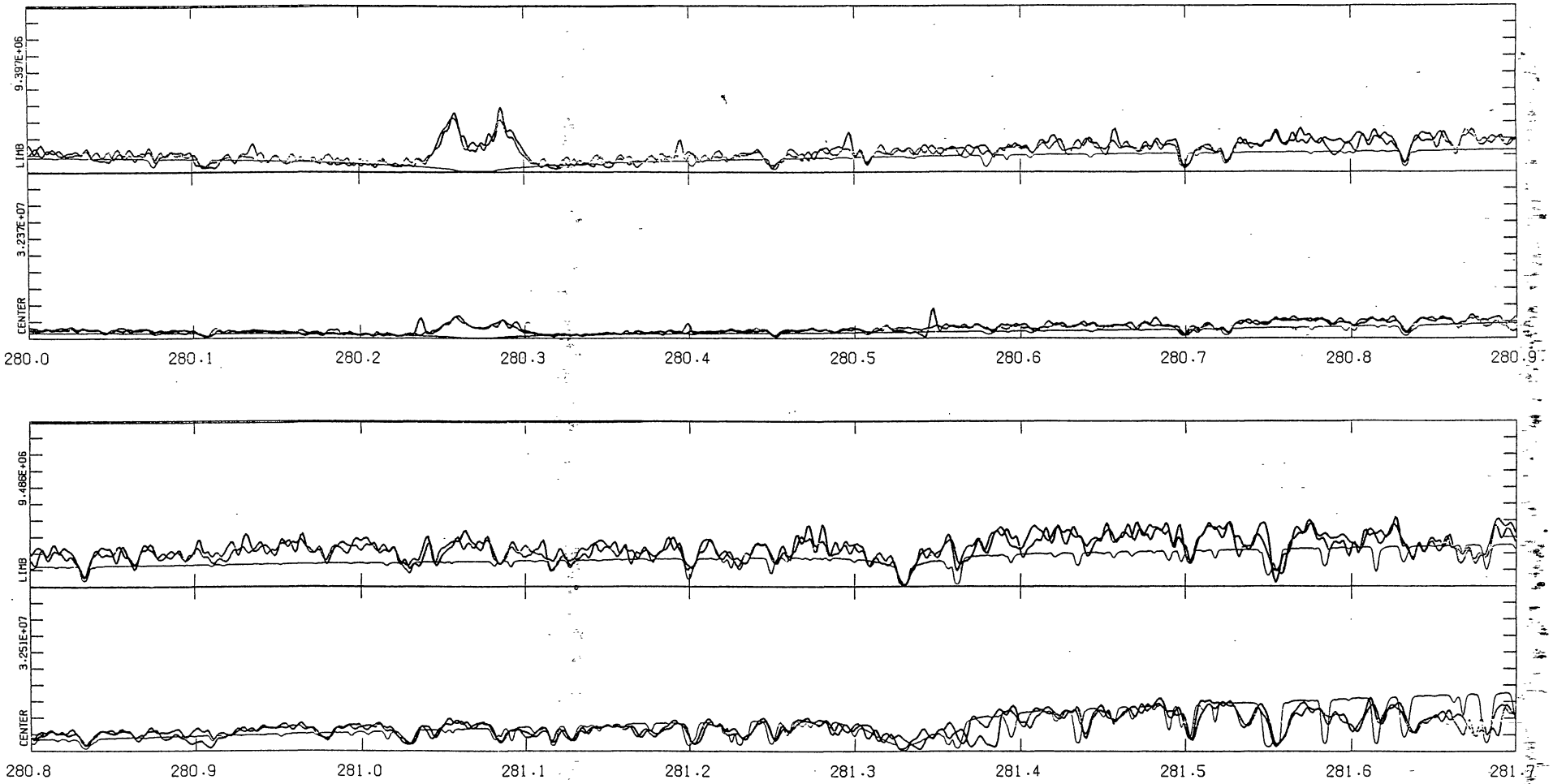

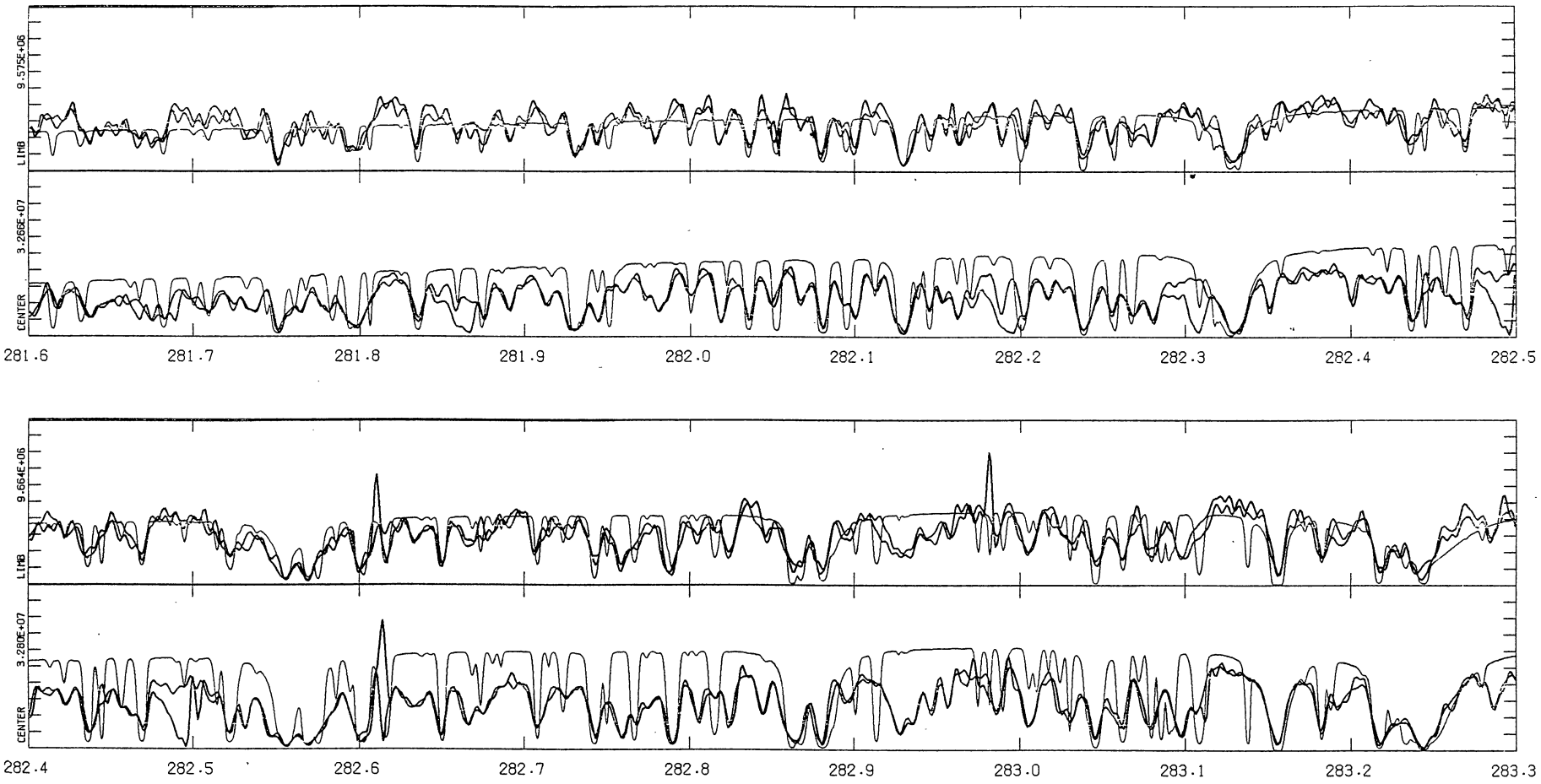

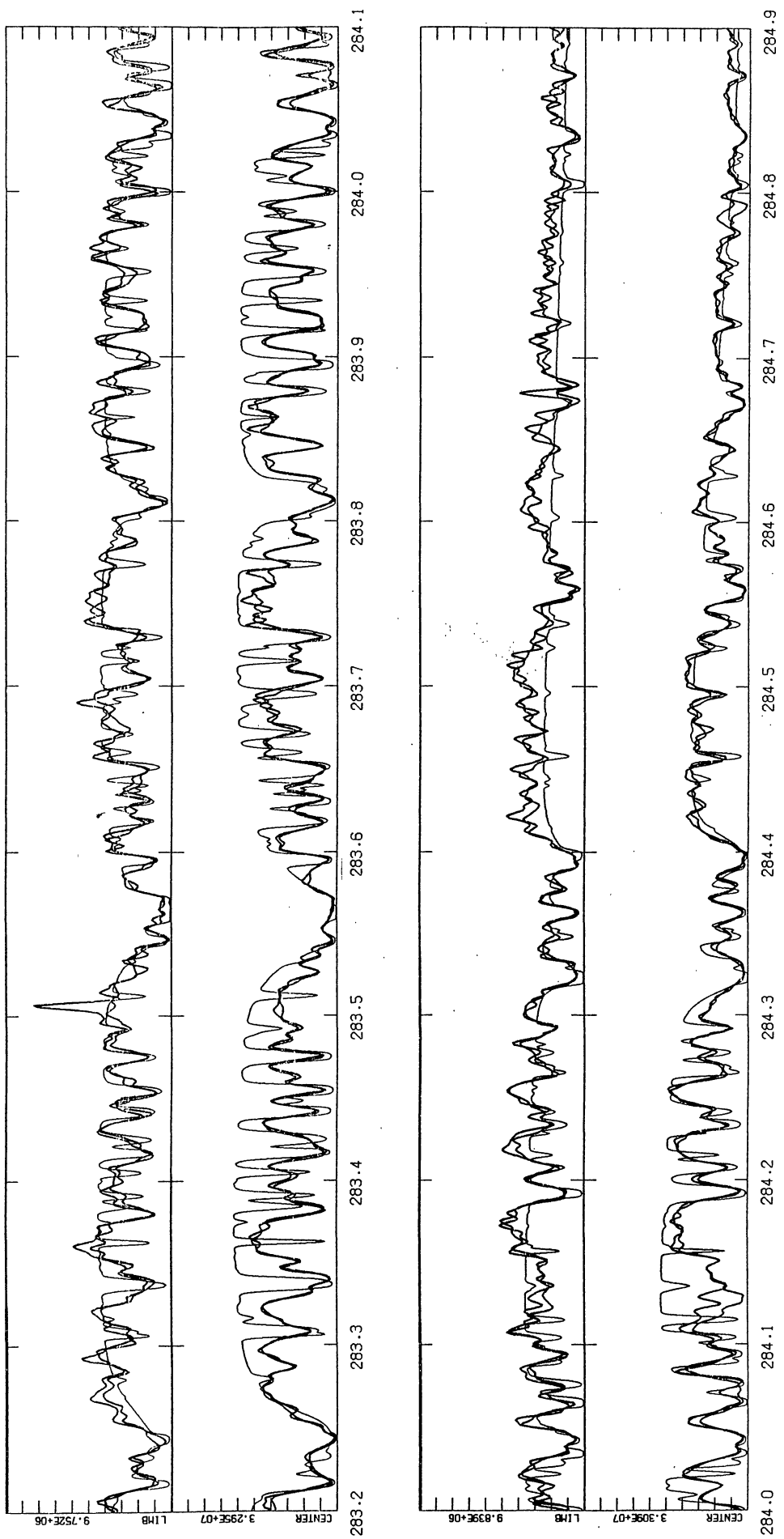

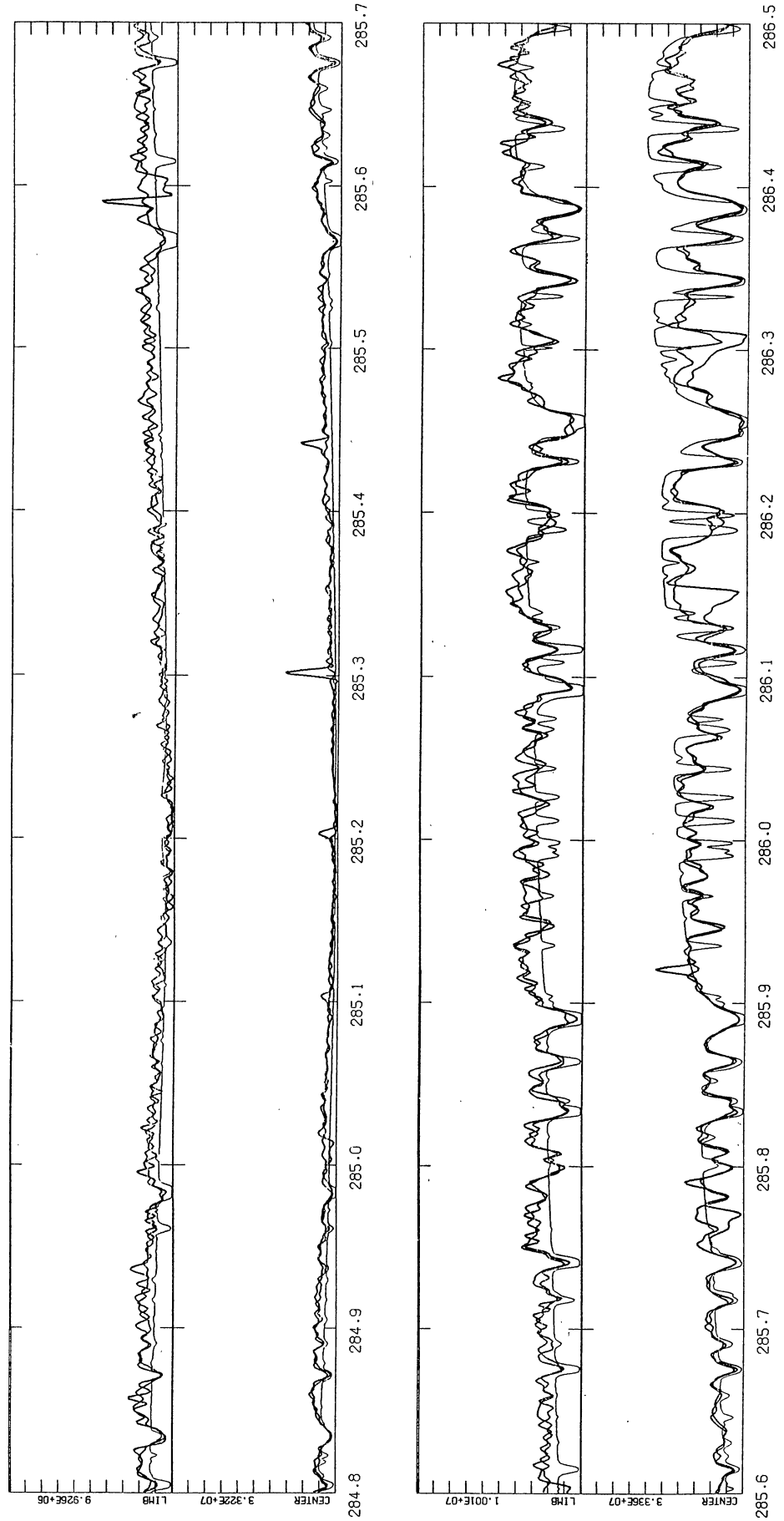

1981SAOSR.391.....K

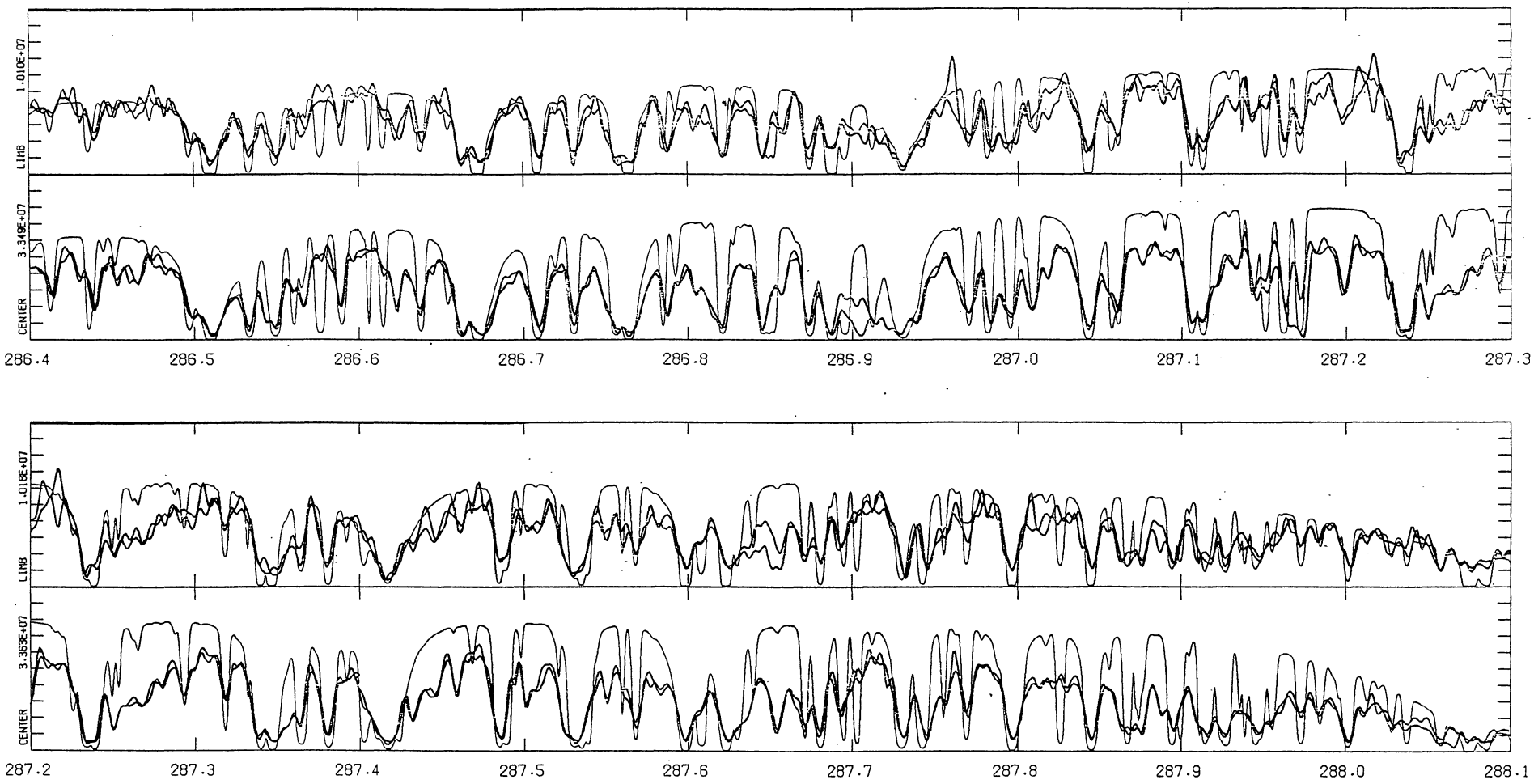

1981SAOSR.391.....K

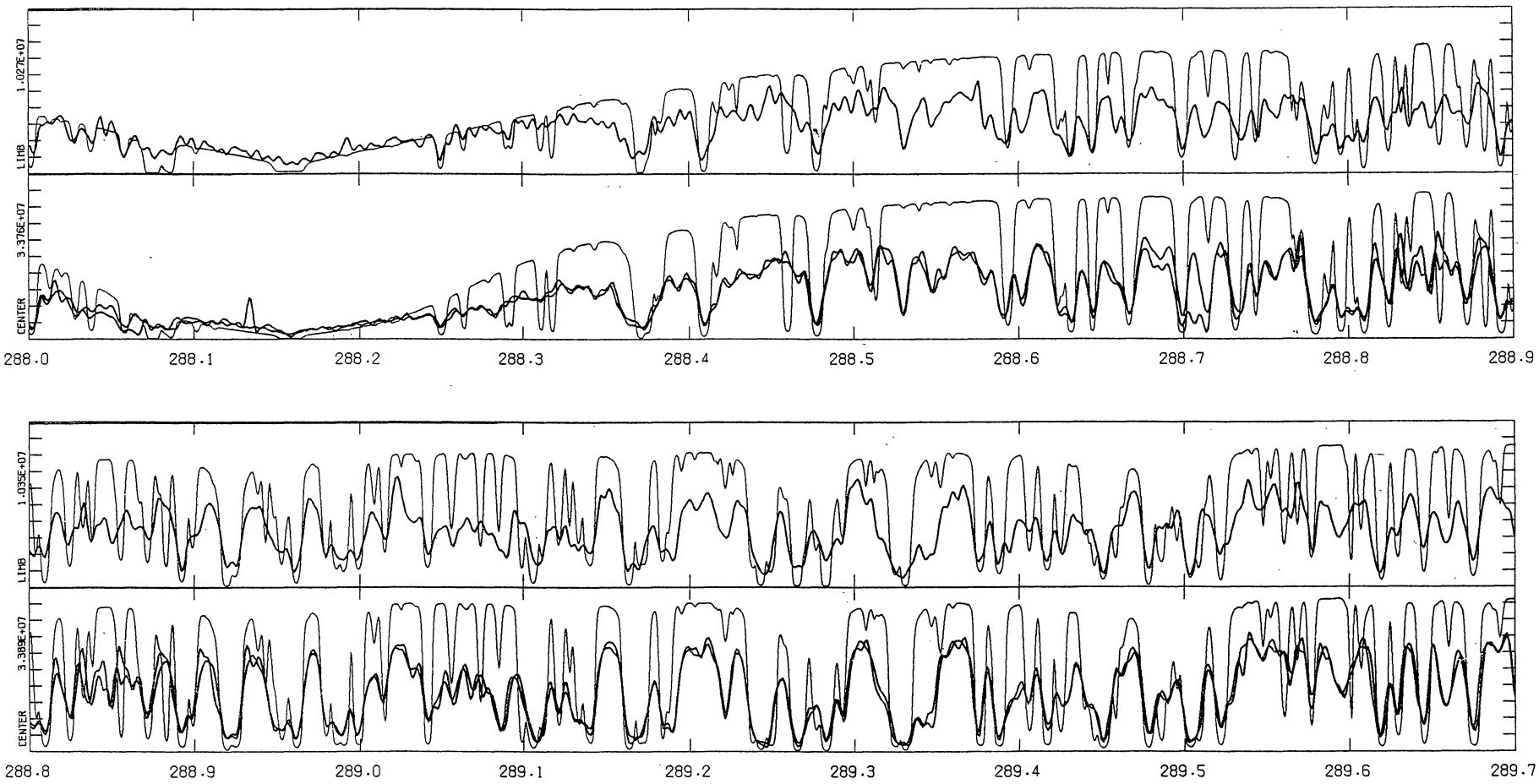

1981SAOSR.391.....K

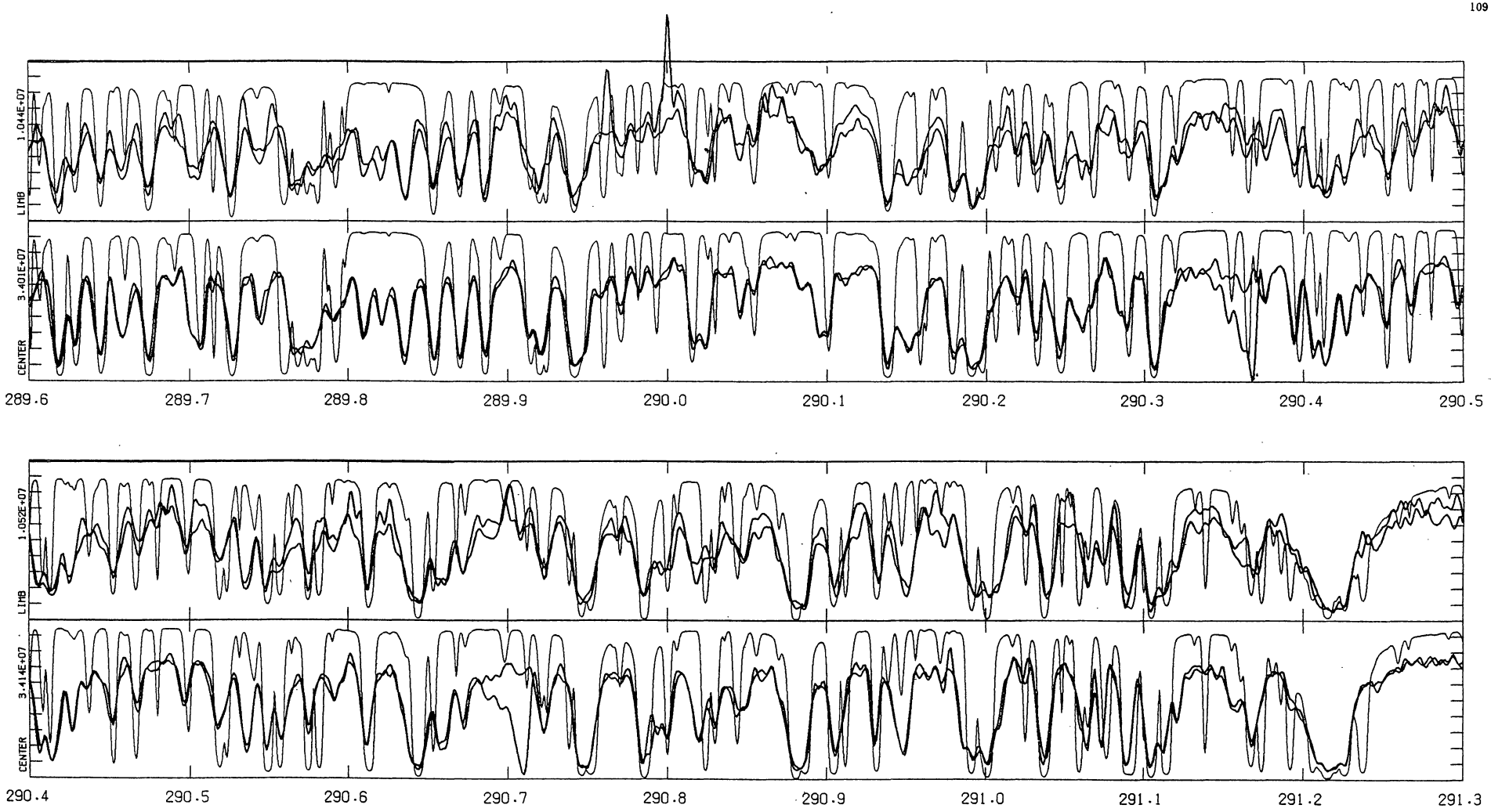

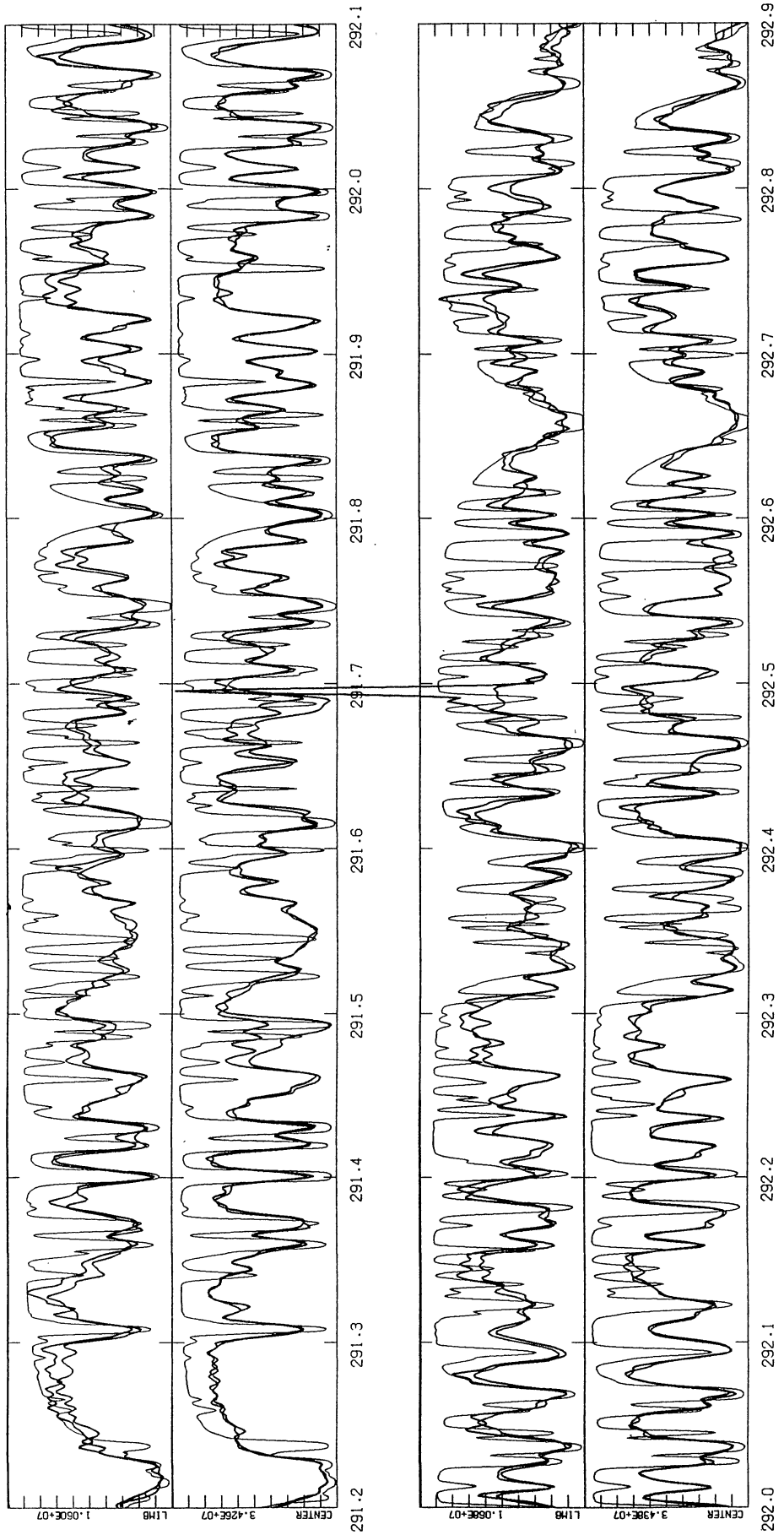

1981SAOSR.391.....K

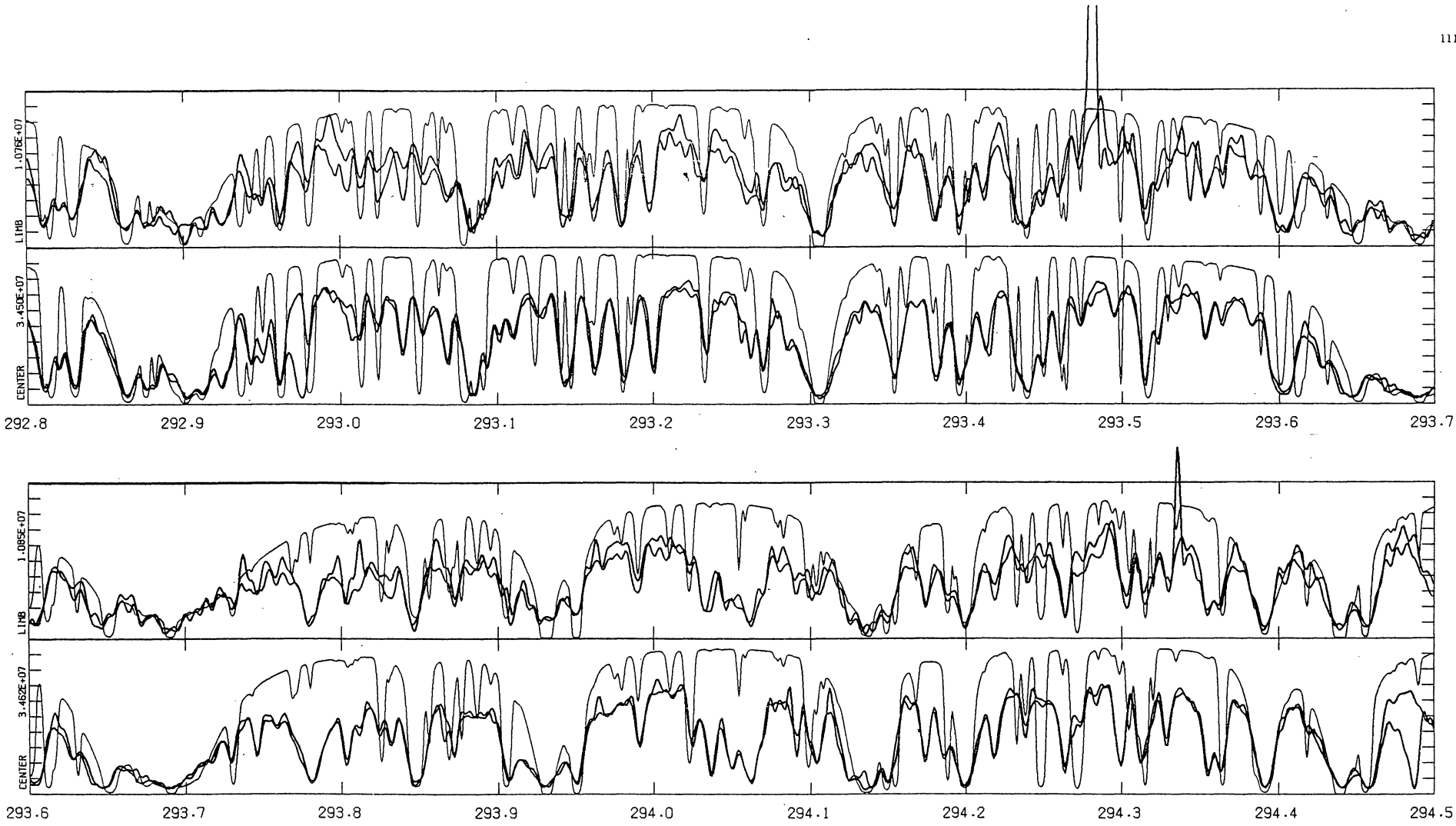

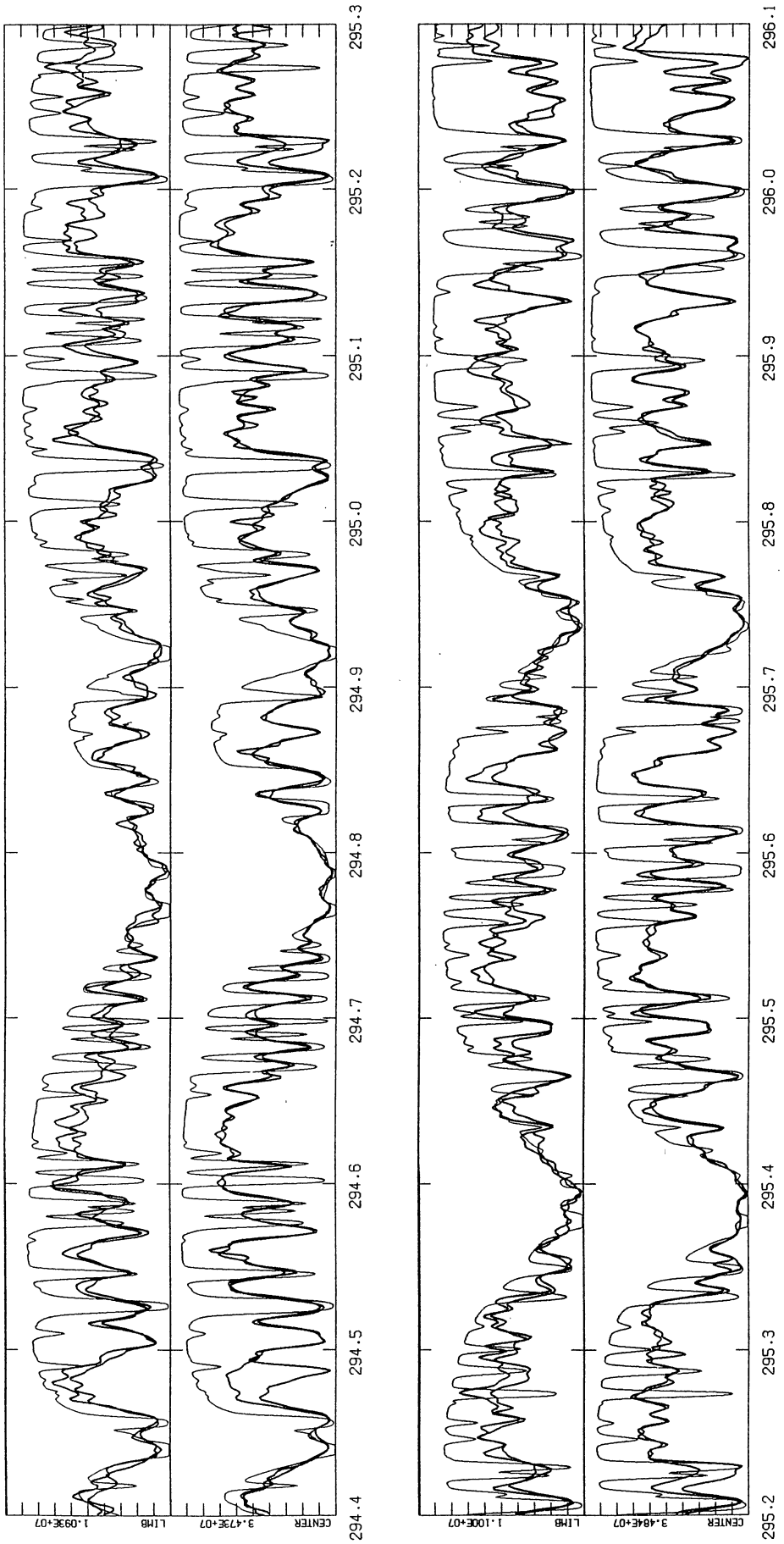

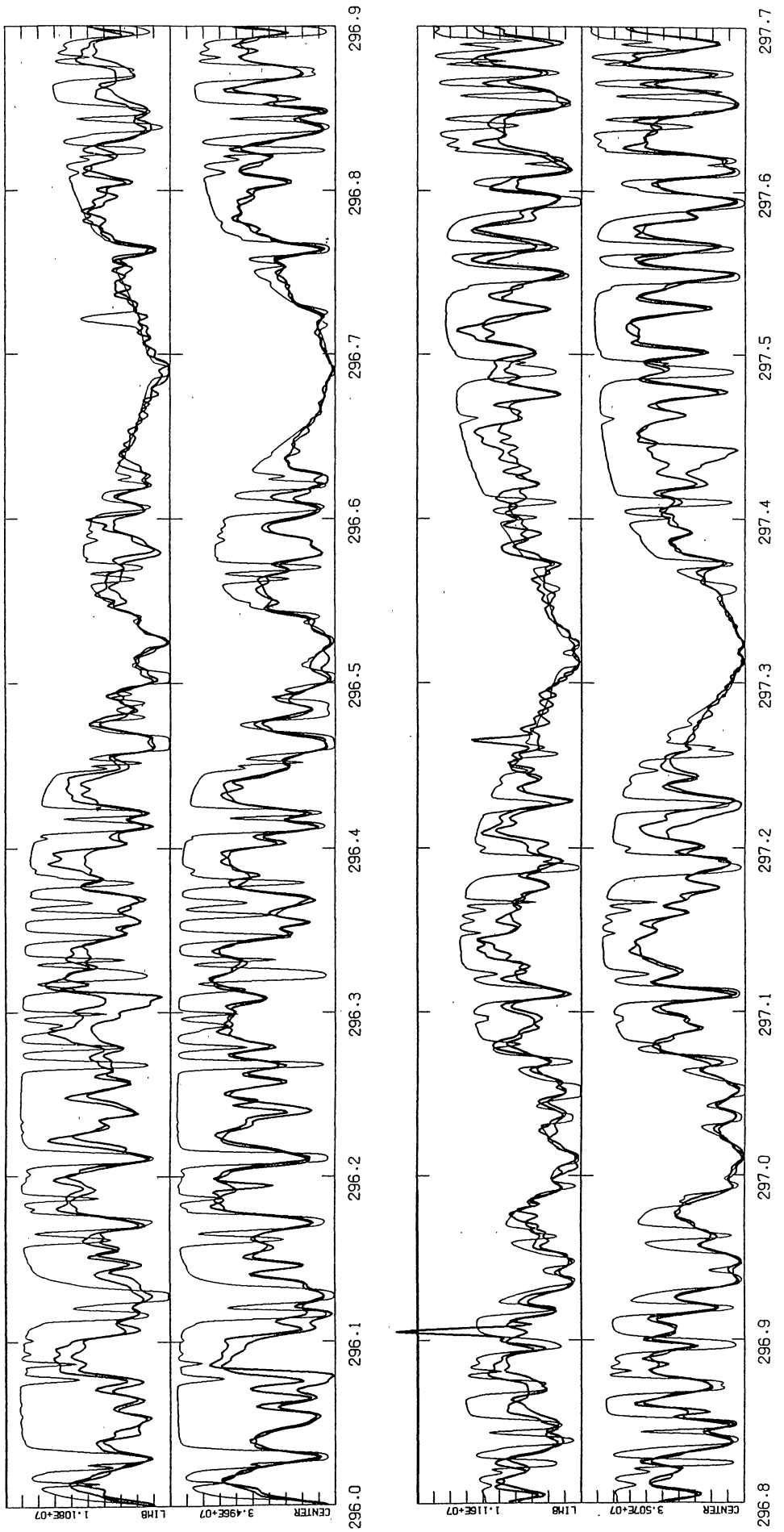

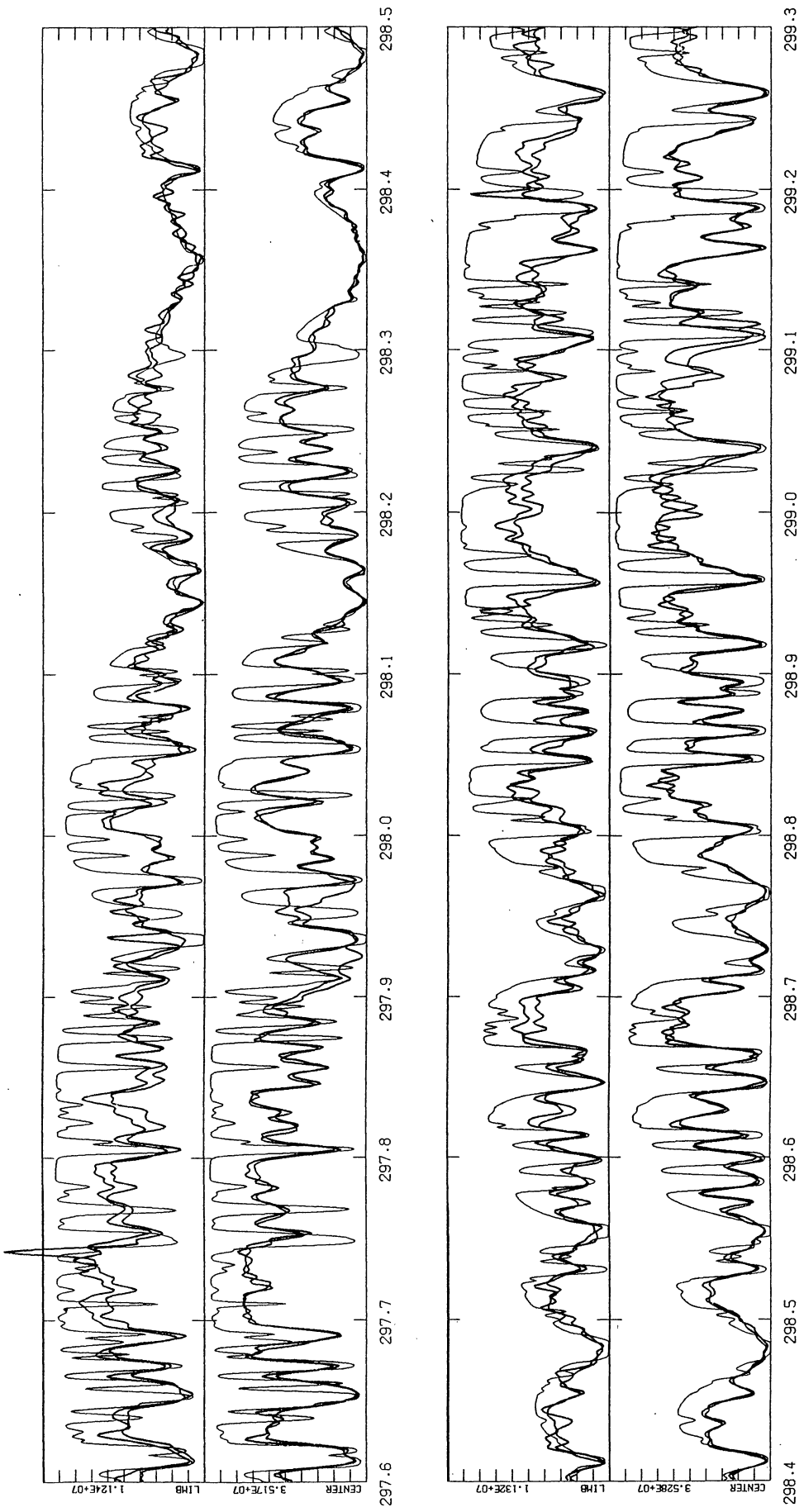

1981SAOSR.391.....K

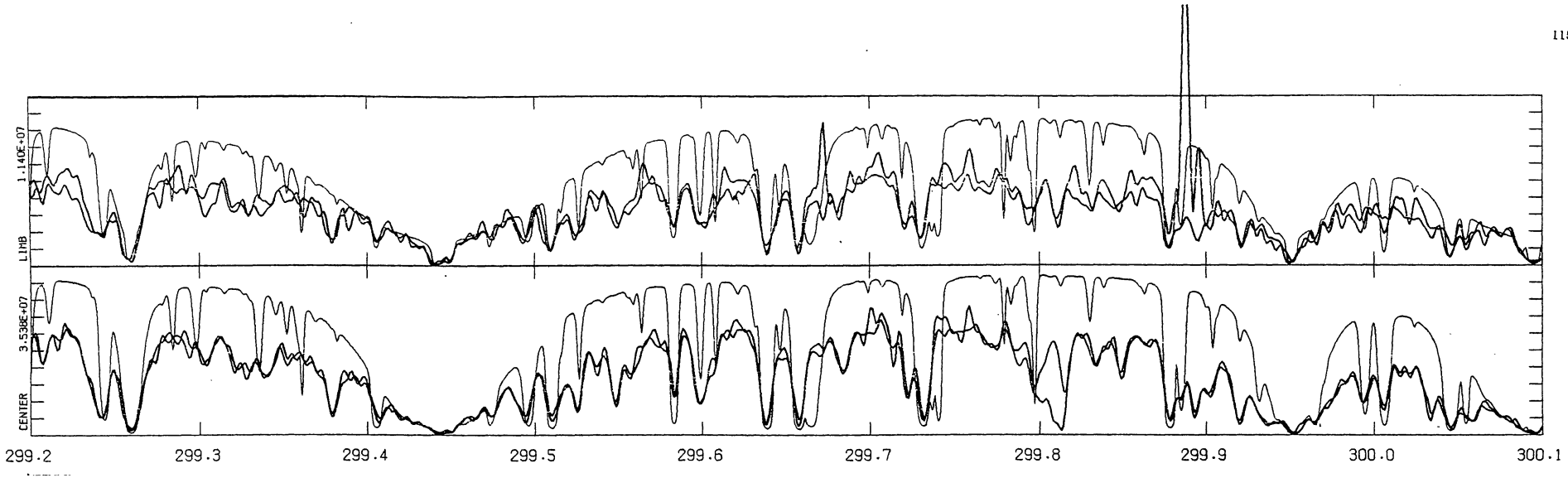

Figure 3. The Hawaii disk center spectrum in the wavelength range 268 to 292 nm compared with our calculated spectrum in the lower half of each panel and compared with the Harvard spectra in the upper half of each panel. The calculated and Harvard spectra are the same as in Figure 1. The heavy line in both the upper and lower half panels is the disk center photographic echelle spectrum of Allen, McAllister, and Jefferies (1978) for which they set the intensity scale to match approximately that of the Harvard spectra. The scale of the upper half panel is arbitrary. The first reliable Hawaii data start at about 268.3 nm.

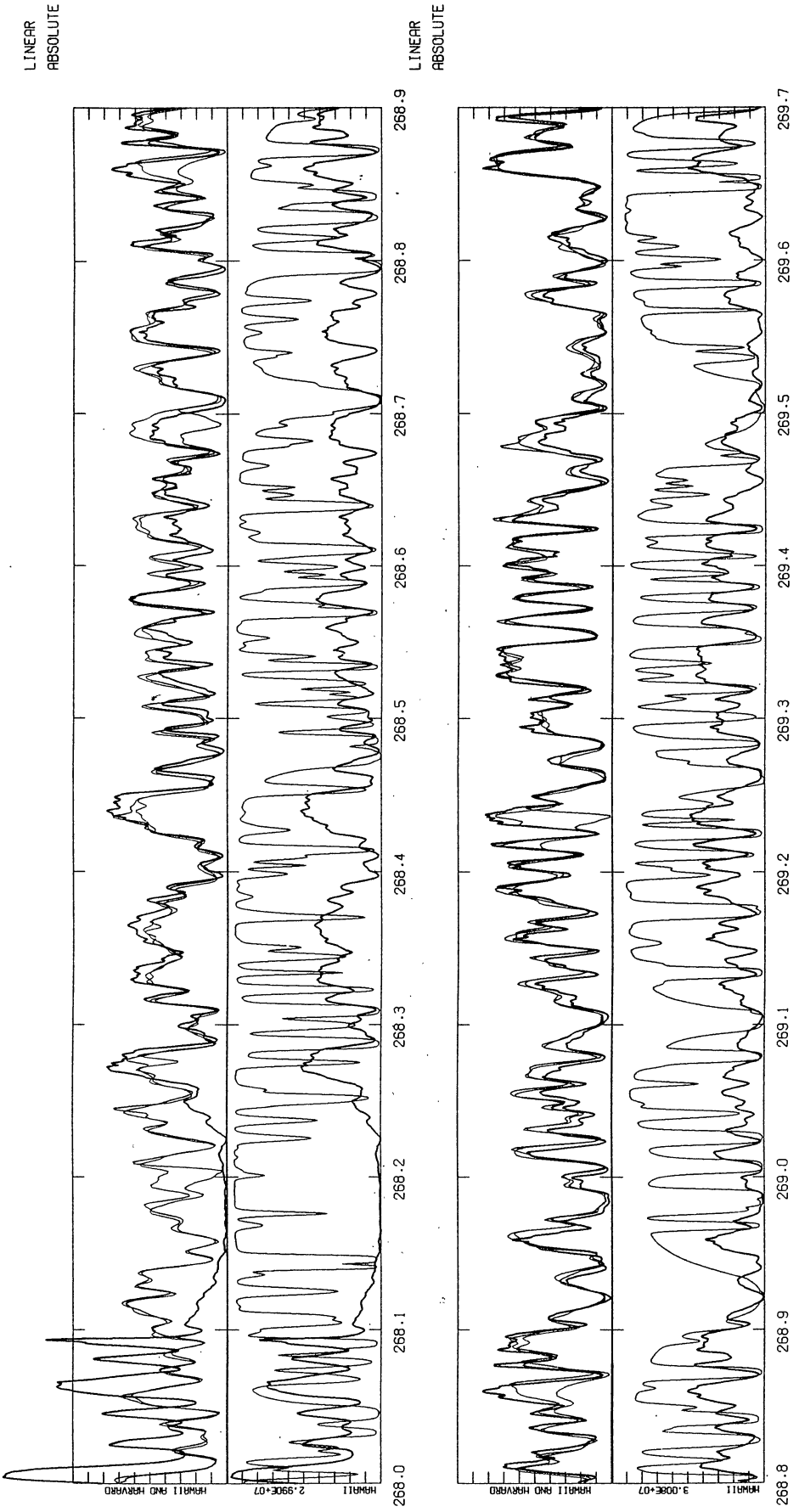

1981SAOSR.391.....K

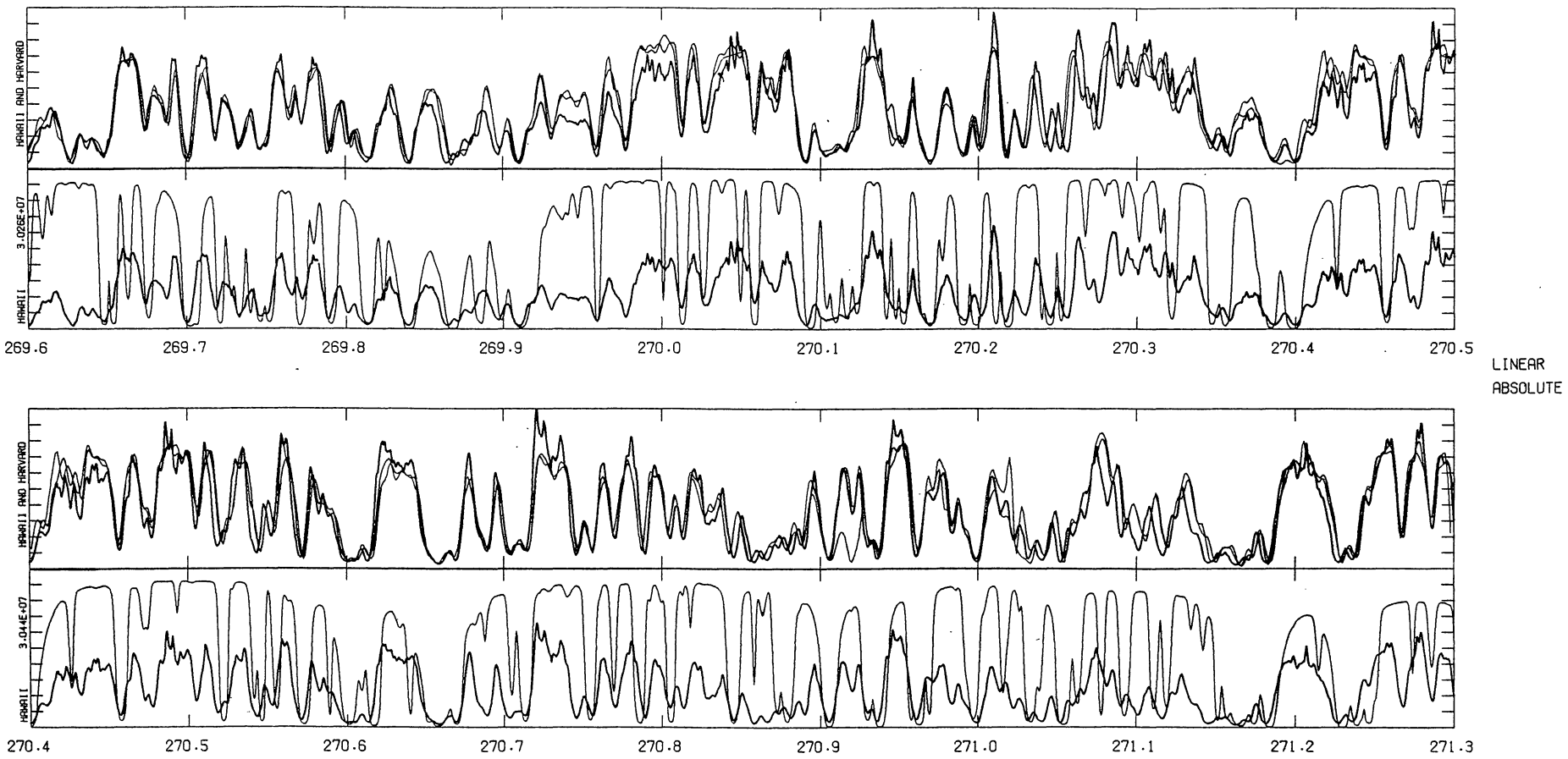

1981SAOSR.391.....K

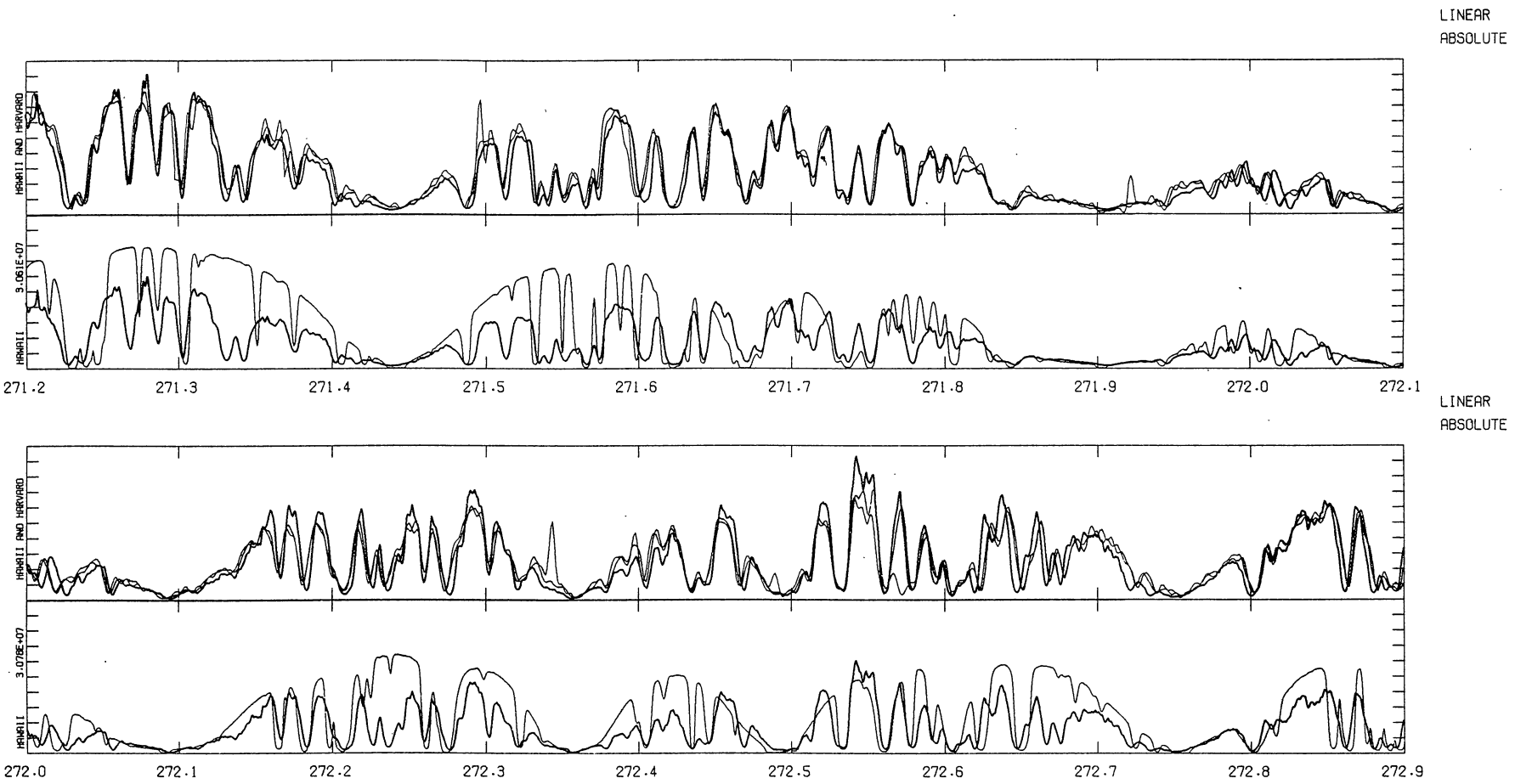

1981SAOSR.391.....K

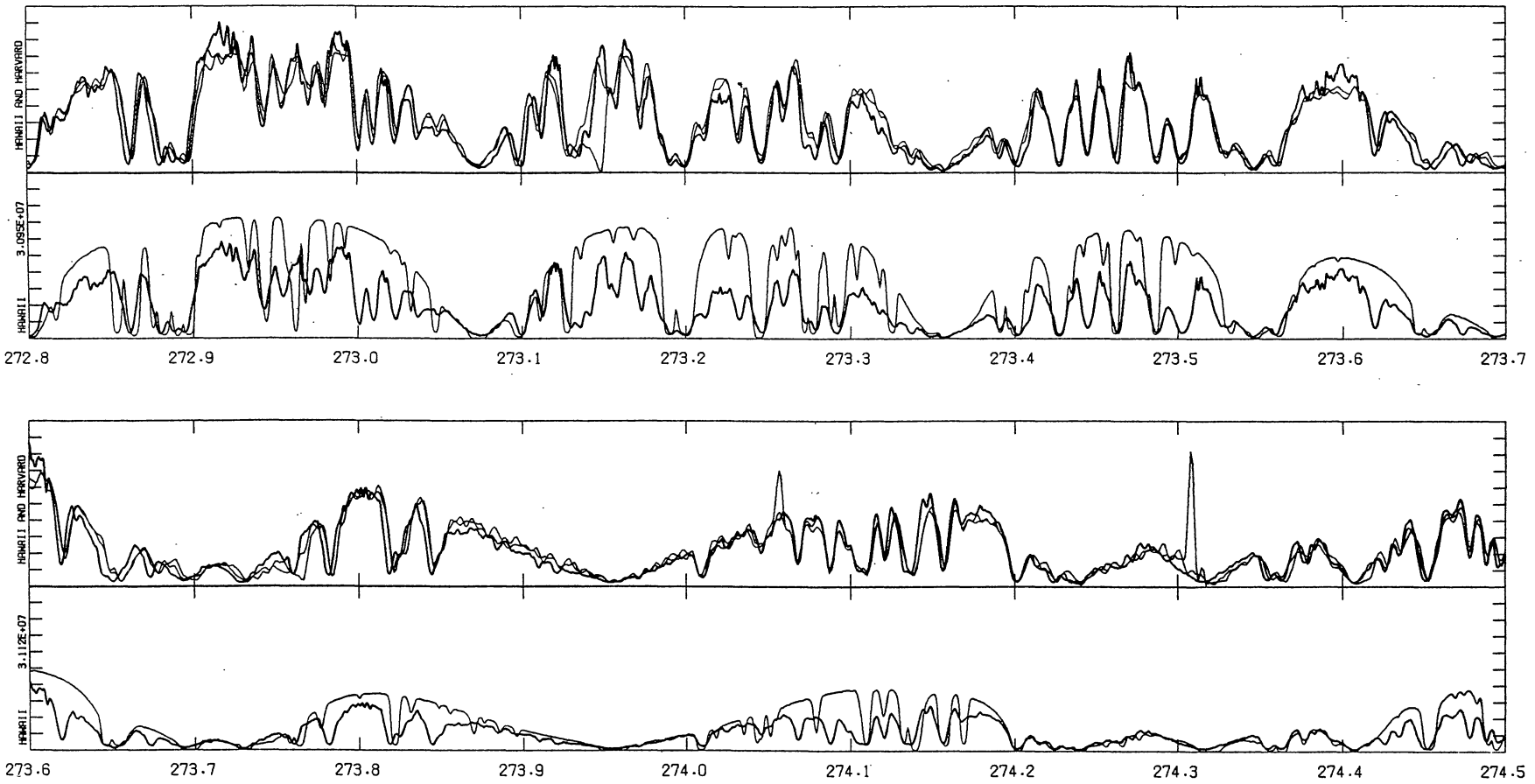

1981SAOSR.391.....K

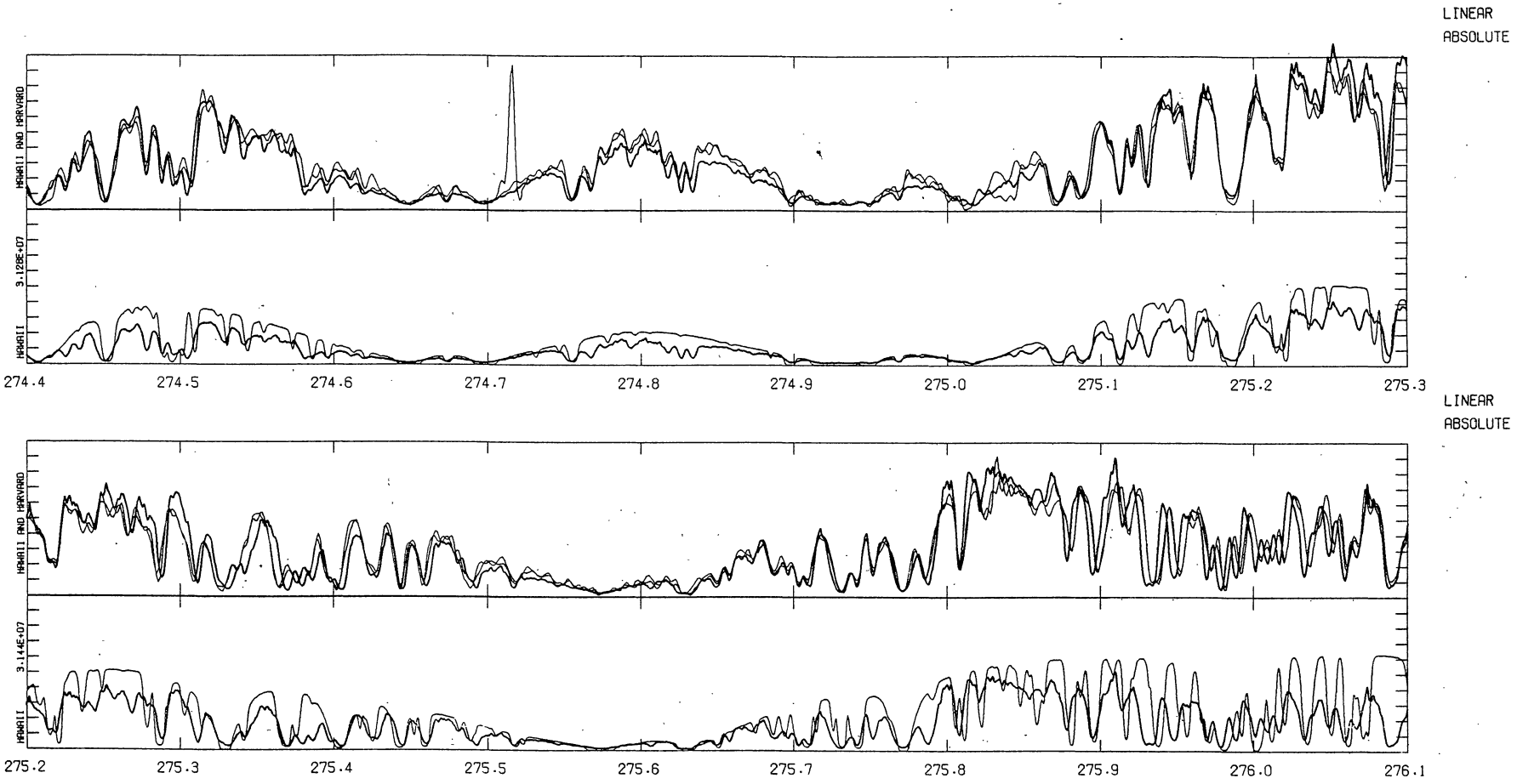

1981SAOSR.391.....K

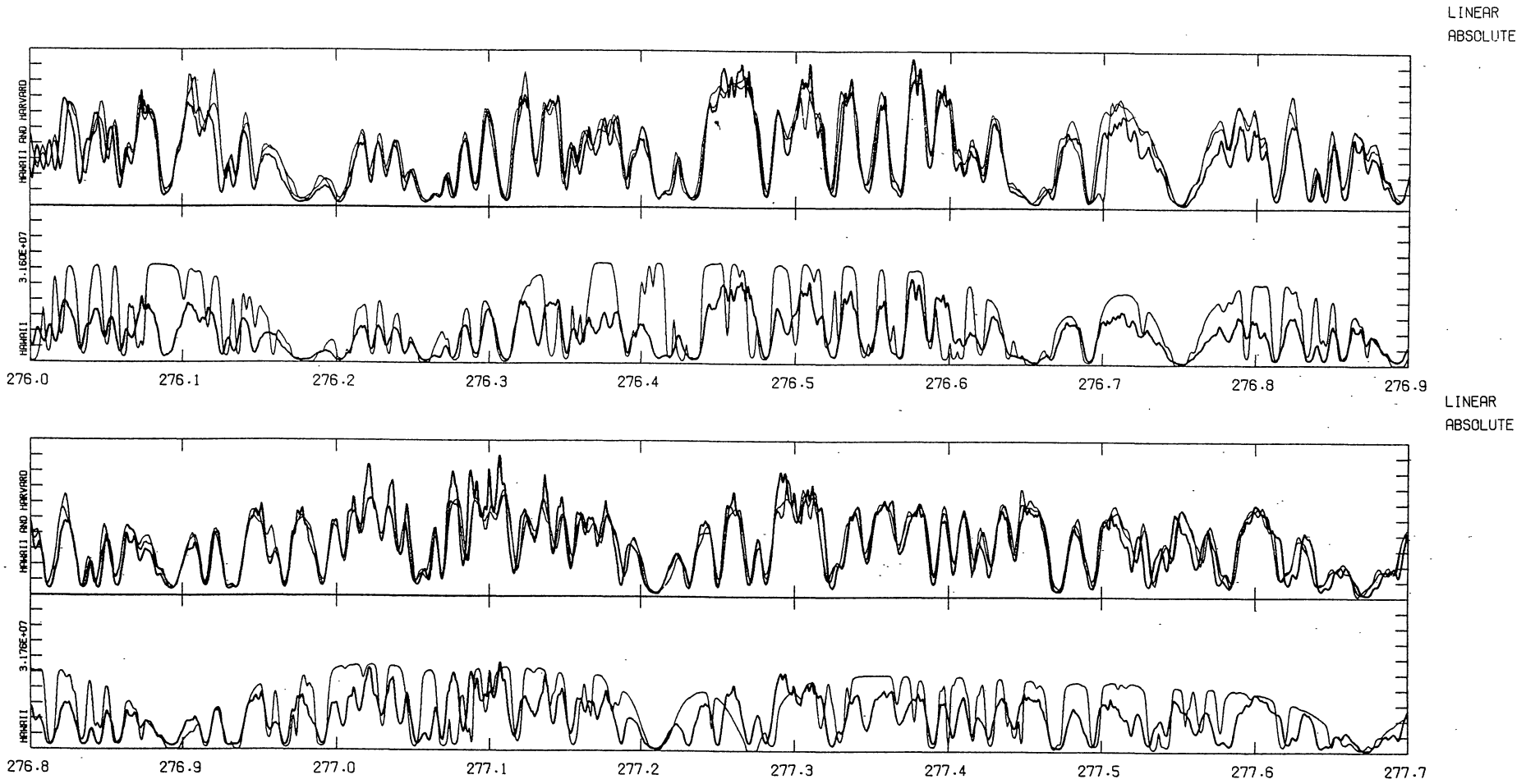

1981SAOSR.391.....K

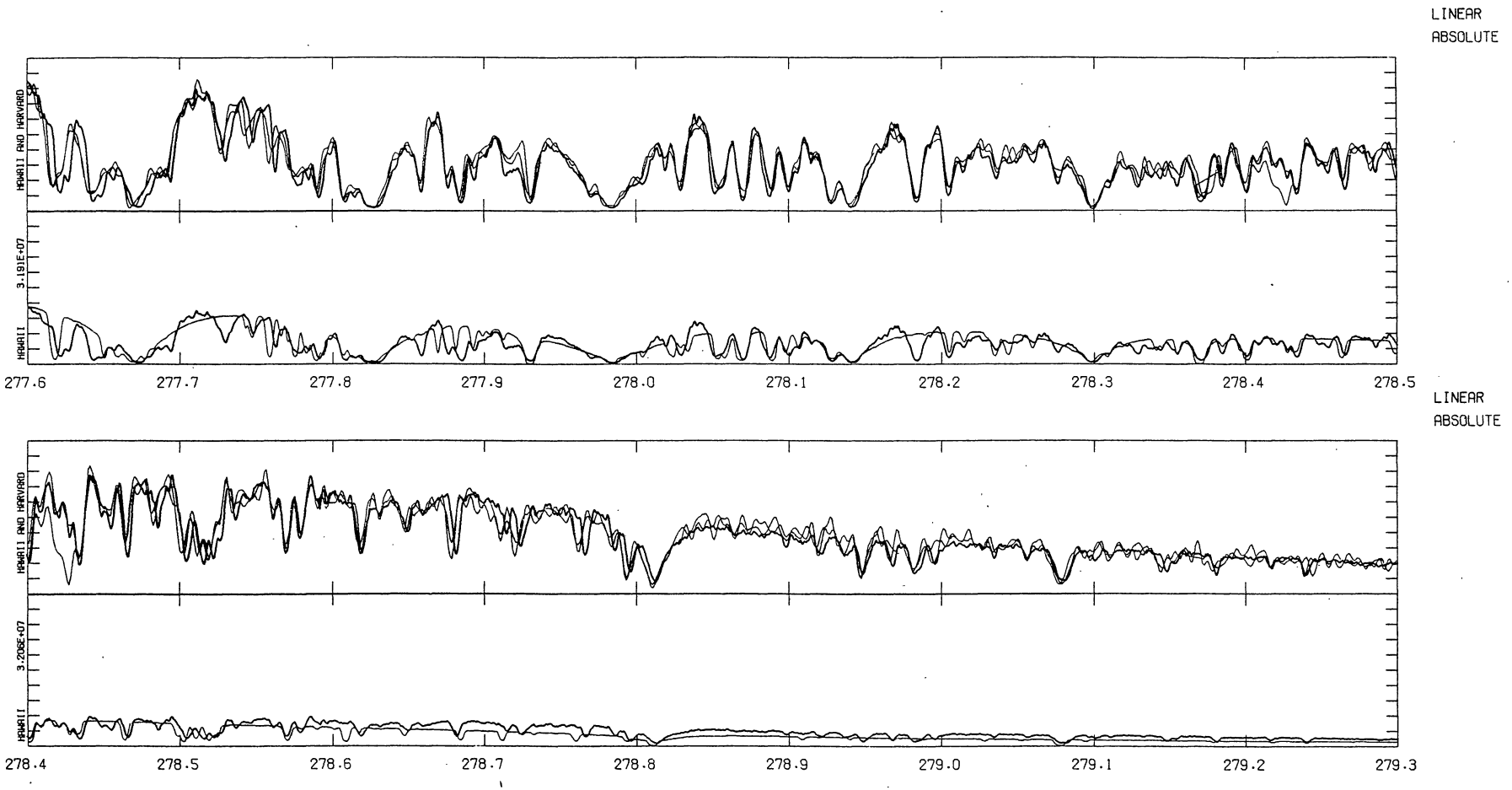

1981SAOSR.391.....K

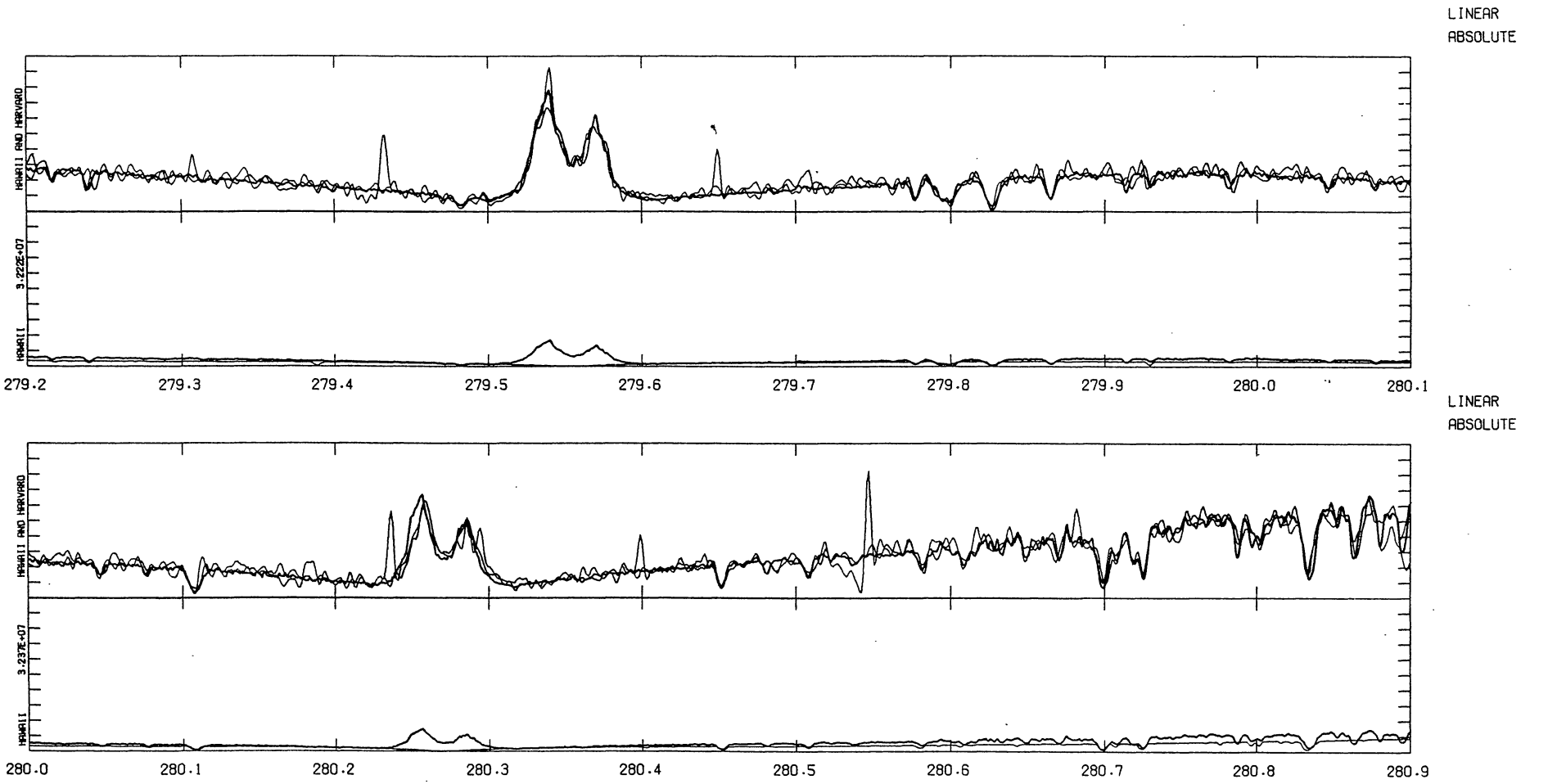

1981SAOSR.391.....K

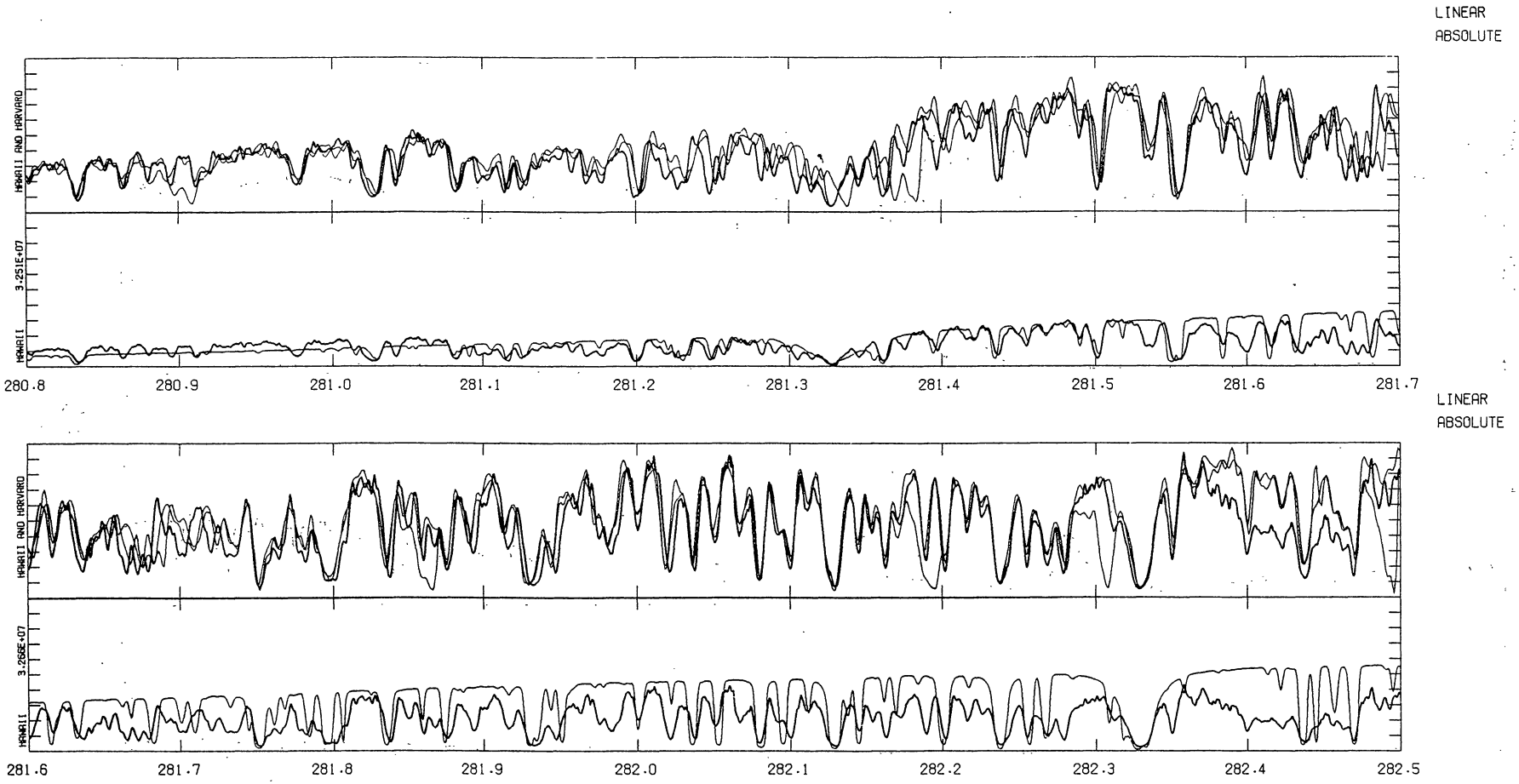

1981SAOSR.391.....K

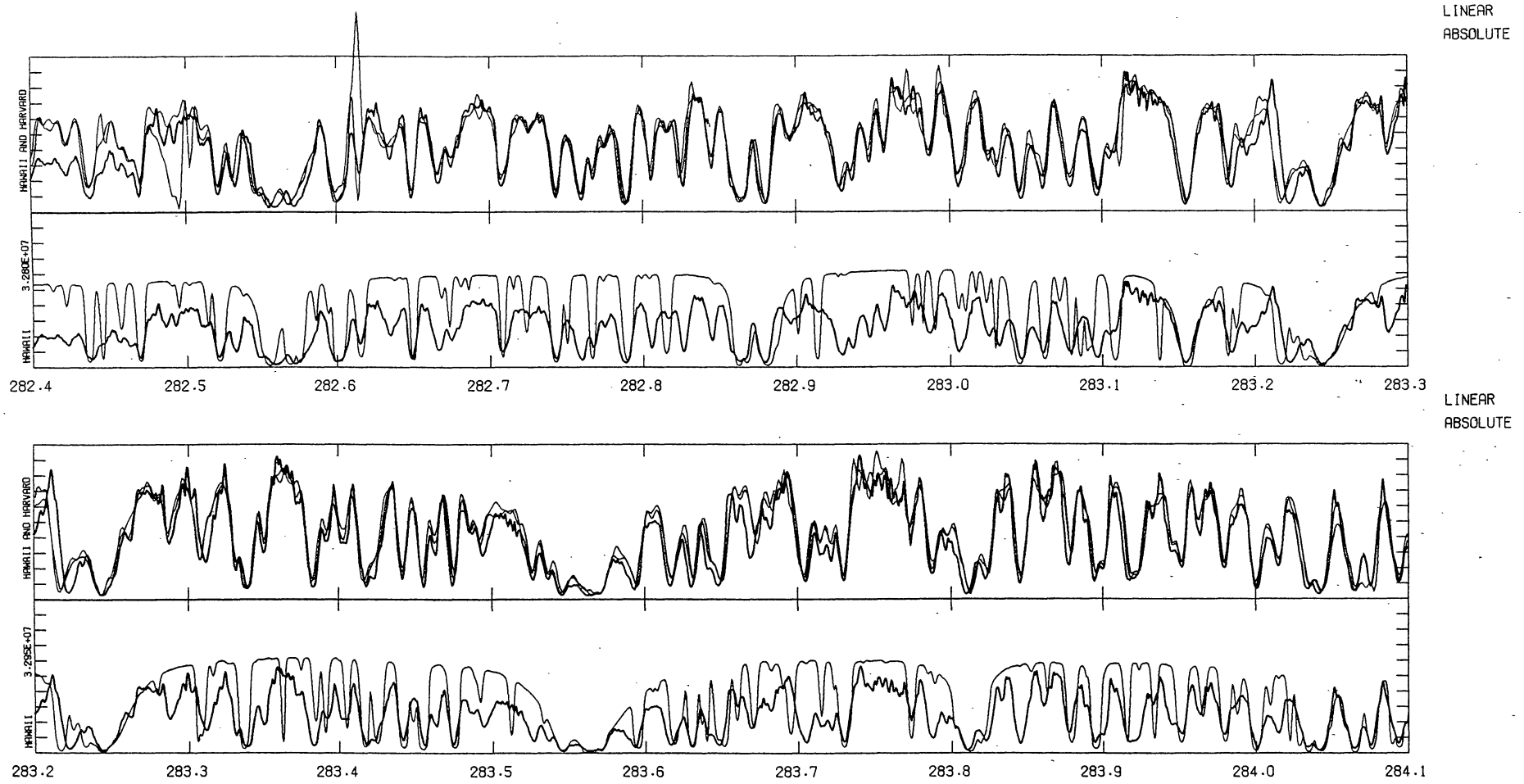

1981SAOSR.391.....K

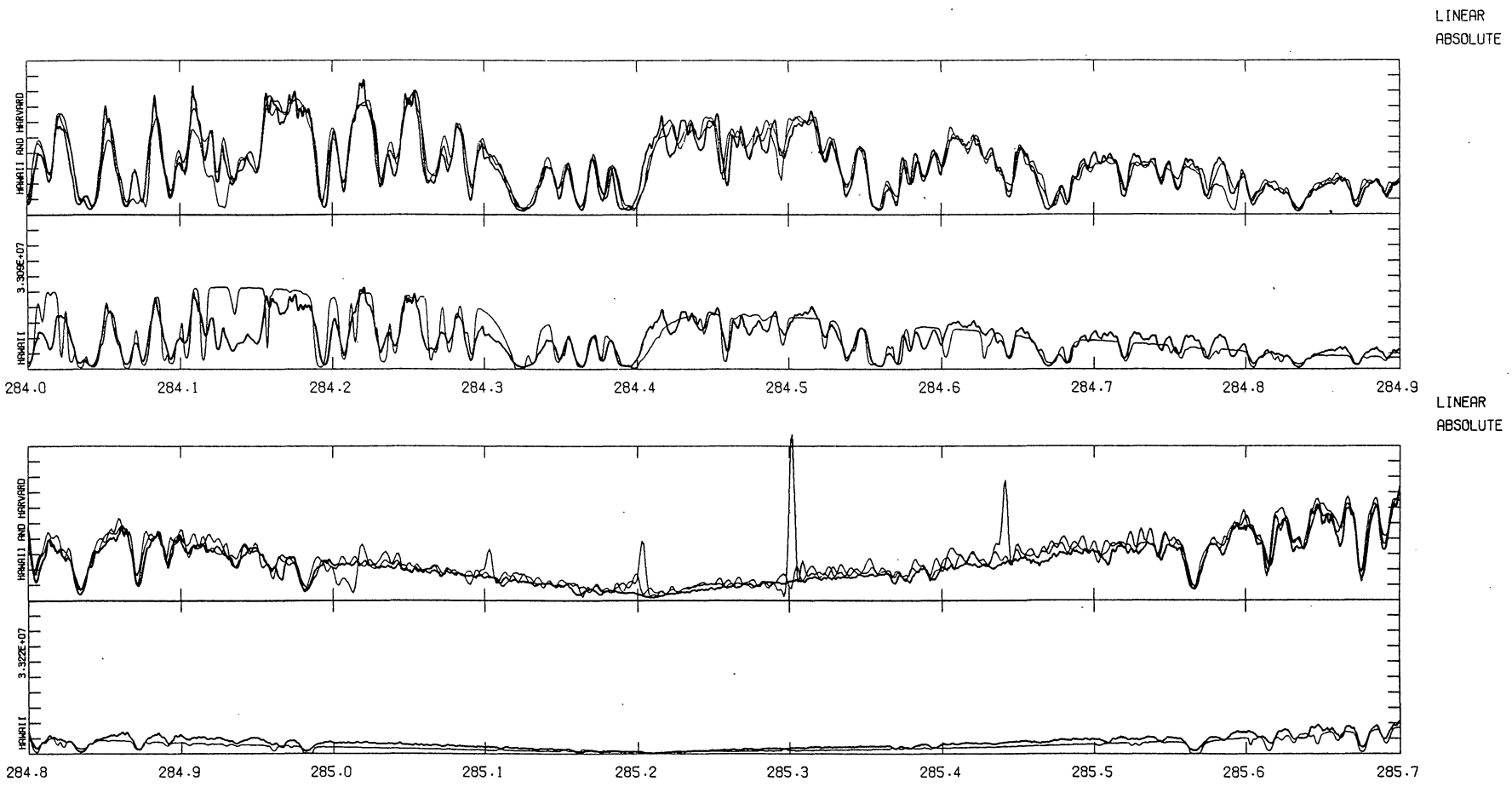

1981SAOSR.391.....K

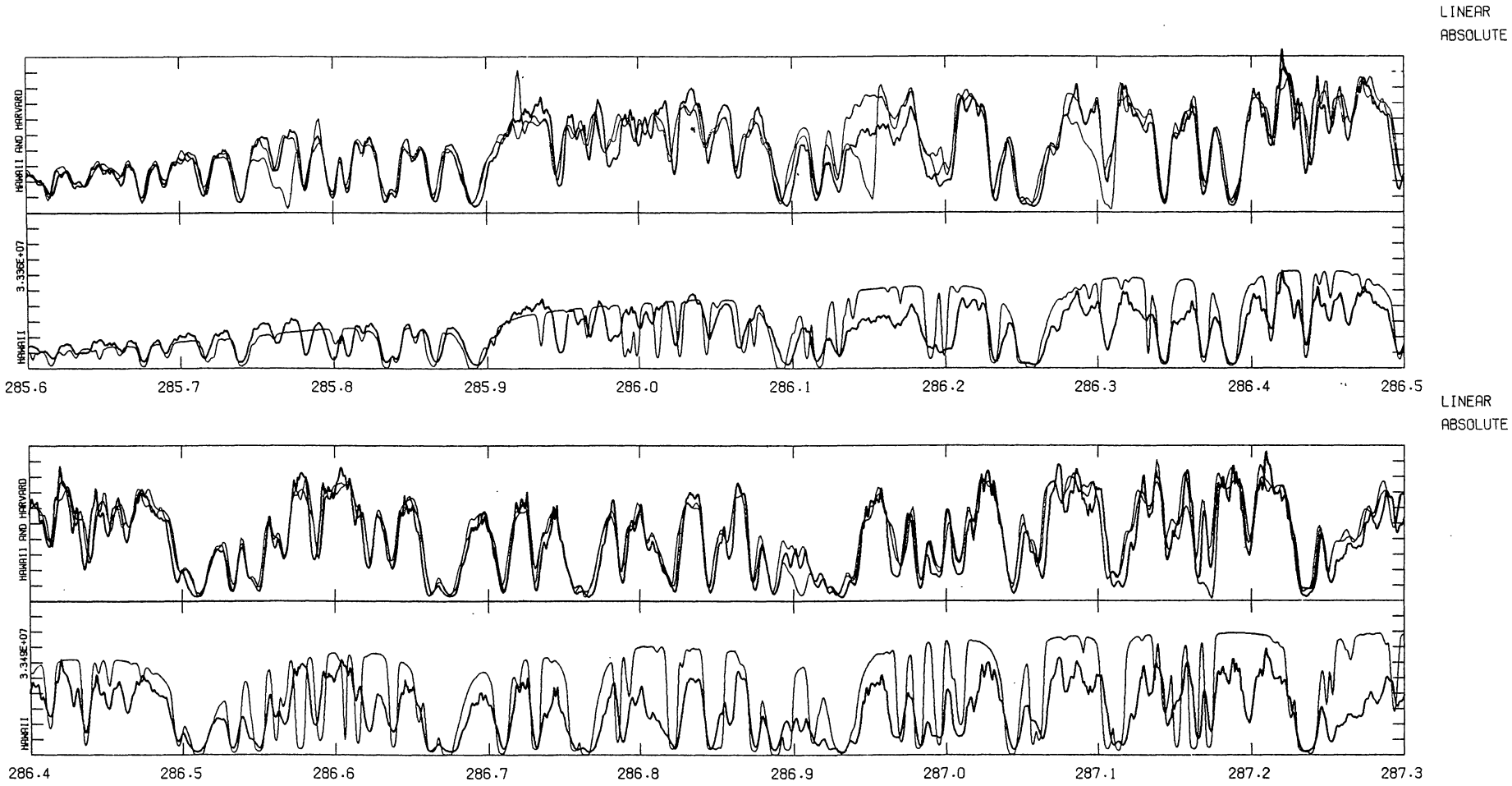

1981SAOSR.391.....K

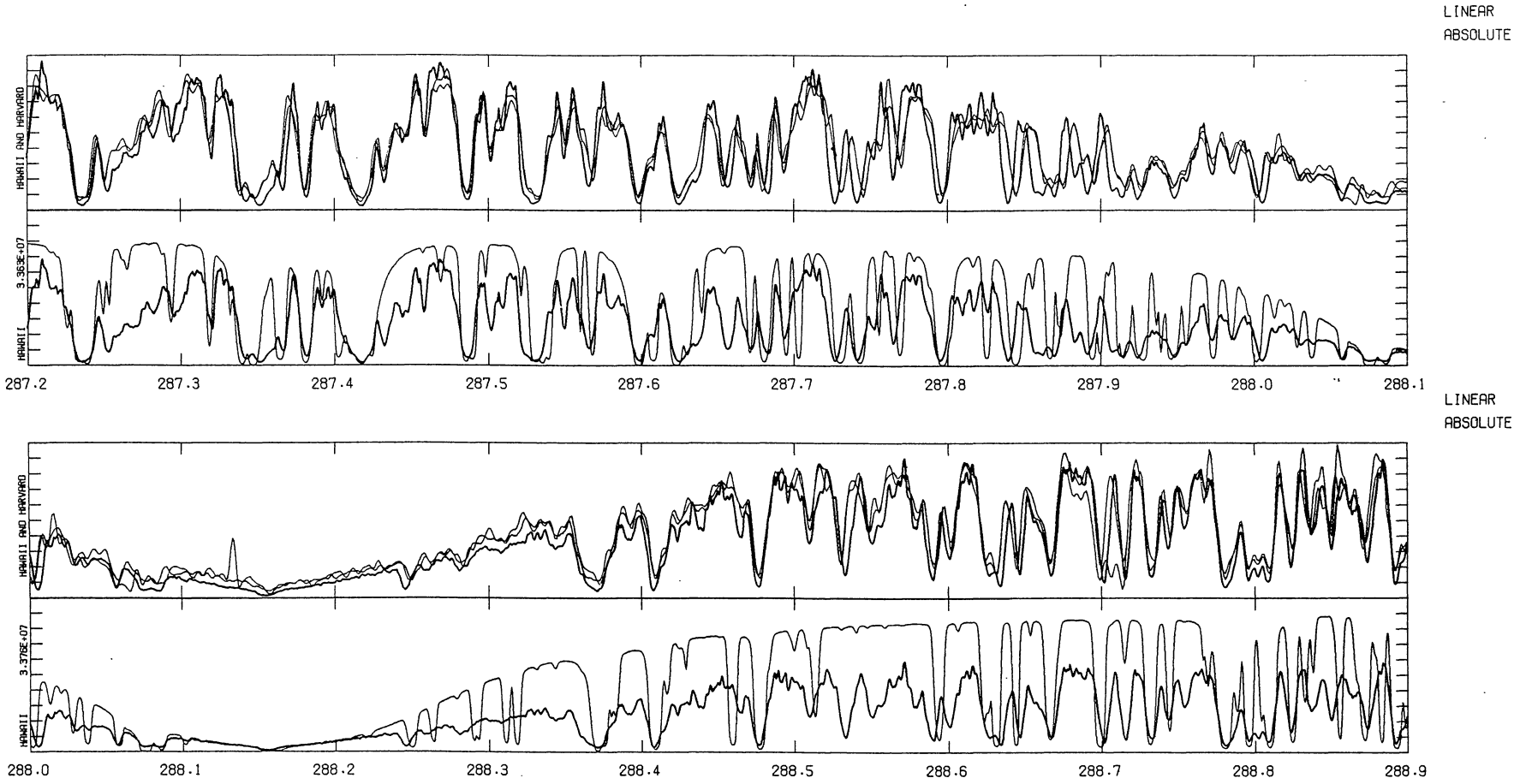

1981SAOSR.391.....K

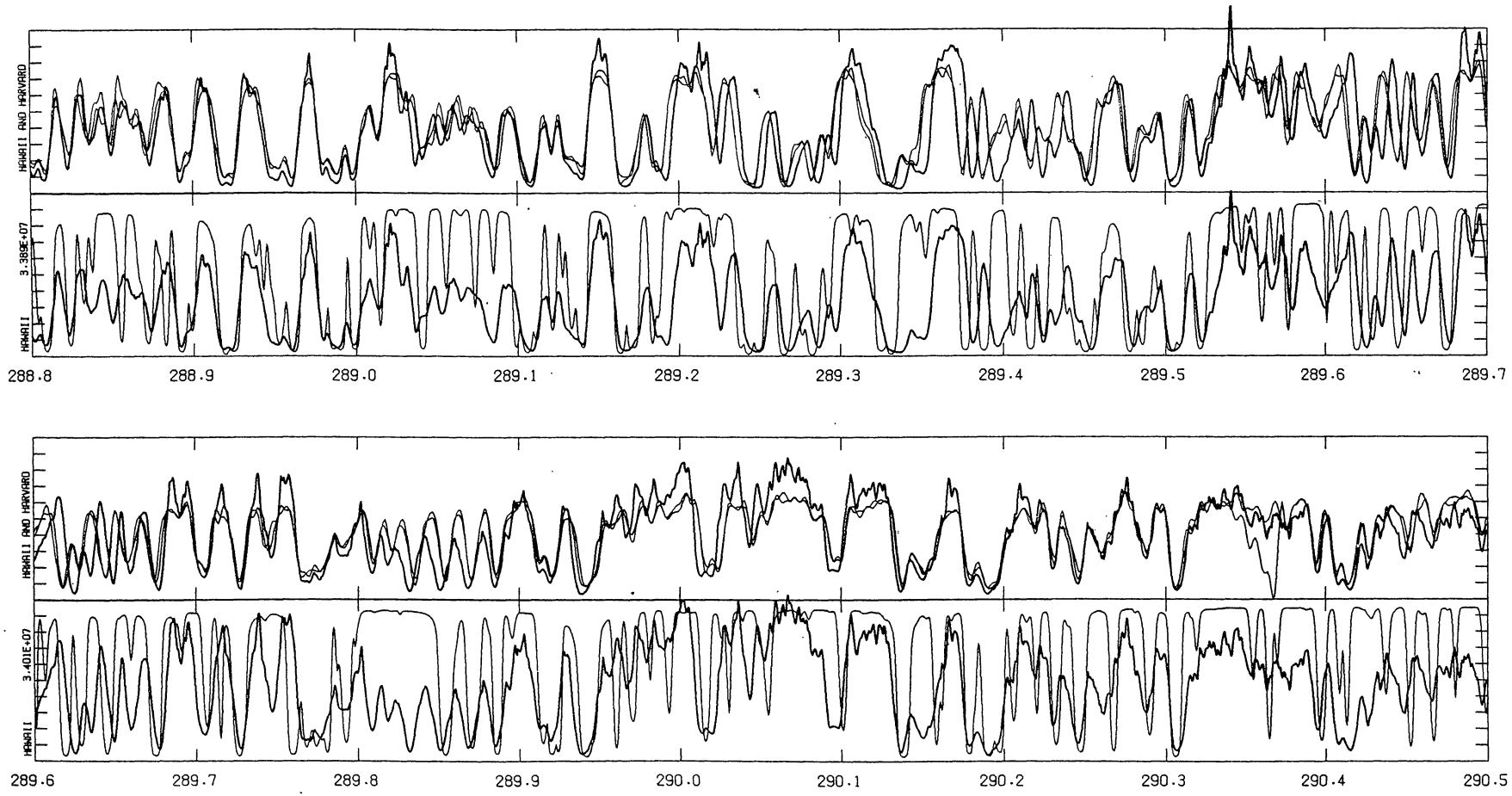

1981SAOSR.391.....K

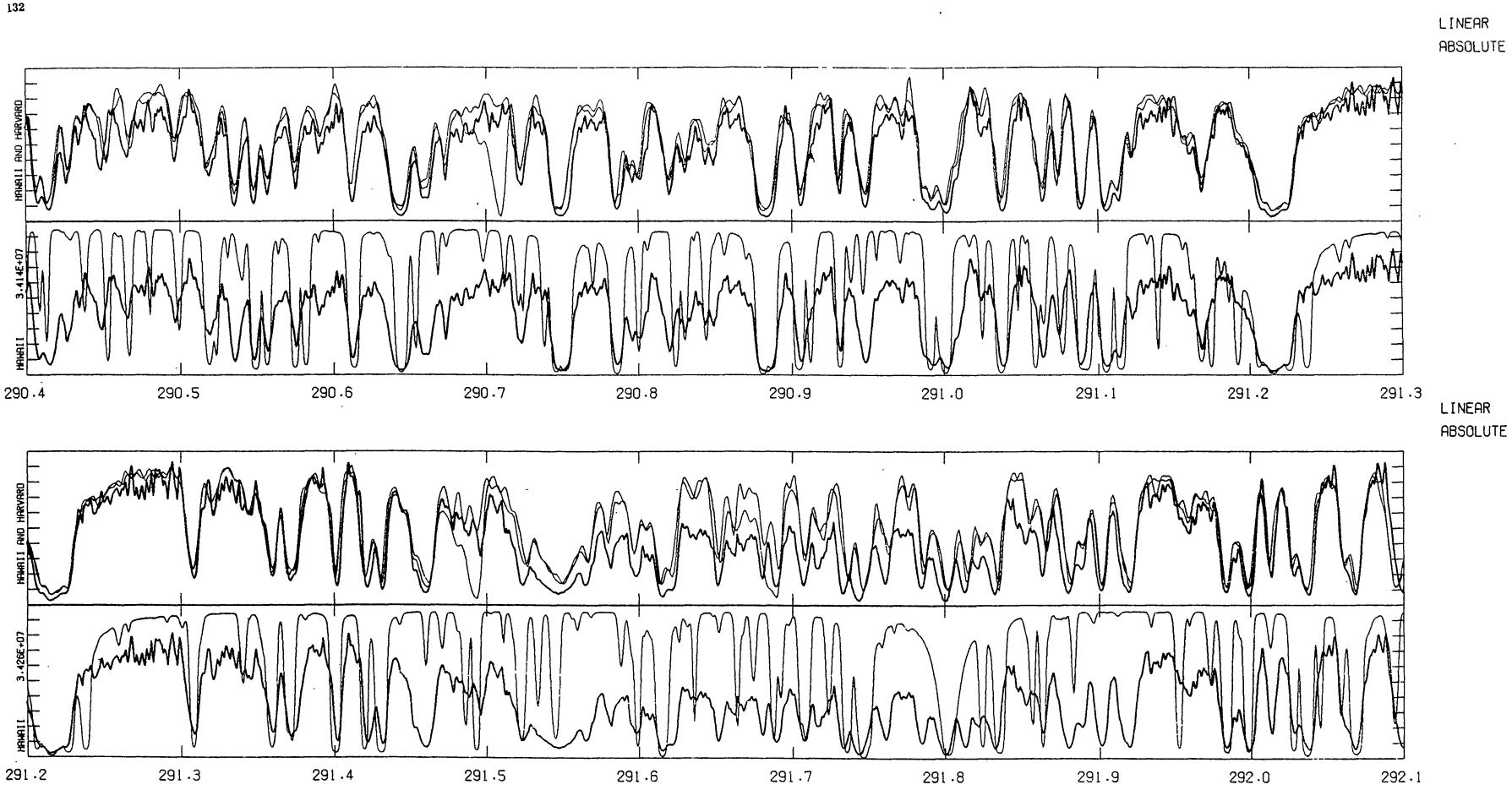

1981SAOSR.391.....K

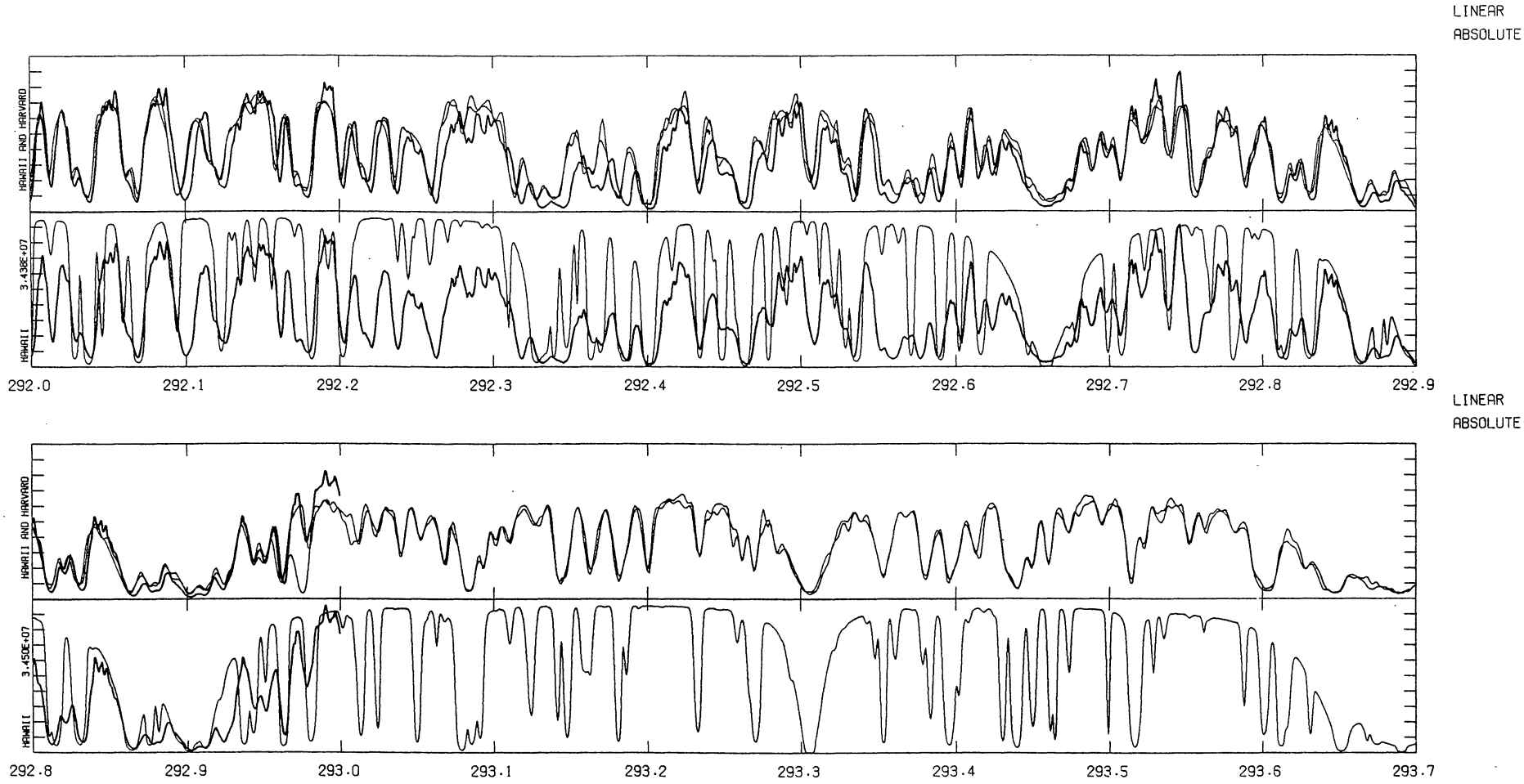

Figure 4. The Kitt Peak disk center spectrum in the wavelength range 294 to 300 nm compared with our calculated spectrum in the lower half of each panel and compared with the Harvard spectra in the upper half of each panel. The calculated and Harvard spectra are the same as in Figure 1. The heavy line is a spectrum scan made from Kitt Peak by Brault and Testerman (1972) for which we have determined an intensity scale by approximately matching that of the Harvard spectra. For wavelengths less than 296 nm, the deepest features in the Kitt Peak data have negative intensities. To eliminate the negative intensities in plotting this spectrum, we have added the intensity ΔI_λ to the Kitt Peak data, where ΔI_λ varies linearly between zero at 296 nm and 5% of the continuum at 294 nm. In future work we will be able to rectify the data more accurately. The scale of the upper half panel is arbitrary.

1981SAOSR.391.....K

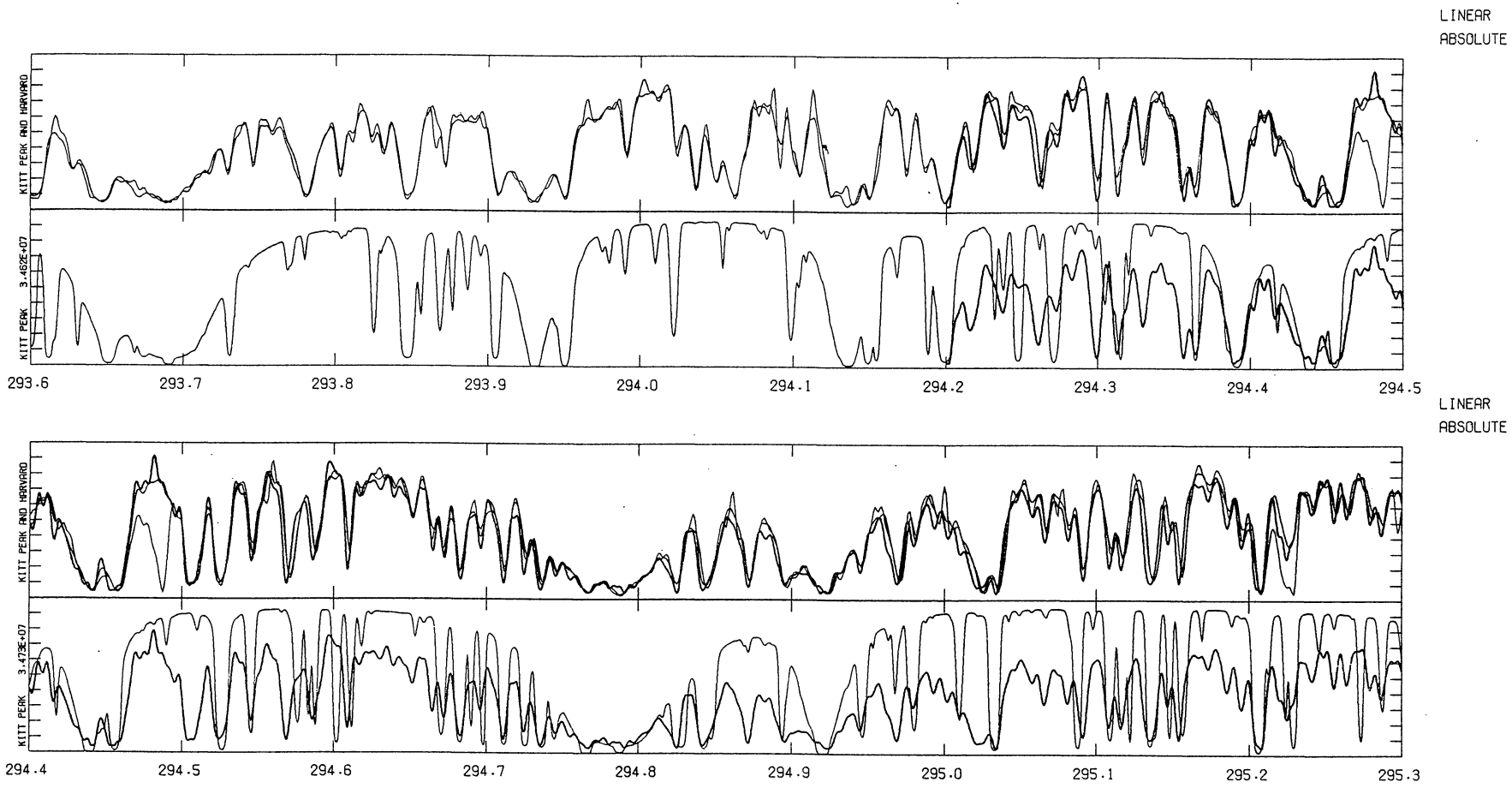

1981SAOSR.391.....K

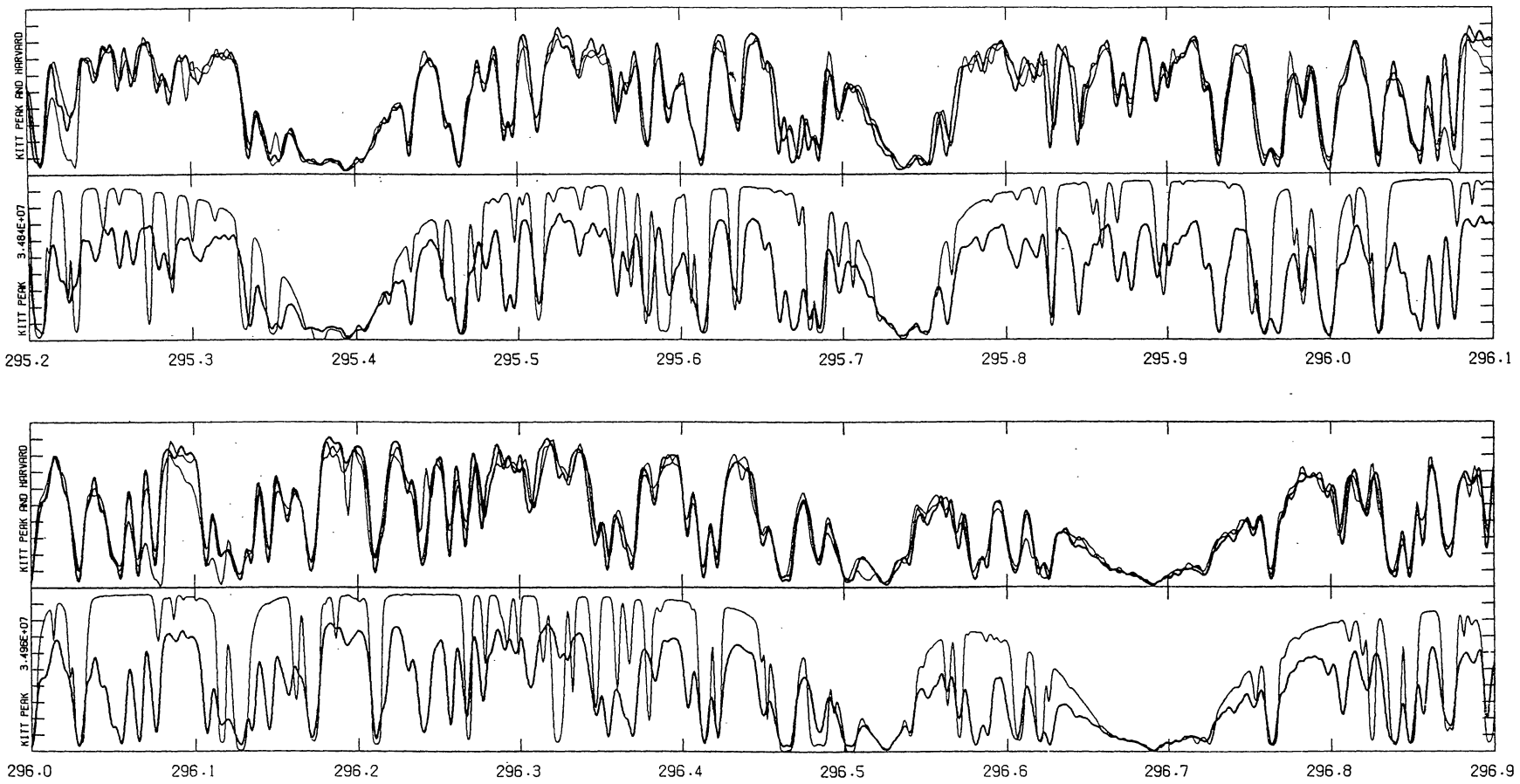

1981SAOSR.391.....K

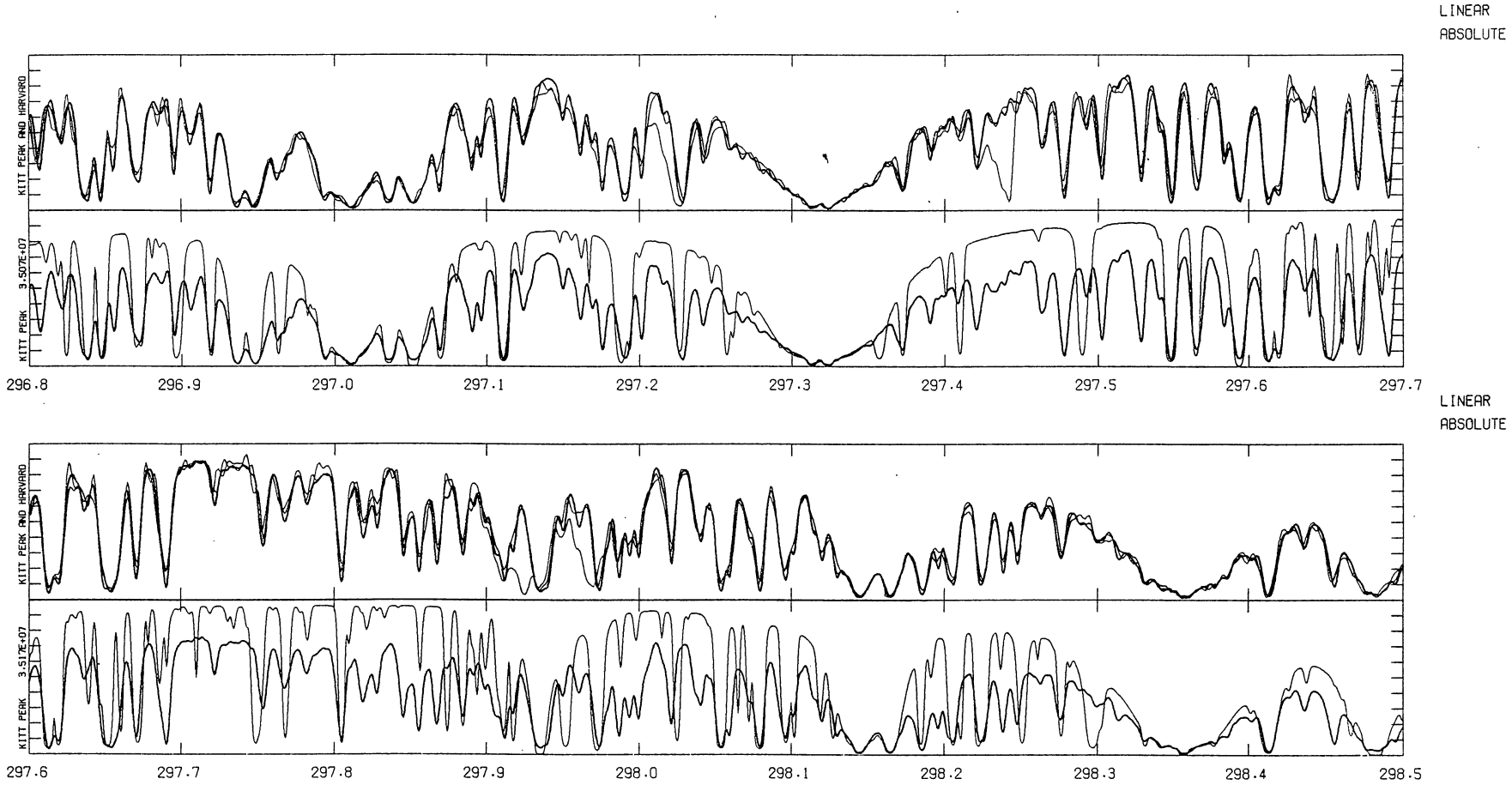

1981SAOSR.391.....K